GEM TN-91-00012

GEM Calorimetry Meeting SSCL

September 4 and 6, 1991

Abstract:

Transparencies and contributions from the GEM Calorimetry Meeting held at the SSCL September 4 and 6, 1991 are presented. A separate volume, GEM TN-91-00009, "GEM Calorimetry Questions and Answers," contains proponents' responses to the questions posed by other people.

Tentative agenda for the September 4/6 GEM Calorimetry Group meeting

Wednesday, September 4

(morning sessions in SSCL Cafetorium)

8 am - 9:45 Technology subgroups meet

9:45 am Begin General Meeting
Introduction - J. Brau

10:00 am Cost estimates/engineering -M. Rennich

10:45 am Liquid Scintillator: Answers to critics - Y. Kamyshkov

11:30 am Lunch

(afternoon sessions in the upstairs conference room)

1:00 pm Silicon: Answers to critics - B. Bugg

1:45 pm Scintillating Fibers: Answers to critics - ? ?

2:30 pm Liquid argon: Answers to critics - H. Gordon

3:15 pm Barium Fluoride: Answers to critics - H. Newman

4:00 pm Liquid xenon: Answers to critics - M. Chen

4:45 pm Scintillating plates: Answers to critics - ? ?

Friday, September 6, 1991

(all sessions in SSCL Cafetorium)

9 am Review and discussion of charge, process, direction

10 am Pre-radiator discussion
general, fibers -P. Cushman
silicon -M. Clemen

11:30 am Lunch

1:30 pm Forward calorimetry
The virutes of forward calorimetry - J. Rutherfoord
Liq. Scintillator - B. Webb
TMS - ??
Liq. argon - ??

3:00 pm Discussion of R/D plans, etc.

4:00 pm Adjourn

September 4 – GEM-CAL

Name	Institution	e-mail (please write clearly)
Jim Brau	U. Oregon	JIMBRAU@SLACVM
Bob Adair	Yale	ADAIR @ YALEHEP
Min Chen	M.I.T.	MITLNS :: CHEN
R. Shuvalov	IHEP	MITLNS :: Shuvalov
W. Bugg	U. Tennessee	BUGG @ SLACVM
Ren-yuan Zhu	CALTECH	ZHU @ CITHEX.BITNE
HANS KOBRAK	UCSD	FNAL:: KOBRAK
Jim Branson	UCSD	BRANSON@UCSDHEP1.UCSD.EDU
Hervey Newman	CALTECH	Newman@ CITHEX.BITNET
Xiaorong Shi	CALTECH	Xrs @ FNAL.BITNET
M. L. Bauer	ORNL	MBB @ ORNLSTC
Frank Plasil	ORNL	FZP @ ORNLSTC
LYLE MASON	MARTIN MARIETTA	LLMASON@SIM.DEN.MMC.COM
Frank Stocker	SSC	Stockes@SSCVX1
Dave Etherton	SSC-PRD	Etherton @ SSCVX1
Craig Wuest	LLNL	WUEST@LLNL.GOV
Alexandre Savine	ORNL	VXCERN:: SAVIN
EVGUENY TARKOVSKY	ORNL	VXCERN:: TARKOVSKY
ANATOLY GOLDEEV	ORNL	VXCERN:: GOLDEEV
ALEXANDRE SMIRNOV	ORAL	
Yur Kamyshkov	ORNL	VXCERN:: KAMYSHKOV
Alexandre Vanyashine	SSC	VANYASHIN@BNLCL1
Hans Cohn	ORNL	COHN@UTKVX
John P. Rutherford	U. of Arizona	[illegible]
Howard Gordon	BNL	BNLCL6:: GORDONH
Veljko Radeka	BNL	RADEKA @ BNL CL1
Hong Ma	BNL	HMA @ BNLCL1
Don Makowiecki	BNL	MAKOWIECKI @ BNLCL1

Name	Institution	e-mail
M. Clemen	Carnegie Mellon Univ.	CLEMEN@CMPHYS
Cliff Eberle	ORNL	ECC@ORNL.GOV EBERLECC@ORNLSTC
Paul M Mockett	Univ. of Washington	Mockett@UWAPHAST
Konstantine Shmakov	ORNL	VXCERN::SHMAKOV SHMAKOV@ORPHA.PHY.ORNL.GOV
Bill Worstell	Boston University	BUPHYC::WORSTELL
MICHAEL SHUPE	UNIV. OF ARIZONA	UAZHEP::SHUPE
Bob Webb	Texas A&M	WEBB@TAMPHYS
LARRY SULAK	BOSTON	BUPHYC::SULAK
William Maier	LANL	MSK@LANL.GOV
HANS PAAR	UCSD	27833::HPAAR
FRANCOIS AYER	CSDL	fnayer@Draper.com
CARL BROMBERG	MSU	MSUHEP::BROMBERG
KON RICHARDS	MSU	MSUHEP::RICHARDS
ROBERT STEINER	ADELPHI UNIV.	RSTEINER@SLACVM

Preradiators

CUSHMAN

Generally employed to

1) Improve Position Resolution
2) e:π separation
3) Recover energy resolution from dead material in front of calorimeter (LAr)

Homogeneous	Thin Sampling (1-2X₀)	Thick Sampling (2
Does not degrade E res.	OK for 25%/√E without E info	Need to add back E OK for 7.5%/√E NOT 2%/√E
Position Resolution	Position Resolution	Position Resoluti and e:π sep
e:π sep	Digital info ⇔ no e:π sep (simpler)	Analog info
Analog Info.		Convert γ's (H → γγ)
Convert γ's		

PAD		STEREO
$\sigma_x \sim 3-10$ cm	(for same ch. count)	$\sigma_x \sim 100-500\,\mu$
No ambiguities		possible ghosts
Could incorporate in trigger - matched to Cal towers		harder to implement in trigger

other issues

Radiation Damage : active medium + electronics

Heat Dissipation (Silicon)

Cracks, cables, readout

Resolution vs speed (Silicon dynamic range for fast clipping?)

Cost (LHC Silicon preRad = 100 M FS)

Position Resolution ← (stereo)

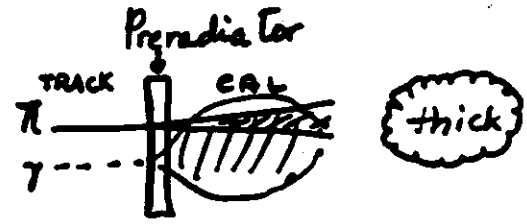

* Distinguish e vs $\pi\gamma$ overlap
  - ⇒ Background of 10^5 (10^3 with isolation cut)
  - ⇒ more important for low B-field
  - ⇒ e.g. UA2 found factor of 200 overlap rejection (track-preshower after cal energy cuts

* $\pi^0 \to \gamma\gamma$ vs γ , γ : jet discrimination ← (Thick)

  ($\Delta x_{min} = \frac{2.6\,mm}{\text{meter flight}}$ for 100 GeV π^0)

  Reduce background (dijets, π^0's) to $H_{Higgs} \to \gamma\gamma$ or $HW \to W\gamma\gamma$ or $Ht\bar{t} \to t\bar{t}\gamma\gamma$

  Also Direct γ physics, structure functions, compositeness etc
  Explore $WW\gamma$ vertex $W\gamma$, $Z\gamma$, $W\gamma$ production.

* Vertex pointing to improve $M_{\gamma\gamma}$ ← (Thick)

* Electron i.d. ← (thin, thick)
  tighter isolation cuts
  perhaps b-tagging : Look for e close to jet
  For 40 GeV jet , $q^* = 2$ GeV $B \to De\nu$
  For $J_t > 1$ GeV (60% of the time)
  the e shower is 7 cm away from jet axis at $R = 0.75$ m
  → Bkgd rejection for $H \to WW \to \ell\nu$ + jets or t-physics. ($q\bar{q} \to t\bar{t} \to Wb\,Wb$)

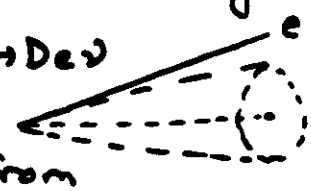

Electron & Hadron Discrimination ← (pad, stereo)

* Early sampling reduces contributions from hadronic showers which charge exchange (Pb is better than BaF_2)
* Not correlated with shower-spread cuts (x15 rejection with 2.7 X_0 for SPACAL after shower cuts - see plot)
* Synchrotron Radiation tags electrons in High Field Option.

Energy Resolution ← homogeneous

* Can recover $7\%/\sqrt{E}$ with realistic $3X_0$ sampling fiber preradiator by adding energy.
* Cannot recover $1.5\%/\sqrt{E}$
* "massless" gaps in LAr to correct for cryostat

Further tracking at large lever arm

Trigger ? ← pad

Sci. Fiber Preradiator

Basic Design: Lead / Fiber ribbon Sandwich

Each Superlayer has 3 stereo views ($\pm 30°, 0°$)
Each view is a double layer of 1mm fibers
with 1.3 mm pitch

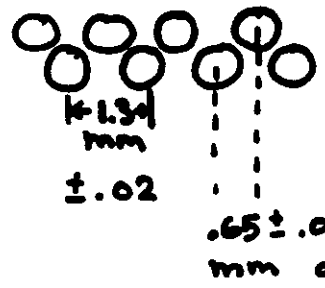

Optimal pitch $= \frac{4}{3} \times$ diam.

$$\sigma = \frac{\text{pitch}}{4\sqrt{12}} = 94\mu$$

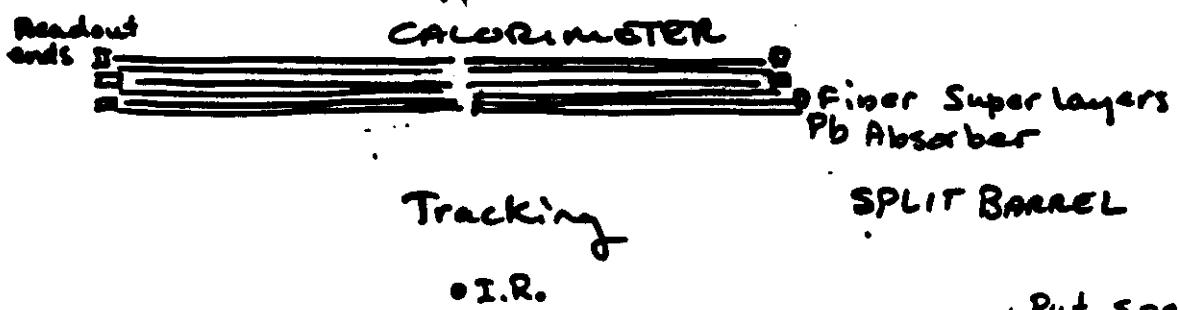

Fibers at $2.0X_0, 2.5X_0, 3.0X_0$ of Pb. (Put spacers between layers to improve angle measurement)

Fiber length = 1.5 m (1.7 m for $\pm 30°$)

Fibers / SL ≈ 20,609 × 2 barrels

Pixel tube 2cm × 2cm with fibers packed at 1.1 mm
⇒ 330 fibers ⇒ 124 tubes / SL (@ $5000 / prototype tube)

(256 channel multianode PMT)
is roughly comparable, just put multiplexing OUTSIDE tube.

4–10 p.e. per fiber per Min I particle

20–600 p.e. " per electron

— compare —
x and y (30cm × .5mm) Si Strips ⇒ 188,500 channels for 1 layer

Fiber Readout

Lots of channels ⇒ ① Multiplexing Scheme to reduce cost

⇒ ② Sparse readout to increase speed

Options

A.) CCD – 1st try at ①, but too slow (5 msec)

B.) Crossed-wire PMT

- ⇒ reduces channel count
- ⇒ fast
- ⇒ But has ambiguities and cross talk

C.) Multi-anode PMT

- ⇒ Too many channels
- ⇒ fast
- ⇒ Phillips XP7022 (64 ch, 96 ch), Hamamatsu new } <1% crosstalk And no ambiguities.
  - old had bad crosstalk
- ⇒ B-field vs Q.E. vs design questions
- → Solution: Design readout chip to do multiplexing
  - PS/SM subsystem: SACLAY work.
  - $5000 / tube PLUS cost of readout

D.) Pixel Tubes

- ⇒ Put silicon and readout chip in a
- ⇒ Proximity-focussed tube (B-field resistance)
  - $4000 / tube is tube + readout
- ⇒ fast and sparse and serial – see next page

Low Occupancy Option

– Rejected for GEM config.

"Smart Pixel Readout"
D. Nygren

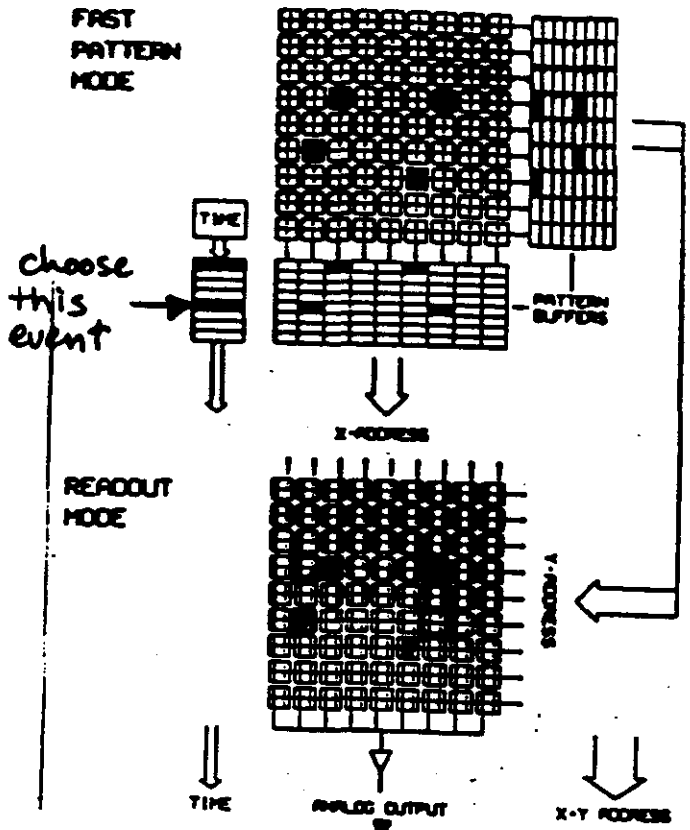

choose this event

pixel size (10μ×100μ)

Only read out addressed pixels of appropriate time stamp above pedestal charge.
(interrogate pixel charge at readout)

One ADC per Tube

Occupancy at $\mathcal{L} = 10^{33}$

1mm fibers at 1m ~ 10^5 Hz
1.5m long
hit every 10 μsec

~300 fibers/tube ⇒ 300 · 100 KHz ≈ 30 hits/tube/μsec

☆ Occupancy too high! — Go to bigger pixels (1mm×1mm) and put memory chip on each.
Clock pointer every bunch crossing.

Pixel Tubes

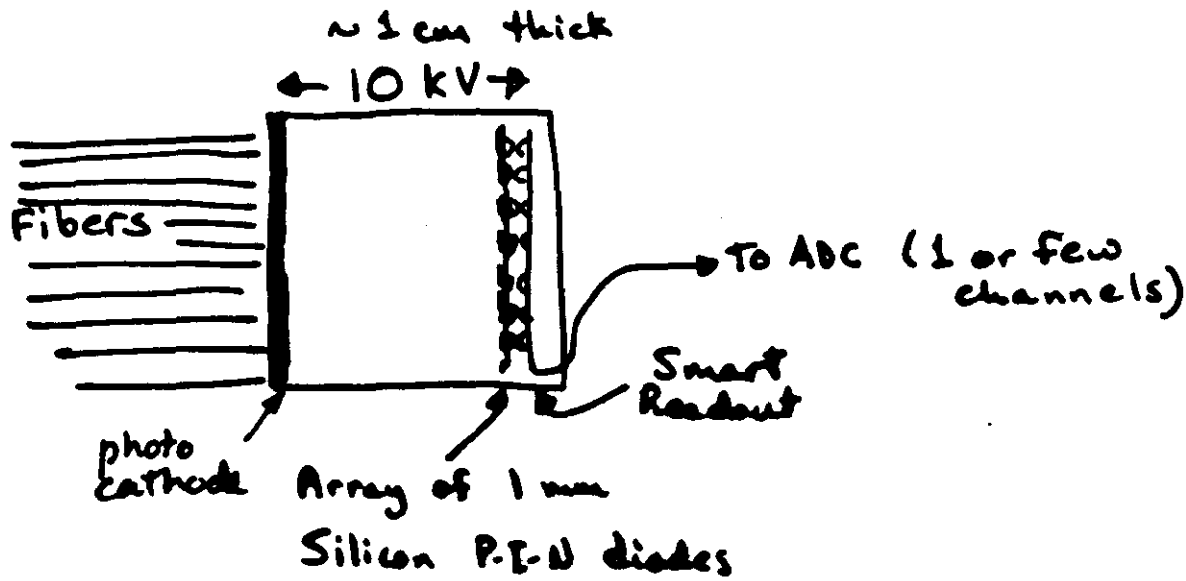

<u>Silicon diodes</u> (similar to Nygren + Shapiro trackers)

* Thick (200-350 μ) ⇒ Capacitance in femto farads
* high resistivity (40 KΩ / sq)
* 500 e⁻ rms measured, 200 e⁻ rms expected soon
* Gain = $\frac{10\ kV}{3.6\ ev}$ = 2778 ⇒ S/N (1 p.e.) ~ 10

<u>Readout</u>

Pixel size matched to fiber ⇒ more room for circuitry

Clock data into memory every bunch crossing (e.g. M. Levy (LBL) has 256 location, 12 bit chip 100μ x 10mm runs at 66 MHz) Effective Pipeline

1st Level trigger at fixed interval, dump data to buffer for 2nd level

<u>Measurements</u>

Single Silicon diode in a GEN 1 PMT (R. de Salvo)

Gain measured = 2000 - 3500 for 7 tubes

<u>Lifetime Test</u> (KeV p.e.s damage surface: worse than vertex detectors with min I which deposit throughout silicon) problem??

corresponds to 1.88 x 10⁹ p.e./sec { 3600 hours with LED (3 μamp, 10 KHz) gave 30% linear reduction in output signal over time.

Max. electron signal 500 p.e. at 40 KHz ⇒ 2x10⁷ p.e., ⇒ No Problem!

Front end read out scheme

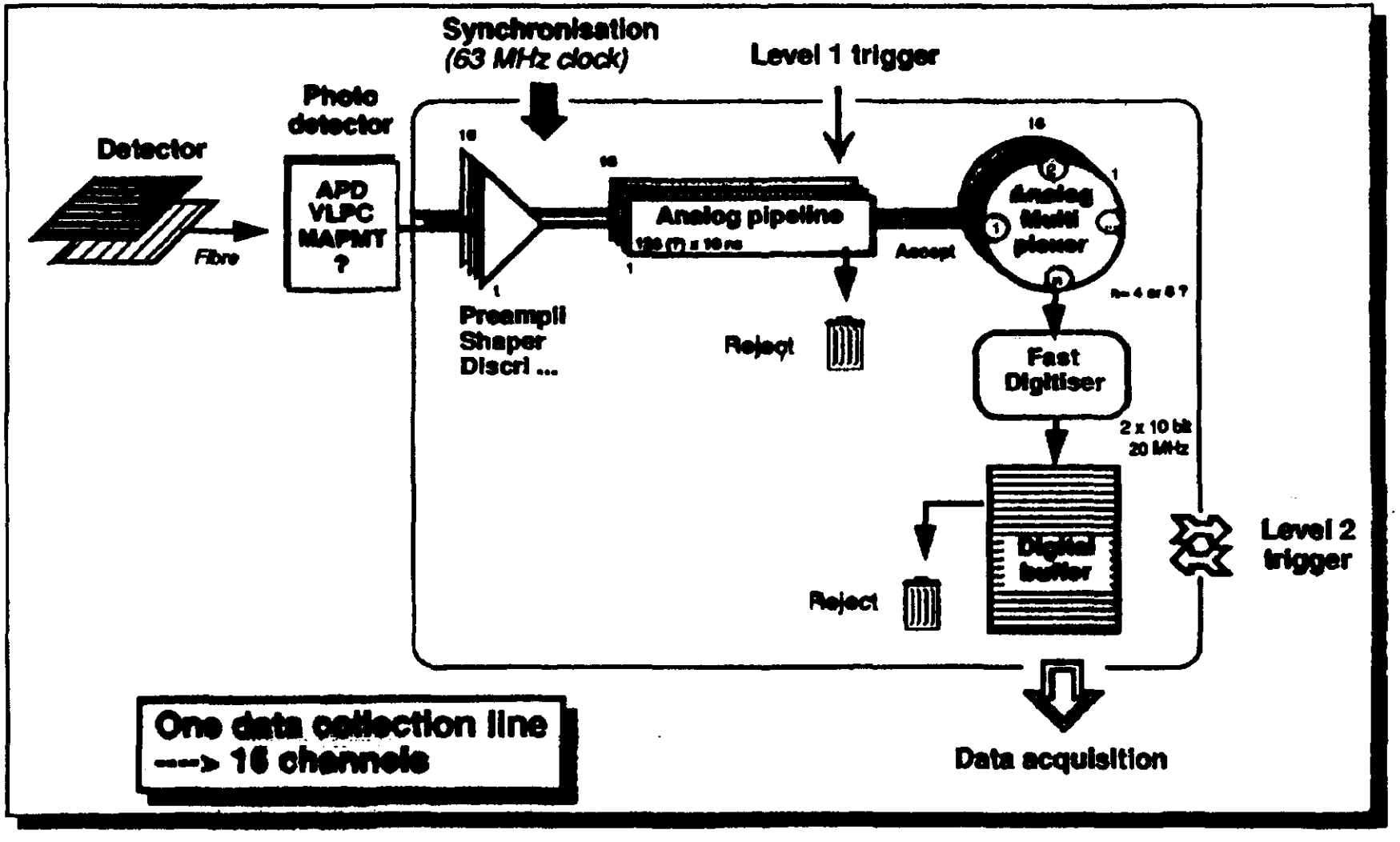

Summary & Cost

Components	Description or type	Number	cost/ unit KFF	cost/ unit K$	Total MFF	Total M$
Photodetector & Cables	APD, VLPC	135168	0.12	0.02	16.220	2.703
Front end						
Front end card	192 ch. digitiser	704	17	2.833	11.968	1.994
Crate	9U Euro-VME	48	18	3	0.864	0.144
Processor (Acquisition)	FIC	48	18	3	0.864	0.144
Synchro & trigger	LTU	48	9	1.5	0.432	0.072
Processor (Monitoring)	FIC	8	18	3	0.144	0.024
Crate interconnection	VIC	48	15	2.5	0.720	0.120
DAQ						
Crate	VME	1	18	3	0.018	0.003
Processors	FIC & RAID	5	30	5	0.150	0.025
Crate interconnection	VIC	3	15	2.5	0.045	0.008
Cables	optical fibres...				0.300	0.050
Workstation & Periph.	SUN4...				0.500	0.083
TOTAL					32.225	5.370
add 10% (protos,spares)					35.448	5.907

120 FF or 20 $ per channel
(Front end + DAQ)

MONTE CARLO

Each view is double layer of close packed fibers, 1 mm in diam. of which 40 μ is insensitive cladding.

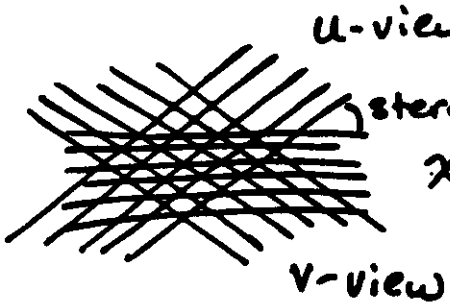

This makes 1 superlayer

3 Superlayers sandwiched between lead.

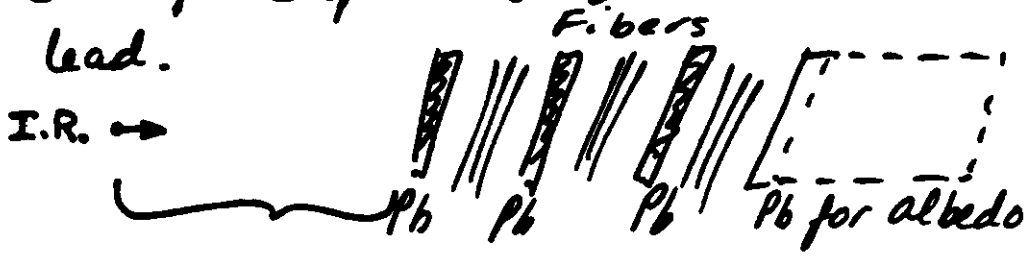

.75 meters
0.8 Tesla

Reality : 1.6 m att. length
15% Quantum Eff.
Poisson Statistics
Polya Distribution for PMT gain
Birk's Law for saturation effects

RESTORE ENERGY RESOLUTION (?)

Assume $\frac{7.5\%}{\sqrt{E}}$ for Calorimeter.

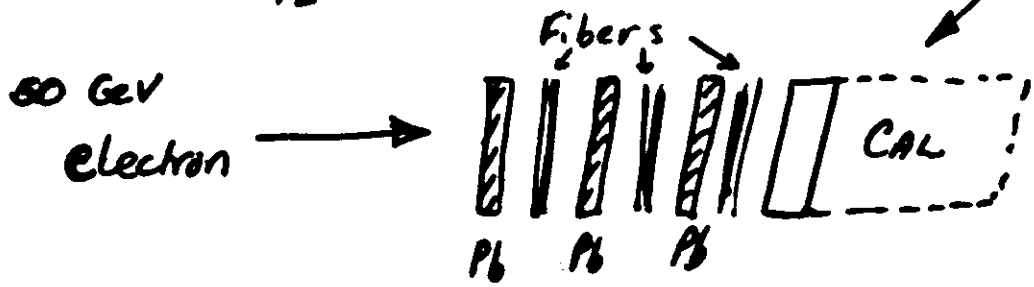

$1X_0$ layers of Pb

After $3X_0$ resolution $\rightarrow \frac{12\%}{\sqrt{E}}$
and $E_{CAL} = 47.7$ GeV

After $2X_0 \rightarrow 10\%/\sqrt{E}$
After $1X_0 \rightarrow 7.7\%/\sqrt{E}$

Add 3rd sampling layer only $\rightarrow \frac{9.1\%}{\sqrt{E}}$

2nd + 3rd S.L $\rightarrow \frac{7.8\%}{\sqrt{E}}$

1, 2, 3 S.L $\rightarrow \frac{8.3\%}{\sqrt{E}}$

uncertainty on 250 events

For $\frac{1.5\%}{\sqrt{E}}$, after $3X_0 \rightarrow 8.9\%/\sqrt{E}$

after $2X_0 \rightarrow 5.1\%/\sqrt{E}$

after $1X_0 \rightarrow 3.8\%/\sqrt{E}$

Hard to get back good resolution – fluctuations in Pre rad are TOO much.

50 GeV Electrons (1mm fibers)

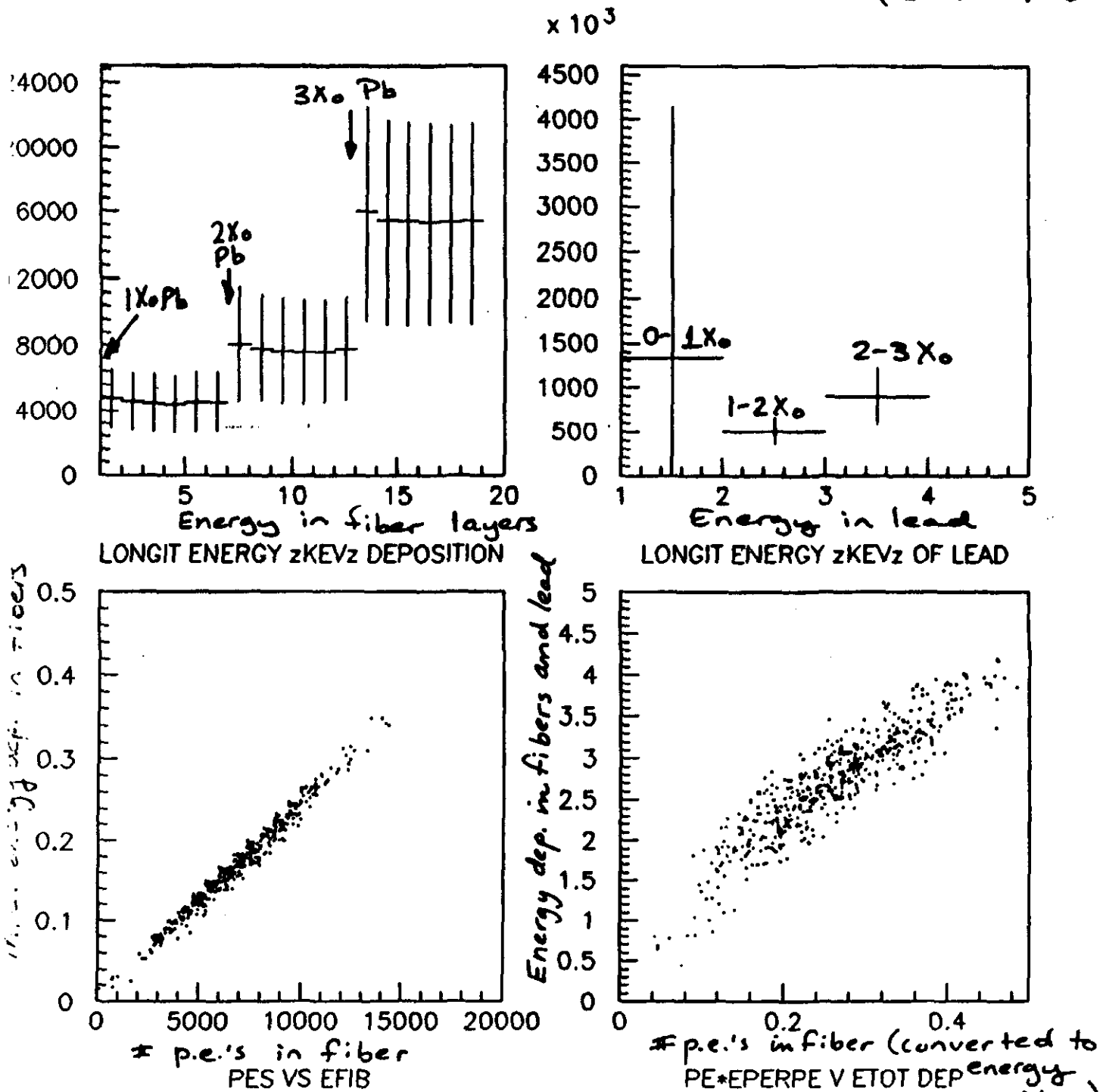

50 GeV Electrons
1mm fibers

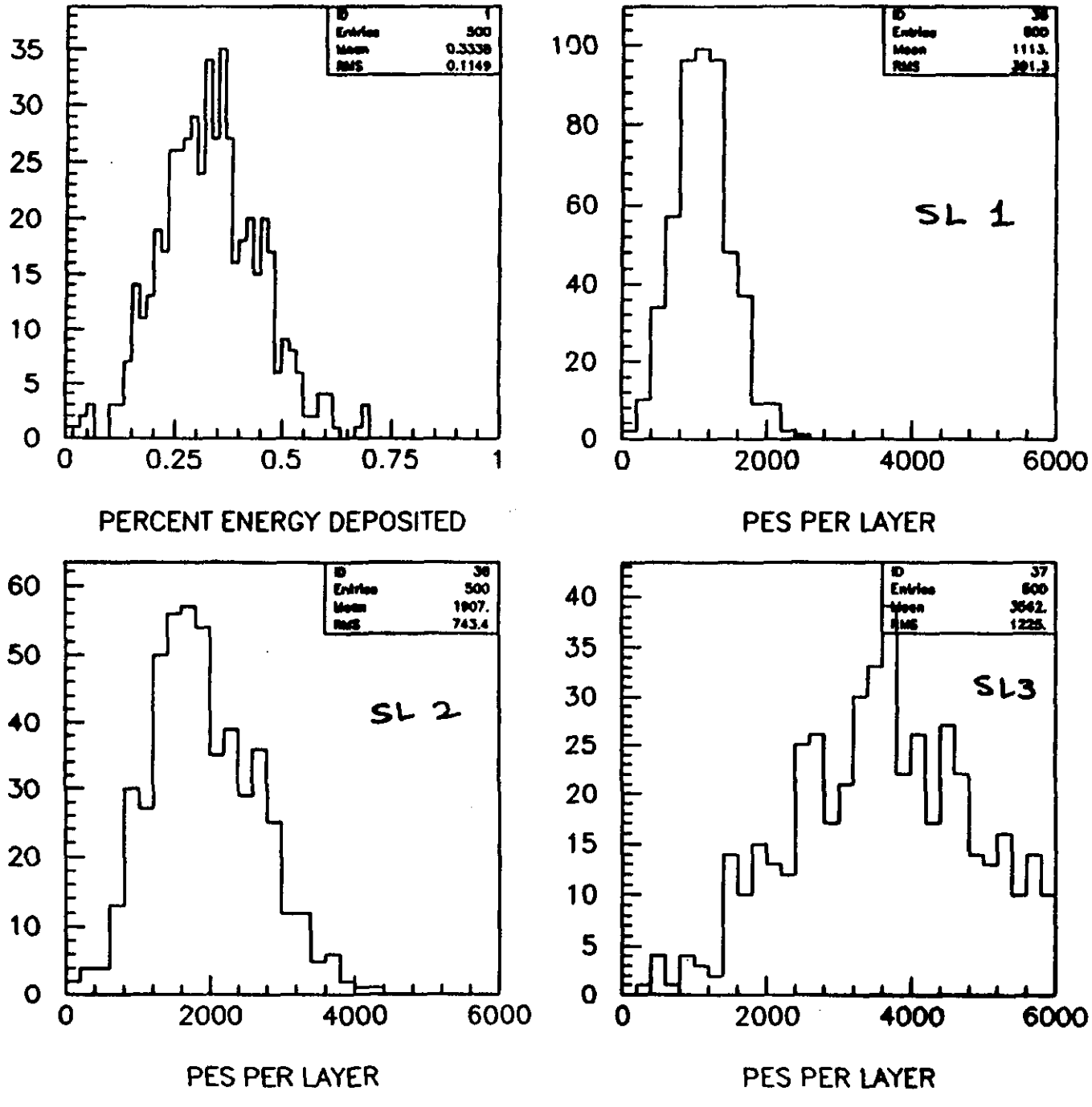

50 GeV Photons
1 mm Fibers

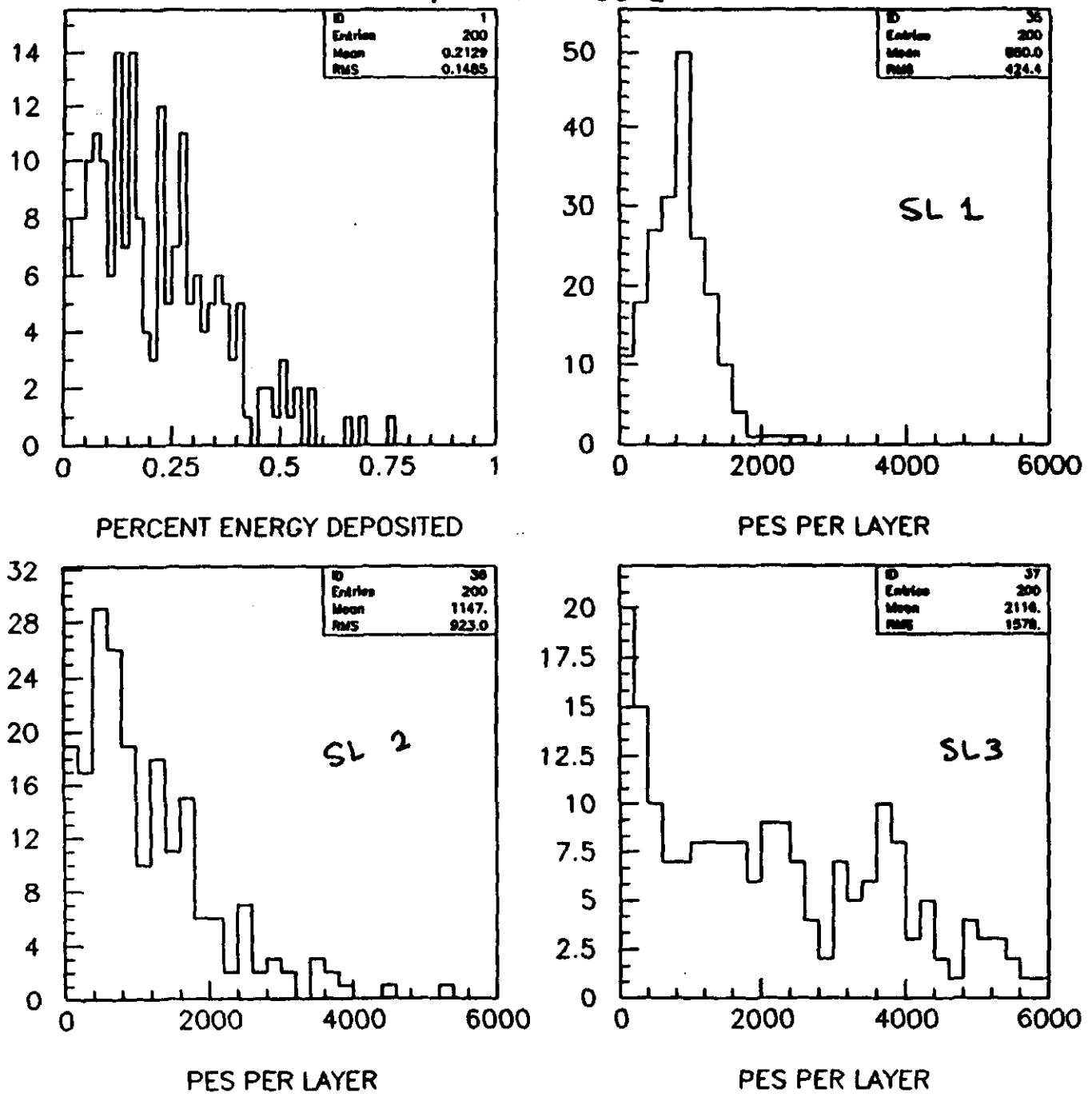

50 GeV electrons

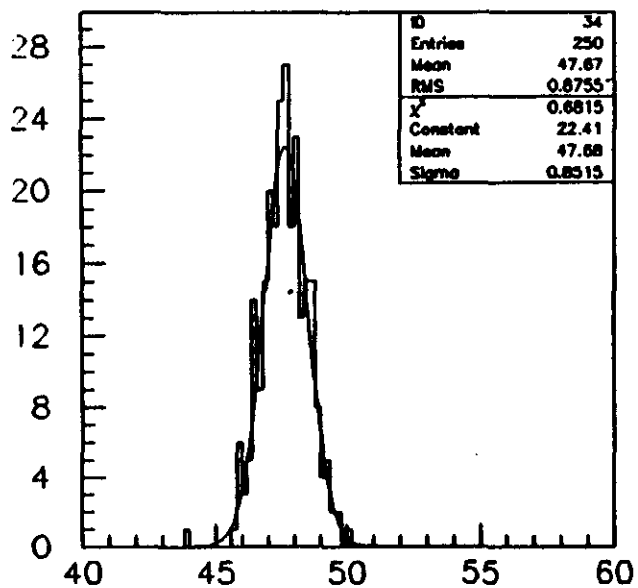

ENERGY IN CAL

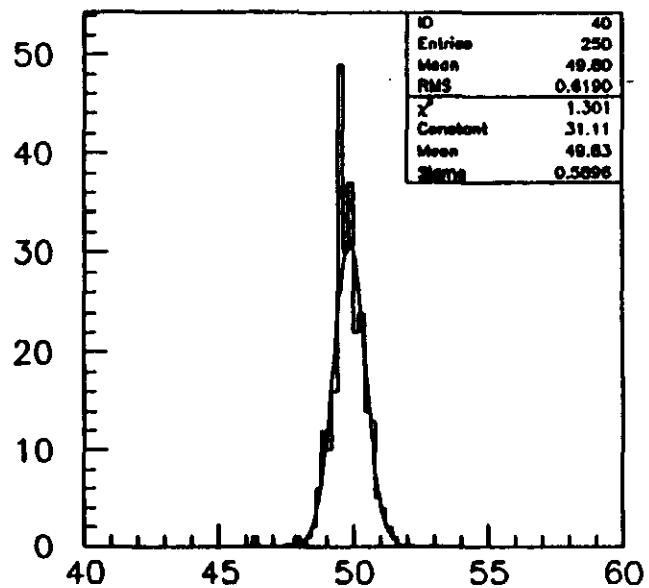

SAMPLE+CAL 3.0RL−1+2+3

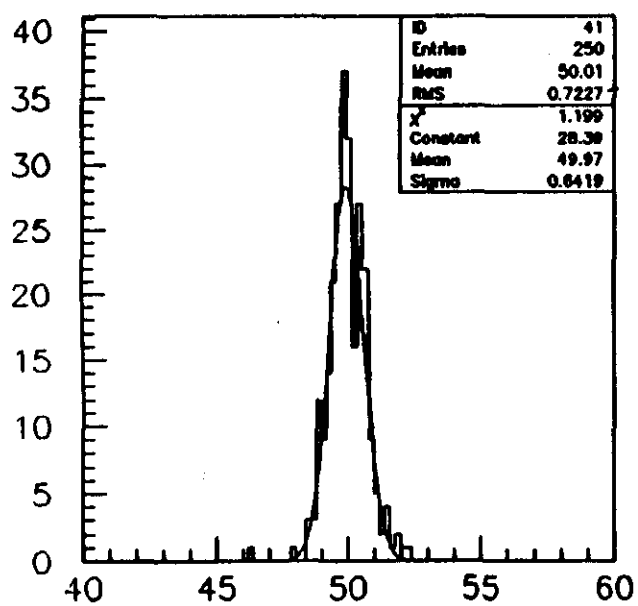

SAMPLE+ CAL 3.0RL−3 ONLY

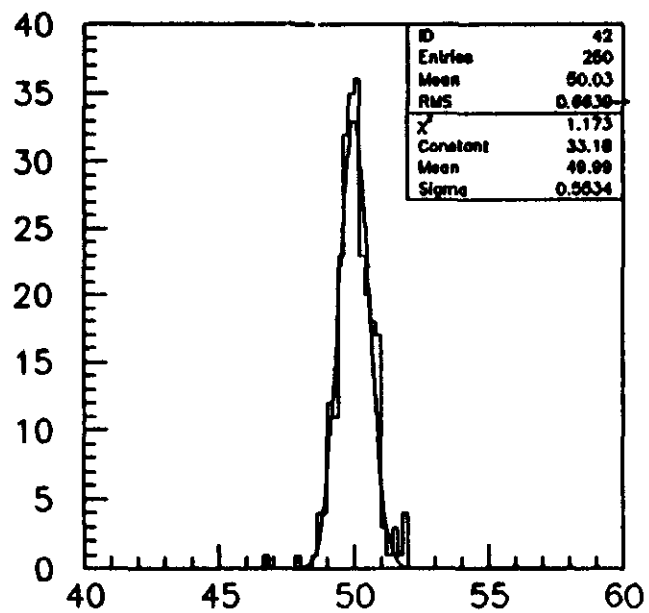

SAMPLE+ CAL 3.0RL−2+3

Assume $7.5\%/\sqrt{E}$ for Cal resolution

Assume $\frac{1.5\%}{\sqrt{E}}$ for Calorimeter resolution

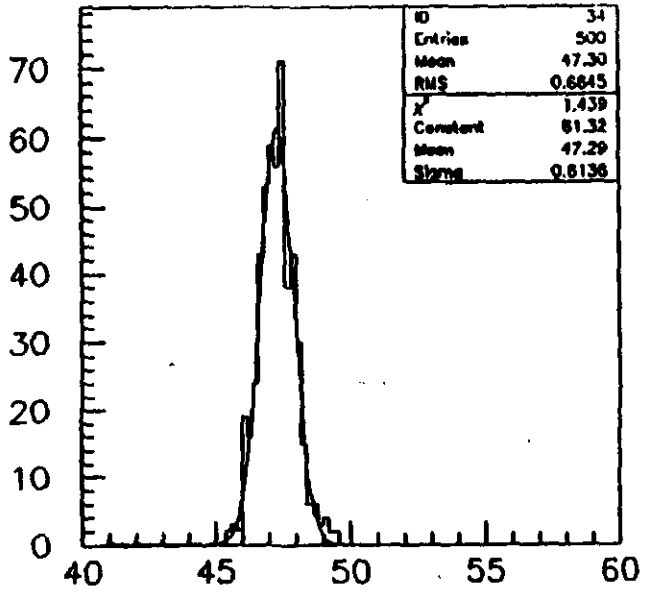

$\frac{8.9\%}{\sqrt{E}}$

After $3X_0$

$5\%/\sqrt{E}$

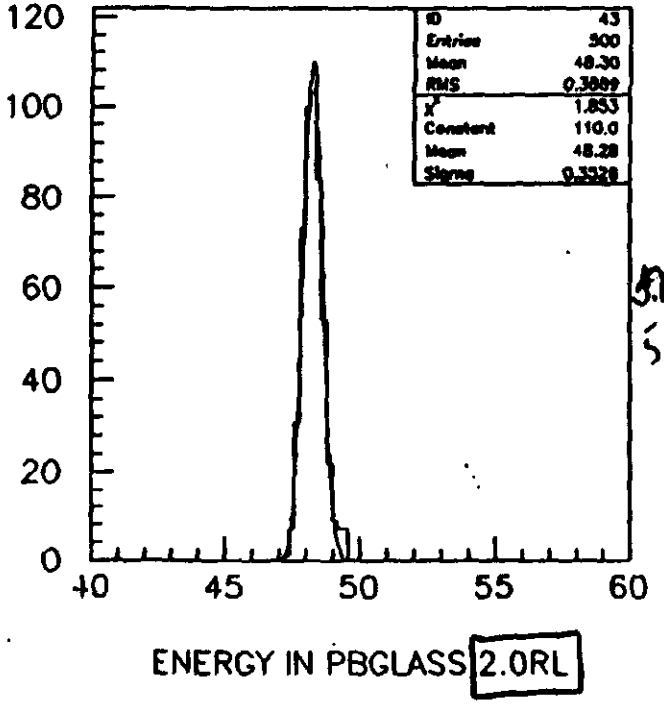

5.1

$3.8\%/\sqrt{E}$

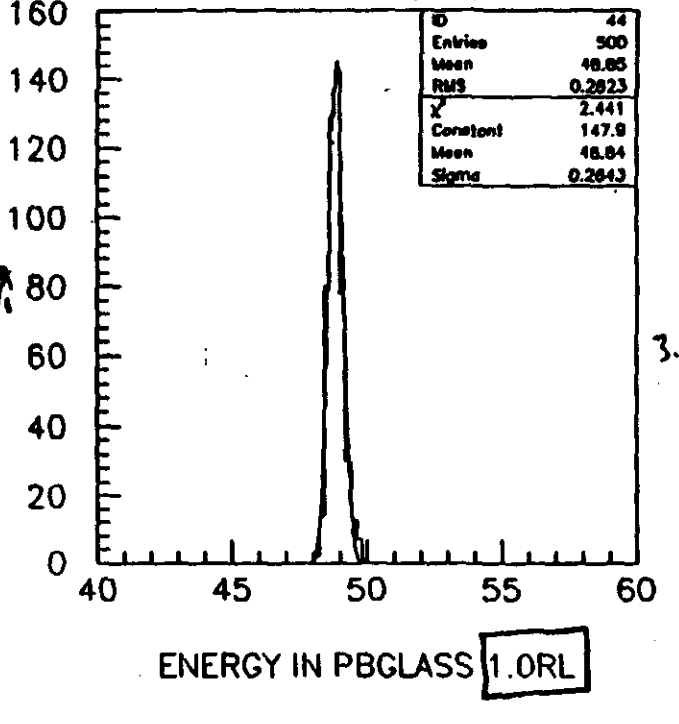

3.8

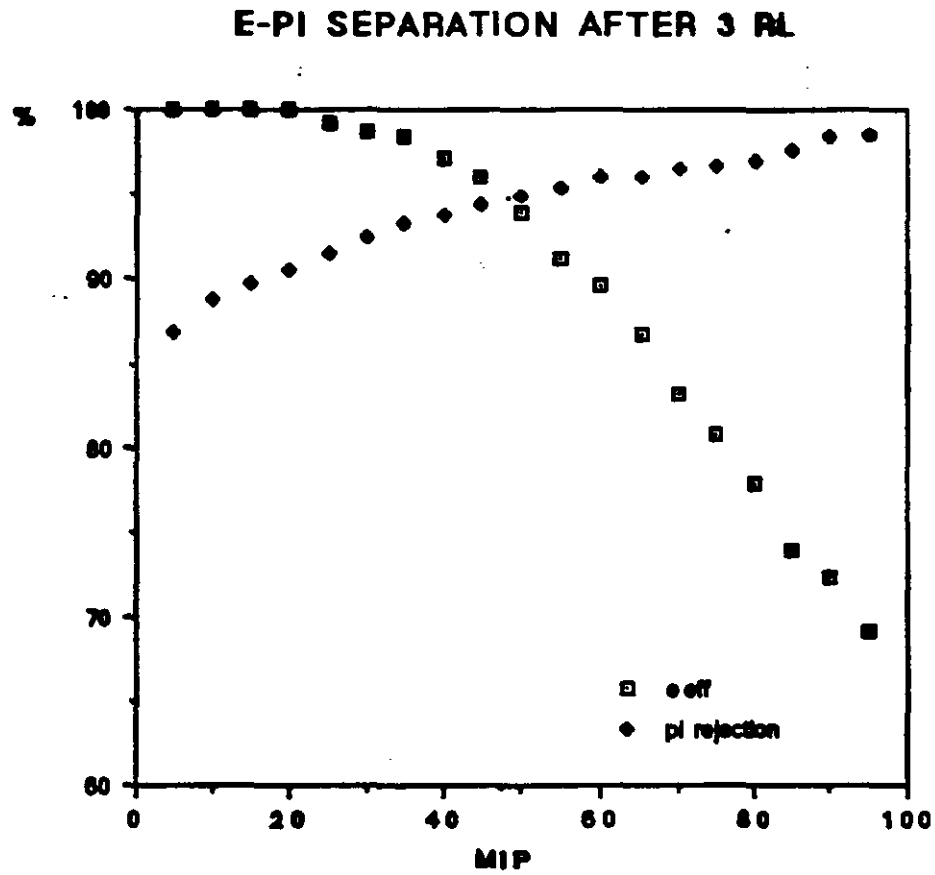

95% π rejection
95% e efficiency (50 GeV e's)
at $E_{cut} > 47$ mip

Reconstruction

1. Find all clusters in each view
   (cuts on min. pulse ht, min. cluster width, "valley" between adjacent clusters)

2. Find a cluster in SL 2 or SL 1 which matches cluster in SL 3 (per view)
   (within ±2 fiber widths)

3. For "matched" clusters, Find all possible space pts. Cut on u,v position along y versus x-fiber determination.

π^0 Upper limit is given by <u>conversion prob</u> at $2X_0$ [for Pb of $1X_0, 2X_0, 3X_0$]

$\Rightarrow$ $2X_0, 2.5X_0, 3X_0$ is better Pb arrangement

$\boxed{2X_0}$ Both γ's convert $\left(1-e^{-\frac{7}{9}(2)}\right)^2 = \boxed{62\%}$

$\boxed{2.5X_0}$ Both γ's convert $= \boxed{73\%}$

And <u>Opening Angle</u>

For 50 GeV π^0, $\Delta X_{min} = 750 \tan\left(\frac{2M_{\pi^0}}{P_{\pi^0}}\right) = 4$ mm

Track - cluster residual $\approx 160\,\mu$

Shower width ~ 2mm core with long tails

$\Rightarrow$ 2-3 half-fibers between peaks.

For 1 mm fibers, 2.0, 2.5, 3 X_0 lead layers

30° stereo angle 50 GeV

Define π^0 as 2 or more clusters

Define γ as 1 cluster

	π^0 (252)		γ (238)	
	1 cluster	≥2 clusters	1 cluster	≥2 clusters
Cuts A (good for π^0)	76 (30%)	155 (61.5%)	119 (50%)	74 (31%)
Cuts B (good for γ)	89 (35%)	136 (54%)	133 (56%)	39 (16.4%)

ϕ 8% 10.7%

ϕ 19% 27.7%

Compare with $P_{\pi^0}(\gamma\gamma \text{ convert}) = 73\%$

$$P_{\pi^0}(\text{no convert}) = \left(e^{-\frac{7}{9}(2.5)}\right)^2 = 2\%$$

$$\Rightarrow P_{\pi^0}(\gamma \text{ convert}) = 25\%$$

M.C. says 30% of the π^0's will fake a γ
and 31% of the γ's will fake a π^0

OR

35% of the π^0's will fake a γ
and 16% of the γ's will fake a π^0

	Cuts A	Cuts B
min. pulse ht on starting fiber	100	200
min. width of cluster	2	2
min. pulse ht of cluster	500	750
Fraction = (valley pulse ht)/(smaller peak ht)	0.33	0.33

01/09/91 16.24

M.C.

50 GEV GAMMAS

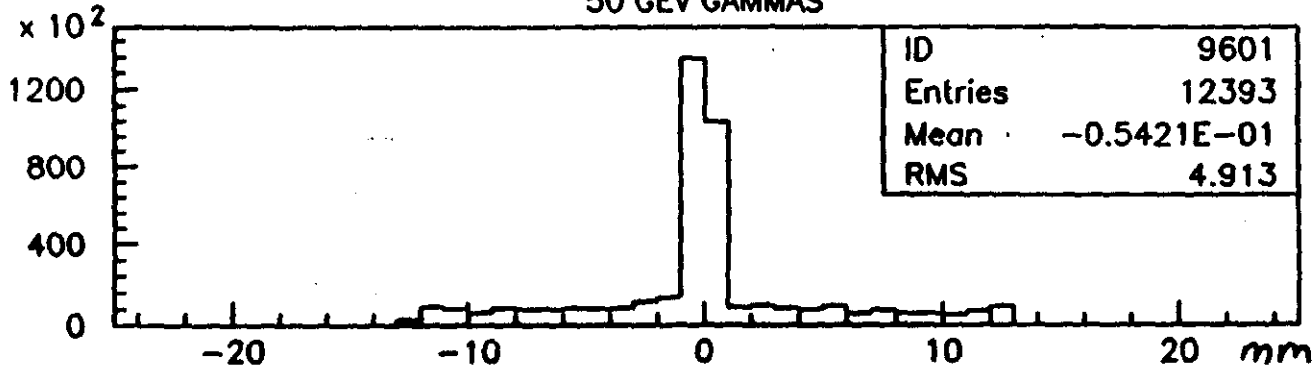

SL 1 – View u Shower Shape

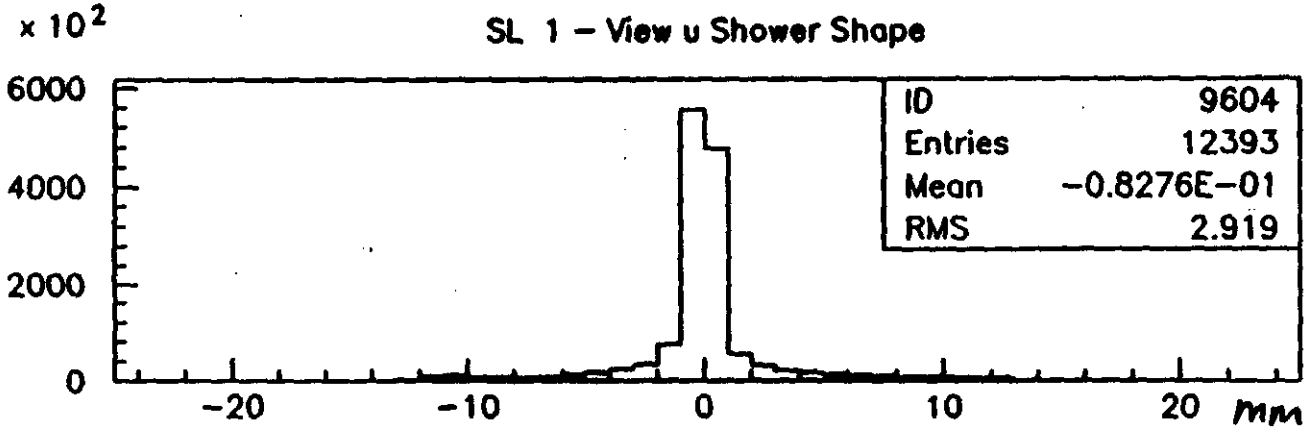

SL 2 – View u Shower Shape

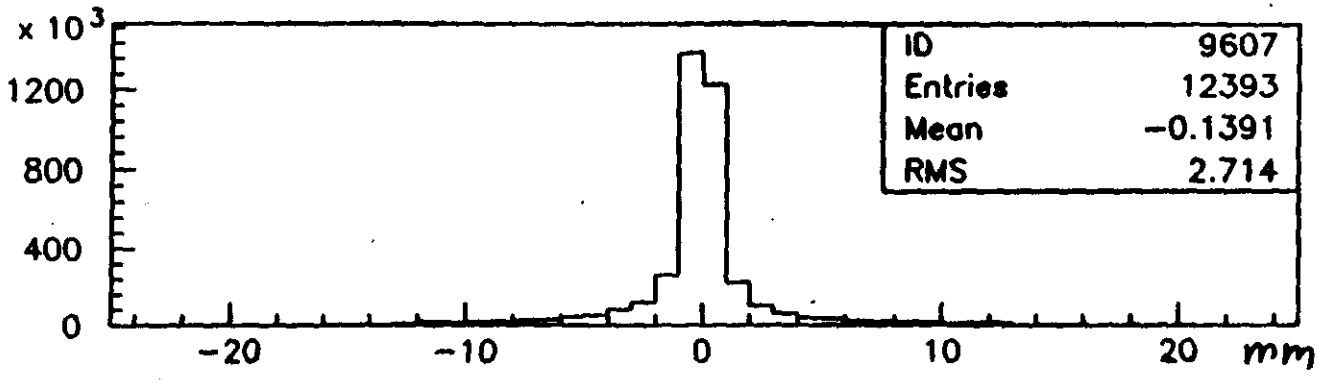

SL 3 – View u Shower Shape

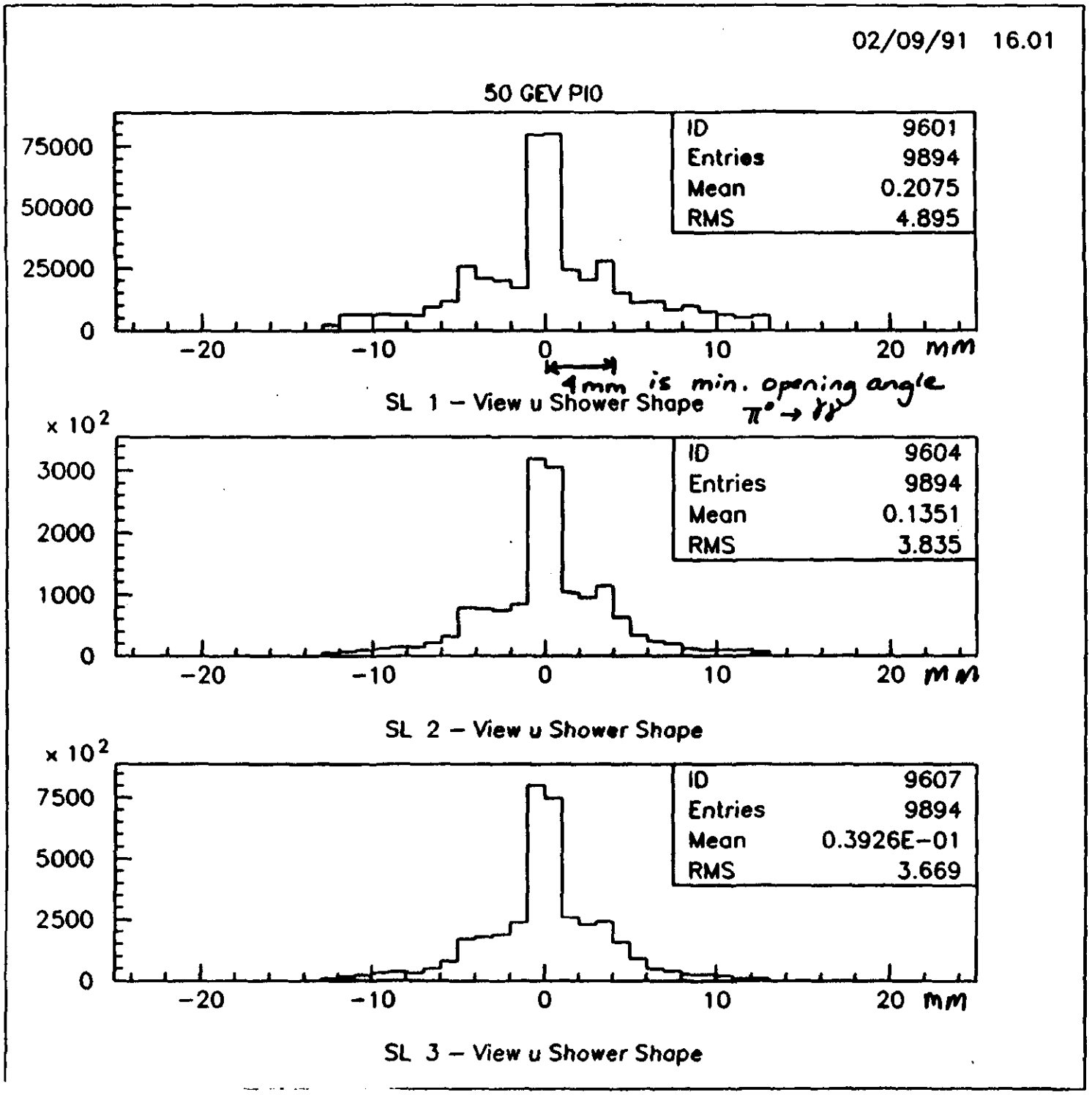
02/09/91 16.01
50 GEV PIO
ID 9601
Entries 9894
Mean 0.2075
RMS 4.895
75000
50000
25000
0
-20
-10
0
10
20
mm
4mm is min. opening angle
$\pi^0 \to \gamma\gamma$
SL 1 – View u Shower Shape
x 10^2
3000
2000
1000
0
ID 9604
Entries 9894
Mean 0.1351
RMS 3.835
-20
-10
0
10
20
mm
SL 2 – View u Shower Shape
x 10^2
7500
5000
2500
0
ID 9607
Entries 9894
Mean 0.3926E-01
RMS 3.669
-20
-10
0
10
20
mm
SL 3 – View u Shower Shape

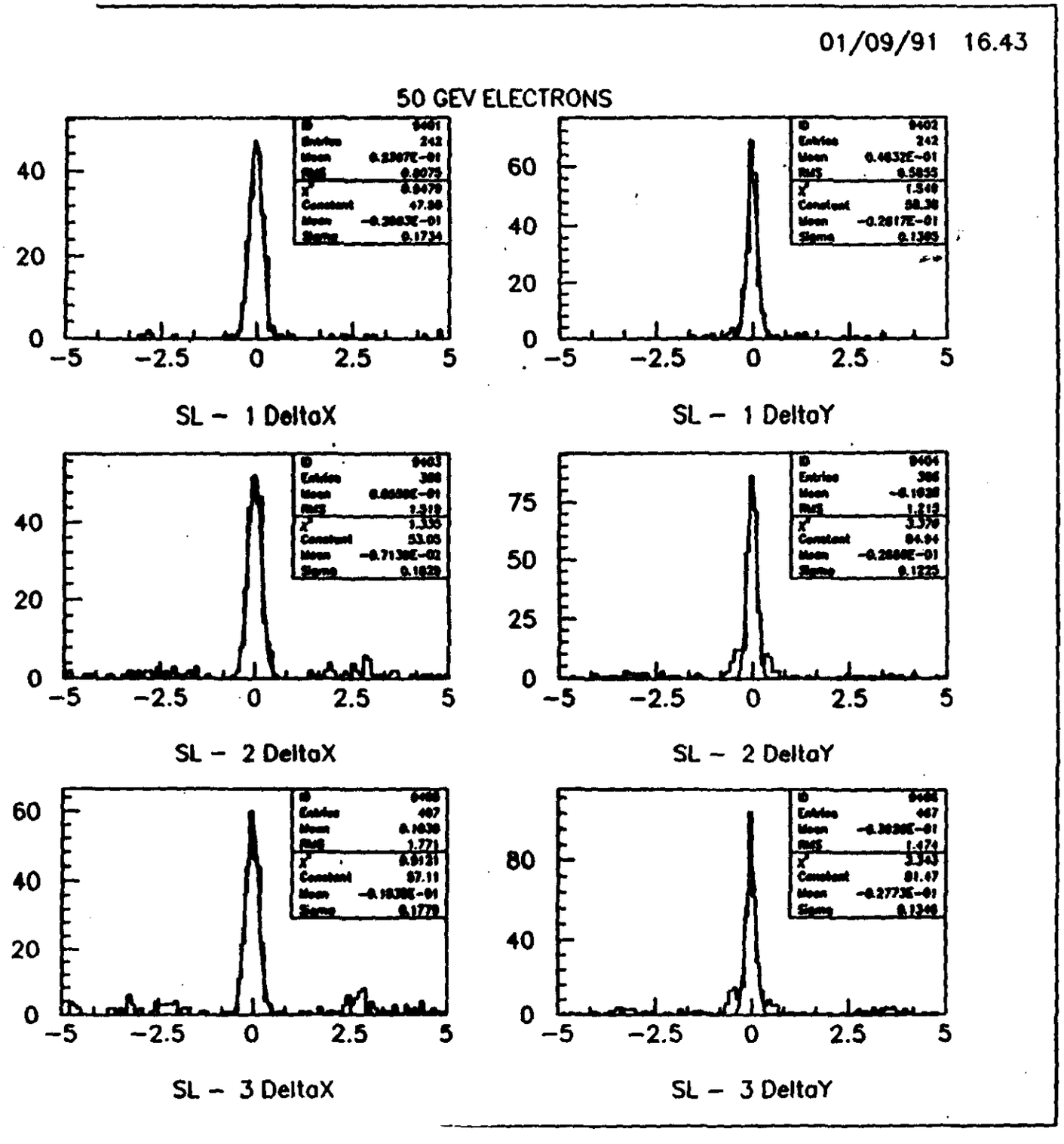

$\sigma_y \sim 130\mu$

$\sigma_x \sim 180\mu$

01/09/91 16.24

50 GEV GAMMAS

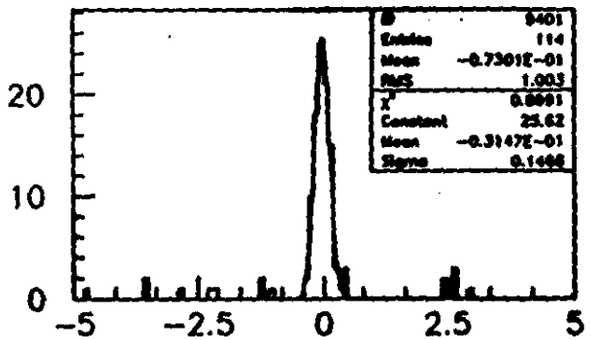

SL − 1 DeltaX

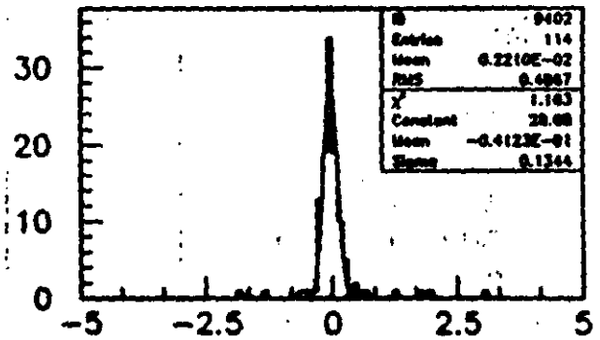

SL − 1 DeltaY

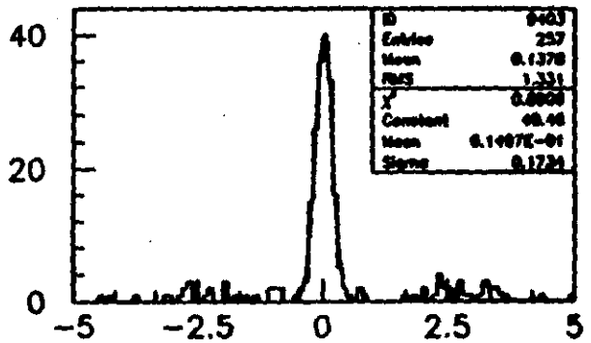

SL − 2 DeltaX

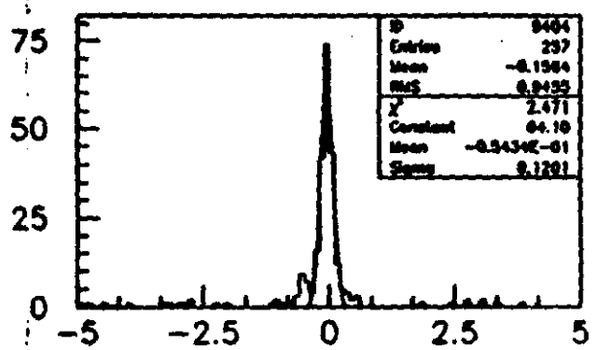

SL − 2 DeltaY

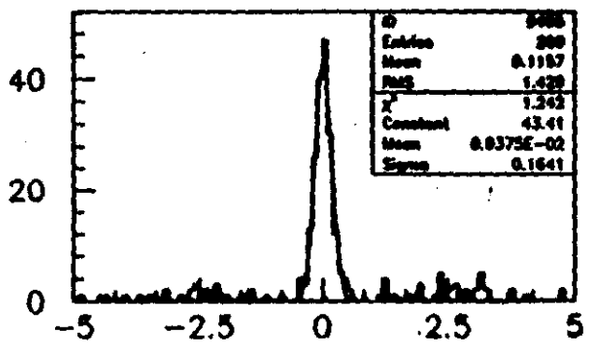

SL − 3 DeltaX

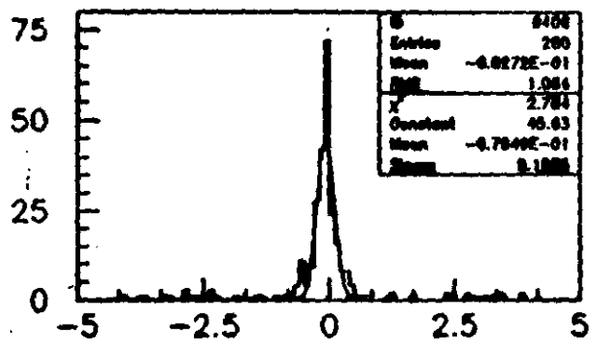

SL − 3 DeltaY

Possible SSC Detector Configuration
High Field (5T) Solenoid. Compact (R = 1 m)

see:
Compact Solenoid
Design Report
Berkeley '87

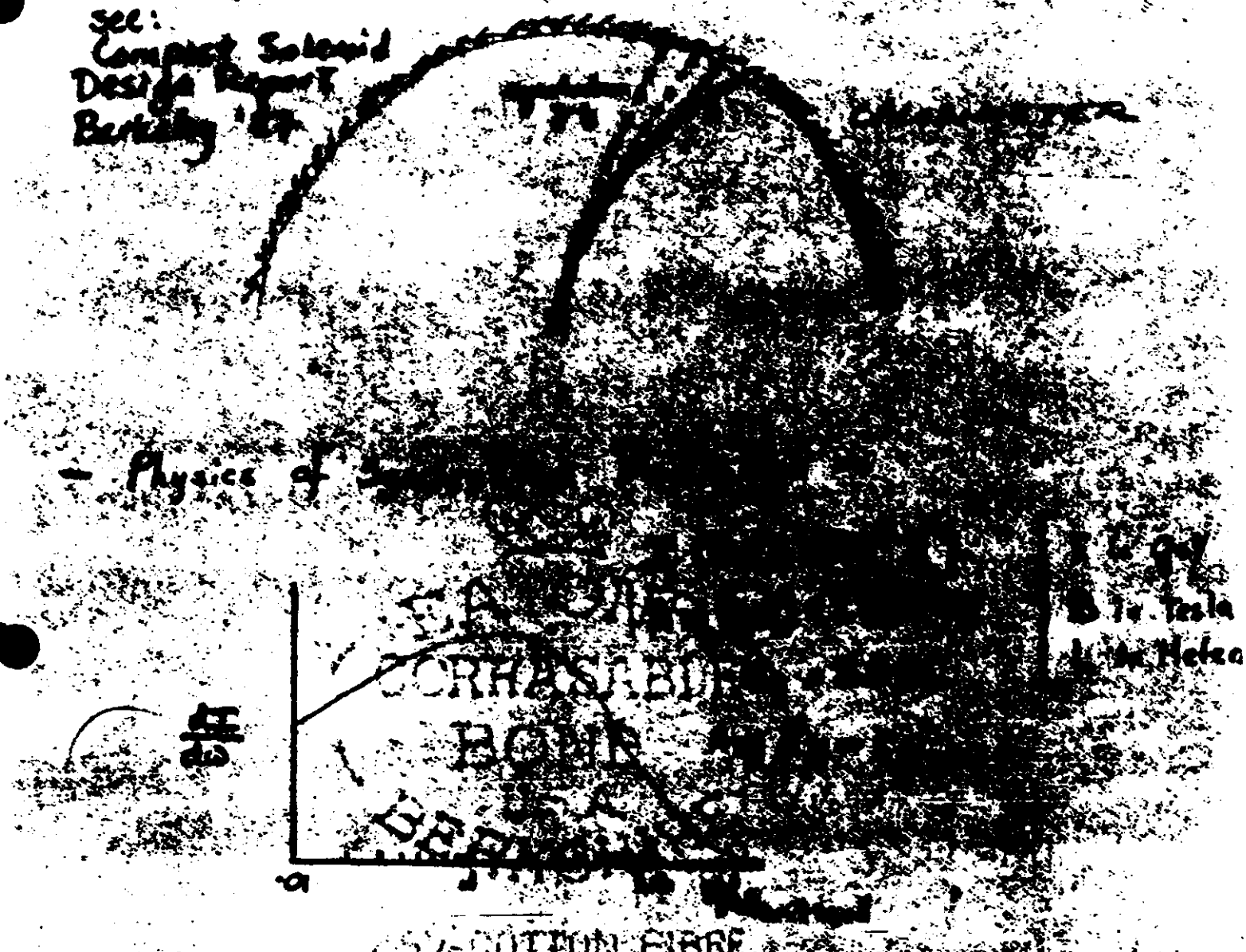

Compact high field magnet config. 5T, 1m	GeV Electron Energy	50	[illegible]	[illegible]	[illegible]	[illegible]
	ΔE_γ (MeV)	16.6	[illegible]	[illegible]	[illegible]	[illegible]
	Δx (mm)	24	[illegible]	[illegible]	[illegible]	[illegible]
Test Beam 2.5T, 1.8m (2 m gap)	ΔE_γ (MeV)	.8	[illegible]	[illegible]	[illegible]	[illegible]
	Δx (mm)	.58	[illegible]	[illegible]	[illegible]	12

$\langle \Delta_\gamma \rangle > .18$

$\langle \Delta_\gamma \rangle = .17$

YALE - P. Cushman, Y. Singh
Rockefeller - R. Rusack, P. Mélèse

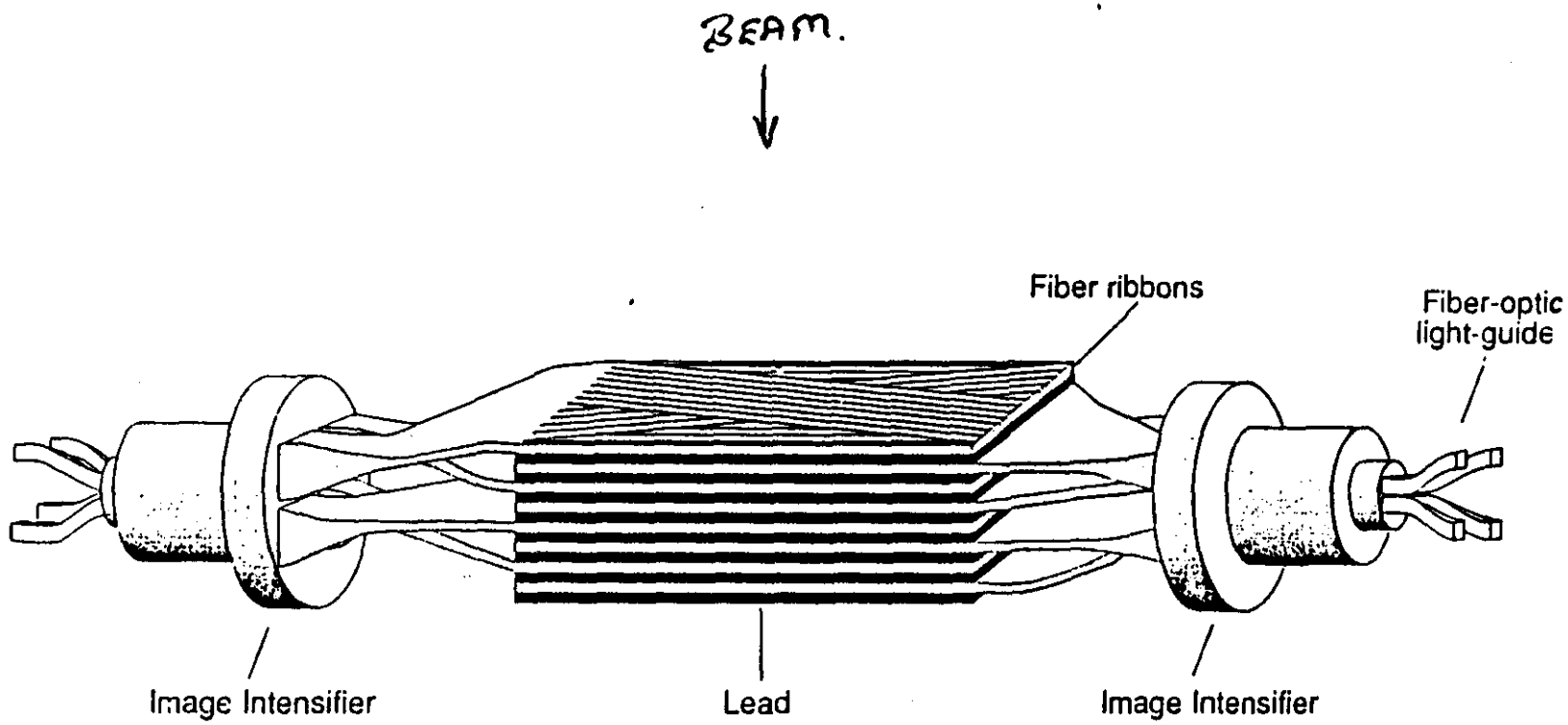

Figure (1)

Yale/Rockefeller Prototype Imaging Preradiator.

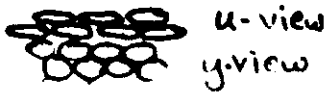

EXP BEAM LINE SETUP

200 GeV electron
$\vec{B} = \emptyset$

Cumulative Pulse height per fiber in Superlayer 4 ($.75\lambda_R$)

26/04/90 23.53

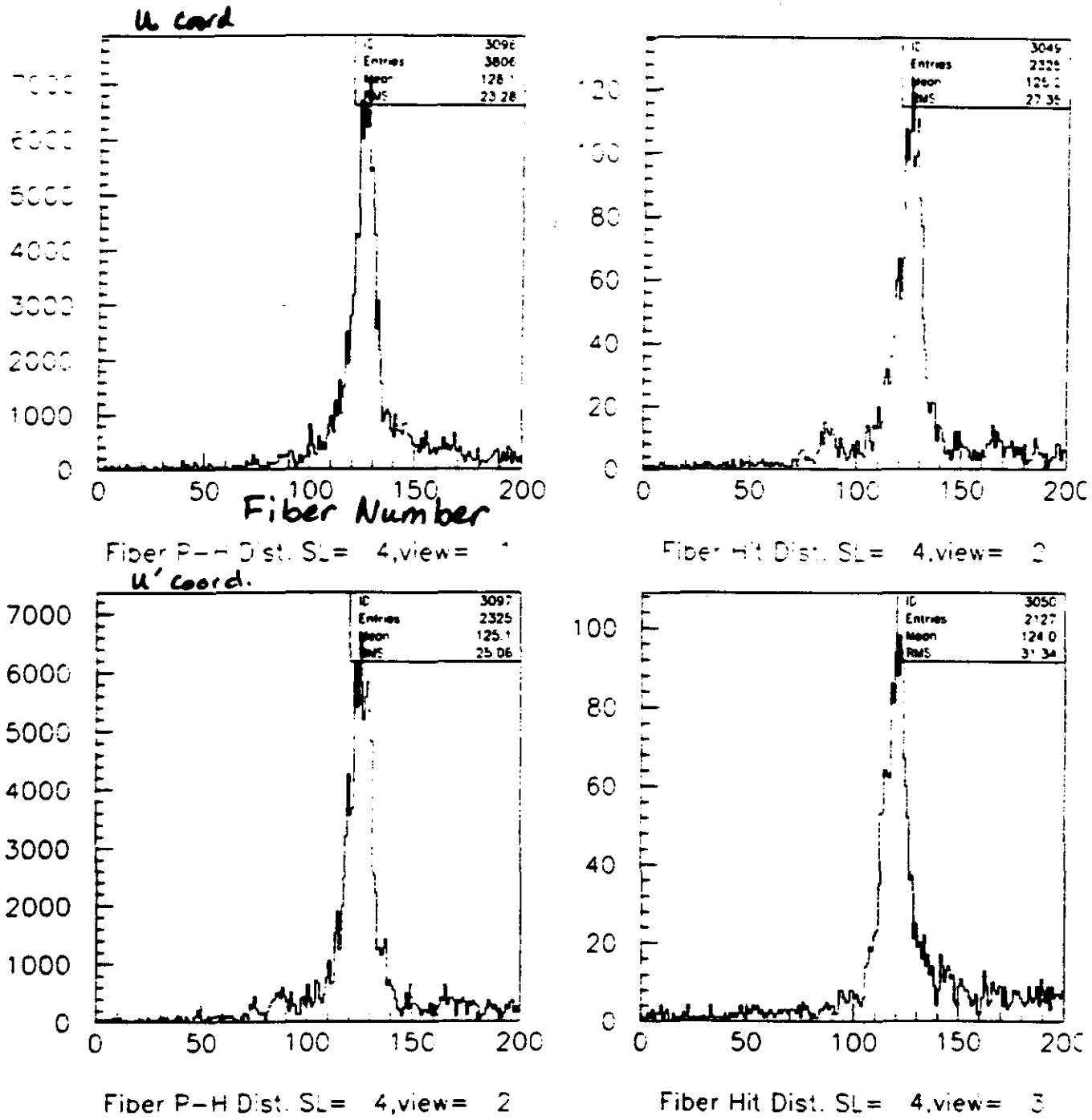

200 gev electron

$\vec{B}$ = 2.5 Tesla

25/04/90 23.53

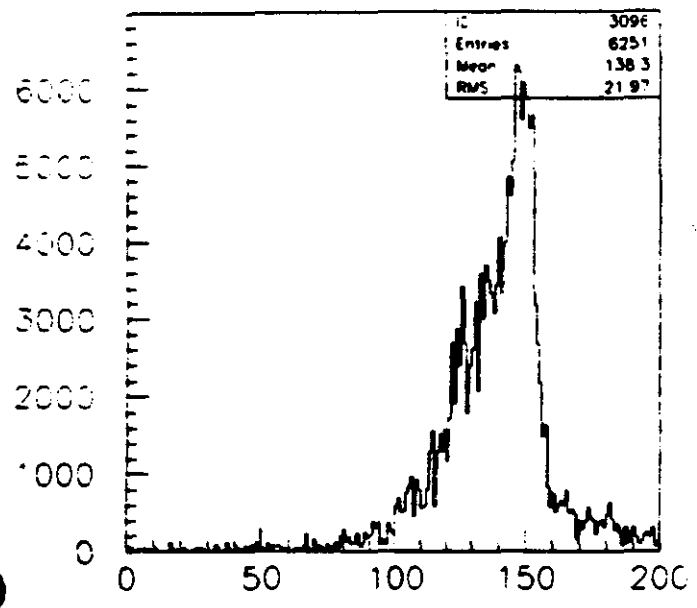

Fiber P−H Dist. SL= 4,view= 1

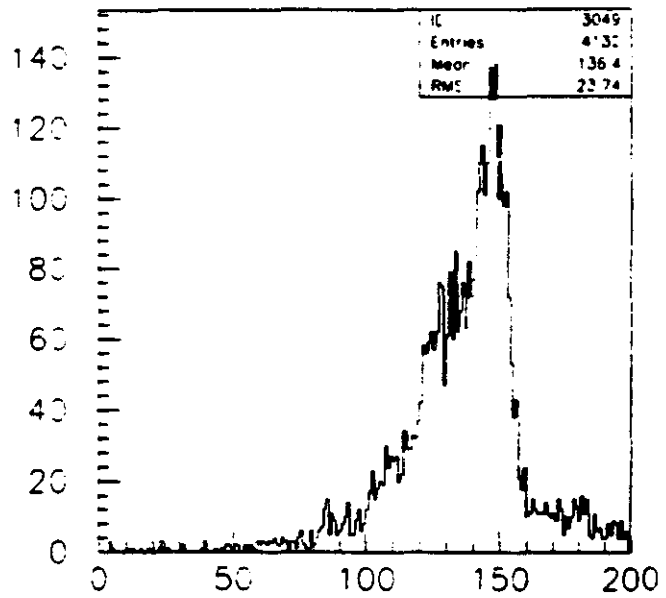

Fiber Hit Dist. SL= 4,view= 2

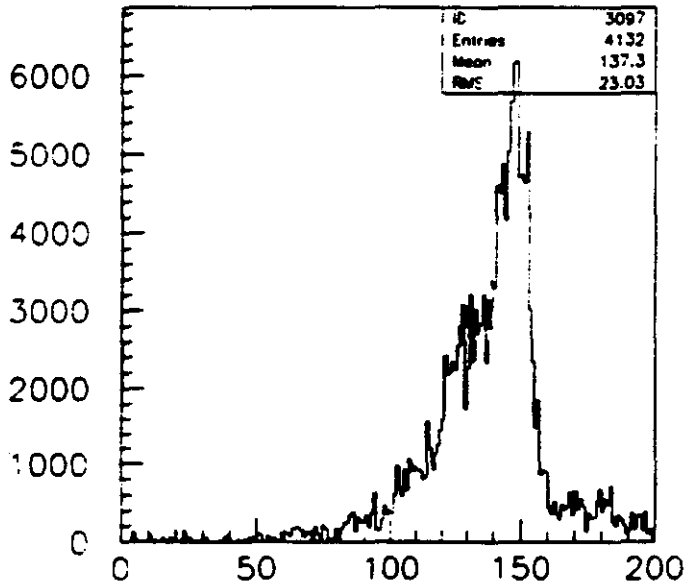

Fiber P−H Dist. SL= 4,view= 2

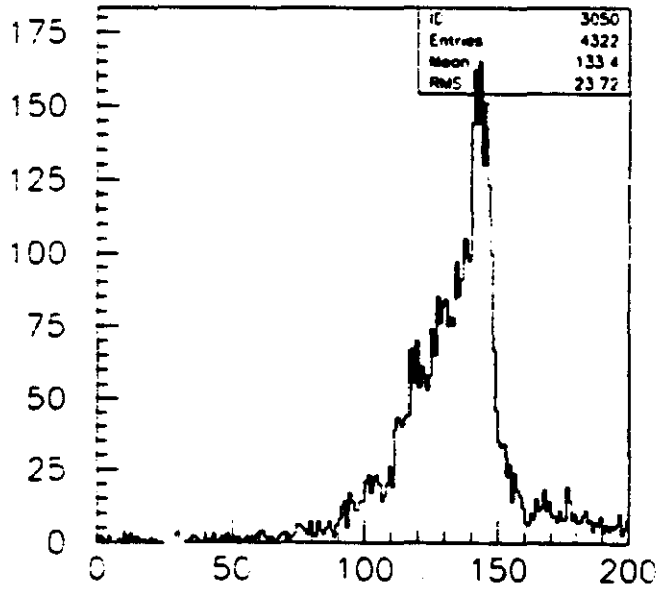

Fiber Hit Dist. SL= 4,view= 3

of shower core..

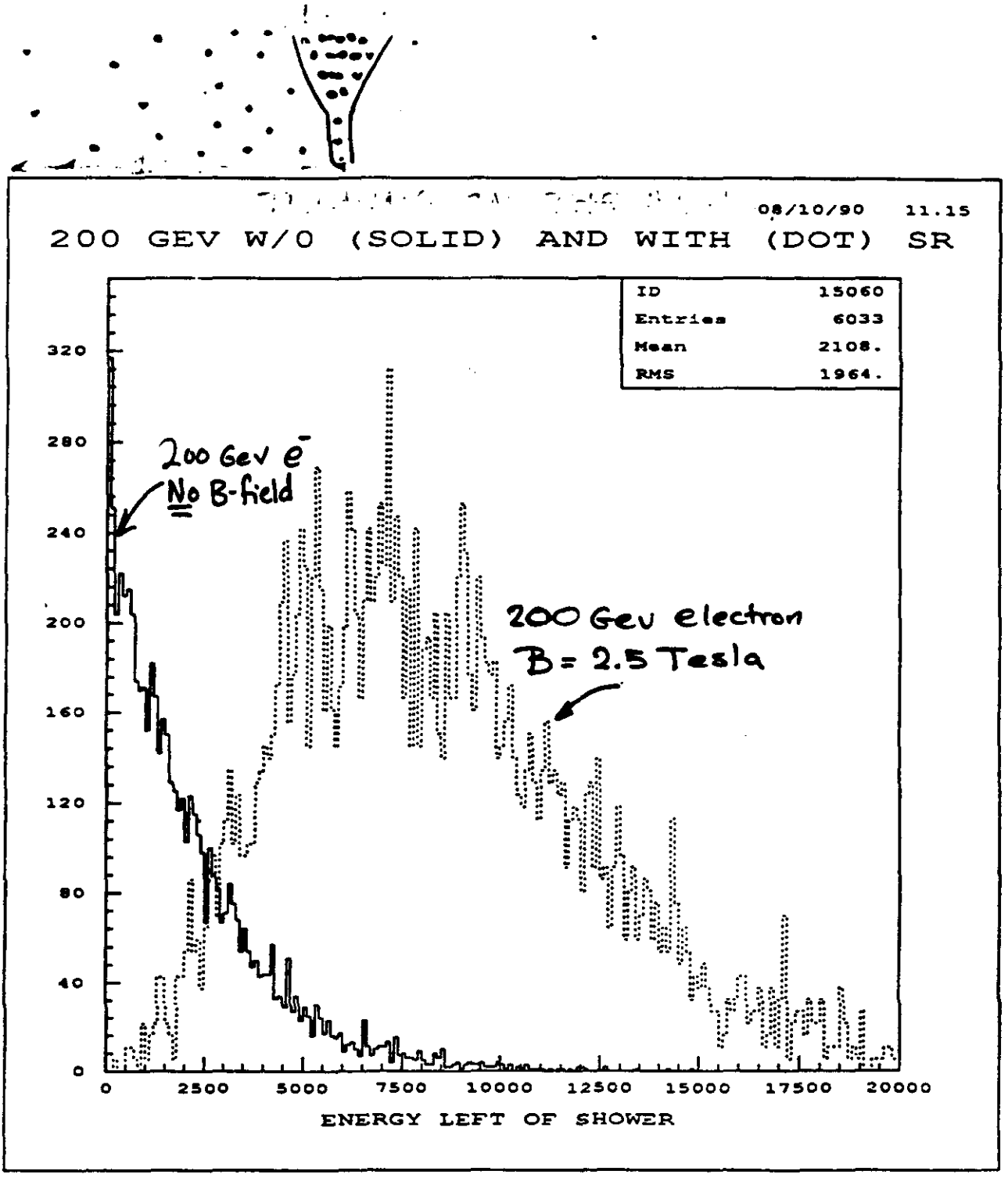

The E(left) variable for different electron energies and for pions.

B = 2.5 Tesla

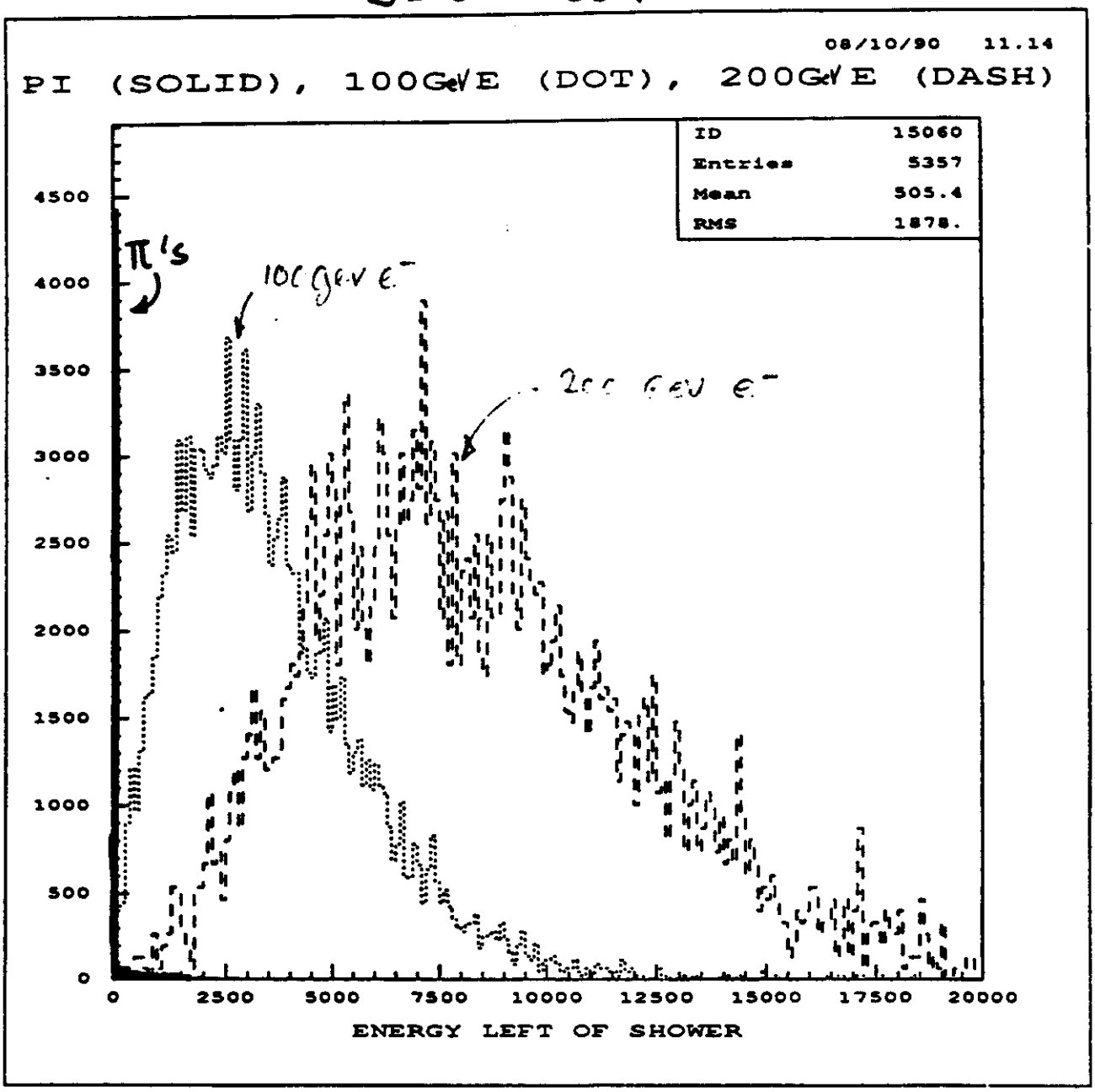

Test Beam Data

π rejection = 94%
10 GeV e eff. = 90%
200 GeV e eff. = 96%

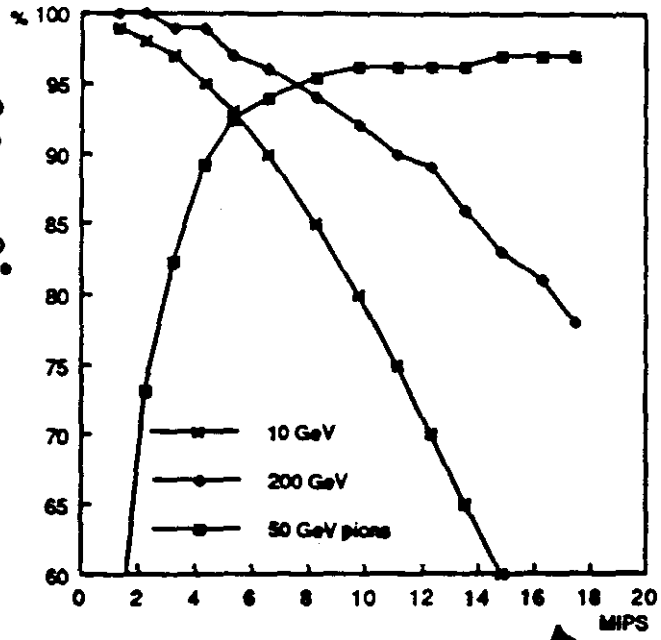

ENERGY IN SUPERLAYER 8 (MIPS)

uncorrelated.
Together get
π rejection = 96%
100 GeV e eff. = 95%
200 GeV e eff. = 100%

π rejection = 93%
100 GeV e eff. = 95%
200 GeV e eff. = 99%

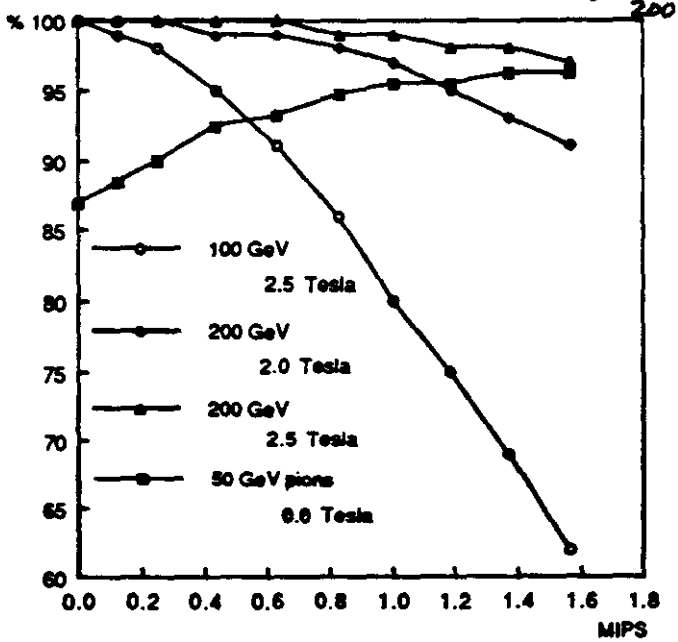

Energy to left of shower cone
(summed over 8 S.L.'s)

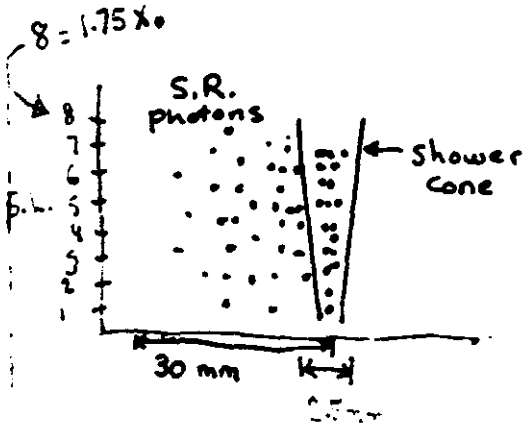

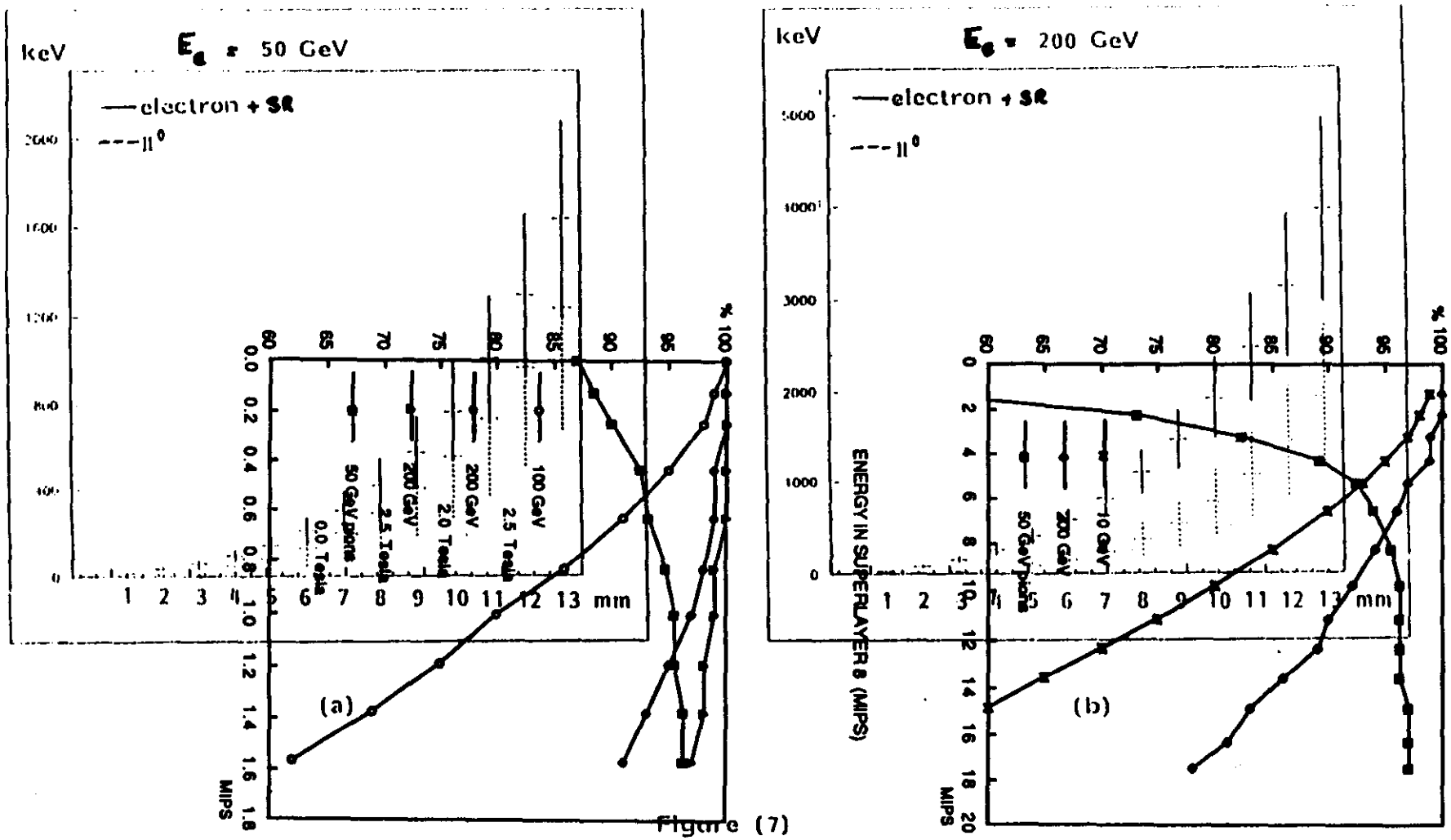

Figure (7)

Cumulative energy deposited in the fibers versus depth in lead.

B= 5 T

Test Beam Data

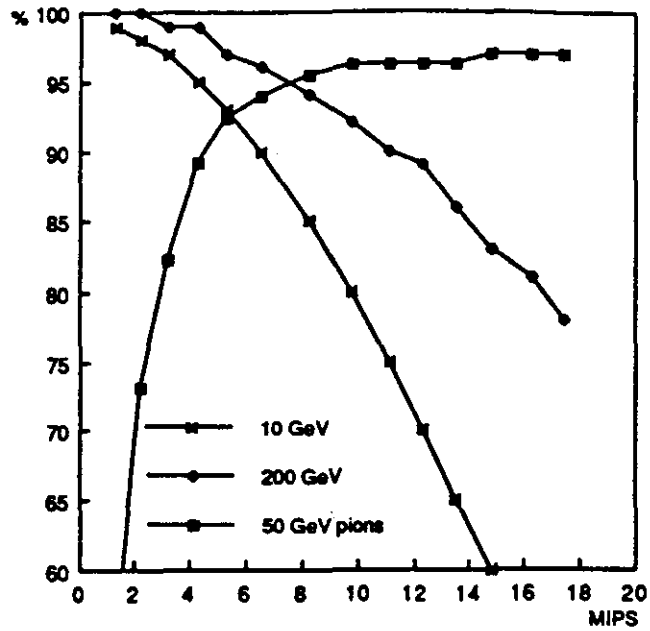

ENERGY IN SUPERLAYER 8 (MIPS)

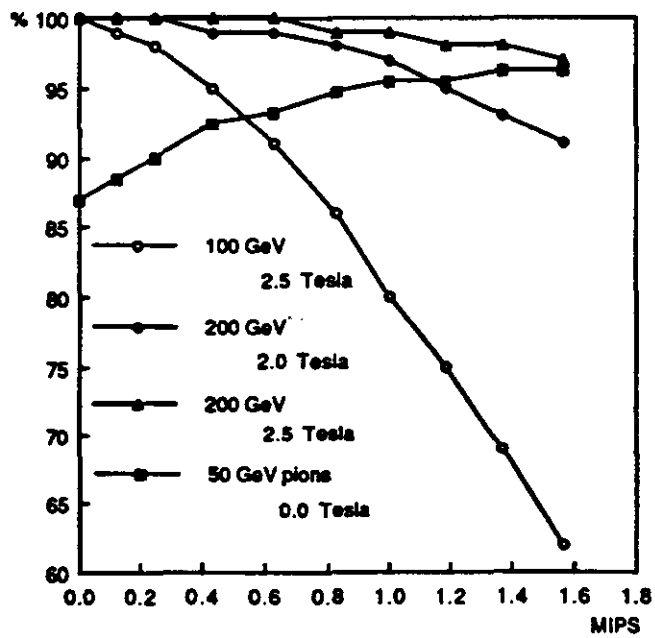

E_{left} =

Synchrotron γ energy
to left of electron cluster

CLEMEN

Silicon Preradiators

Requirements $\gamma/e/\pi$ discrimination

and at a higher level

$\pi^0 \leftarrow \gamma\gamma$ identification

$P/E \Rightarrow$ momentum resolution with large lever arm, small σ_x

⋮

<u>trigger</u> x-y space point to compare against other detectors ?

Preradiator - Demands

① Integrates well with central tracker

② Integrates well with fast trigger

Monte Carlo: GEANT 3.14/07

GHEISHA

GEOMETRY

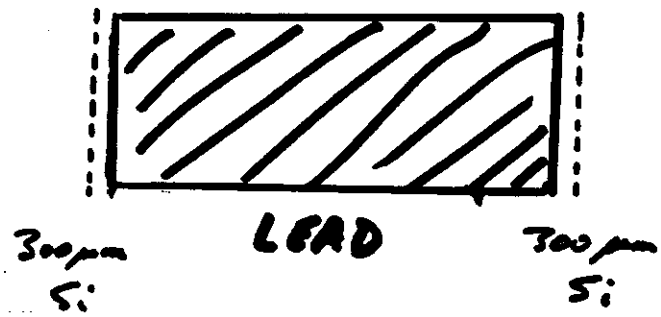

no gaps!

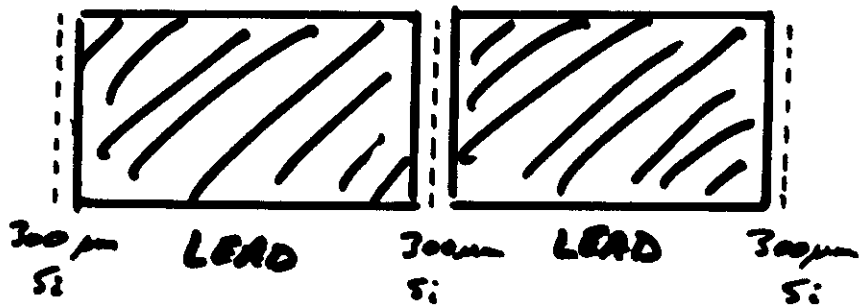

GOAL: ESTIMATE $\varepsilon_e/\varepsilon_\pi$ with simple cuts,

Easily implemented at trigger level

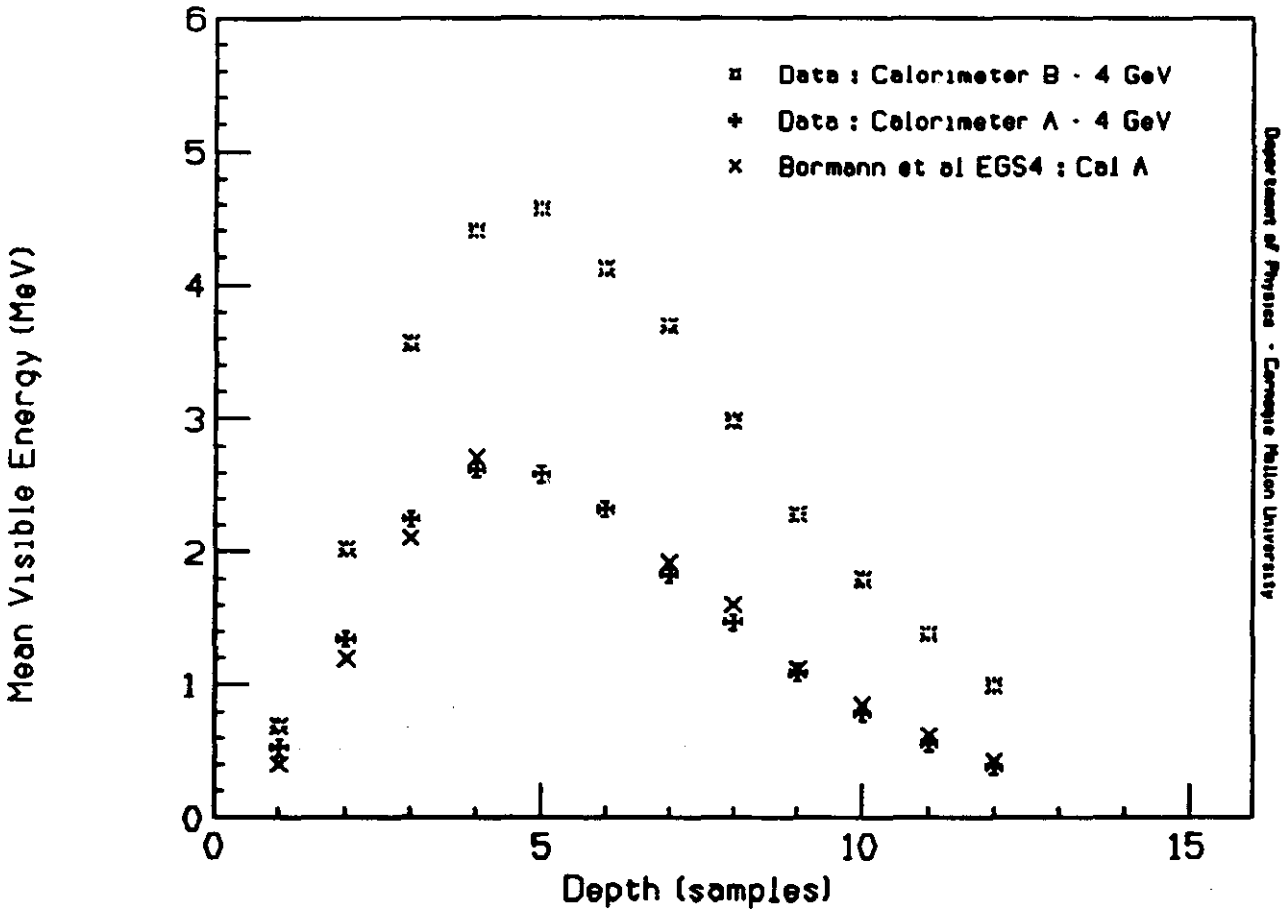

M. Bormann et al

"Beam Tests With Large Area Silicon Sandwich Calorimeters for Electron Energies Between 1 and 6 GeV"

NIM A 257 (1987) pp 479-487.

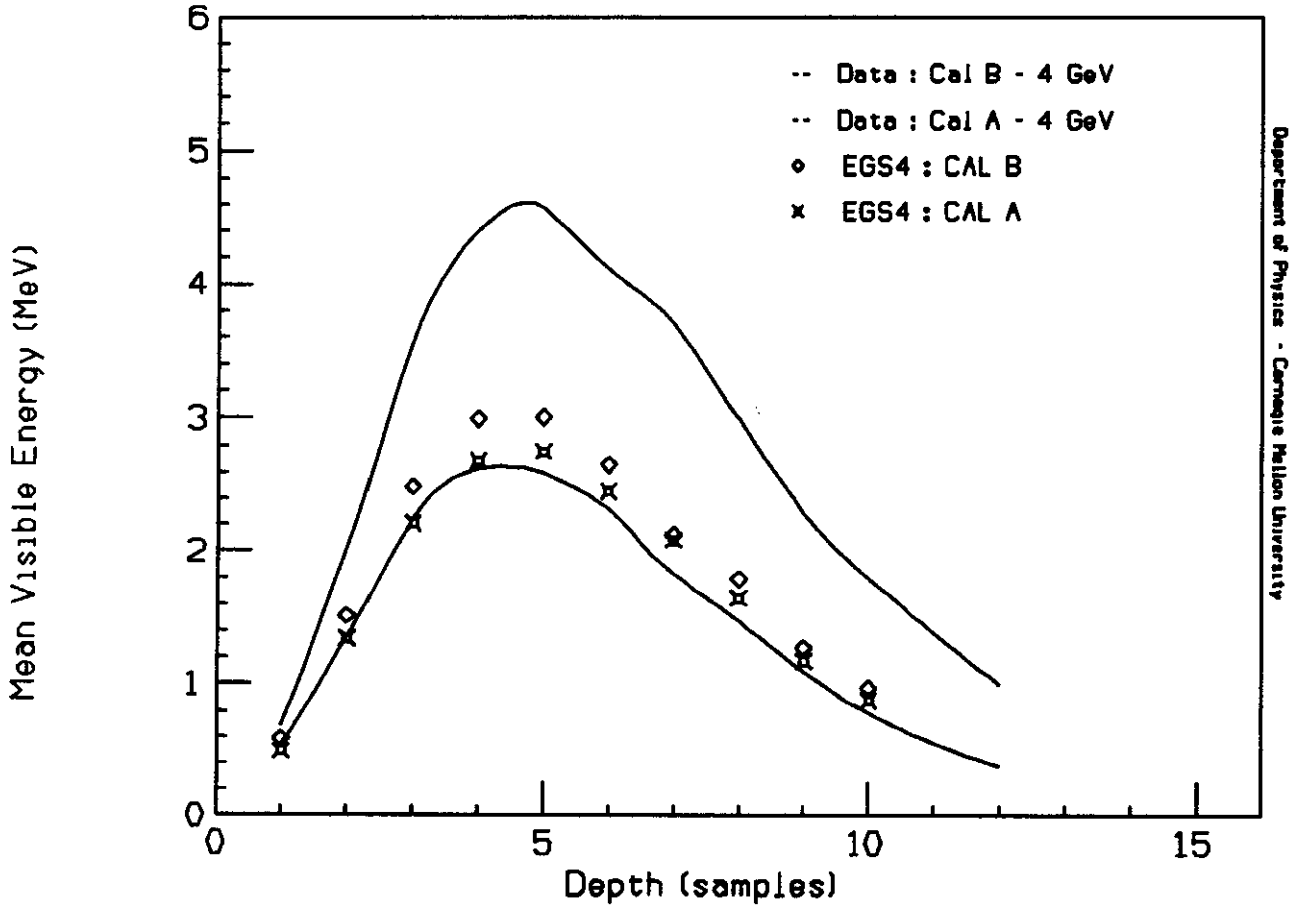
Mean Visible Energy (MeV)
Depth (samples)
-- Data : Cal B - 4 GeV
-- Data : Cal A - 4 GeV
EGS4 : CAL B
EGS4 : CAL A
0
1
2
3
4
5
6
0
5
10
15
Department of Physics - Carnegie Mellon University

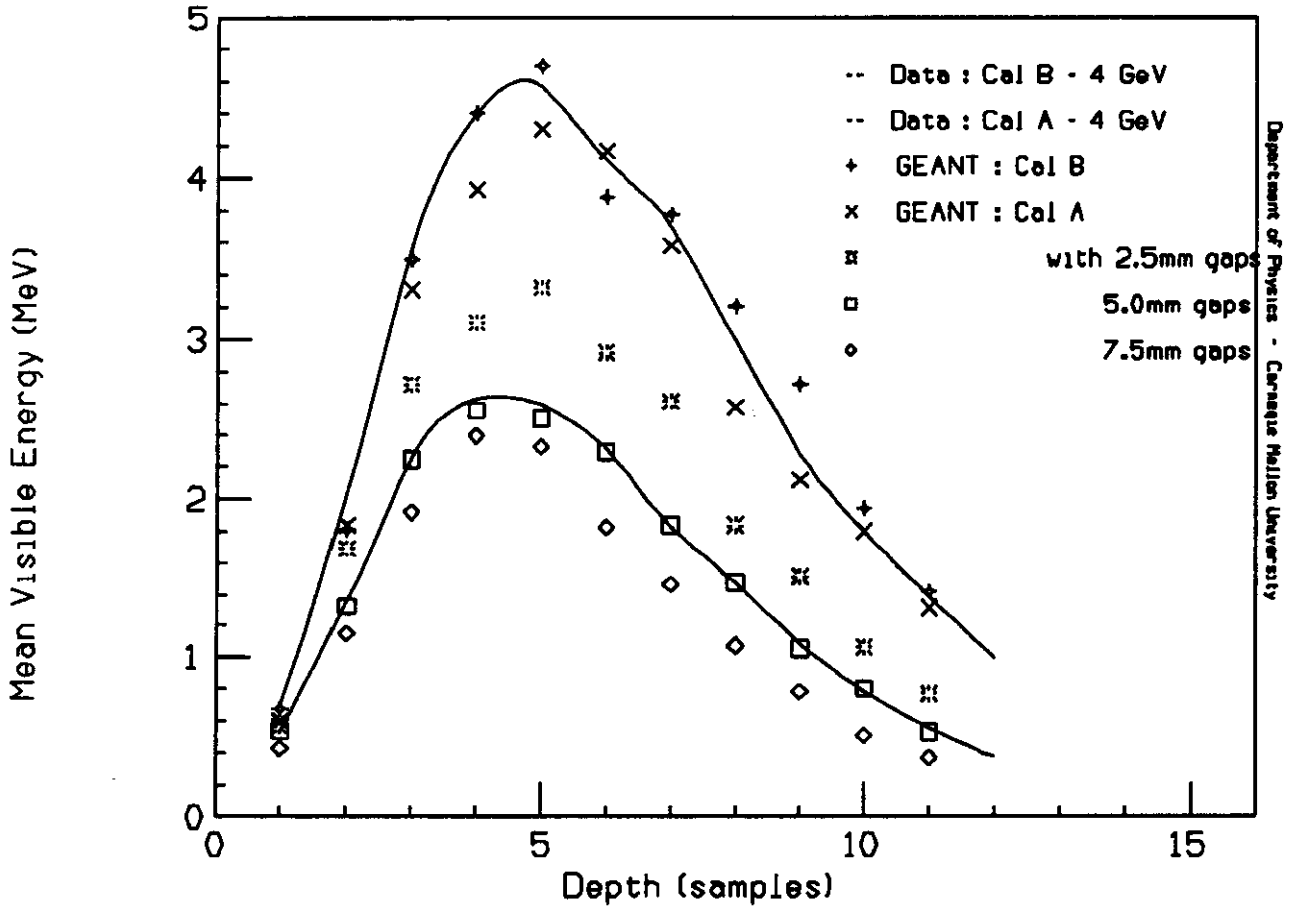
Mean Visible Energy (MeV)
Depth (samples)
0
1
2
3
4
5
0
5
10
15
-- Data : Cal B - 4 GeV
-- Data : Cal A - 4 GeV
+ GEANT : Cal B
× GEANT : Cal A
with 2.5mm gaps
5.0mm gaps
7.5mm gaps
Department of Physics - Carnegie Mellon University

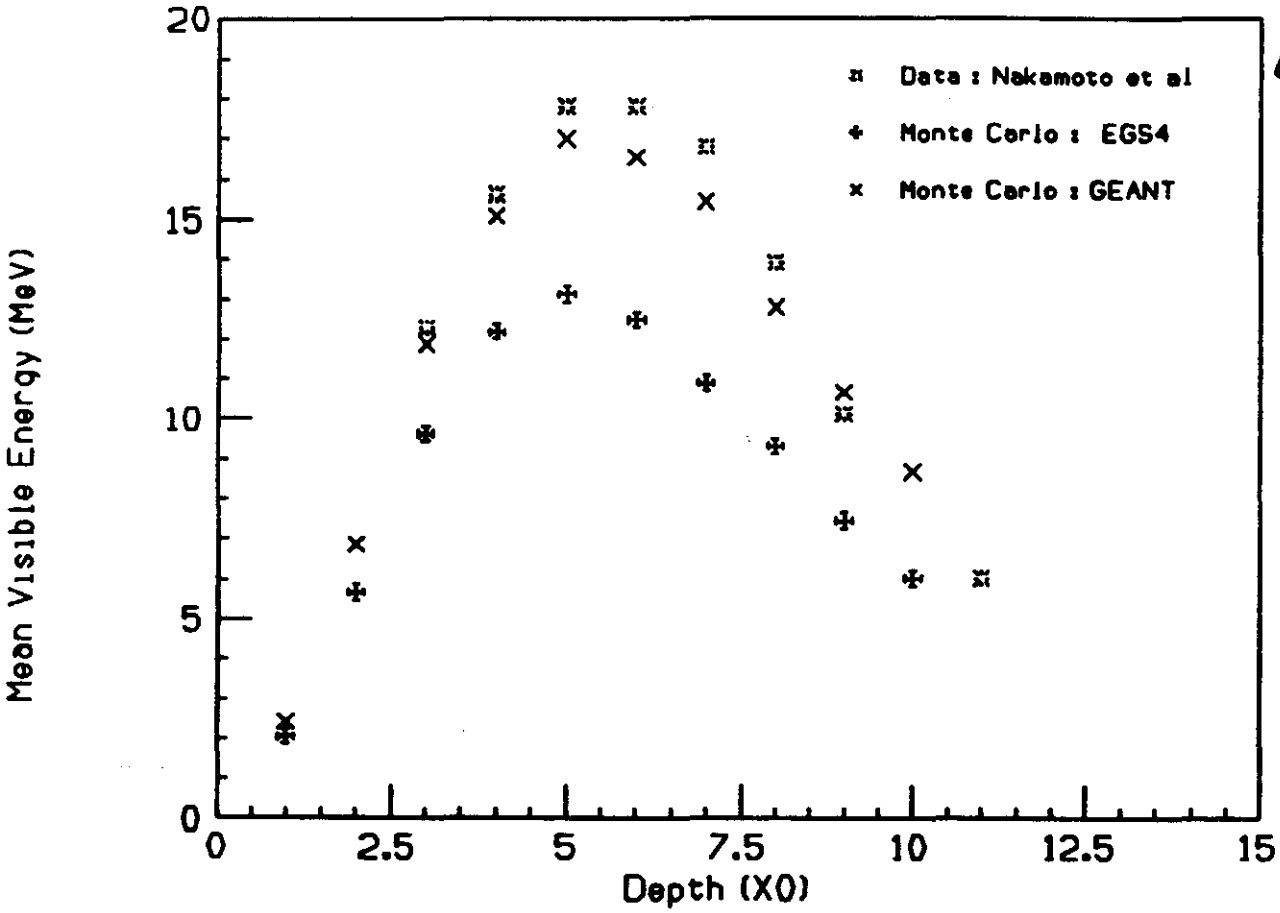

4.5 GeV

Nakamoto et al
"A Si(Li)-Pb Shower Calorimeter for $p\bar{p}$ Collider Experiments"
NIM A238 (1985) pp 53-60.

in general: Need high energy test beam data!

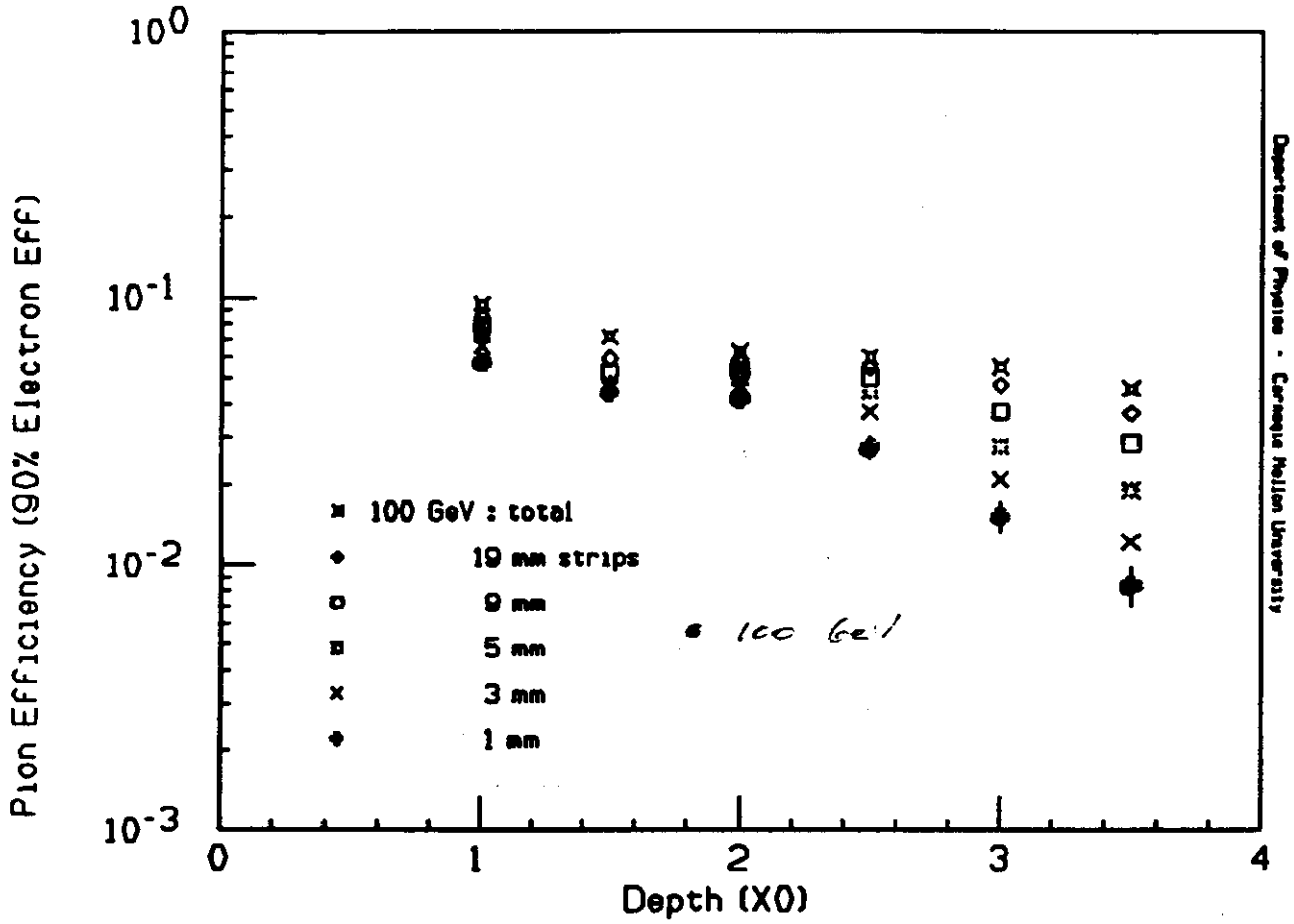

Cut: Total Energy deposit in a strip in last Silicon plane.

Varied: Thickness of lead

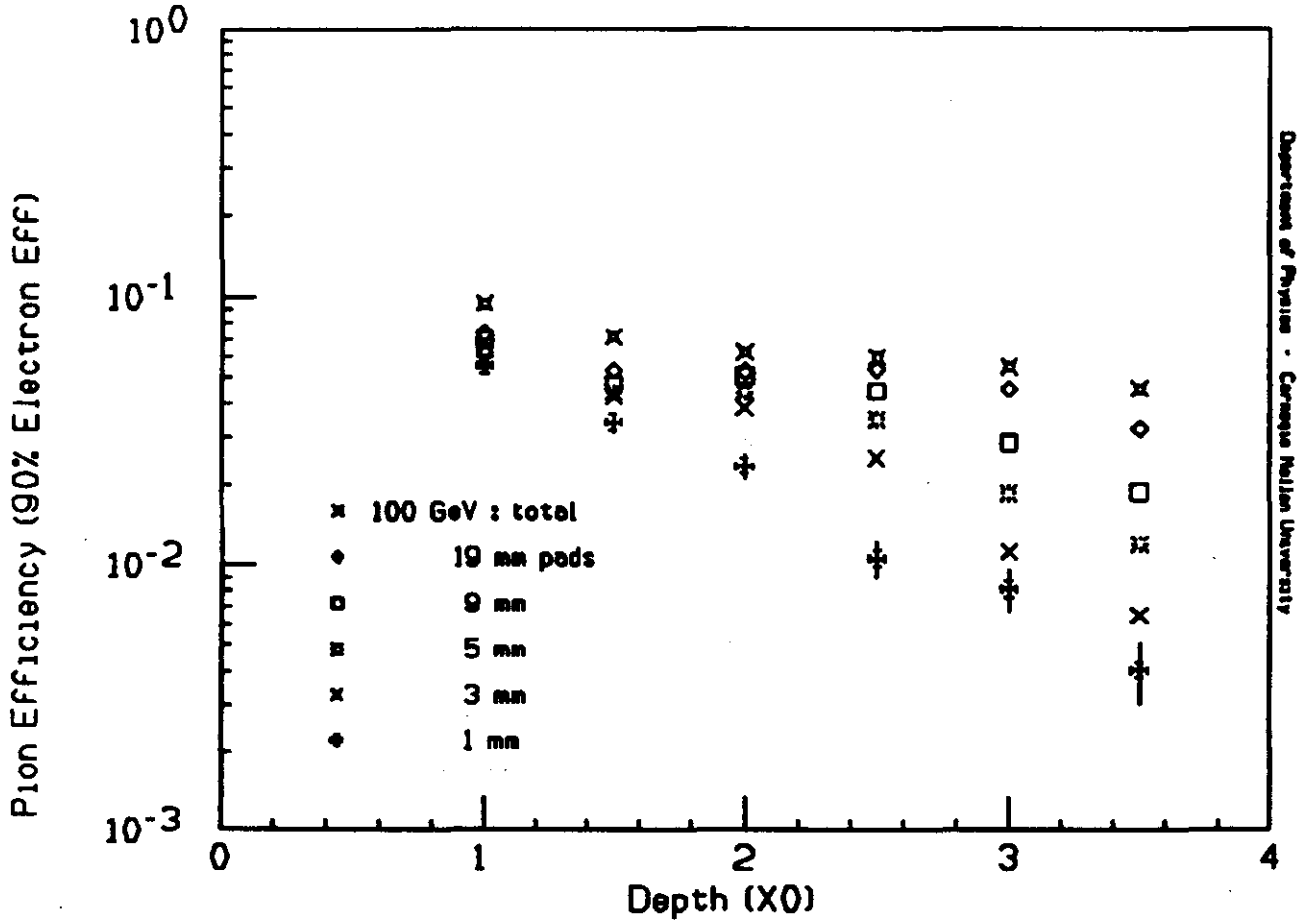
Pion Efficiency (90% Electron Eff)
10^0
10^{-1}
10^{-2}
10^{-3}
0
1
2
3
4
Depth (X0)
100 GeV : total
19 mm pads
9 mm
5 mm
3 mm
1 mm
Department of Physics - Carnegie Mellon University

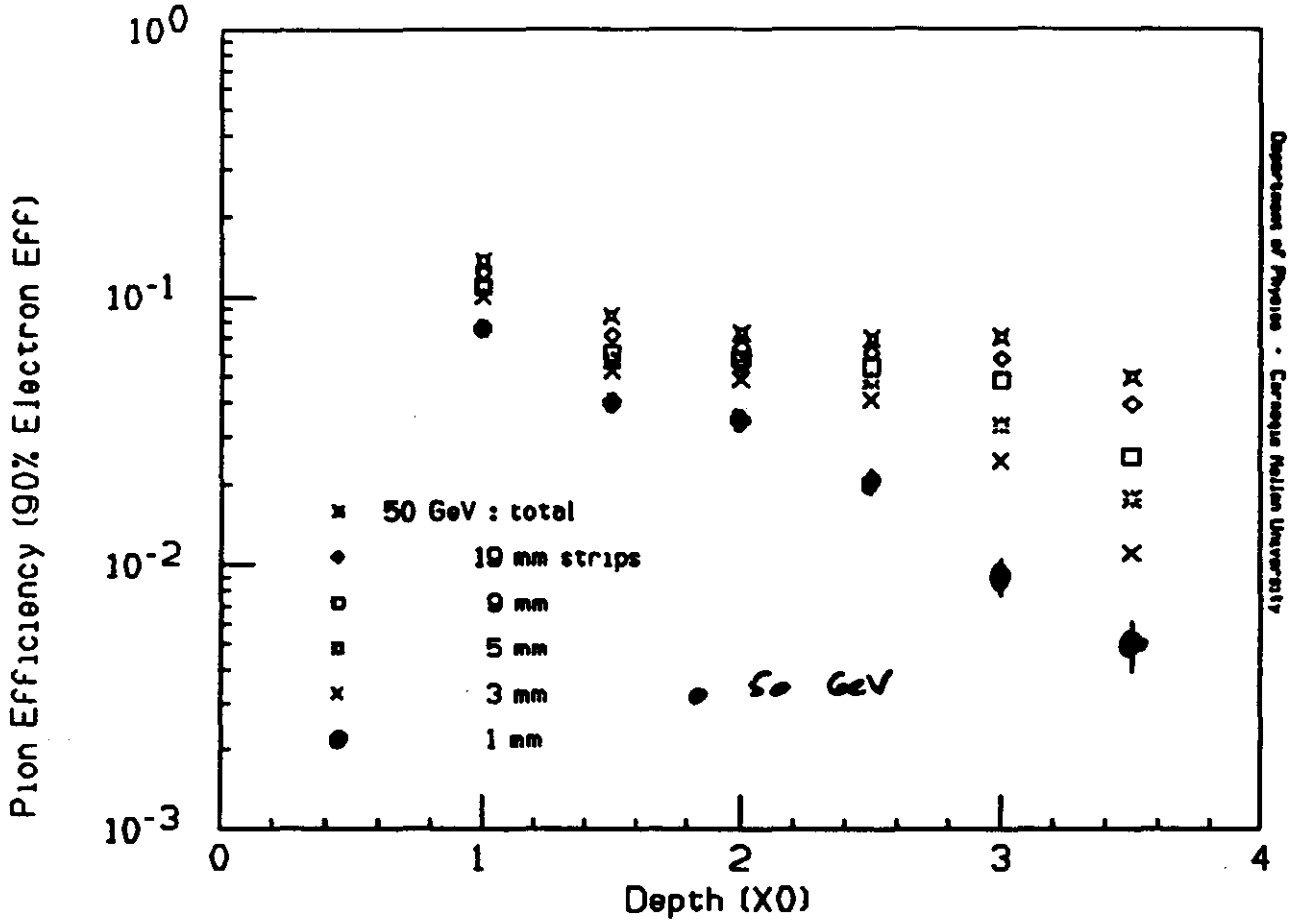
Pion Efficiency (90% Electron Eff)
Depth (X0)
50 GeV : total
19 mm strips
9 mm
5 mm
3 mm
1 mm
50 GeV
Department of Physics - Carnegie Mellon University

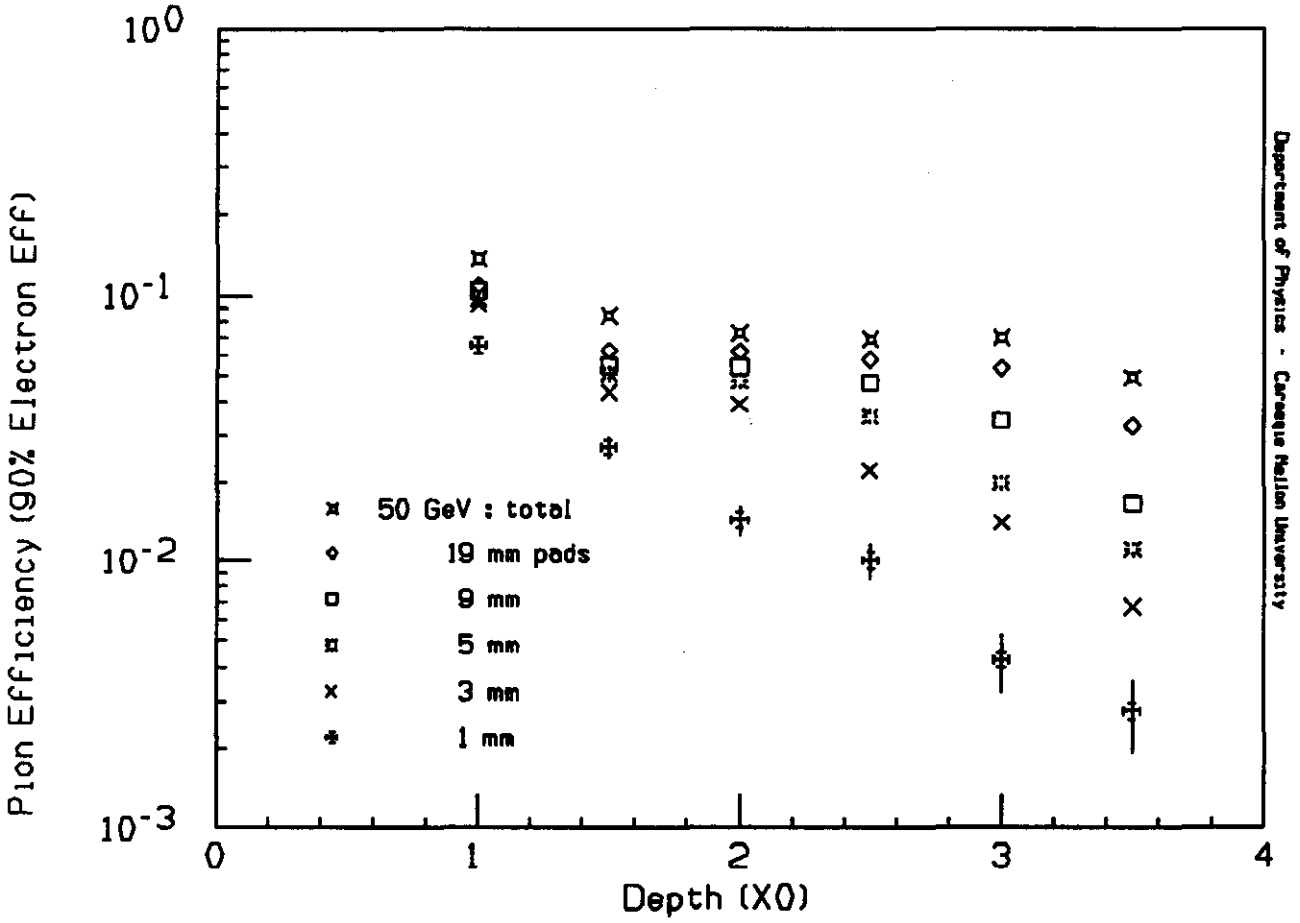
Pion Efficiency (90% Electron Eff)
10^0
10^{-1}
10^{-2}
10^{-3}
0
1
2
3
4
Depth (X0)
50 GeV : total
19 mm pads
9 mm
5 mm
3 mm
1 mm
Department of Physics - Carnegie Mellon University

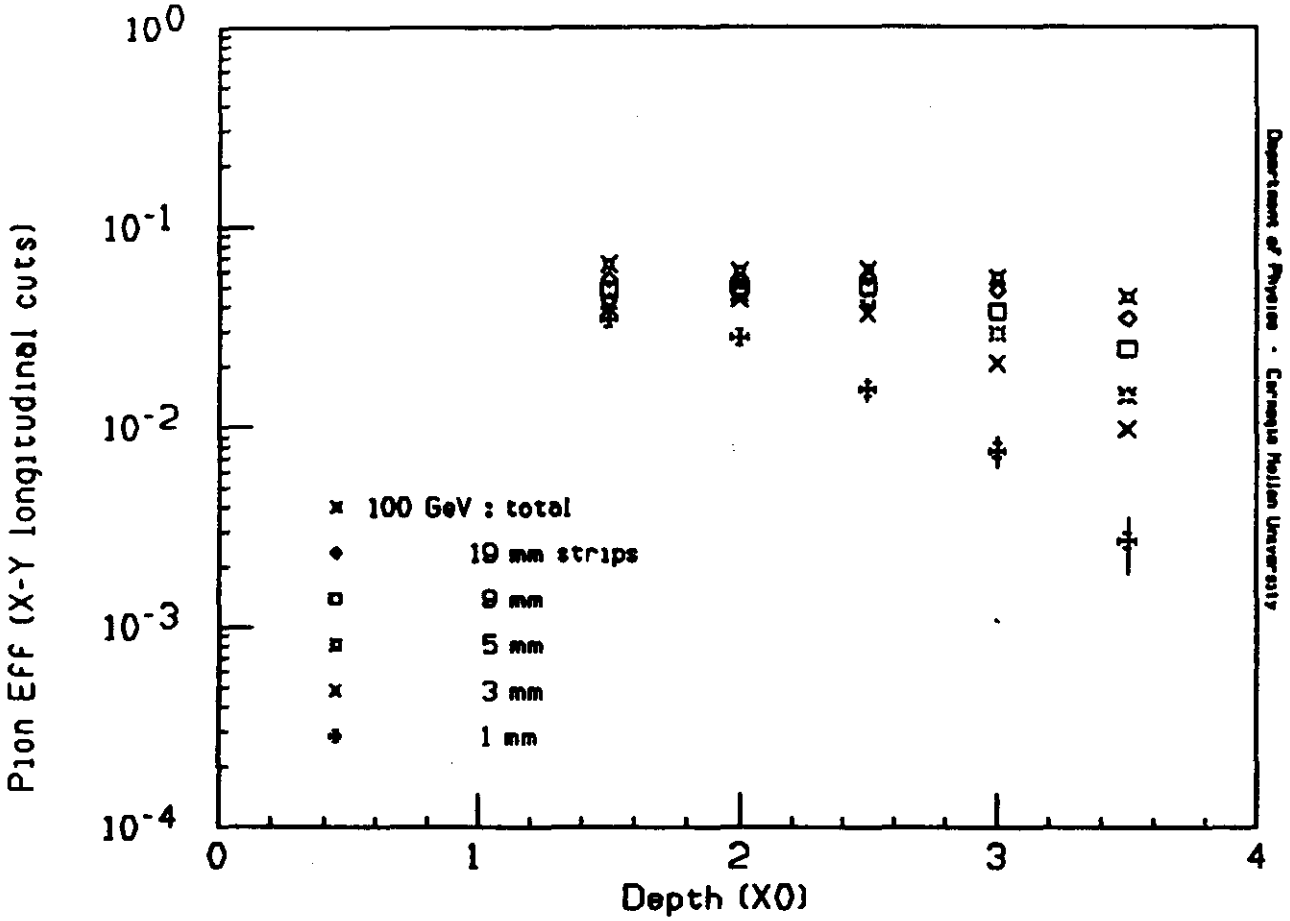

CUT 1: Total Energy Deposit in Last Silicon Plane, such that $\varepsilon_e = 90\%$

CUT 2: Total Energy Deposit in Silicon Plane $\frac{1}{2} X_0$ before last, such that $\varepsilon_e = .9 \times .9$

VARIED: Lead Thickness

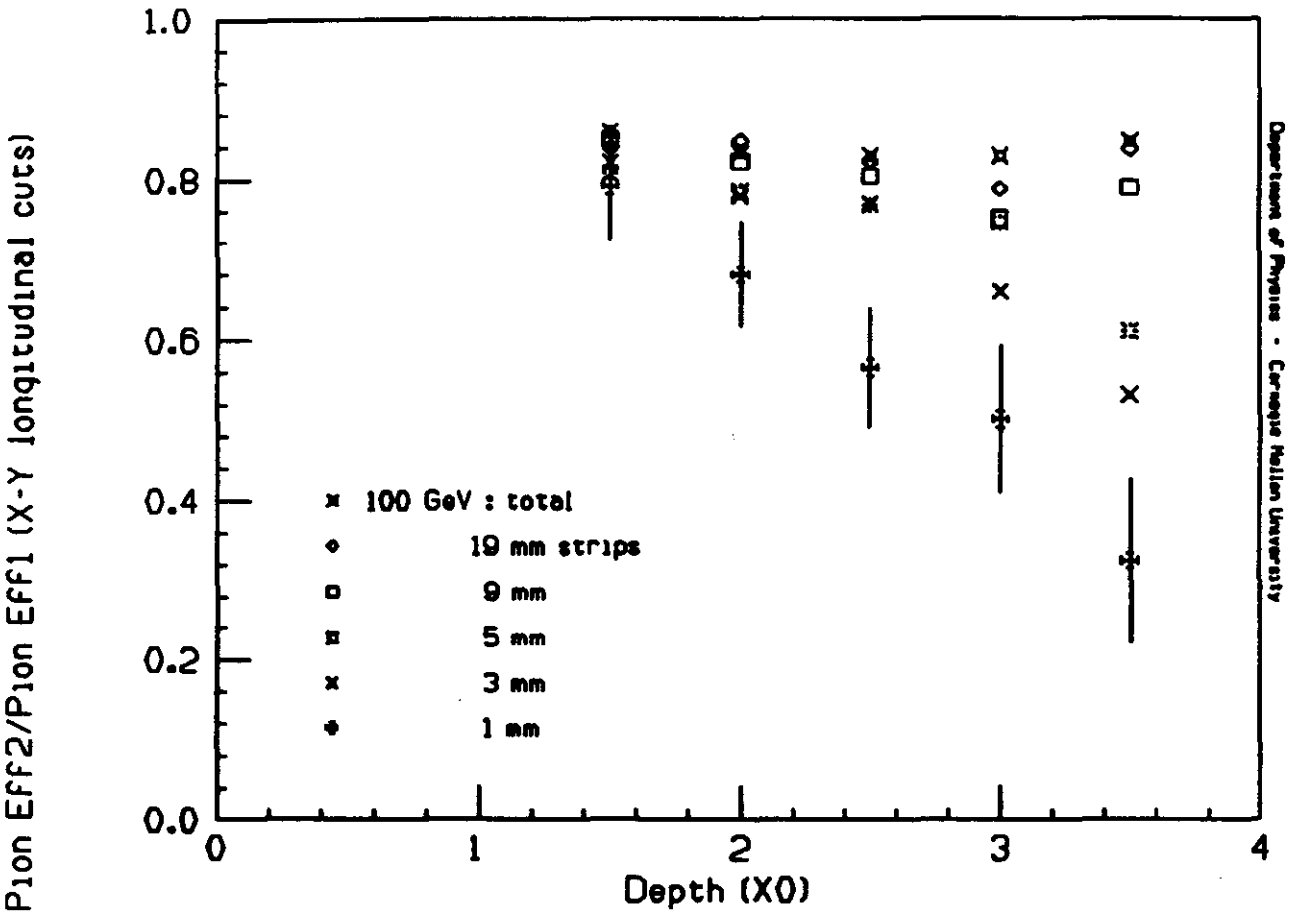

CUT 1: Total Energy in last Silicon plane, such that $\varepsilon_e = 90\%$

CUT 2: Total Energy in Silicon Plane ½ X_0 before last, such that $\varepsilon_e = 0.9 \times 0.9$

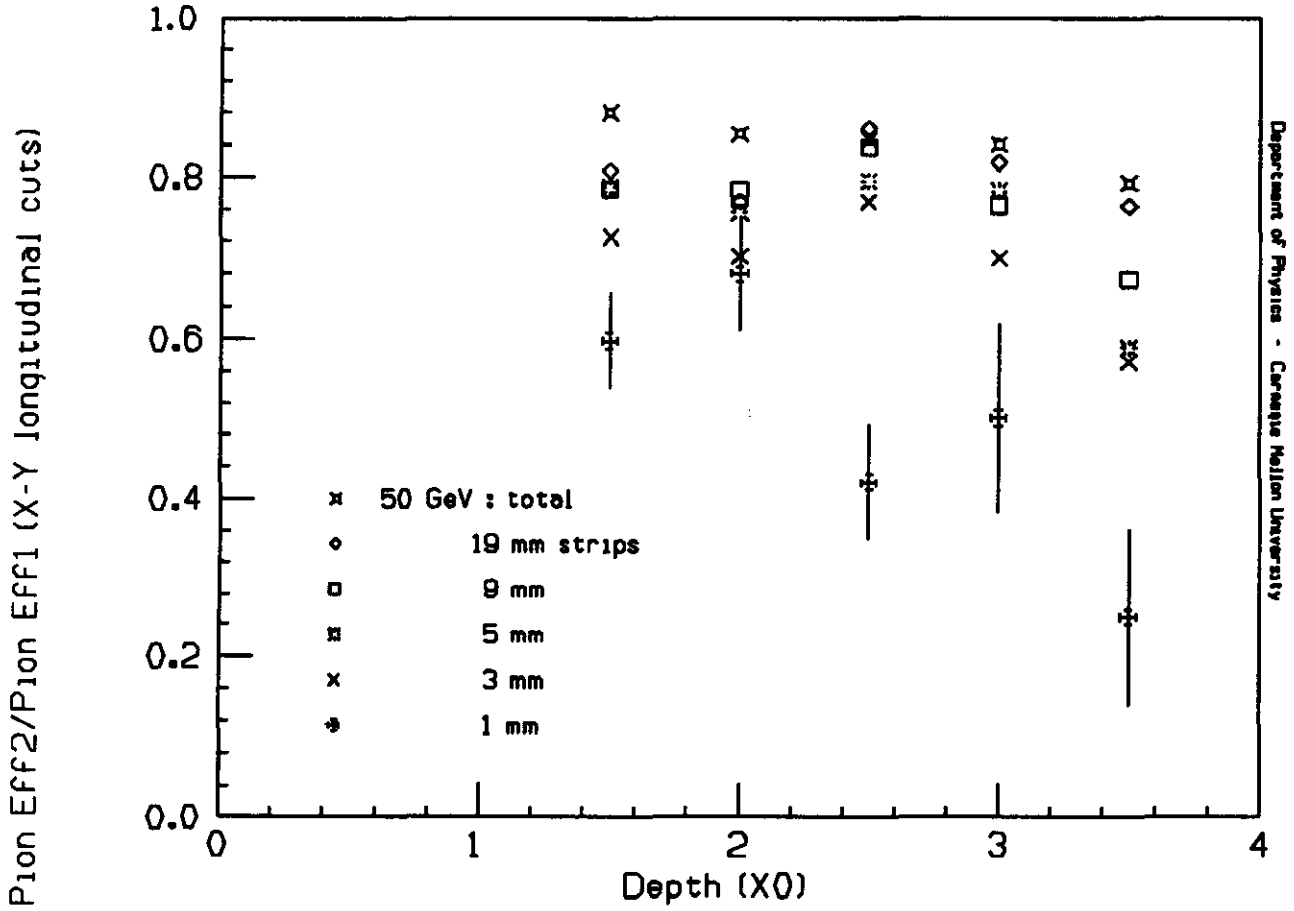
Pion Eff2/Pion Eff1 (X-Y longitudinal cuts)
1.0
0.8
0.6
0.4
0.2
0.0
0
1
2
3
4
Depth (X0)
50 GeV : total
19 mm strips
9 mm
5 mm
3 mm
1 mm
Department of Physics - Carnegie Mellon University

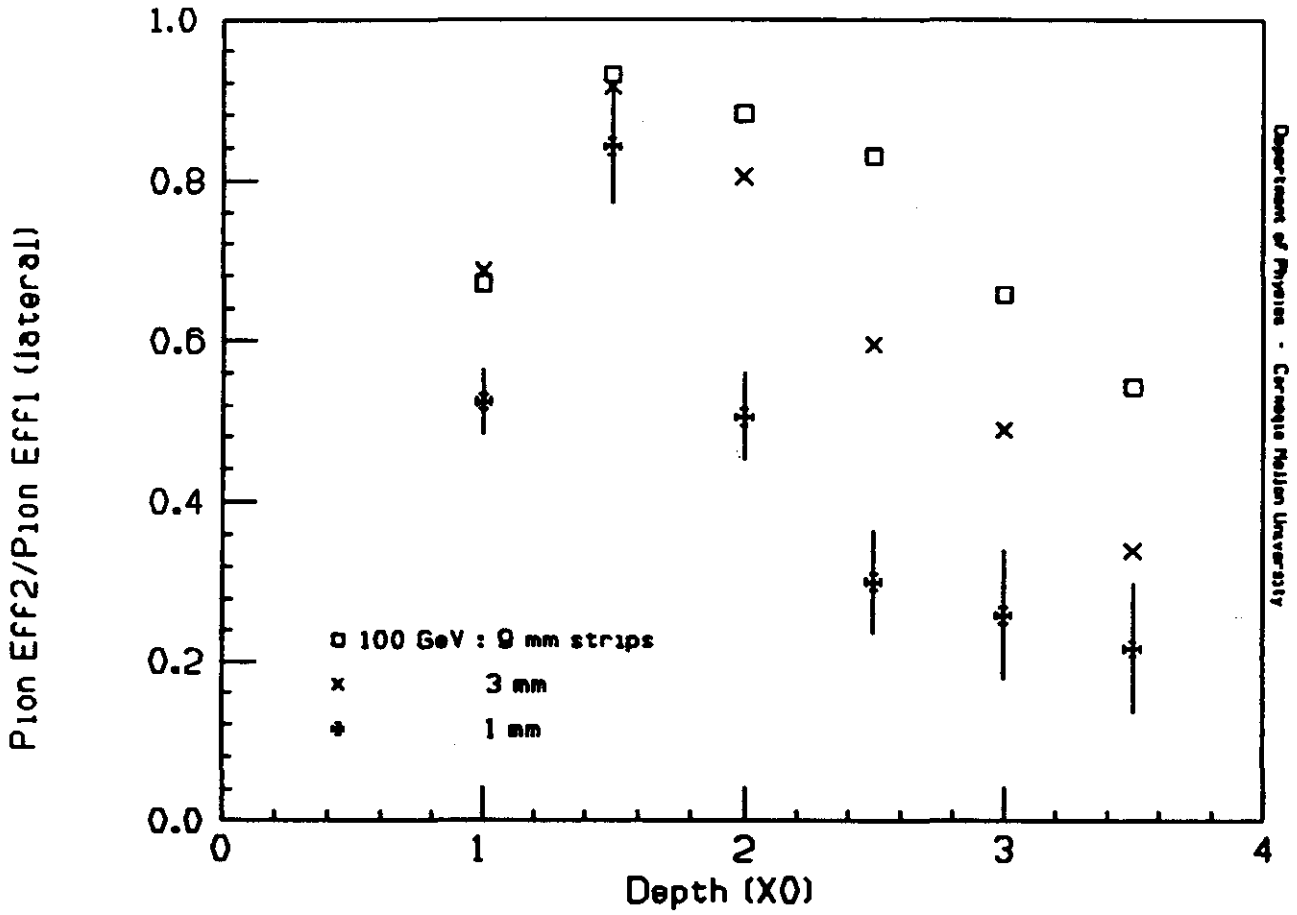

CUT 1: Total Energy in last Silicon Plane, such that $\varepsilon_e = 90\%$

CUT 2: Total Energy in Last Silicon Plane, in 3 strips, such that $\varepsilon_e = .9 \times .9$

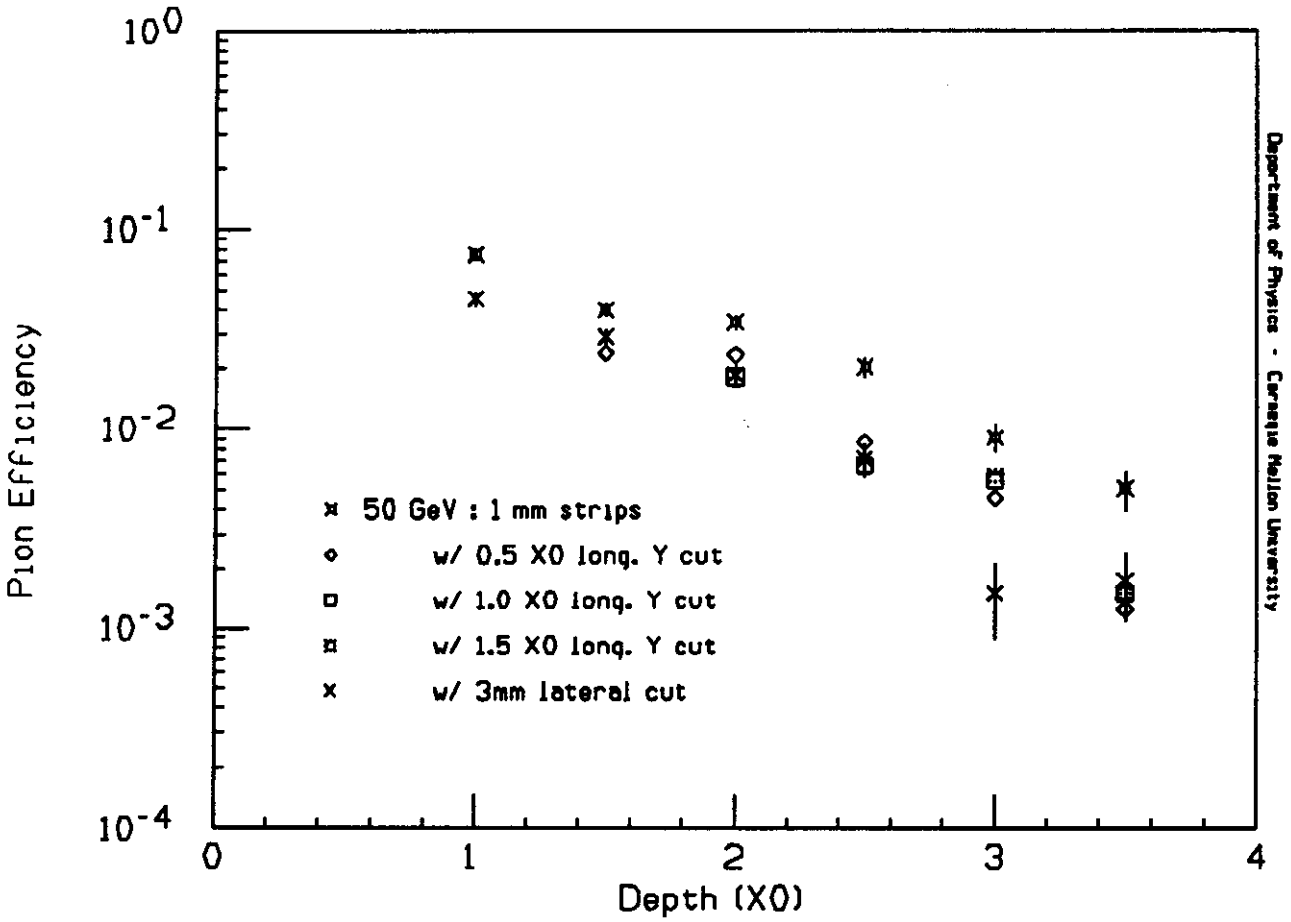
Pion Efficiency
Depth (X0)
50 GeV : 1 mm strips
w/ 0.5 X0 long. Y cut
w/ 1.0 X0 long. Y cut
w/ 1.5 X0 long. Y cut
w/ 3mm lateral cut
Department of Physics - Carnegie Mellon University

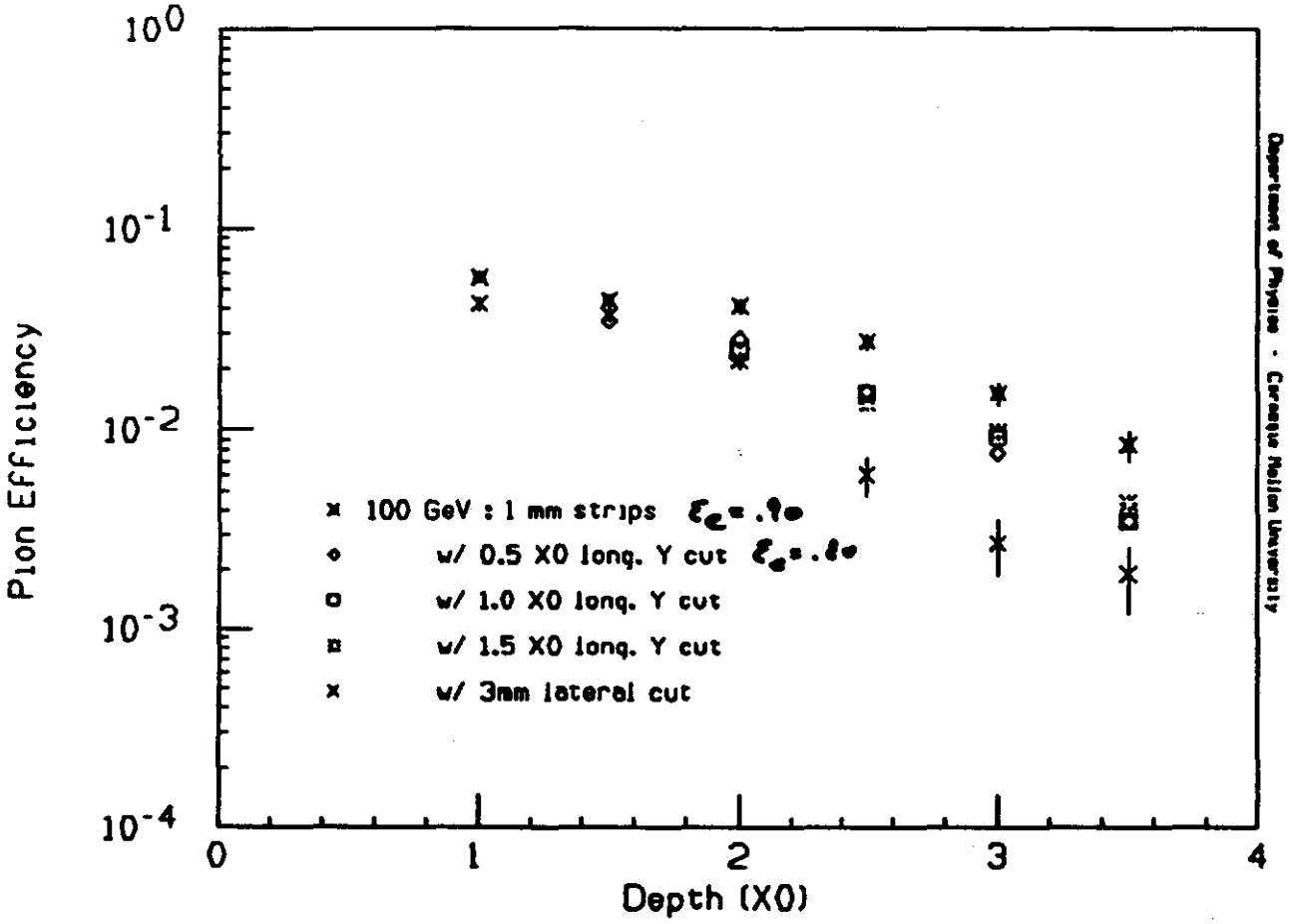
Pion Efficiency
Depth (X0)
100 GeV : 1 mm strips
w/ 0.5 X0 long. Y cut
w/ 1.0 X0 long. Y cut
w/ 1.5 X0 long. Y cut
w/ 3mm lateral cut
Department of Physics - Carnegie Mellon University

Conclusions

Preradiator may as well just sample at the very end of its volume, and, in the case of X-Y strips, seperated by small thickness of absorber near the end

1 mm strips: $\frac{\varepsilon_e}{\varepsilon_\pi} \sim \frac{1}{20}$ at $1 X_0$

$\frac{1}{500}$ at $3\frac{1}{2} X_0$

(no pileup noise)

Strips : 3 Silicon Planes Minimum

Pads : 2 Silicon Planes Minimum

ID= 70

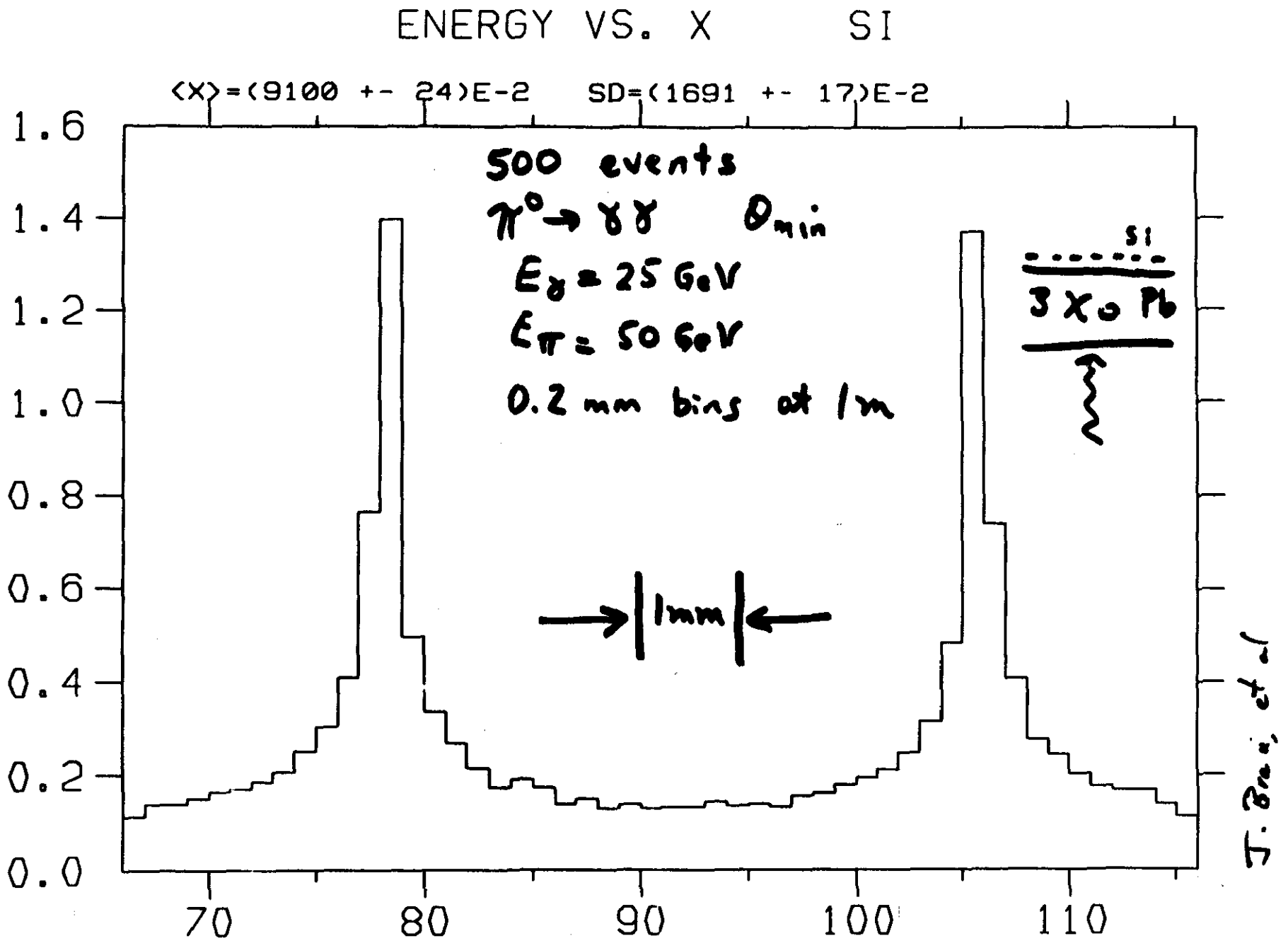

J. Brau, et al

HANDYPAK X1A14:53 30AUG91

ID= 78

ENERGY VS. Y SI

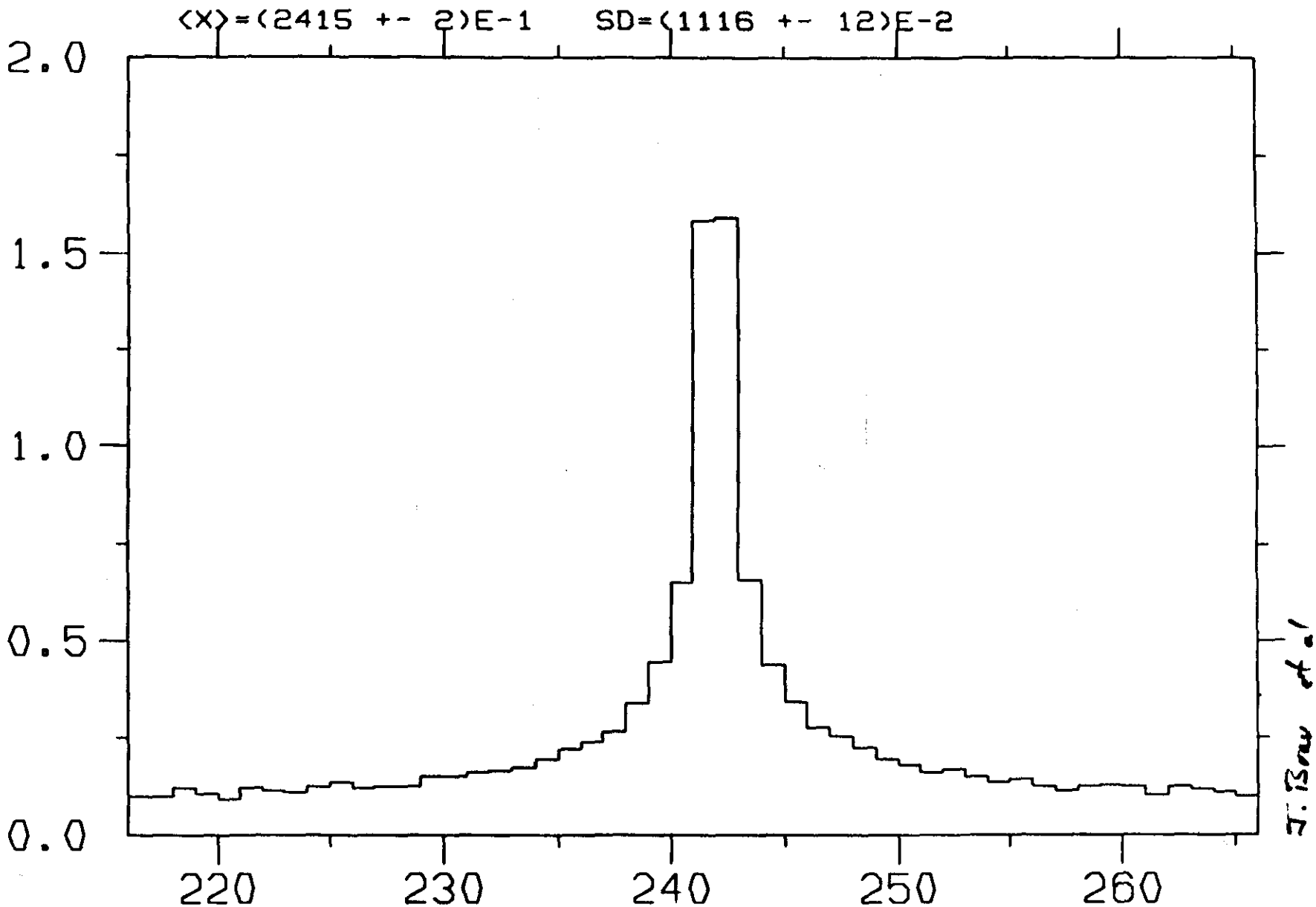

T. Bow et al

HANDYPAK X1A14:53 30AUG91

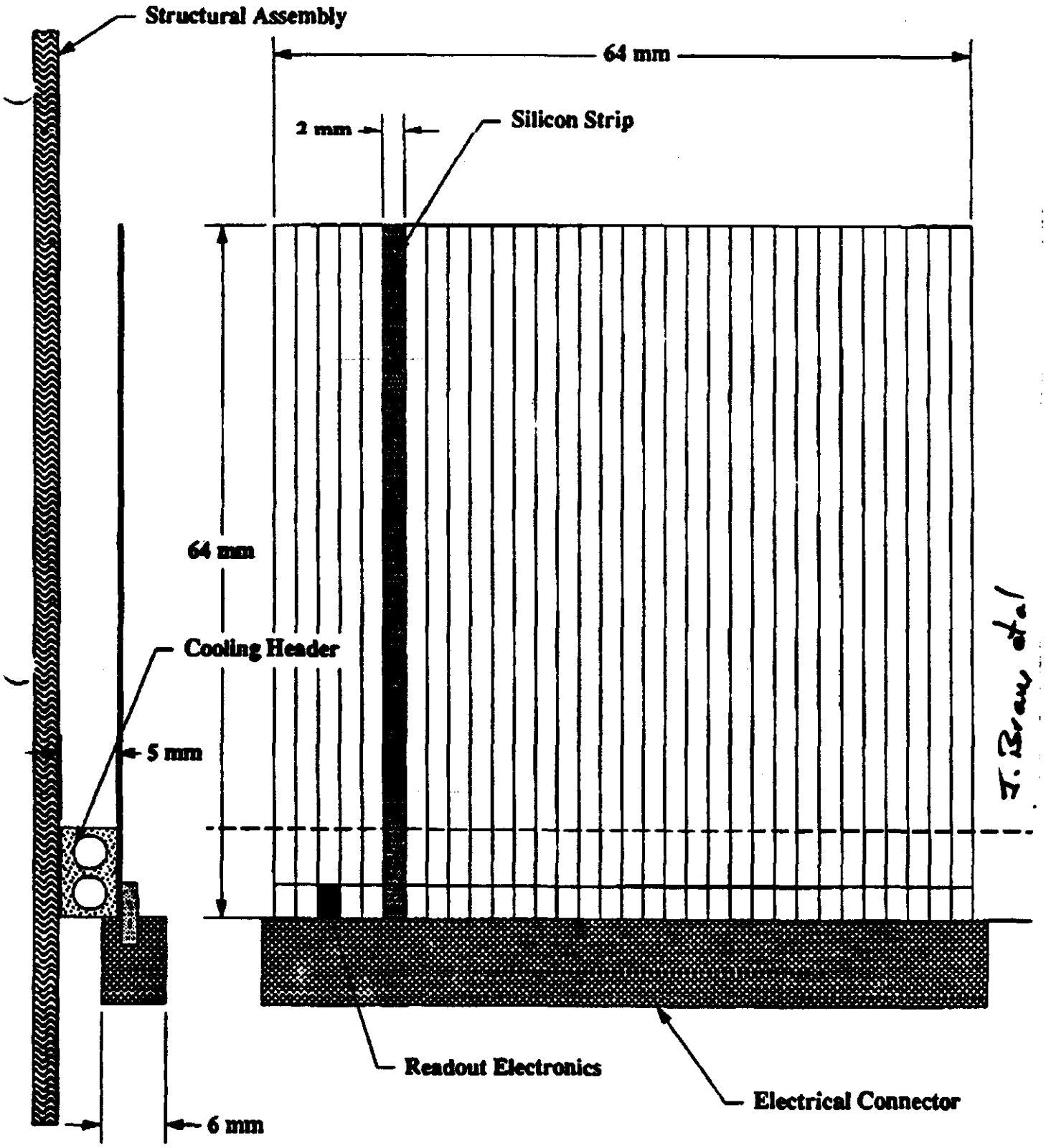

Silicon Preradiator "Chip" Assembly

LS.03.PR.00013

Rennich

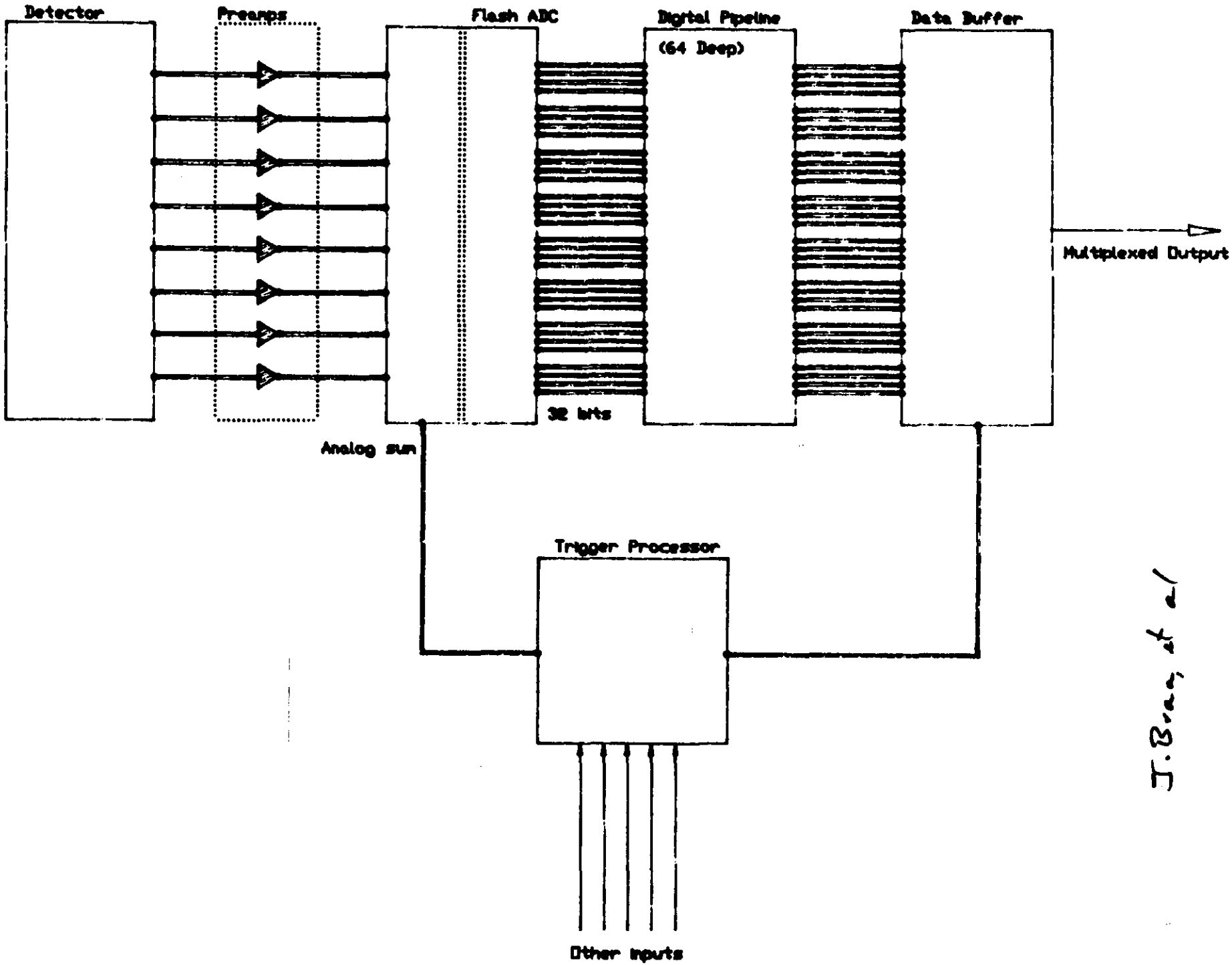
Detector
Preamps
Flash ADC
Digital Pipeline
(64 Deep)
Data Buffer
Multiplexed Output
32 bits
Analog sum
Trigger Processor
Other inputs

J. Bran et al

GORDON

STUDY OF PUNCHTHROUGH RATES IN AN IRON TOROID

A. Dell'Acqua
K. Jakobs
J. Wotschack

- Motivation
  Description of the Simulation
- Punchthrough rates as a function of λ_{int}
- Study of μ-Reconstruction and trigger possibilities
  (muons inside jets)

Motivation:

(a) Study the problem of μ-reconstruction (trigger) for non isolated muons "muons inside jets"

(b) what is the minimal thickness (in λ_{abs}) for the hadron absorber (calorimeter) in front of the first muon stations

$\Downarrow$

is it possible to use the iron toroid O as "tail catcher" for the hadronic calorim

$\Rightarrow$ split hadron calorimeter in two parts

H1 $\sim 7-10\ \lambda_{abs}$

H2 instrumented iron toroid

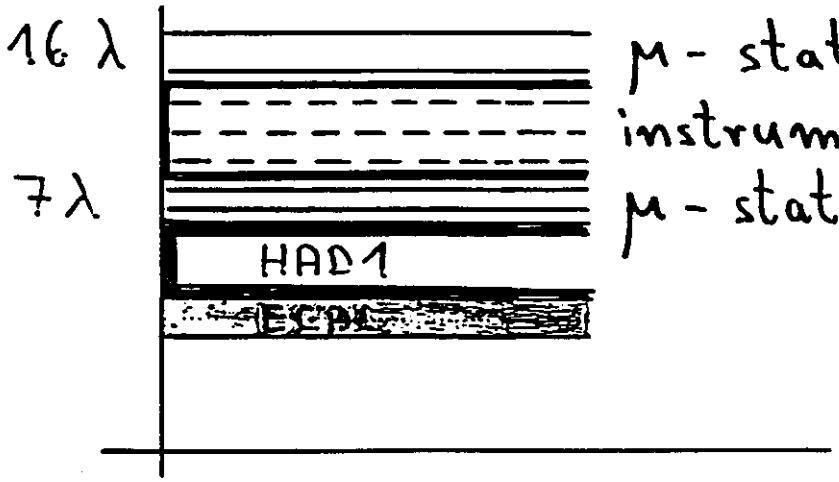

Problem: reconstruct muon hits in inner muon stations (confusion proble

advantage: make detector more compact

Sources of Punchthrough.

(a) underlying event (minimum bias)
- soft particle spectrum at central rapidities
  $\Longrightarrow$ should be no problem

(b) - high-P_T hadrons appear mainly inside the fragmentation products of high-P_T jets
- single, isolated high P_T hadrons are rare

  $\Longrightarrow$ problem can be reduced to punchthrough studies for high-P_T jets

---

Remark:

- Punchthrough probabilities for single hadrons ($\pi^{\pm}$) have been evaluated for Aachen workshop
  (see contribution by H. Fesefeld)
- good agreement between GEISHA simulation and testbeam measurements

P_T – Spectrum of particles in min. bias events $\sqrt{s} = 16$ TeV

GENCL Monte Carlo (UA5)

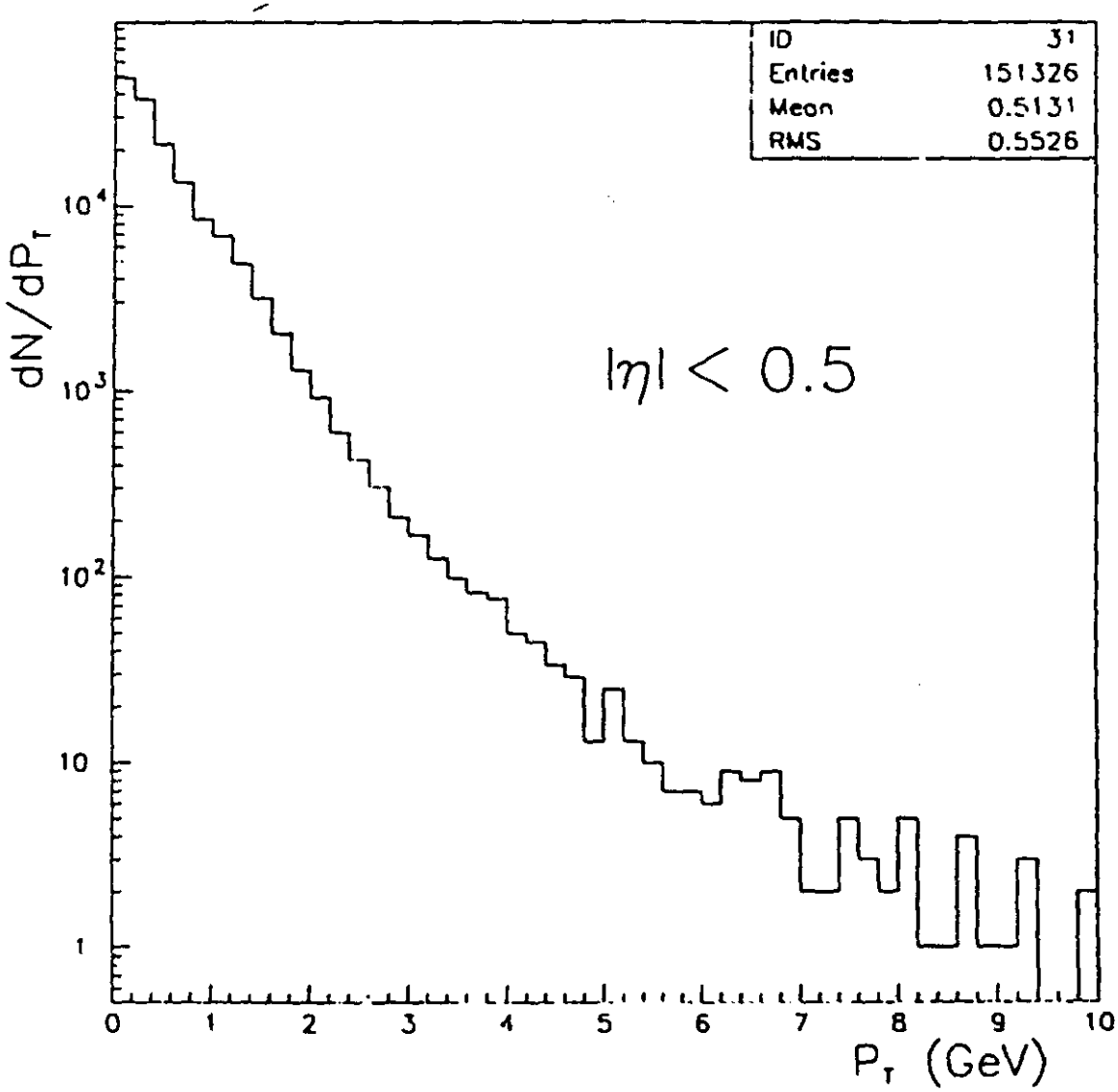

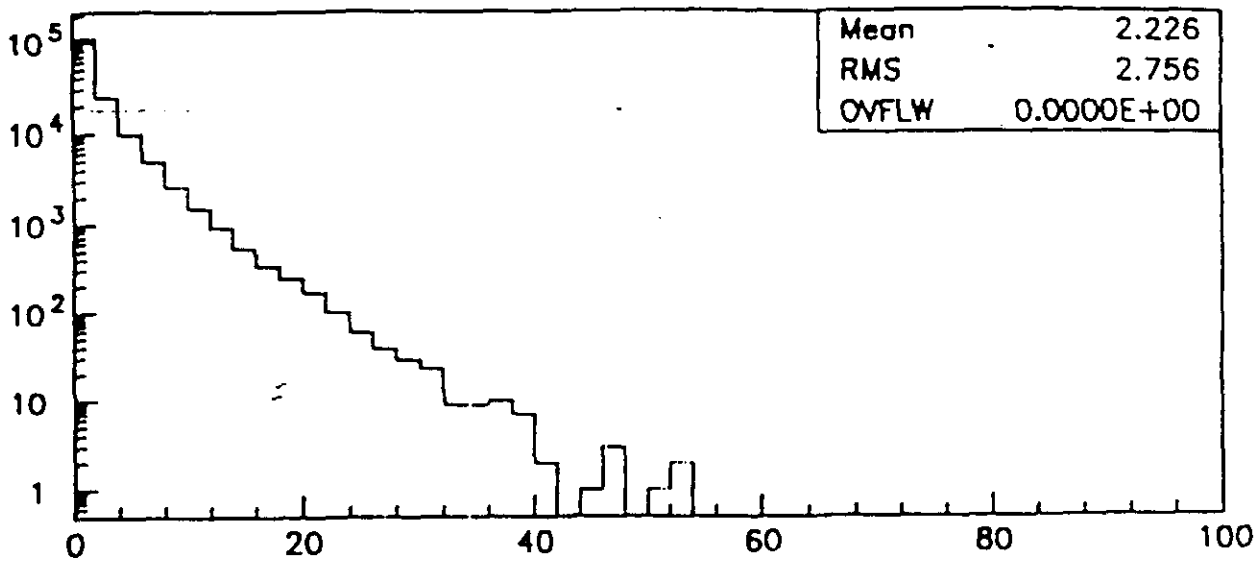

E–frag. products 50– 70 GeV

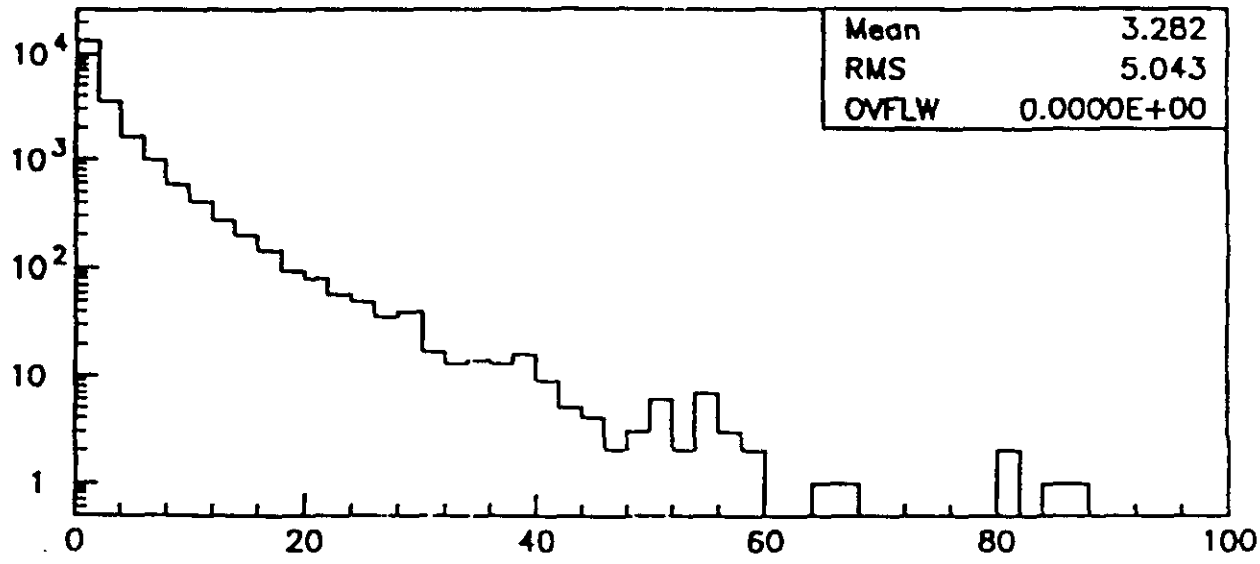

E–frag. products 100–150 GeV

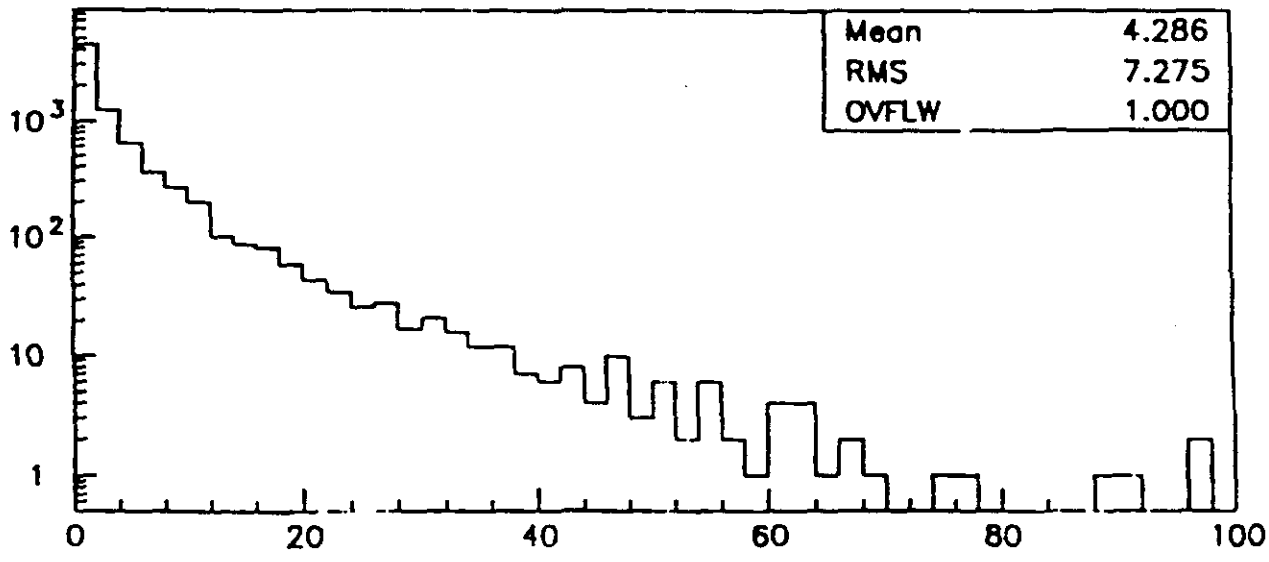

E–frag. products 150–250 GeV

GEISHA / DICE simulation

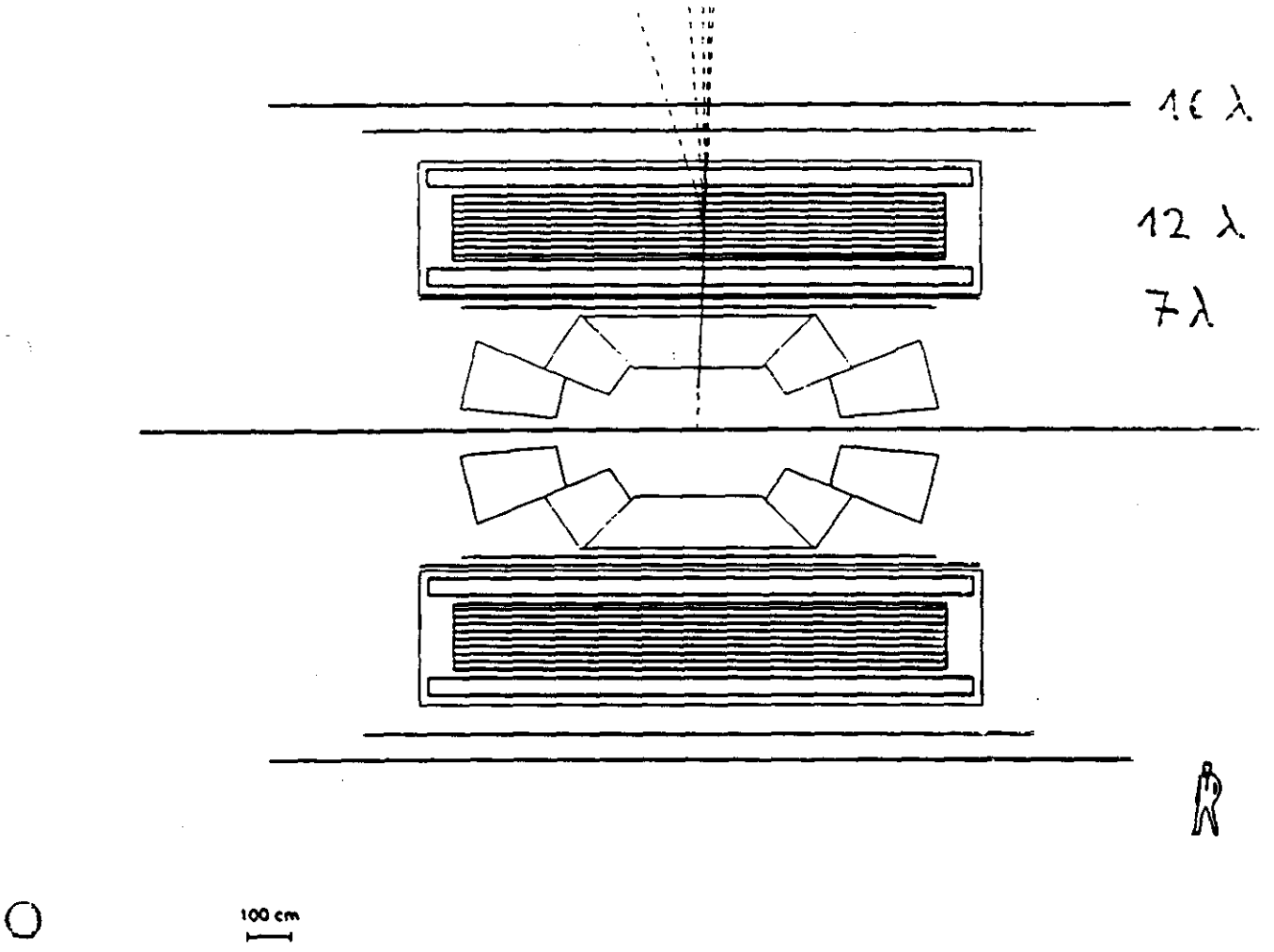

- superimpose muons of different energies (10, 20, 50, 100, 500 GeV) on high-E_T jet
  muon direction = original parton dir.
- store hits after each $\lambda_{abs.}$
  (in range between $7 < \lambda_{abs} < 16$)

Results:

fraction of events with more than one hit in inner muon station

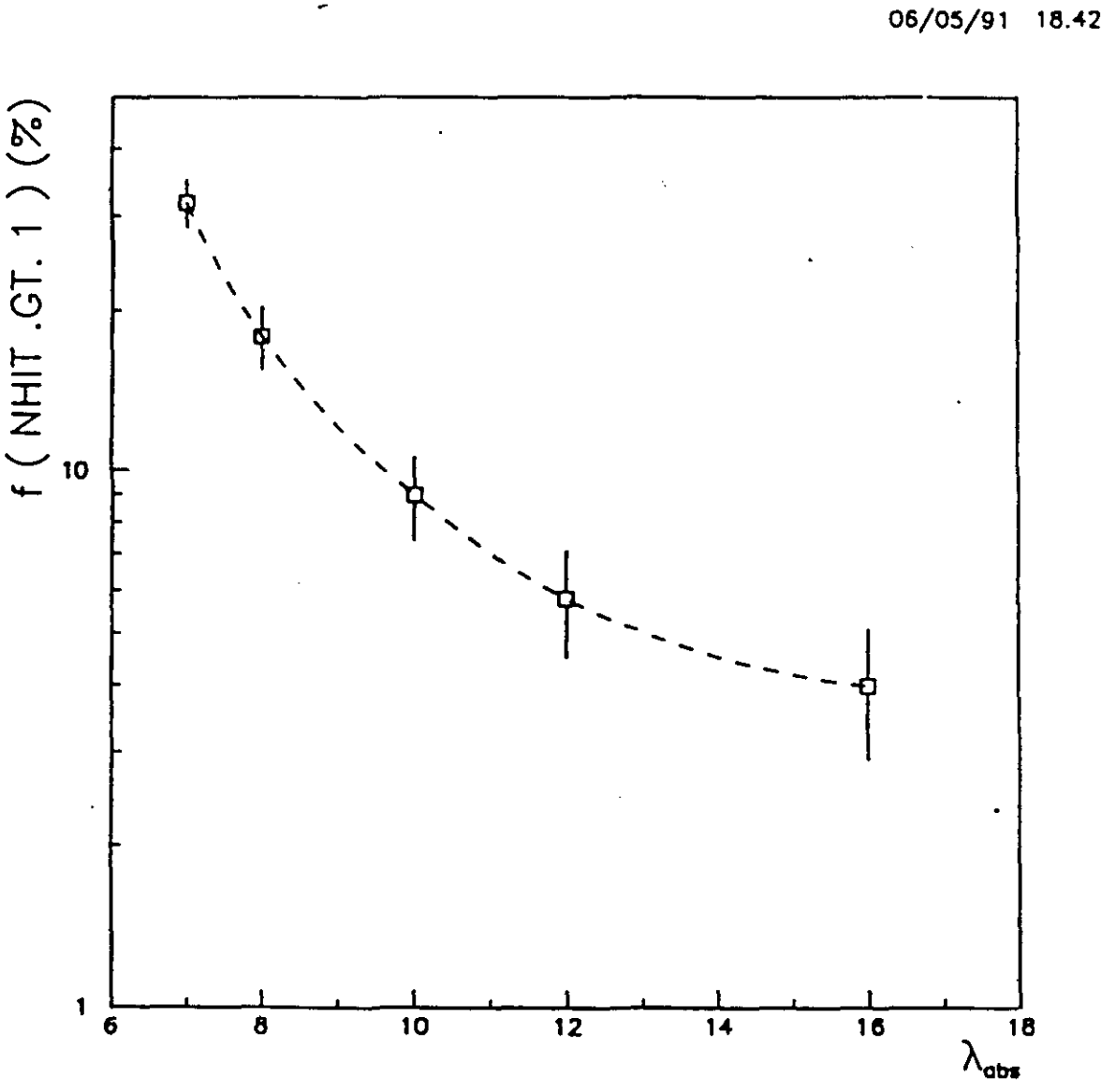

$\lambda_{abs} = 7.$ $f = 31.7 \pm 3.3$ %

$\lambda_{abs} = 10.$ $f = 9.0 \pm 1.6$ %

$\lambda_{abs} = 16$ $f = 4.0 \pm 1.1$ %

contributions from secondary muons (π, K-decays) in the punchthrough:

06/05/91 18.42

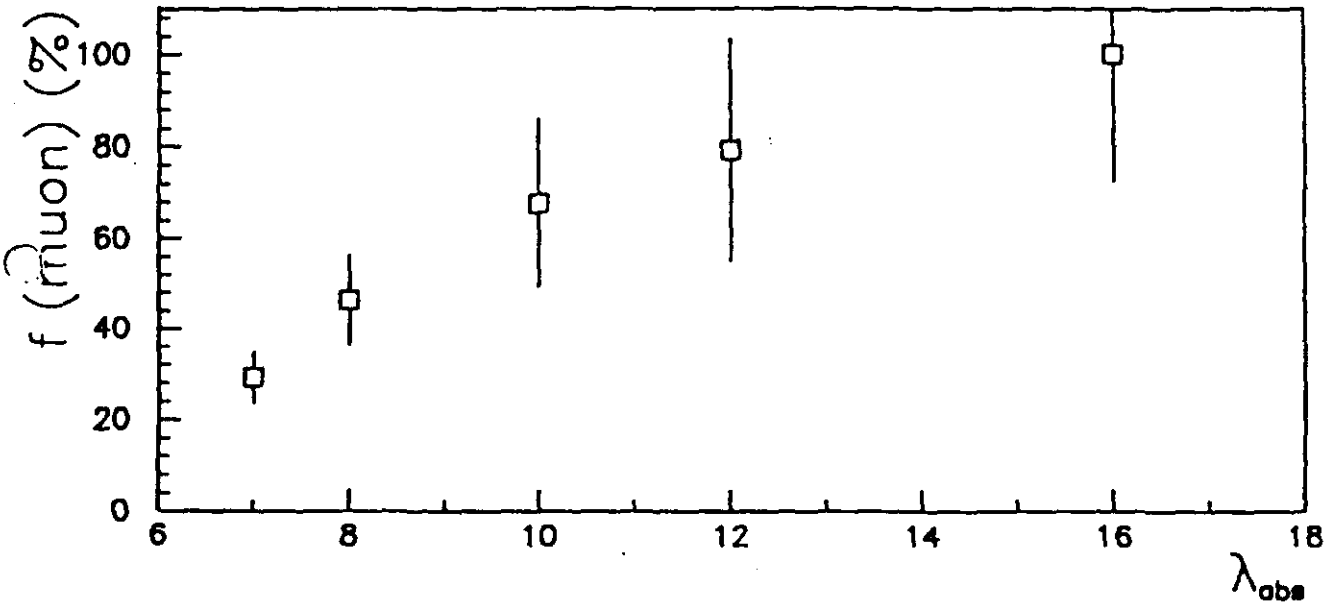

O

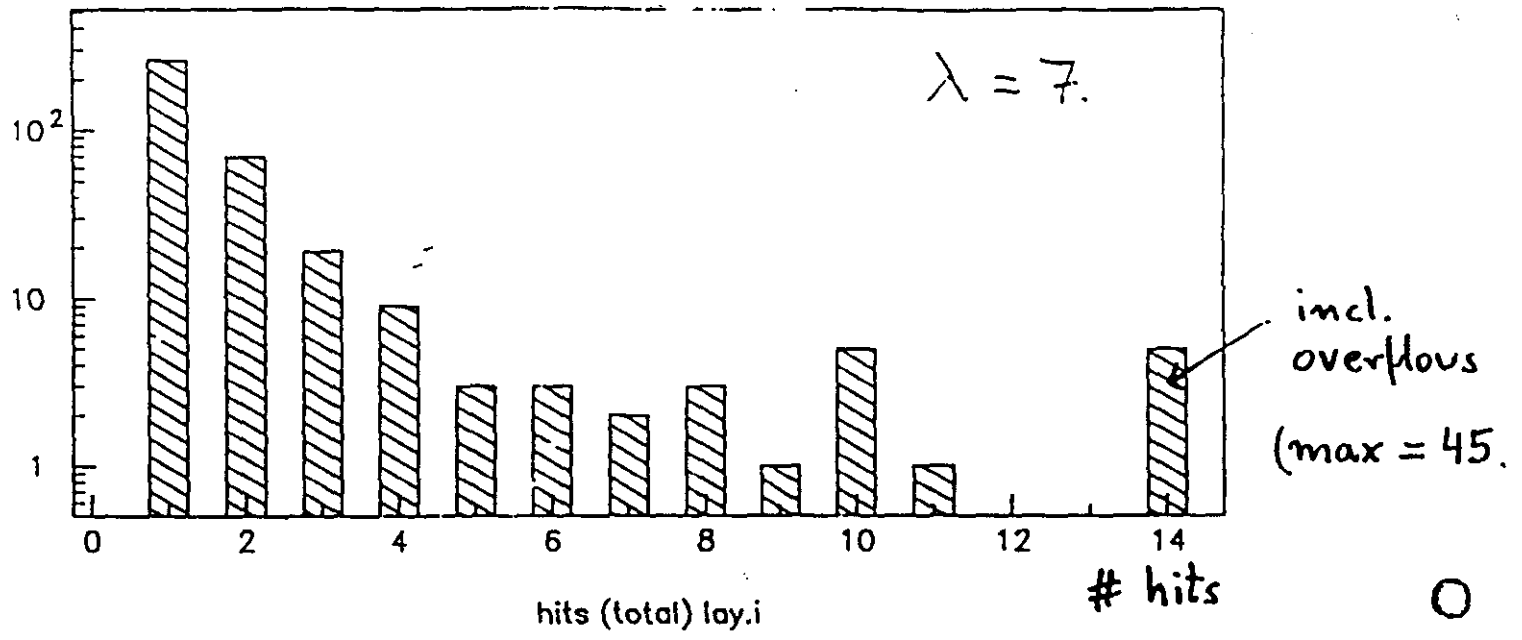
λ = 7.
incl. overflows
(max = 45.
hits (total) lay.i
hits

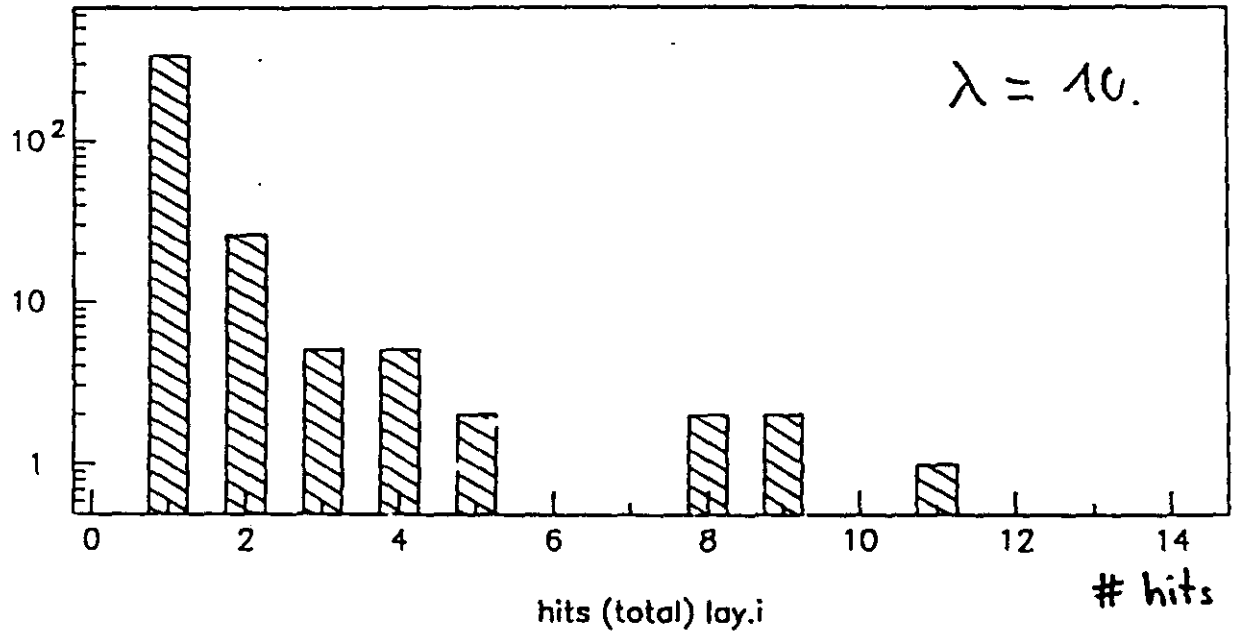
λ = 10.
hits (total) lay.i
hits

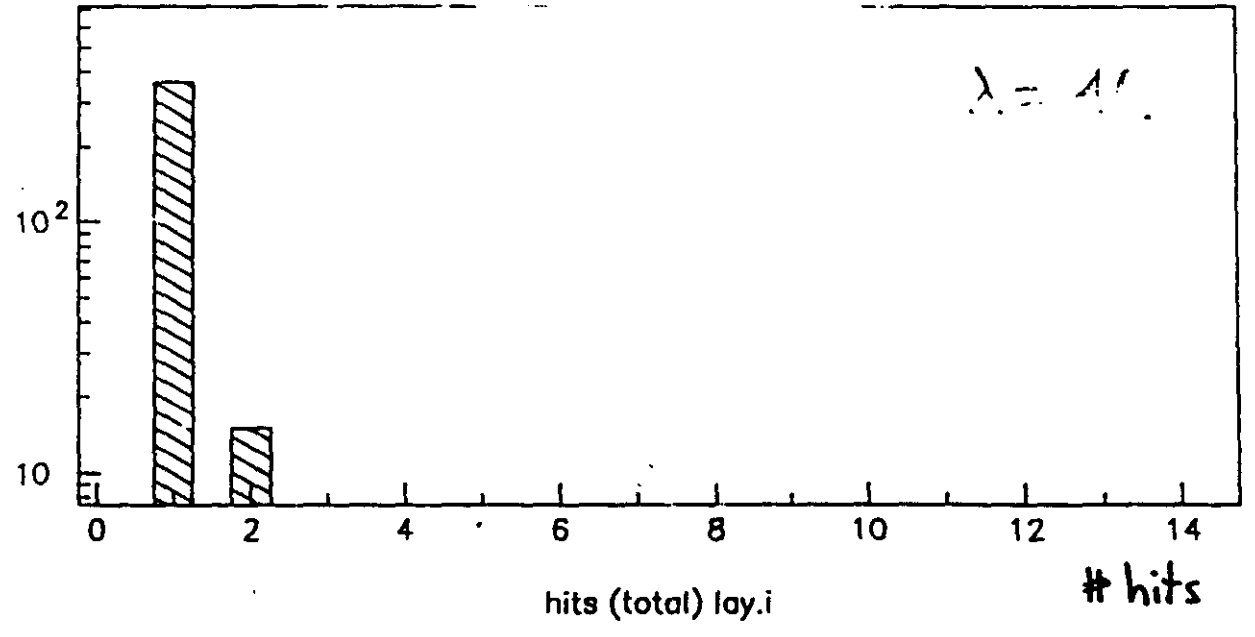
λ = 41.
hits (total) lay.i
hits

momentum distributions hadrons

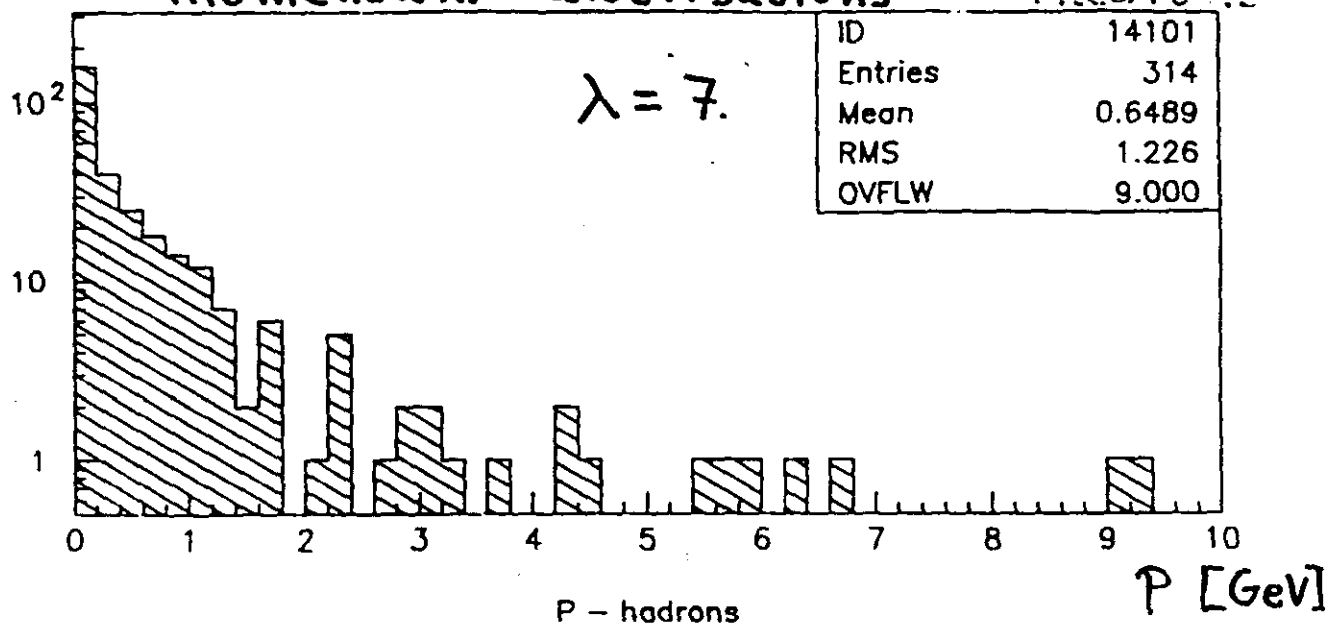

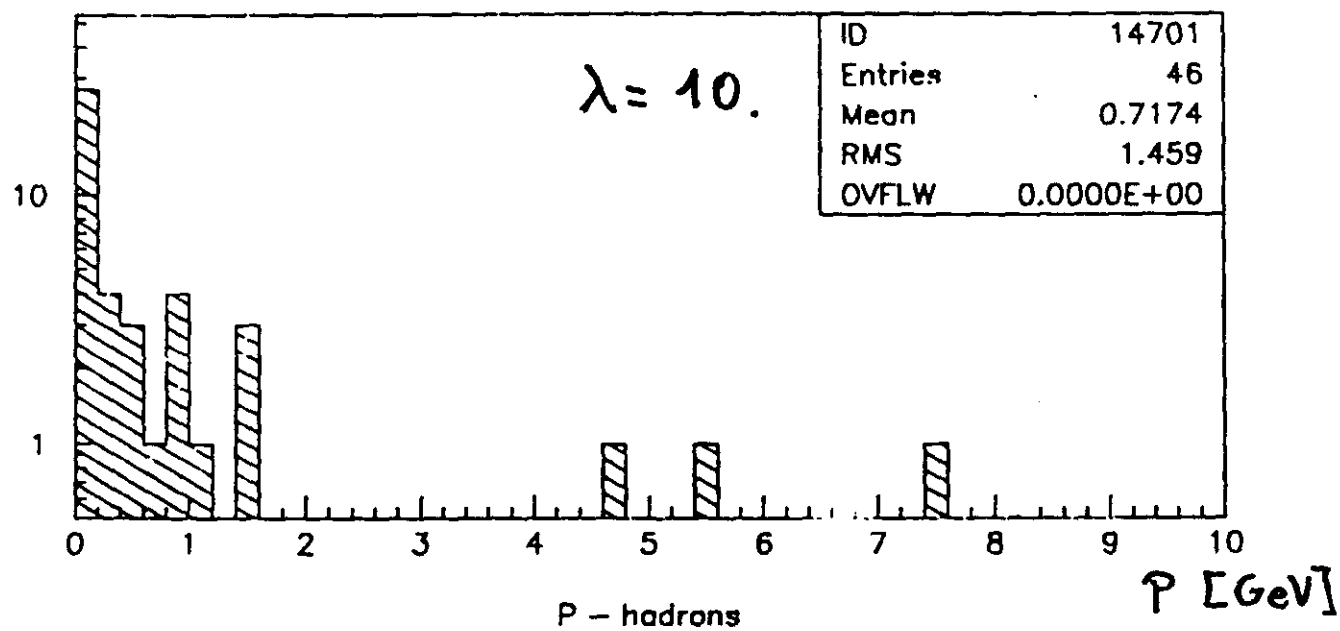

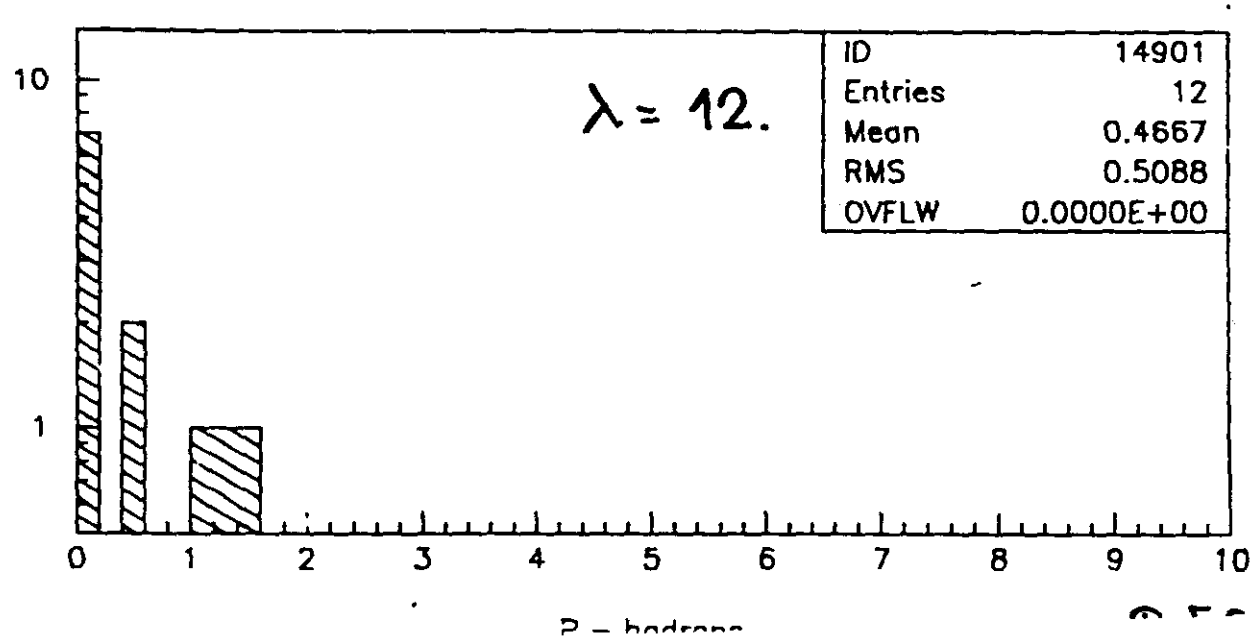

momentum distributions Muons

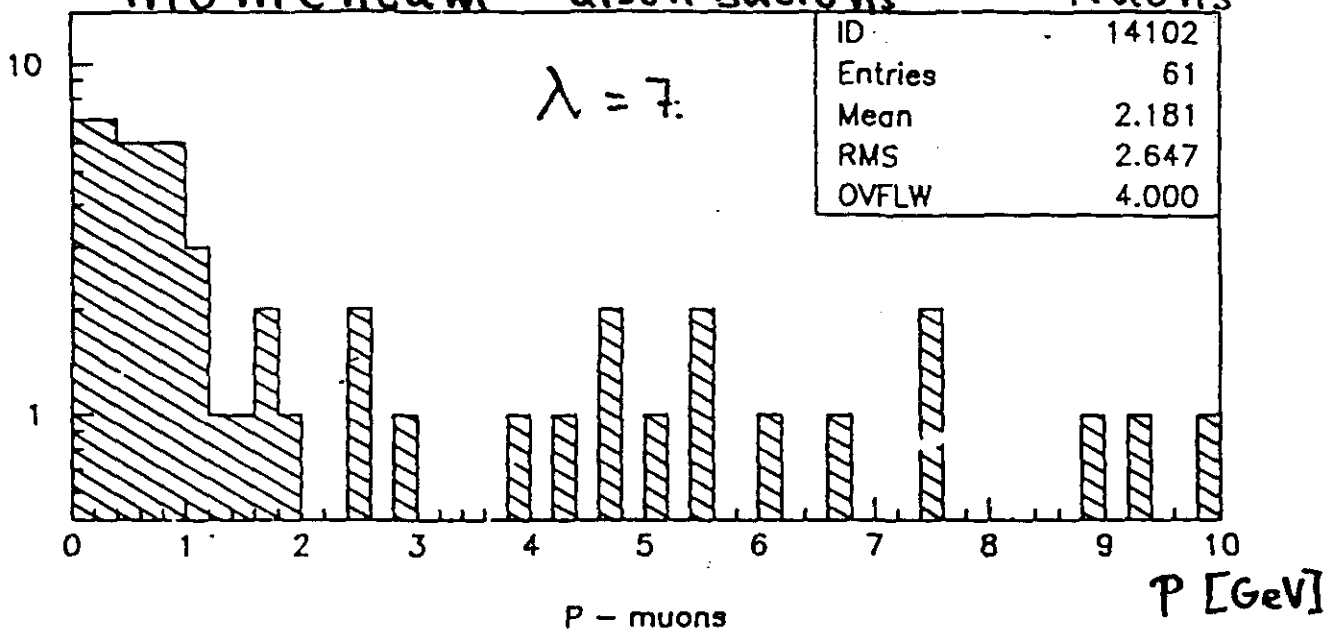

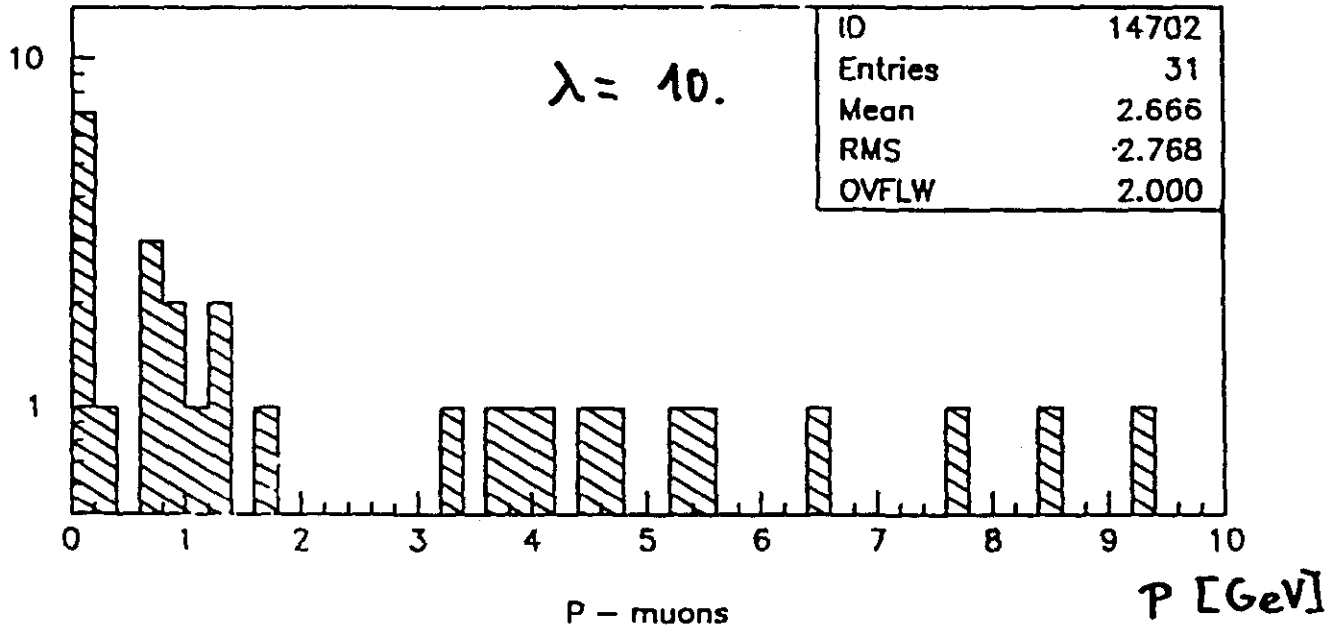

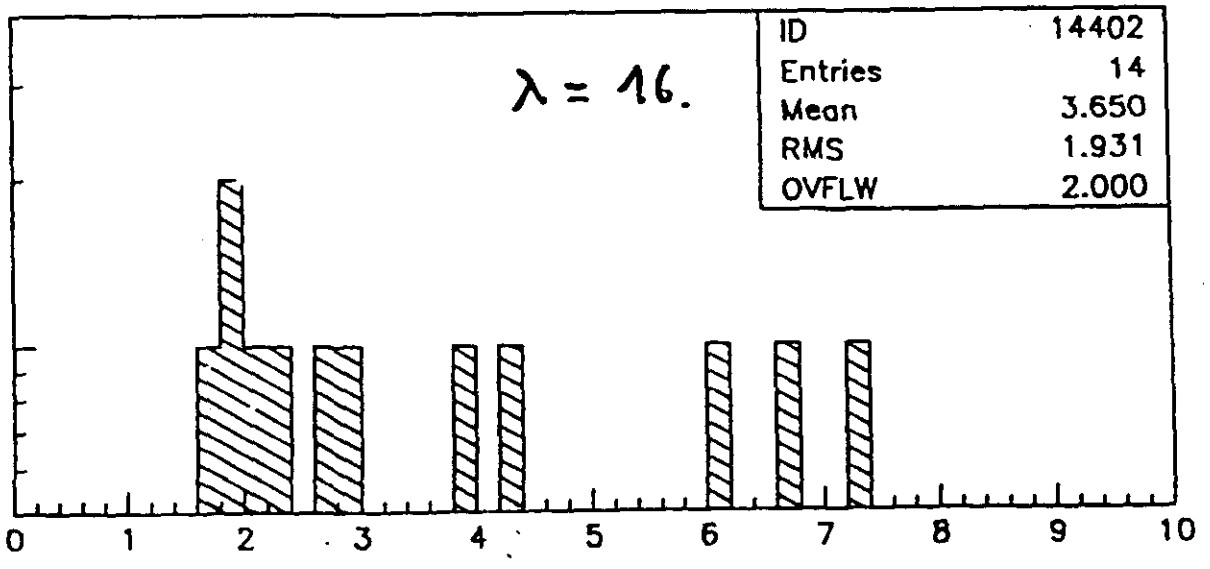

MUON RECONSTRUCTION

- start with outer muon chambers (hits in these chambers are necessary to set the muon trigger)

- use φ-constraint to associate hits in the inner chambers

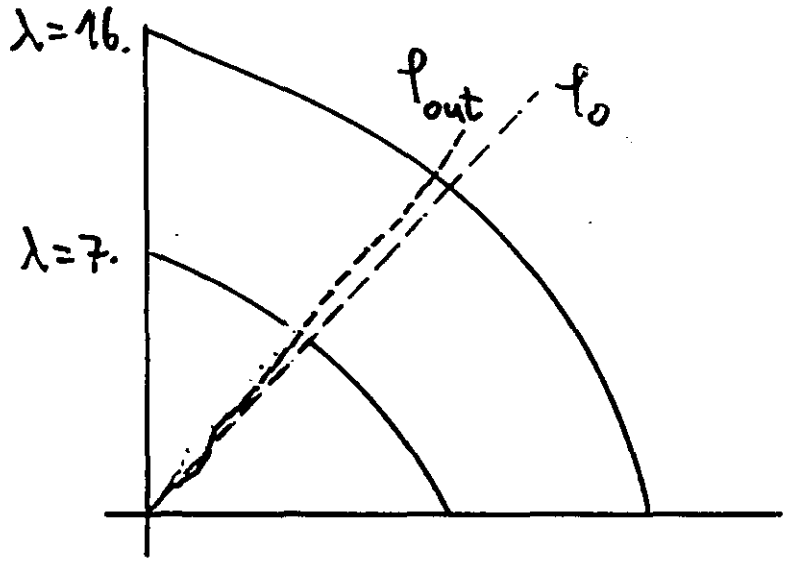

--- muon track

measure φ_{out}

select those hits in the inner chambers in a given interval of $\Delta(R \cdot \phi_{out})$

interval determined by multiple scattering

$\Longrightarrow$ if association is unique

$\Rightarrow$ get P_T measurement of muon (from angular deflection in R-z plane

$\Longrightarrow$ trigger on high P_T-muons

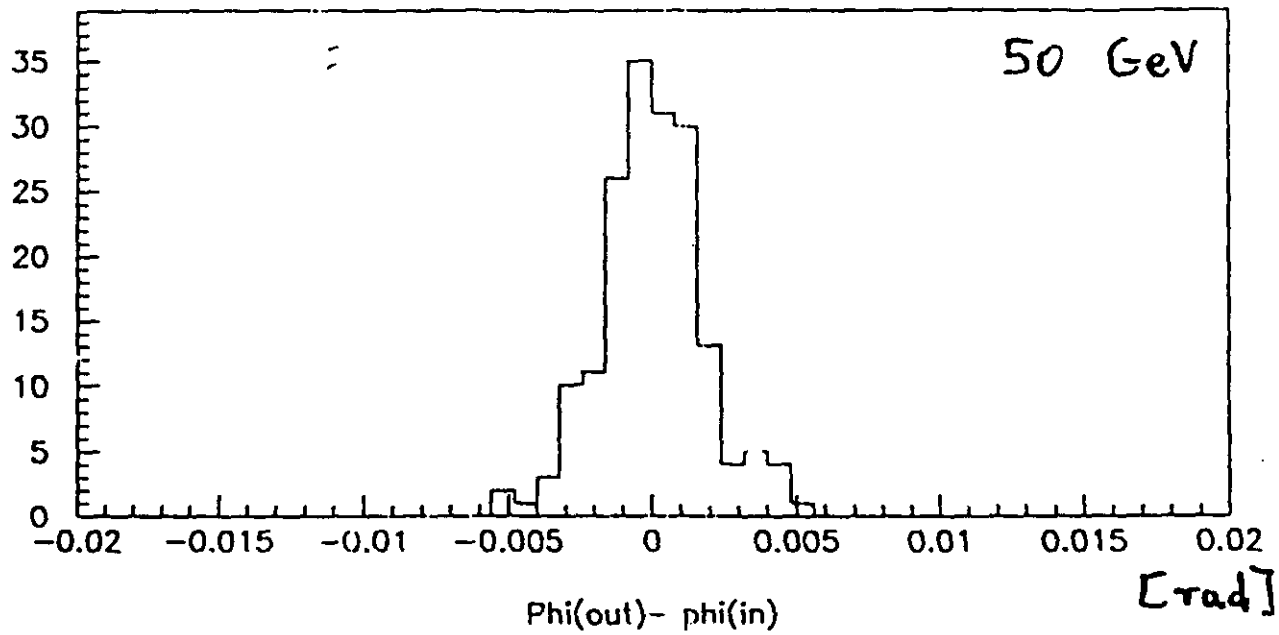
50 GeV
35
30
25
20
15
10
5
0
−0.02
−0.015
−0.01
−0.005
0
0.005
0.01
0.015
0.02
Phi(out)− phi(in)
[rad]

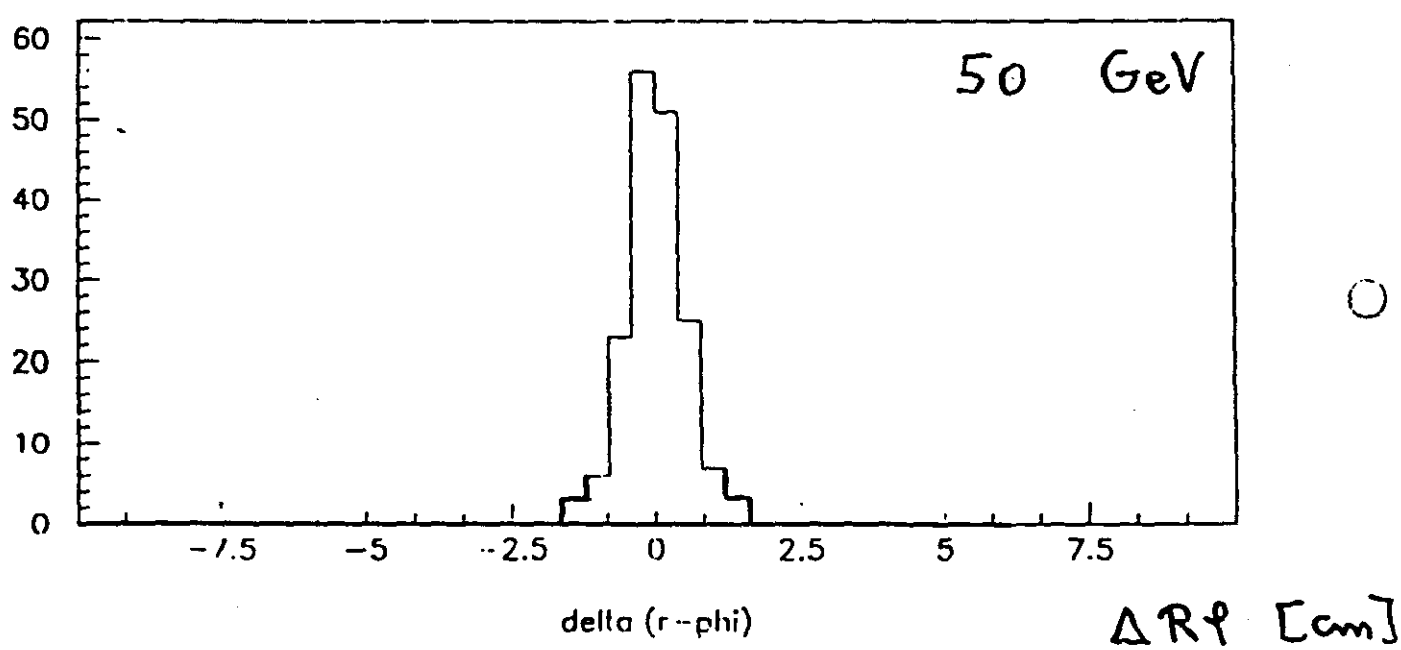
50 GeV
60
50
40
30
20
10
0
−7.5
−5
−2.5
0
2.5
5
7.5
delta (r−phi)
ΔRφ [cm]

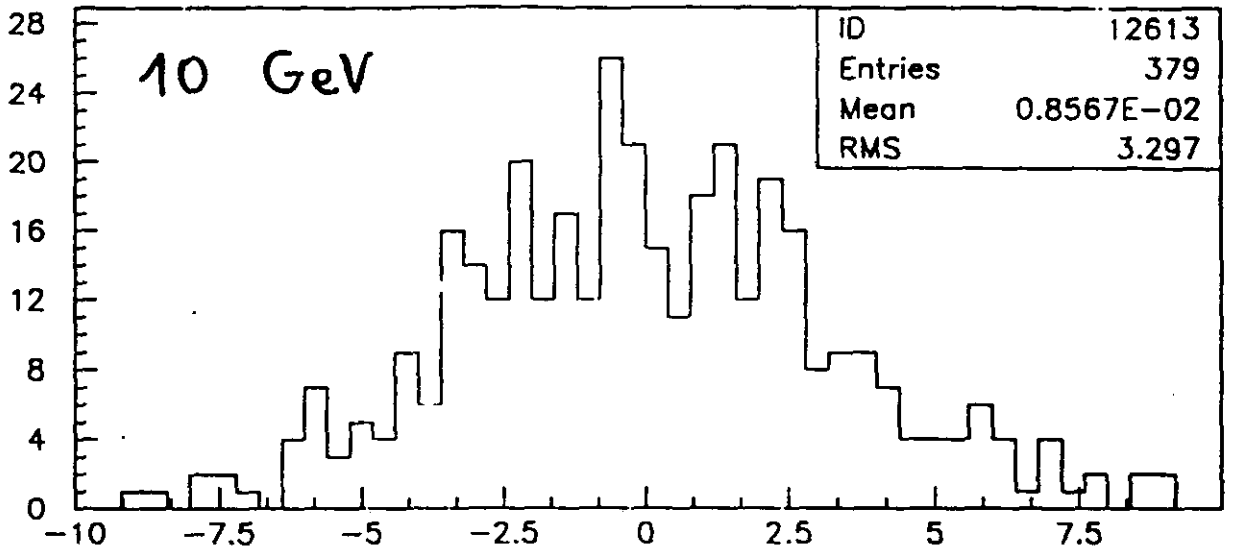

delta (r−phi) 10 GeV

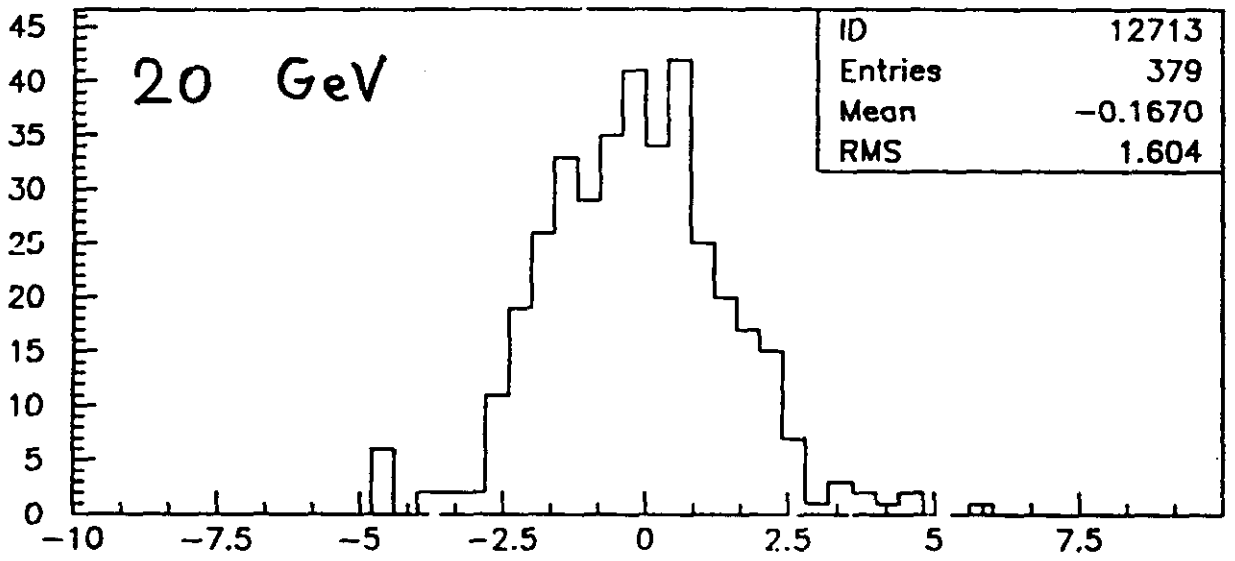

delta (r−phi) 20 GeV

⇒ • use cut of $\Delta R\phi = \pm 10$ cm to select associations (muon hits)

• high efficiency for high-P_T muons ($P_T > 10$ GeV)

• study rejection against punchthrough

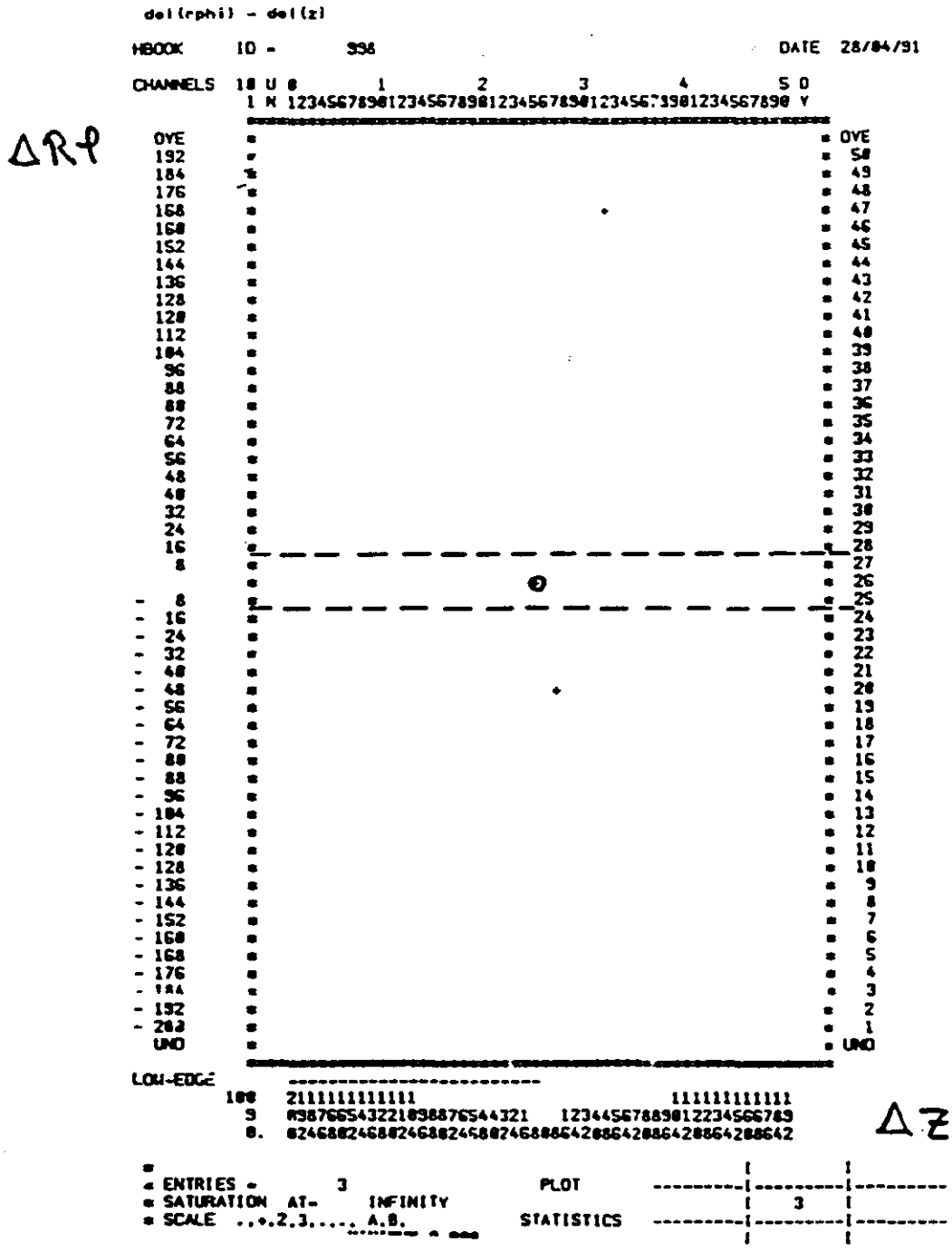

Δφ - cut is very effective in rejecting punchtrough from isolated hadrons / muons

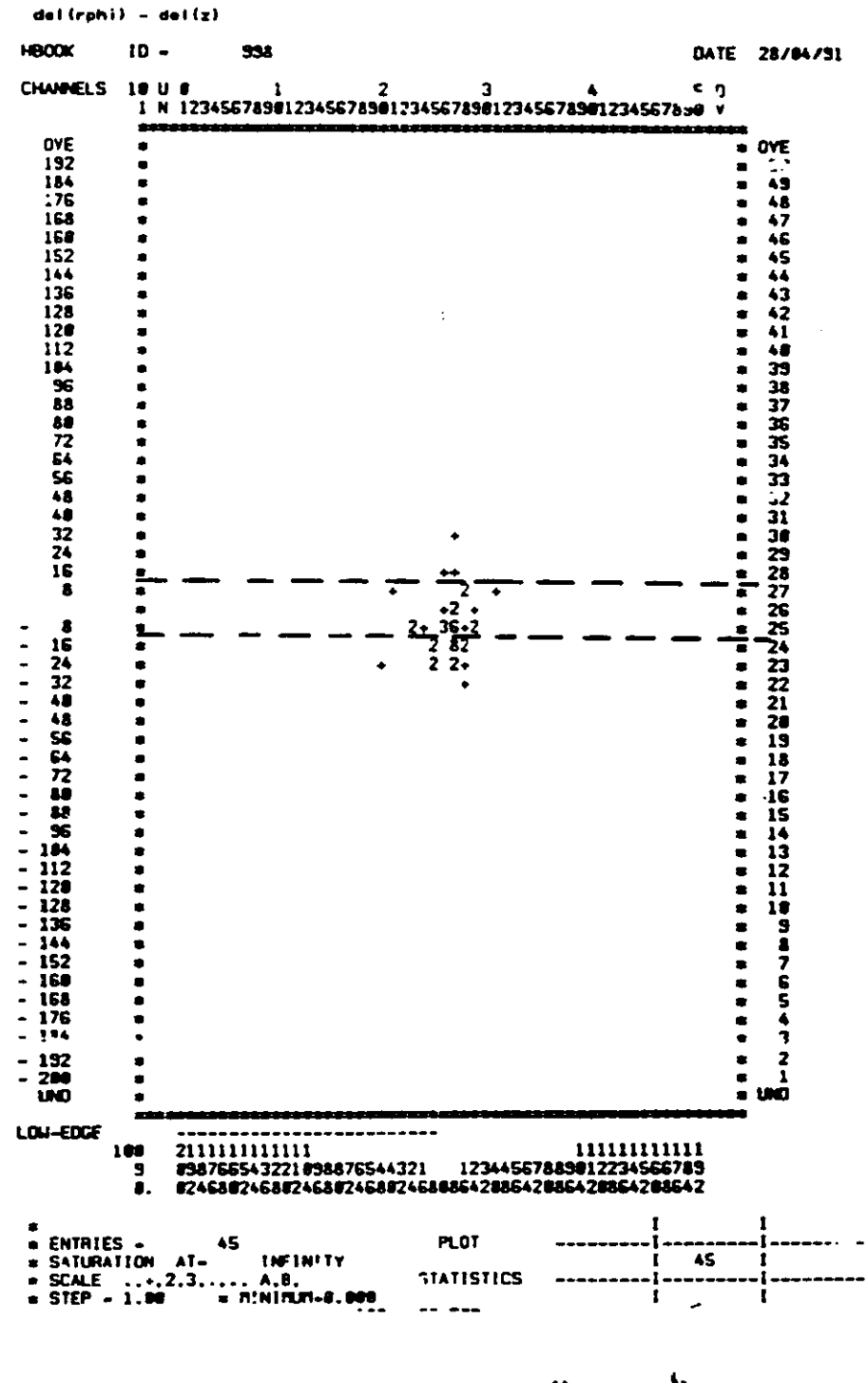

hopeless against "jet"-punchthrough!

Results:

for a cut at $R \cdot \Delta\phi = 10$ cm ambiguities remain for:

~ 10 %	of the events	$\lambda_{abs} = 7.$
~ 2.5 %		$\lambda_{abs} = 10.$
<1 %		$\lambda_{abs} = 12.$

In those events high-P_T muons can be faked by a superposition of

- a low-P_T muon $\oplus$
- hadronic punchthrough

$\Longrightarrow$ increased trigger rate

These configurations can be rejected by using measurements inside the toroids.

additional "clean" muon station at $\lambda_{abs} = 12.$

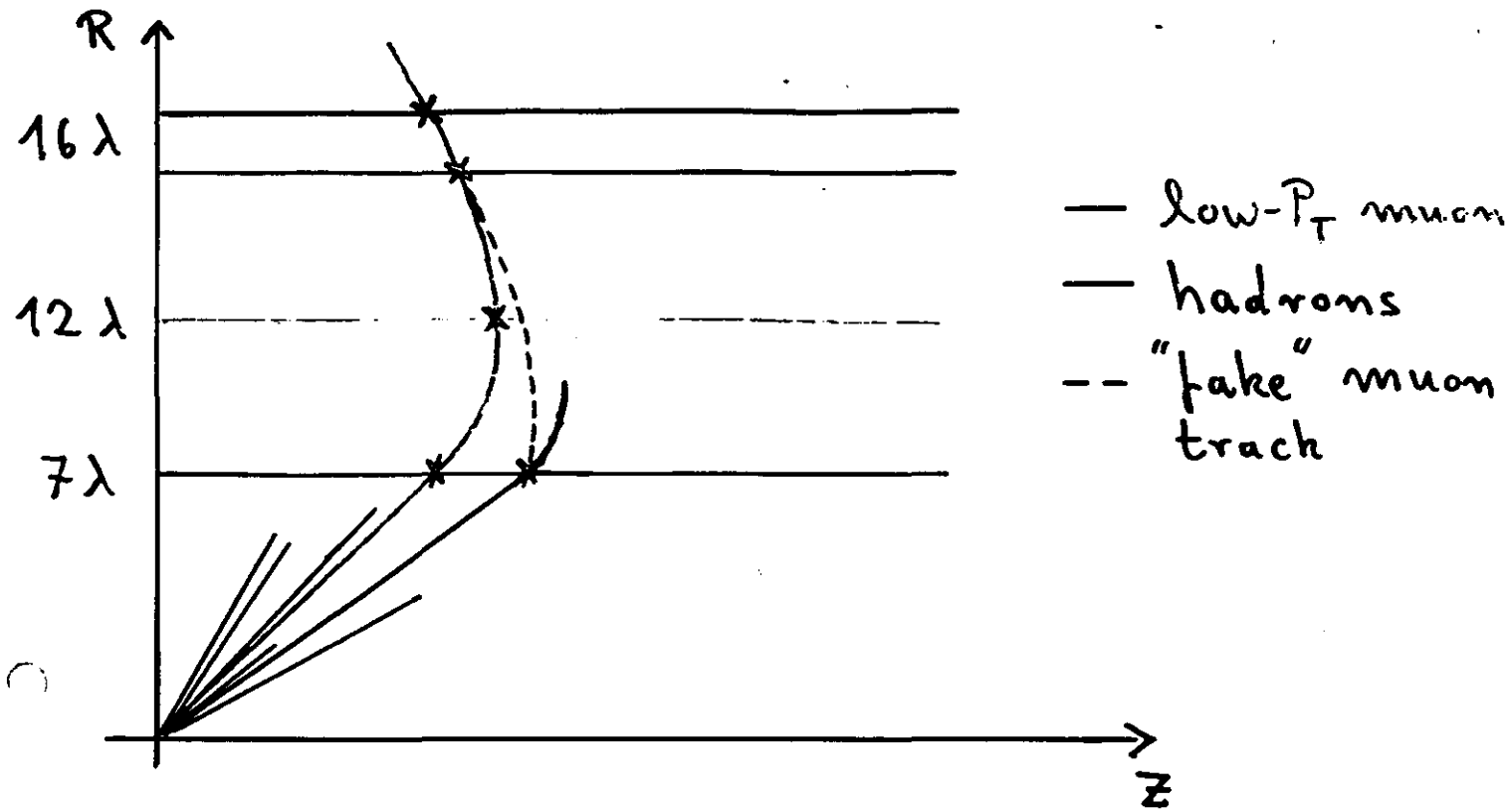

- add. muon station in iron toroid can be used to obtain momentum measurement

$\Rightarrow$ ambiguities in inner chambers can be resolved

Effect of energy loss in calorimeter / iron toroid

efficiencies to get muon hits in various planes

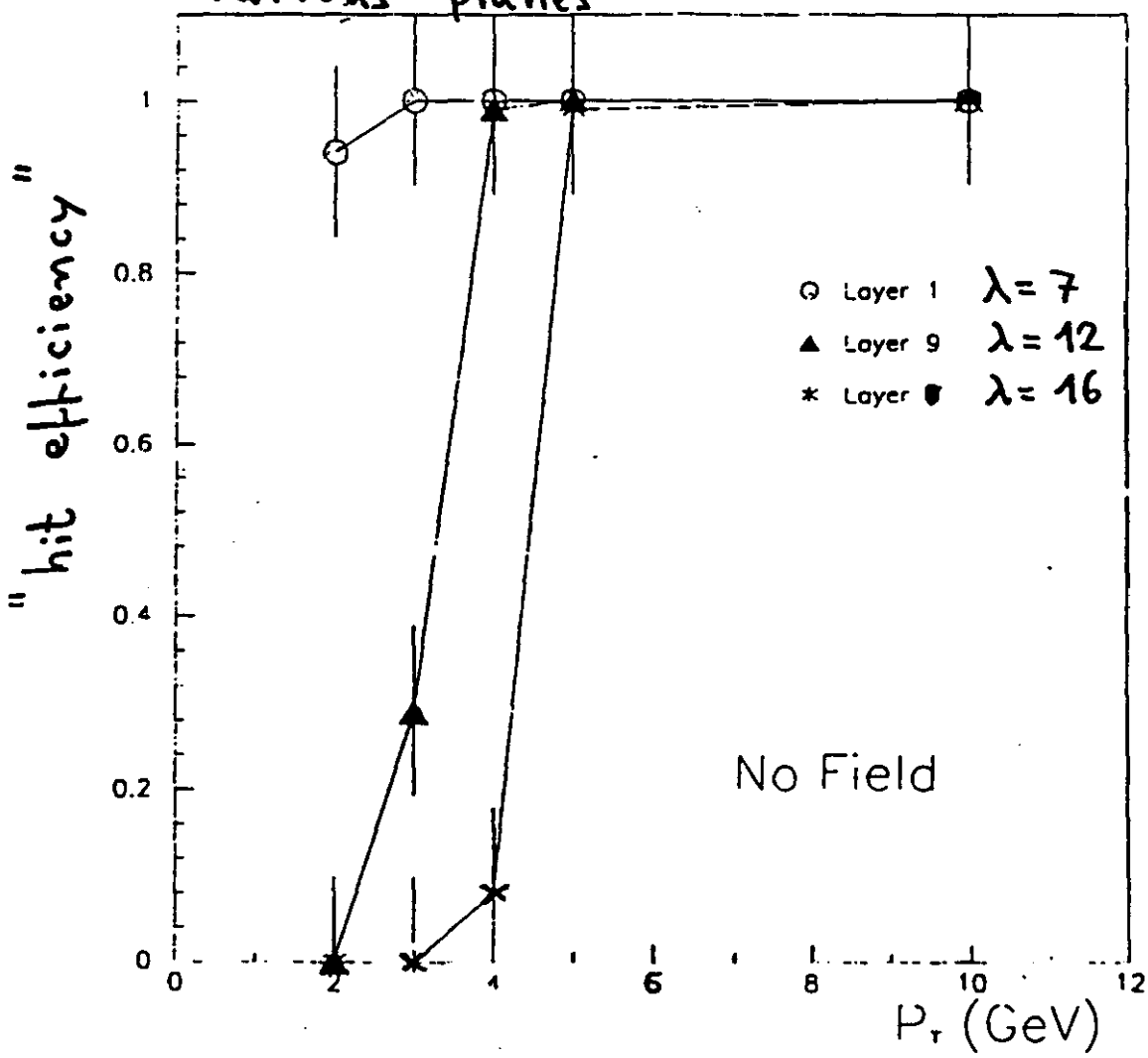

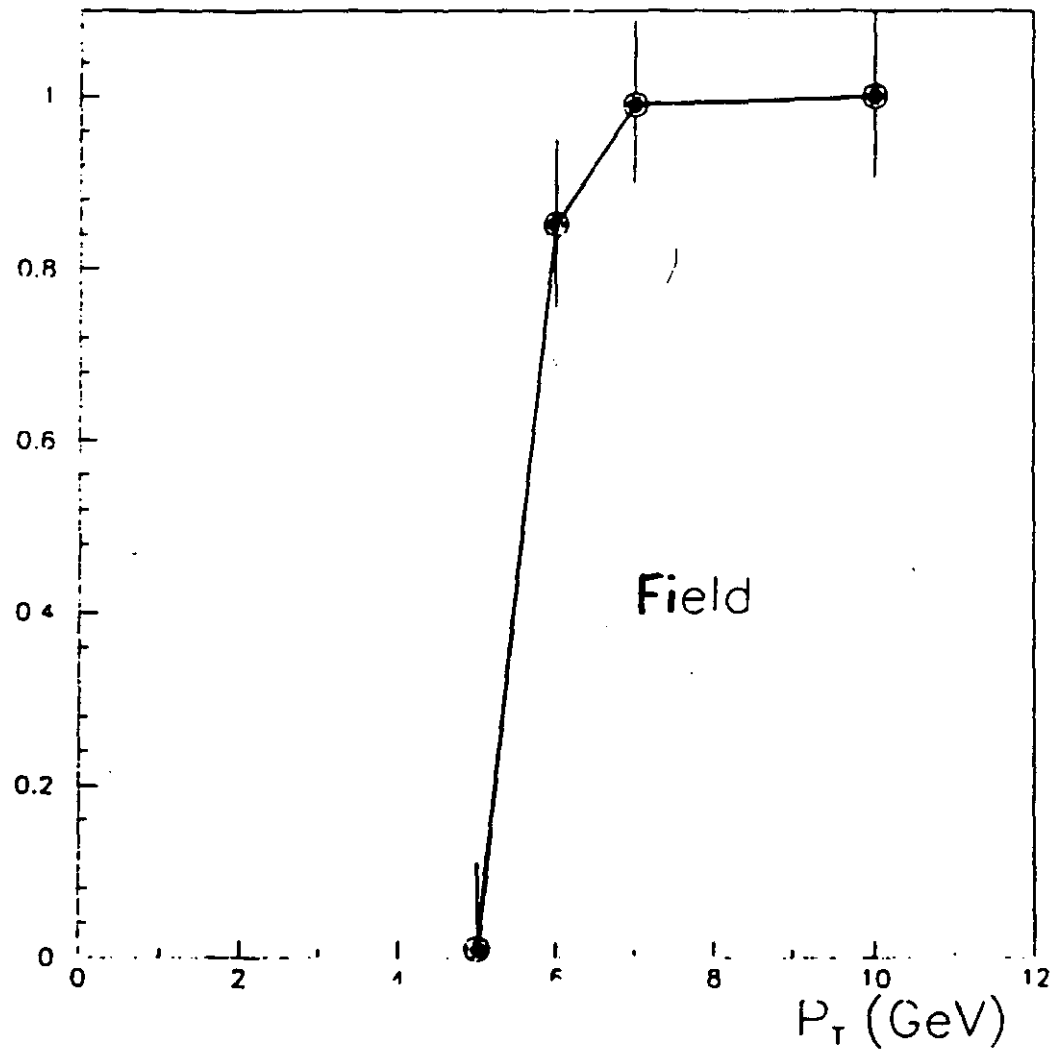

O

$\Rightarrow$ implicit cutoff $P_T^{\mu} \sim 5$ GeV

Summary:

- for jets with $E > 100$ GeV the punchthrough probabilities are found to be:

$P \simeq 0.30$	for 7λ	30 % muon
$P \simeq 0.04$	for 16λ	100 % muon

- punchthrough can be rejected by $\Delta\varphi$ cut; leaves a confusion problem at the level of

~ 10 %	after 7λ	
~ 2.5 %	10λ	
< 1 %	12λ	(no problem)

- the idea of a splitted hadron calorimeter (instr. iron toroid) can work

however: - additional muon station in the toroid is desirable (trigger level)

7/16/91

HOWARD A. GORDON

DEPTH REQUIREMENTS IN SSC CALORIMETERS

The FNAL SDC Simulation Group
(D. Green, A. Beretvas, K. Denisenko,
N. Denisenko J. Marraffino, A. Para, W. Wu)
Fermilab

1. Introduction

The depth requirements for a calorimeter to be used at the SSC are herein explored. Obviously, this parameter is a crucial cost driving element as it defines the size of the muon system, and the materials cost of the calorimeter itself. For this reason, it is imperative to make the calorimeter depth as shallow as possible. Balancing this tendency, the depth must be of a sufficient thickness so as not to compromise a variety of Physics issues. Among those topics are jet energy resolution, the size of the cross section for missing transverse momentum, and the filtering of hadrons before they enter the muon system.

2. Longitudinal Leakage in Calorimeters

The first task to be accomplished is to collect data on longitudinal leakage and leakage fluctuations in calorimeters. This data could then be parametrized and the parameterization used in a Monte Carlo program. It was thought to be important to use an ensemble of data sets since they would differ in energy range, beam tagging, transverse containment, longitudinal containment, and perhaps other systematic factors.

It is also true that in extrapolating to the SSC one must go beyond the region of validity of the data. A variety of functional fits allows one some idea of the systematic errors in this case.

2.1 CITF Model

As a first step, the data from the CITF collaboration[1] are parameterized so as to make a model to extrapolate to all energies. Some of the data are shown in Fig. 1. The approximation is made that the fluctuation in the contained energy fraction f, scaling as $\sqrt{f}$, causes a degradation in energy resolution, r =

$dE(f)/dE(1)$, which is energy independent. It is further assumed that the depth of absorber needed for a containment fraction f scales logarithmically with the incident energy E, see Fig. 1b. This assumption is obvious, given the general properties of hadronic showers.[2] The parameterization given below, Eq. 1, is shown as dashed curves in Fig. 1. The energy, E, is in GeV units.

$$\begin{aligned} (1 - 1/r) &= a\sqrt{1-f} \\ D &= D_o \exp(-b\sqrt{1-f}) \\ D_o &= c\ (1 + d\ln E). \end{aligned} \tag{1}$$

The parameters are, a = 0.9, b = 3.2, d = 0.43, and c = 3.51 absorption lengths in steel. Note that in what follows, an absorption length is defined to be 16.76 cm of steel. This form provides a reasonable representation of the data given in Fig. 1. Shown in Fig. 2 is the value of r as a function of depth at fixed energy. Again the parameterization given in Eq. 1 works fairly well. Other data sets have been checked against this formulation. A data set spanning the same energy range is well represented by the f = 0.95 curve analogous to those data shown in Fig. 1b.[3] Similarly, the curve analogous to Fig. 2 is well represented at lower energies.[4] However, as a note of caution, some data[5] for r as a function of E are not well matched to Eq. 1, at least at energies above 100 GeV.

2.2 WA1 Model

The form given above will be used in all the work which follows. It is convenient for hand calculations and for incorporation into Monte Carlo simulations. Note, however, that this formulation represents only the Gaussian part of the error. There is a long asymmetric tail which has not been parameterized. In order to answer this objection to the model and to obtain an ensemble of data sets a second form was also studied. Having several forms allows one to check that the conclusions are stable under variations of the input assumptions. This second model uses an averaged shower shape.[6]

$$dE = c_1\ fo\ t^{a-1}e^{-bt}dt + c_2(1-fo)D^{a-1}e^{-gD}dD. \tag{2}$$

The energy has an electromagnetic, (fo), and an hadronic, (1 - fo), component. The depth is in radiation length, t, units and absorption length, D = λ/λ_0, units. The normalization is, $c_1 = Eb^a/\Gamma(a)$ and $c_2 = Eg^a/\Gamma(a)$.

Assuming that the electromagnetic energy is rapidly absorbed, the hadronic energy fraction leakage from a depth v = gD, $\Delta E/E$, and the corresponding energy error (using an asymptotic expansion), dE/E, due to fluctuations in electromagnetic fraction, dfo, and conversion point, dD, is,

$$\Delta E/E = -(1\text{-fo})\ \Gamma(a,v)/\Gamma(a)$$
$$dE/E \sim (\Delta E/E)\ (1/[1\text{-fo}])\ dfo\ \Theta\ [-1 + (a-1)/v]\ dD. \qquad (3)$$

In Eq. 3 $\Gamma(a,v)$ is the incomplete gamma function and only the first term in an asymptotic expansion has been retained in estimation the error. Using the parameters a, b, g, and fo given in Ref. 6, this form was checked against the form given in Eq. 1a, i.e. 15 f = $\Delta E/E$? The agreement is quite good. The advantage of this second scheme is that the fluctuations in the hadron conversion point, dD, and in the electromagnetic fraction, dfo, will lead to an asymmetric distribution in $\Delta E/E$ and hence to a tail in the resolution dE due to the fluctuations in ΔE. In Eq. 3 only the Gaussian error is quoted.

2.3 CDHS Model

A third technique uses the data on resolution due to leakage given by the CDHS group.[7] A reasonable representation of the data, after deconvoluting the calorimeter resolution itself, is

$$(dE/E) = 1.6\ e^{-(D/DEFF)}$$
$$D_{EFF} = 0.93\ (1 + 0.49\ \ln E). \qquad (4)$$

Thus, at any depth D, for any energy E, one can find the effective interaction length D_{EFF}, and then the leakage contribution to the energy resolution.

For example, at 1.0 TeV, for a depth, D, of 10, D_{EFF} = 4.08 and (dE/E) due to leakage is 14%. By comparison, using Eq. 1, the first method yields D_o = 13.94. Since the first two methods have depths referred to the interaction

point (Eq. 1, Eq. 2), while the third method refers to the physical calorimeter depth, roughly 1 absorption length should be removed in comparing Eq. 1 to Eq. 4. Thus, D = 9 in Eq. 1, the containment factor f is 0.98, and r = 1.14. Since r refers to the ratio of resolution with respect to $dE(1) \equiv 1.1/\sqrt{E} \oplus 0.03 = 0.046$, the deconvoluted leakage error is (dE/E) 2.5%. At first glance, these two formulations do not seem to be compatible.

In fact, the discrepancy is only apparent. The CDHS fit uses rms for a distribution which is distinctly not a Gaussian. We have compared the data of Sections 2.3 and 2.4 analyzed in comparable ways and convinced ourselves that no contradiction exists. That being the case, we drop reference to the CDHS model in what follows since we do not have available a convenient Gaussian fit to be parametrized.

2.4 Lab E Model

In order to improve the energy range and containment properties available in the models, Lab E test beam data was used.[8] This data spans the range 15 to 450 GeV, which we will see is a range almost sufficient for the maximum transverse energy jet accessible at the SSC. The energy seen upstream of a given depth was fit to a Gaussian, and the width was characterized as in Eq. 4. Since the algorithm was different, compared to the CDHS RMs calculation, the values were, therefore, rather different. The parameterization was, $dE/E = 0.5 \exp(-D/D_{EFF})$ with $D_{EFF} = 0.88\ (1 + 0.35 \ln E)$. The contained energy fraction, f, was found to be well represented by the form given in Eq. 1. The values of the parameters for the Lab E data, b = 2.4, c = 5.5, and d = 0.19 result in values of D and D_0 which are compatible with those of the CITF model over the range of energies spanned by the data.

These three models were used in all subsequent work. The spread among them is an indication of the "systematic error" to be found among the existing published data on depth and energy resolution in hadron calorimeters.

3. Dijets and Depth Requirements

One possible physics topic which might drive the design of an SSC calorimeter is the measurement of dijet masses. The question to be answered is;

what is the highest possible dijet mass which can be measured at SSC design luminosity? From the answer follows the highest jet energy which must be well measured.

3.1 Maximum Accessible Mass

The question of QCD jets has been addressed many times in the context of the SSC.[9] Curves are given in Ref. 9. A rough parameterization is needed to extrapolate from these curves to the cases of interest. The simple form[10] shown below has been adopted to do this extrapolation:

$$d\sigma/dM = g(1 - M/\sqrt{s})^{12}/M^3. \tag{5}$$

The constant g is roughly 1.2 mb $(GeV)^2$, M is the dijet mass, and s is the square of the CM energy. This form is an adequate representation of the exact calculation[9] for dijet transverse momenta, $P_t \sim M/2$, in the range 2 to 4 TeV. Using this form one finds that at design luminosity, in a one year, = 10^7 sec, $\pm 1\sigma$, there are ~ 150 events in a ±2% mass bin for a 10 TeV dijet mass (P_t = 5.0 TeV). Hence, one runs out of statistics at a dijet mass around 10 TeV in that the statistical error is 8% in a bin set by the 2% resolution.

3.2 Fragmentation

The next task is to make the connection between jet energy containment and the energy containment of individual hadrons. For the purposes of hand estimates and building up intuition, a simple form[11] of the jet fragmentation function, D(z), is adopted. This function specifies the probability that a jet of momentum P fragments into a hadron of momentum k; z is the momentum fraction carried off by the hadron:

$$\begin{aligned} k_i &= z_i P, \ \Sigma\, z_i = 1 \\ D(z) &= [(h+1)\ (1-z)^h]/z \\ \langle n \rangle &= (h+1)\ [\ln(1/z_0) - (h-h[h-1]/4+\ldots+1/h)] \\ z_0 &= m_\pi/P. \end{aligned} \tag{6}$$

This form is a reasonable parameterization of the existing e^+e^- data[12] for the charged multiplicity if one assumes that the total multiplicity is a factor 3/2 higher and if h is ~ 6.0. This form also provides a good representation of the CDF data.[13] The shape of D(z) as a function of z is given in Fig. 3. The dashed and dashed-dotted curves are the approximate forms, D(z) = 7/z and D(z) = 125 exp (-13z) respectively. Since the integral of D(z) is the multiplicity, Eq. 6, one can find the average location of particles in the fragmentation chain. The locations are also indicated in Fig. 3. For example, the "leading" fragment exists between z = 1.0 and z = 0.174. Although the fluctuations are enormous, one can assign a mean z location for the leading fragment.

$$\begin{aligned} \langle z_1 \rangle &\sim 0.23 \\ k_t &\sim \langle z_1 \rangle P_t. \end{aligned} \tag{7}$$

This point, $\langle z_1 \rangle$, is defined to be the point where the mean multiplicity starting from the end point of z at z = 1 is = 0.5. Hence, it is the mean location of the "leading" fragment.

The estimate for $\langle z_1 \rangle$ allows us to estimate the angular scaling of an SSC detector immediately. A glance at Eq. 1 shows that, for a given containment fraction f, the required depth ratio depends only on energy and not f. Picking a fixed P_t = 5.0 TeV, set by the maximum accessible dijet mass, $k_t = \langle z_1 \rangle P_t$. The dependence as a function of rapidity, y, is quite weak (logarithmic). The approximate relation, $y = -\ln [\tan (\theta/2)]$ has been assumed:

$$D(y)/D(0) = (1 + d \ln [k_t/\sin \theta])/(1 + d \ln[k_t]). \tag{8}$$

The ratio is displayed in Fig. 4. Clearly there is only a minor thickness increase in the calorimetry as the result of increasing y from y = 0 to y = 3. Note that this result is independent of which value of f is ultimately deemed necessary.

3.3 Estimate, f = 0.99

As a first guesstimate, one can ask for f = 0.99 for a jet of transverse momentum P_t. As seen in Fig. 1a, this requirement would insure that the dijet

mass would be well measured on the scale of the calorimeter energy error, which at high masses would be a few percent. Individual particles in the jet would be measured to 4% error or less due to leakage. Using $\langle z_1 \rangle$ and taking as an upper limit M = 10 TeV, one gets the curve of 99% containment depth as a function of P_t which is shown in Fig. 5. This Figure is made by assuming that the f = 0.99 criterion applies to the leading fragment. Using this criterion, one gets a very crude estimate that ~ 10 to 11 absorption lengths are required.

3.4 Mass Errors Due to Calorimeter Resolution

There are many sources of mass error. For "low" masses, 0.1 TeV and 1.0 TeV, the mass resolution is not determined by the energy measurement but by fluctuations in the jet fragmentation and in the underlying event.[14] As discussed below, at high enough mass, this will not be the case. In the equation which follows it is assumed that the vector sum of momenta is roughly the scaler sum (Eq. 6). One further assumes that, as in low P_t jets, the mass resolution is dominated by momentum errors. Finally, one assumes that the calorimeter granularity is sufficiently fine that individual hadrons are independently measured. If the calorimeter energy resolution, dE, determines the mass resolution, dM, then;

$$\begin{aligned} dE/E &= s/\sqrt{E} \oplus t \\ dM/M &\sim s/\sqrt{M} \oplus t\langle z_1 \rangle/\sqrt{2}. \end{aligned} \tag{9}$$

The second formula follows from the first using Eq. 6 and propagating the errors. It is assumed that the sum of the sqaures of z_i can be ~~see~~ approximated by the leading term z_1^2.

For example, a typical hadronic calorimeter resolution might be s = 0.5, t = 0.03. These values of the parameters have been used in the Monte Carlo studies described below. This single particle resolution leads to a dijet mass resolution as given in Eq. 9. The resolution, dM/M, as a function of calorimeter depth, at fixed mass = 10 TeV, is shown in Fig. 6. In this figure, the value of r in Eq. 1 was assumed to refer to the quoted resolution of Ref. 1 folded in quadrature with a leakage term, as discussed above.

Clearly, the constraints on depth are rather soft, given the logarithmic dependence. Note that $D_0 \sim 14.1$ absorption lengths for the leading particle fragment. Note also that dM/M is ~ 1% at great depths which is very small on the scale of "low" mass errors.[14] Obviously, a detailed Monte Carlo is required to quantify these estimates and to elucidate the size of the fluctuations due to fragmentation, the underlying event, and the existence of heavy flavors in the jet. For this purpose, the package SSCSIM, a FNAL supported product,[15] was used.

3.5 Monte Carlo Results

There are several effects in addition to measurement error which are important to dijet mass resolution. The underlying event contains a fluctuating amount of transverse energy which may fall into a "cone" containing the jet. With a density of 8 particles per inelastic event per unit of rapidity, where each particle contains roughly 0.6 GeV of k_t, one has 4.8 GeV per unit of y. This means roughly 1.1 GeV within a cone of radius, $R = \sqrt{(\Delta y)^2 + (\Delta\phi)^2} = 0.6$ for "minbias" events. Hard scattering events have a higher density; the SSCSIM result is that there is ~ 5.0 GeV within a cone of radius R = 0.6 for 10 TeV dijet events.

The jet contains many soft fragments as shown in Fig. 3. For a cone of radius 0.7, and $k_t \sim 0.6$ GeV, all fragments with momenta less than $k_{min} = 0.86$ GeV will fall outside the cone radius and be lost. Given the form of D(z), this means that ~ $(h+1)k_{min} \sim 6.0$ GeV falls outside the search cone. One can optimize the search cone; but a smaller size loses more fragments, while a larger size adds more extraneous underlying event energy. Thus, there is an optimal cone. In this work the magnetic field effects are not studied. Presumably, they would act so as to increase the fluctuations.

Fluctuations set a scale $P_{fluc} \sim 5$ GeV for fluctuations into or out of that cone as we have seen above. One expects, very crudely, that this error contributes to dM/M a term to be added in quadrature to Eq. 9.

$$(dM/M)_{fluc} = \sqrt{2}\, P_{fluc}/M. \tag{10}$$

A fixed value of P_{fluc} means that at high masses fluctuations are less important and that the "intrinsic" calorimeter resolution may begin to be the

dominant term in the dijet mass resolution. The scale for P_{fluc} to cause a 1% error, dM/M, is estimated to be M = 0.7 TeV in the case that P_{fluc} is caused by fluctuations due to fragmentation and the underlying event.

First one needs to optimize the cone radius defining the jet. In Fig. 7 is shown the standard deviation of the reconstructed to generated dijet mass ratio, δ, as a function of cone radius. If only jet fragments are used, the error decreases smoothly till it reaches a value ~ 0.01 at R ~ 1.0. When the underlying event, and its fluctuations, are added the minimum error occurs at R ~ 0.6. The error is then increased to ~ 2%. This simple clustering algorithm has been checked against a more complete approach.[14] The results given here are stable with respect to the treatment of clustering. Note that in order to contribute to dM/M by 1.4% the scale of momentum fluctuations must be ~ 100 GeV. This size for P_{fluc} is well above the ~ 5 GeV scale which was previously estimated. The origin of this scale for P_{fluc} is "hard" non-colinear gluon radiation and neutrino losses from heavy flavors as will be discussed below in Section 4.

A histogram of the ratio of reconstructed to generated dijet mass is shown in Fig. 8. The bin width is 1%, and the error is 1.3% for the case of R = 0.6 with only dijet fragments used. Note the long "radiative" tail which is due to gluon radiation and neutrinos, as will be discussed later. We assume that this "radiative tail" is soft enough That it cannot be tagged amidst the general debris of the dijet event.

A histogram of the energy of the leading hadronic fragment is given in Fig. 9. Note that the mean $\langle z_1 \rangle$ is 0.26 with a standard deviation of 0.14. These results are consistent with the expectations drawn from consideration of Fig 3.

The result for the mass error as a function of calorimeter depth is shown in Fig. 10. By comparison with Fig. 6 one can see that a purely resolution dominated (Fig. 6) calorimeter with a mass error of ~ 0.7% shifts to a mass error of ~ 2% (resolution and fluctuations) in the case of a very thick calorimeter. The shift in asymptotic resolution means that 10 absorption lengths is more than adequate. The uncertainty is roughly I 1 unit due to the spread in the data sets. This is an estimate of the extrapolation and systematic errors.

4. Missing P_t and Calorimeter Depth

A signal for the existence of high transverse momentum neutrinos in an event is a large missing transverse momentum. Clearly, this signal can be mimicked by a lack of "hermeticity" caused by holes in coverage at small angles, cracks due to leads or supports, or "leakage" due to inadequate depth of calorimetry. Thus an SSC calorimeter should be deep enough that leakage should not dominate the real sources of neutrinos. A limit to the required depth is provided by the evolution of a gluon jet into a heavy quark pair. The semileptonic decay of either quark provides a source of neutrinos which will "leak" out of the calorimeter undetected. It is in comparison to the scale of this leakage that the scale of calorimeter depth should be evaluated.

4.1 $J \to Q\overline{Q} \to ql\nu$

First, what is the physics source of neutrinos? Obviously there are many. What concerns us here are sources topologically similar to those caused by calorimeter leakage. A gluon jet has a finite probability to vacuum fluctuate into a heavy quark antiquark, $Q\overline{Q}$, pair which then semielectronically decays in the core of a jet.[16] This process acts as an irreducible physics background source of neutrinos in the vicinity of jets. It is assumed that a muonic decay is tagged ($l = \mu$) but that in an electronic decay ($l = e$) the e will be lost in the core of the jet. A rough estimate of the probability is given in Eq. 11. The strong coupling "constant" is taken, for purposes of hand estimates, to be = 0.1. This value is not unreasonable given the mass scales involved and the slow, logarithmic "running" of α_s. The value for the semiloptonic branching ~~θ~~/ratio, $B(Q \to gl\nu)$ is taken to be 20%.

$$\alpha_s/\pi \ \ln(2M_Q/P_t) \ B(Q \to ql\nu)$$
$$(P_t)_{miss} \sim P_t/6. \tag{11}$$

The cross section for jets, Eq. 5 in arbitrary units, and for the neutrinos, Eq. 11, is shown in Fig. 11. At a fixed P_t, the missing P_t due to neutrinos is down by a factor ~ 10^{-5} with respect to the jet cross section. This factor has 2 components. First, as shown as a vertical dashed line, the probability for $g \to Q\overline{Q}$, $Q \to q\,\mu\,\nu$ is about 1%. Second, the reduced P_t of the neutrino with

respect to the gluon, coupled with the steep gluon P_t spectrum, reduces the cross section by another factor of ~ 1000 at fixed P_t. This six-fold reduction going from P_t to $\not{P}_t$ is shown as the horizontal dashed line in Fig. 11.

4.2 Jet Leakage

In comparison, a calorimeter of finite depth will leak some fraction, 1-f, of its energy out the back. This leakage will cause one to miss some of the energy.

$$\not{P}_t = (P_t)_{miss} \sim (1\text{-}f)\ P_t. \tag{12}$$

The resulting spectrum for 95% containment is shown in Fig. 11. One obtains it by using the jet cross section and derating P_t by a factor of 20 to get $\not{P}_t$ due to incomplete containment. Clearly, this loss of energy leads to a missing P_t cross section quite comparable to the irreducible rate due to the decays of heavy flavors in jets.

The design criterion is to make the calorimetric leakage < the physics leakage at all accessible (luminosity dependent) dijet masses. An estimate for 10 TeV dijet mass, $P_t \sim 5.0$ TeV, $k_t \sim \langle z_1 \rangle P_t$, is that ~ 7 ± 1 absorption lengths are needed. Thus the limit on depth placed by the dijet mass resolution appears to be more stringent than that imposed by leakage. Note that this limit has been estimated using only the leading QCD hard $Q\bar{Q}$ fragmentation. It is also true that the response function has been assumed to be a Gaussian characterized by a standard deviation. There are, however, tails which, if not removed, lead to missing transverse momentum which may dominate over real physical processes.[17] We defer discussion of the tails until longitudinal segmentation is discussed.

4.3 Leakage and Calorimeter Resolution

It is interesting to note that the evolution of gluons into heavy flavor fragments places an upper limit on the accuracy of any calorimeter. Thus, one must note that the "leakage' of a jet limits the ultimate "constant term" which one can attain for jets. The probability for a dijet to produce a neutrino can be roughly estimated, in perturbative QCD, from leading fragmentation to be:

$$P\ (\nu) \sim (4\ \alpha_s/\pi)\ \ln\ (2M_Q/P_t)\ B(Q \to q l \nu). \tag{13}$$

For a 10 TeV dijet, P_t = 5.0 TeV, this is ~ 8% for b or c decays into electrons and neutrinos. When that decay occurs, the jet loses ~ 1/6 of its total energy on average or, roughly, 5000 GeV (0.08)/6 = 66 GeV is lost per jet or 1.3%. This loss leads to an error on the jet energy which places a lower limit on the accuracy of energy measurement. The long tail and asymmetric broadening of the mass peak in Fig. 8 is partially due to the presence of neutrinos in the jets.

4.4 Monte Carlo Results

The Monte Carlo program with dijets was used to study the neutrino leakage. A plot of the ratio of the mean leakage energy to the mean neutrino energy for 10 TeV dijets is shown in Fig. 12 as a function of calorimeter depth. At ~ 12 absorption lengths the leakage energy falls below the "intrinsic" leakage due to neutrinos from heavy flavor decays. This result is more restrictive than that which is inferred from Fig. 11, which reflects the effect of an entire chain of fragmentation fluctuations to $Q\bar{Q}$ within the jet. Note that Fig. 11 assumes only "leading" fluctuations.

This cascade effect is displayed in Fig. 13 where the distribution of the fraction of the jet energy possessed by the neutrino is plotted. Most neutrinos are quite soft; the mean energy fraction for all events is 1.6% with a spread of ± 1.4%. However, only 18% of the events have a neutrino, and for these events they carry away approximately 5% of the energy. Clearly, the neutrino leakage effect contributes substantially to the resolution of a thick calorimeter for very high mass dijets.

Assume that the mass error is due to the effects of resolution, fluctuations due to fragmentation and underlying event, neutrino leakage, and depth leakage folded in quadrature. For depths above 10 absorption lengths, the depth leakage is not important. The fluctuation term, Eq. 10, falls as 1/M, and is small for large masses. The effects of stochastic contributions to the energy resolution fall as $1/\sqrt{M}$, Eq. 9, while the neutrino leakage rises as ln(M), Eq. 13. Finally, the effects of non-colinear gluon emission dominate at high masses.[18] This latter effect has a very soft (logarithmic) decrease with mass. At 10 TeV, the gluon radiation fluctuation is most important, followed by neutrinos, while the energy measurement errors are only third most important.

5. Depth Required for Muon Identification

The calorimeter also serves as a preliminary filter for the muon identification system. Clearly, one should examine whether the total depth of the calorimeter is also sufficient for this task. The total depth of the muon system is set by global considerations for muon identification.[19] The calorimeter depth should be sufficient to insure that the rate from hadronic punchthrough is less than the irreducible rate from pion decays in the tracking volume. In order to explore this criterion, the source of pions was taken from CDF data for transverse momenta, P_t, below 10 GeV.[20] The cross section was scaled up to give a rapidity space density of 8 particles per unit of y. The resulting rate, at SSC design luminosity, at $y = 0$, for pion decays into muons, with a 2m decay radius, is shown as a function of P_t in Fig. 14a. Clearly, after 10 absorption lengths, the rate integrating over all P_t is roughly 10^5 Hz per unit of rapidity.

The pions from minbias events also occasionally punchthrough the calorimeter into the region occupied by the inner muon detectors. The rate of punchthrough is estimated using a parameterization of the WA1 data.[21] The rates for punchthrough are given in Fig. 14b, along with the pion decay rate. Clearly, real muons dominate over punchthroughs for a calorimeter thickness > 7 absorption lengths. Since this thickness is less than that which has already been considered on the basis of resolution and leakage studies, one concludes that no more stringent requirement appears to be imposed by considerations of the muon system.

6. Longitudinal Segmentation and Depth

6.1 Energy Asymmetry and Resolution

Until now the calorimeter has been considered to be a unitary object. However, at some point the fact that the cost of materials scales as D^3 means that depth segmentation may become an attractive alternative to adding more depth. In the context of the WA1 model (Section 2.2), dividing a $D = 10$ calorimeter into $D1 = 6$ and $D2 = 4$ segments allows one to measure the interaction point and therefore estimate and/or tag the leakage.

The interaction point is determined, on average, by the energy asymmetry δ which is correlated with the energy leakage fraction γ:

$$\begin{aligned} \delta &= (E_1 - E_2)/(E_1 + E_2) \\ \gamma &= EL/E. \end{aligned} \tag{15}$$

A plot of the numerical results for the mean values of δ and γ at representative energies and interaction points is given in Fig. 15. The form of Eq. 2 was used, but the additional smearing due to the fluctuation in shower shapes, dfo (Eq. 3), was not put in. The relationship is sufficiently well parameterized by the form

$$\begin{aligned} \delta &= 1.0 - \gamma/\gamma_{EFF} \\ 1/\gamma_{EFF} &= 4.2\ (1 - 0.095 \ln E). \end{aligned} \tag{16}$$

Clearly, in the absence of any other fluctuations in the shower, the energy leakage can be corrected for using the depth segmentation. This correction should improve the energy resolution by correcting for the interaction point smearing (see Eq. 3).

The containment and resolution of a D = 10.1 calorimeter longitudinally segmented into D1 = 6.6 and D2 = 3.5 were studied using the Lab E data. Representative data are shown in Fig. 16. In Fig. 16a is shown the distribution of containment fractions, f, for 450 GeV beam incident on the calorimeter. Note the long tail caused by fluctuations in the hadronic shower development. These fluctuations defeat attempts to use the energy asymmetry δ to make the calorimeter thinner while preserving the resolution. It was found that no improvement in the Gaussian part of the resolution could be obtained using information from the two depth segments.

6.2 Back Section Veto and Containment

The non-Gaussian tails in the resolution due to fluctuations can still be reduced. In Fig. 16b, is shown the same distribution except that the cut on Δ, the ratio of D2 energy to total incident energy, $\Delta < 0.18$, was made. Clearly, the long tail is much reduced while preserving the events in the $f \simeq 1$ region with good efficiency. The cut passed ~ 85% of all events. Harder cuts on Δ improved the containment fraction average.

The segmentation studies were then extended to cover different energies and total depths. After some inspection of the events it was decided to keep a D2 = 3.5 depth back segment. The reason for this is that the low f hadronic showers often appear "disconnected" with initial clumps of energy, a gap, and then a second energy clump. The width of these gaps roughly dictates the value of D2.

In Fig. 17a is shown the efficiency for events as a function of Δ. The efficiency falls roughly logarithmically with the cut. At a fixed depth, D, the efficiency falls with energy at fixed Δ as expected since showers penetrate deeper into the calorimeter with increasing energy. At fixed energy the efficiency at fixed Δ falls as the total calorimeter depth is decreased.

The fraction of events, F, with less than 95% containment as a function of Δ is shown in Fig. 17b. At an energy of 450 GeV, using the resolution that has been assumed so far ($dE/E = 0.5/\sqrt{E} \oplus 0.03$) the error is $dE/E = 0.038$ which sets a scale which should be comparable to F. This fraction, F, falls as a power of Δ as one expects since that is the purpose of the Δ cut. It also rises with energy at fixed Δ, as expected. At fixed Δ, F rises as D decreases since a thinner calorimeter will leak more.

Comparing the Figures, one can establish the tradeoffs. First, some longitudinal segmentation cut is needed in order to control the tails lest the real missing transverse momentum signal due to neutrinos be swamped by leaking hadrons.[17] Second, can the calorimeter be made thinner to save costs? As shown above, for $D < 10$, a thinner calorimeter degrades jet energy measurements at the highest accessible jet energies. Third, the fluctuation tail can be controlled with a thinner calorimeter, but at the cost of an inefficiency. For example, if F = 0.05, i.e., 95% containment for 95% of the events, then for 450 GeV, $\Delta = 0.36$ for $D = 10$ with $\epsilon = 1.0$ while $\Delta = 0.14$ for $D = 8.7$ with $\epsilon = 0.5$. Since 450

GeV corresponds to $z \sim 0.09$ for a 10 TeV dijet, which is $< z_1$, one expects that the rare high-mass dijets will be vetoed by the leakage cut on Δ leading to a large inefficiency if $D < 10$.

7. Summary and Conclusions

The requirements of SSC Physics on calorimeter depths were studied. First an ensemble of data sets at energies < 450 GeV were assembled and parametrized. This ensemble, when extrapolated to SSC energies, indicates the range of systematic errors.

The Physics process which was chosen was dijets at the highest accessible (rate limited) mass, M = 10 TeV. The leading fragment in such an event has $z_1 \sim 0.2$ or $k \sim 1$ TeV. Using the parametrizations, one finds that $D(y = 3)/D(y = 0) = 1.2$. Only a 20% increase in thickness is needed as pseudorapidity goes from zero to three.

A Monte Carlo study of the dijet mass resolution indicated $dM/M \sim 2\%$ for $D > 10$. For thinner calorimeters, the Gaussian part of the resolution was increased due to leakage errors. The dijet mass resolution was found to depend mostly on fragmentation fluctuations, which reduced the sensitivity of dM to calorimeter resolution and leakage effects.

Neutrinos from $Q\bar{Q}$ pairs which evolve in the jet begin to become important for dM at the highest masses. Defining the criterion to be that missing P_t due to leakage be less than missing P_t due to neutrinos in jets leads to the requirement $D < 11$.

The calorimeter also removes hadrons as the front filter for the muon system. Defining the criterion to be that the rate behind the calorimeter due to punchthrough (leakage) be less than the rate due to pion decays in a 2 m radius upstream of the calorimeter leads to the requirement $D < 7$.

Longitudinal segmentation was found not to be useful in improving resolutions. However, it is extremely useful in vetoing the long tail in the resolution corresponding to poor containment/large leakages. A cut of $\Delta = 0.18$ effectively removes the non-Gaussian leakage tail for energies < 450 GeV in that the fraction with 95% energy containment is = 97% (450 GeV), > 98% (< 100

GeV), if D = 10. The loss of real events with this cut is < 15% for E < 450 GeV.

In conclusion, given a systematic error spread due to the extrapolation of existing data, a calorimeter with depth D = 10 segmented into D1 = 6.5, D2 = 3.5 will not degrade jet measurements, muon systems, or missing transverse momentum measurements at the SSC.

REFERENCES

[1]F.J. Sciulli, *Calorimeter Workshop*, May 1975, Fermilab.

[2]S. Iwata, DPNU-3-79, February 1979, Nagoya Japan.

[3]M. Holder, Nuc. Inst. Meth. 108, 54 (1978).

[4]K. Rauschnabel, KEK-EXT 3/78-5.

[5]D.L. Cheshire, Nuc. Inst. Meth. 126, 253 (1975).

[6]R.K. Bock, Nuc. Inst. Meth. 186, 533 (1981).

[7]E. Hughes in *International Conference on Calorimetry in High Energy Physics* October 1990, Fermilab.

[8]F.J. Sciulli et al., Unpublished data from hadron test beam exposures of the full sized neutrino detector. The detector dimensions insure negligible transverse or longitudinal leakage in distinction to other test modules. W.K. Sakumoto et al., Nuc. Inst. Meth. A294, 179, (1990).

[9]J.F. Owens et al., *Design and Utilization of the SSC, proceedings of, Snowmass 1984*, 218 (1984).

[10]D. Green, *$P\overline{P}$ Collider Physics*, FNAL-CONF 89/70.

[11]D. Green, *Dijet Spectroscopy at High Luminosity*, FNAL-CONF-90/151.

[12]Review of Particle Properties, Phys. Lett B, 239 1-516 (1990).

[13]R. Plunkett and F. Abe et al., *Jet Dynamics at the Tevatron Collider*, FNAL-Conf-89/261-E, Phys. Rev. Lett. 65, 968 (1990).

[14]W. Wu. SSC-SDC-F60, SSC-SDC-F63 Internal Notes.

[15]A. Beretvas et al., SSCSIM User Guide, SSC-SDC-F31.

[16]R.K. Ellis, *An Introduction to the QCD Parton Model*, FNAL-CONF-88/60-T.

[17]J. Hauptman, M. Pang. SDC Note, (1989).

[18]G. Sterman and S. Weinberg, Phys. Rev. Lett. 39, 1436 (1977).

[19]D. Green and D. Hedin, Nuc. Inst. Meth. A297, 111-120 (1990).

[20]F. Abe et al., Phys. Rev. Lett. 61, 1819 (1988).

[21]D. Green, *In Workshop on Triggering, Data Acquistion, and Off-line Computing For High Energy/High Luminosity Hadron-Hadron Colliders*, FNAL Nov. 11-14, 1985.

FIGURE CAPTIONS

1. Dashed curves refer to the parameterization described in the text. Solid curves refer to a model described in Ref. 1.

   a. Resolution ratio as a function of energy for several energy containment fractions, f.

   b. Distance in steel required for a given energy containment fraction as a function of energy for 3 values of f.

2. Resolution ratio with respect to total thickness at fixed energy, 200 GeV, as a function of calorimeter depth. Dashed curve is a parameterization as described in the text.

3. Fragmentation function D(z) as a function of z. The points are taken from Eq. 6., while the dashed and dashed-dotted curves are approximate forms which are discussed in the text. Also indicated are the z values appropriate to multiplicities 1 through 5.

4. Ratio of depths required at y = 0 and at variable y as a function of y for a 10 TeV dijet mass.

5. Required calorimeter depth, in steel absorption length units, to achieve f = 0.99 as a function of the P_t of the jet.

6. Fractional dijet mass resolution for a 10 TeV dijet mass as a function of calorimeter depth. Note that the resolution at great depths is only that due to energy resolution of the jets; fluctuations in fragmentation and the underlying event have not been included.

7. Standard deviation of the ratio of the reconstructed to generated dijet mass for 10 TeV dijets as a function of containment cone radius R. The points, o, refer to the case where only jet fragments are used. The points, •, refer to the case where all particles in the event are used if they fall within the cone.

8. Histogram of the ratio of reconstructed to generated mass for 10 TeV dijets using a cone of radius R = 0.6. Only jet fragments are used in the calculation.

9. Histogram of the energy of the "leading" hadronic fragment for a 10 TeV dijet. The energy units are GeV.

10. Error on the ratio of reconstructed to generated dijet mass as a function of the depth of the calorimetry for 10 TeV dijets; CITF •, WA1 o, Lab E, □, parametrizations.

11. Cross section (arbitrary units) for missing P_t due to jets. For jets, the horizontal axis is the jet transverse momentum, P_t. The two possibilities which are shown are semileptonic decays of heavy quarks from leading fragments of gluons and leakage of jet fragments due to finite calorimeter depth.

12. Ratio of mean leakage energy to mean neutrino energy as a function of the calorimeter depth. The hatched region corresponds to "leakage" dominated by neutrinos.

13. Histogram of the fraction of the jet energy carried away by neutrinos. For leading fragmentation this fraction would be equal to 1/6.

14. Rates behind the calorimeter germane to muon detection.

    a. Rate for muon decays as a function of P_t at $y = 0$. The shaded area corresponds to the range cut of 10 absorption lengths of steel.

    b. Reduction factors with respect to pion rates for decay muons, •, punchthrough at 7 absorption lengths, ⊙, and at 8 absorption lengths, o, as a function of P_t at $y = 0$.

15. Energy depth asymmetry, δ, calculated using the WA1 parametrization as a function of leakage ratio, γ, for various energies; 100, 200, 400, 800 GeV corresponding to •, o, □, and ▽, respectively. The calorimeter depths are D = 10, D1 = 6, and D2 = 4. The electromagnetic fraction, fo, is fixed at the WA1 value.

16. The distribution, for 1000 events, of the containment fraction f for 450 GeV incident beam.

   a. D = 10.1 calorimeter, no longitudinal segmentation.

   b. D = 10.1 calorimeter with D1 = 6.6 and D2 = 3.5 longitudinal segmentation. The fractional beam energy, Δ, in the back, D2, segment must be < 0.18.

17. In this Figure lines are drawn to guide the eye. Solid lines refer to 100 GeV data while dashed lines refer to 450 GeV data. The meaning of the symbols is that:

   • = 100 GeV, D = 10.1, D1 = 6.6, D2 = 3.5
   o = 450 GeV, D = 10.1, D1 = 6.6, D2 = 3.5
   ▽ = 450 GeV, D = 9.4, D1 = 5.9, D2 = 3.5
   □ = 450 GeV, D = 8.7, D1 = 5.2, D2 = 3.5

   a. Efficiency of event acceptance as a function of Δ, the fractional beam energy cut in the back segment.

   b. Fraction of events, F, with containment fraction, f, < 95% as a function of Δ.

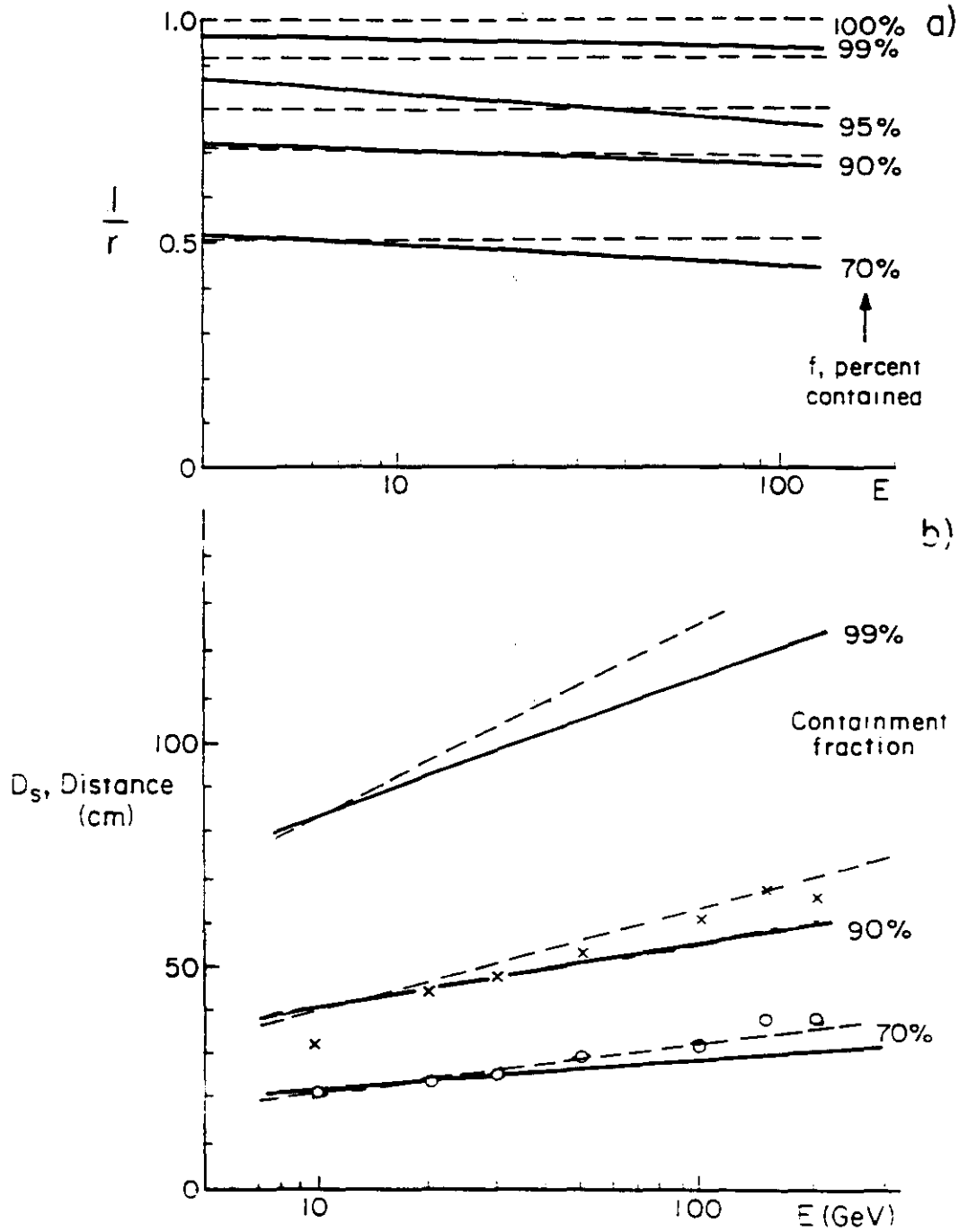
a)
1.0
0.5
0
1/r
100%
99%
95%
90%
70%
f, percent contained
10
100
E
b)
100
50
0
D_s, Distance (cm)
99%
Containment fraction
90%
70%
10
100
E (GeV)

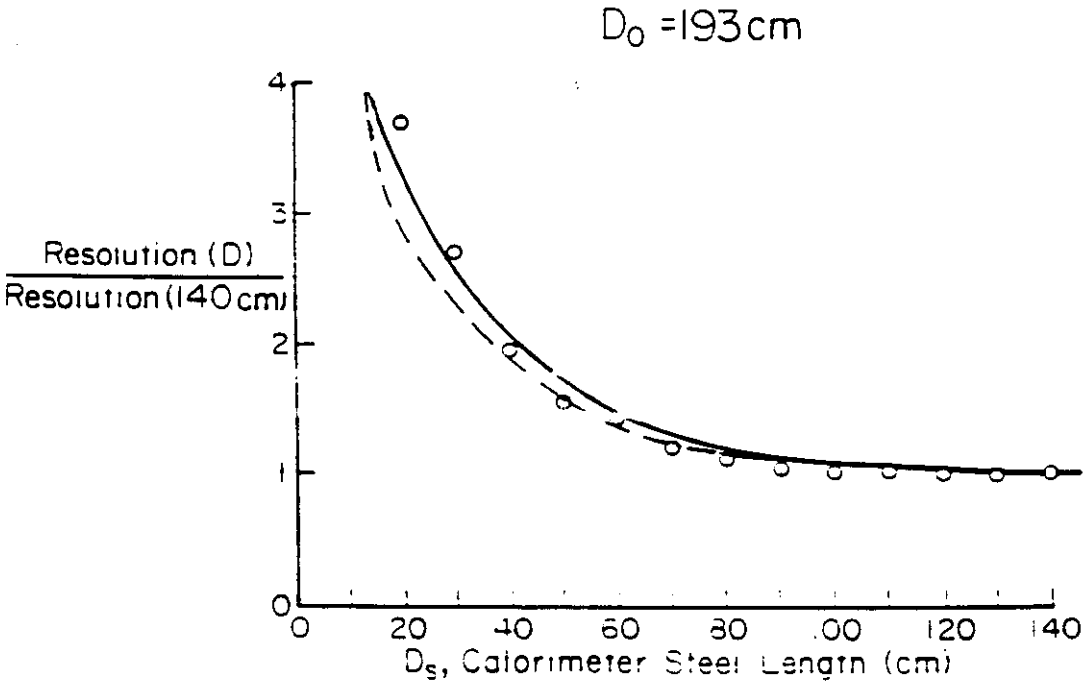
D_0 =193cm
Resolution (D) / Resolution (140 cm)
4
3
2
1
0
0
20
40
60
80
100
120
140
D_s, Calorimeter Steel Length (cm)

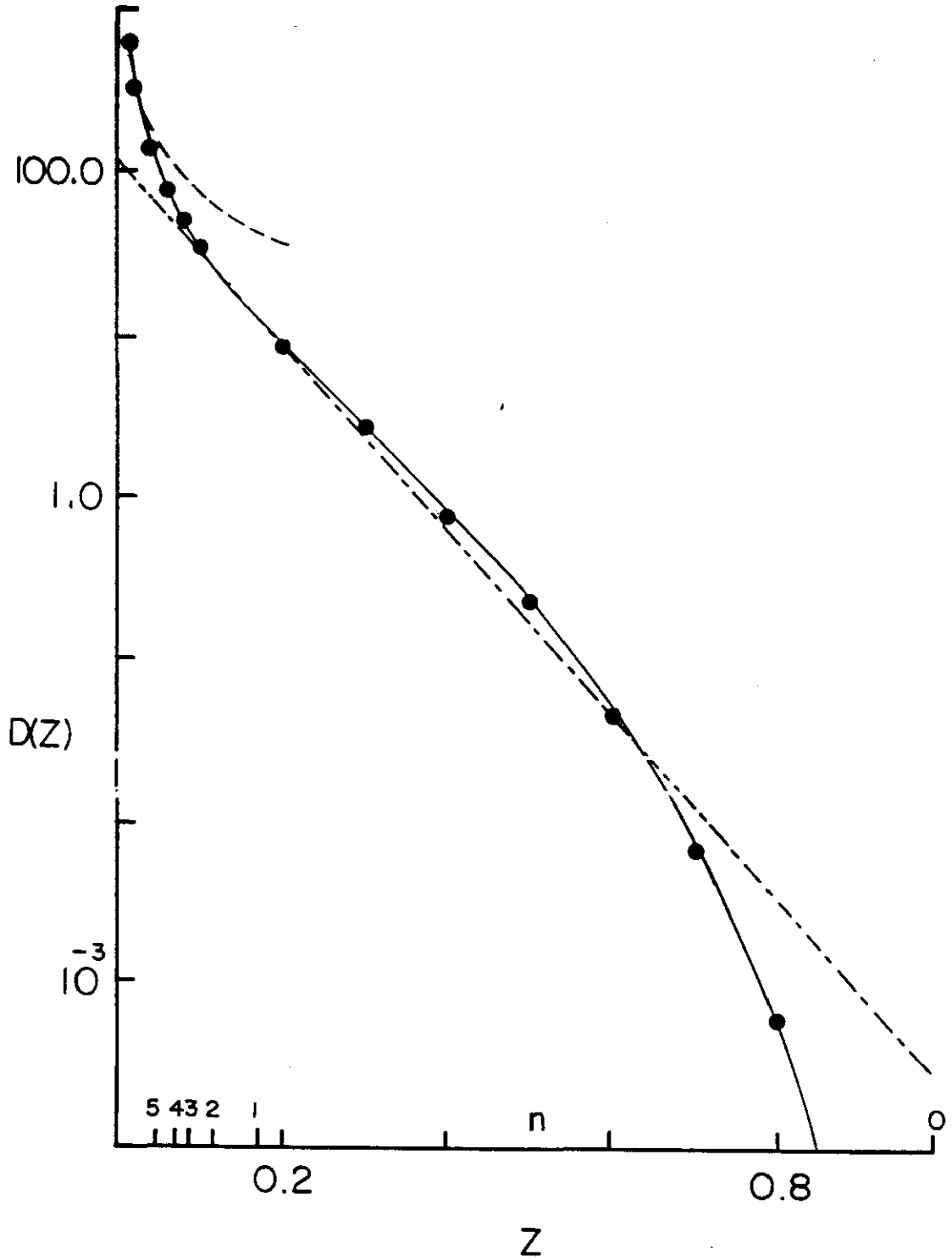
100.0
1.0
D(Z)
10^{-3}
5 4 3 2 1
n
0
0.2
0.8
Z

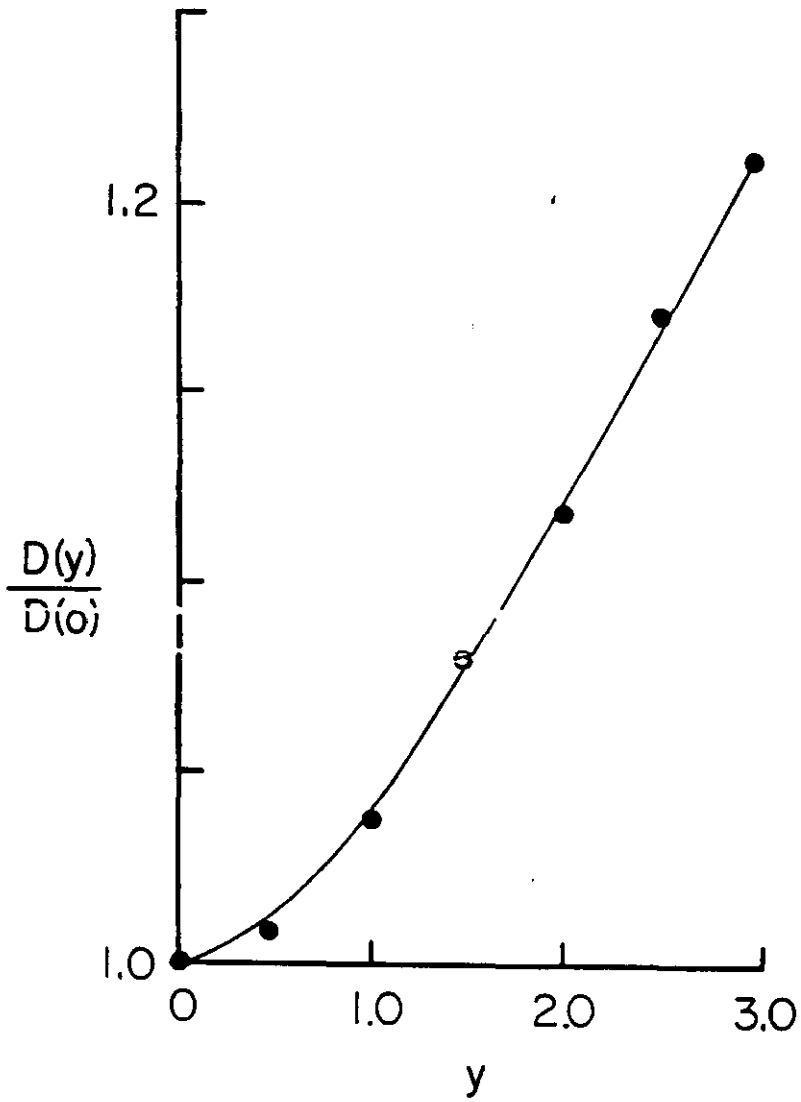
1.2
D(y)
D(o)
1.0
0
1.0
2.0
3.0
y

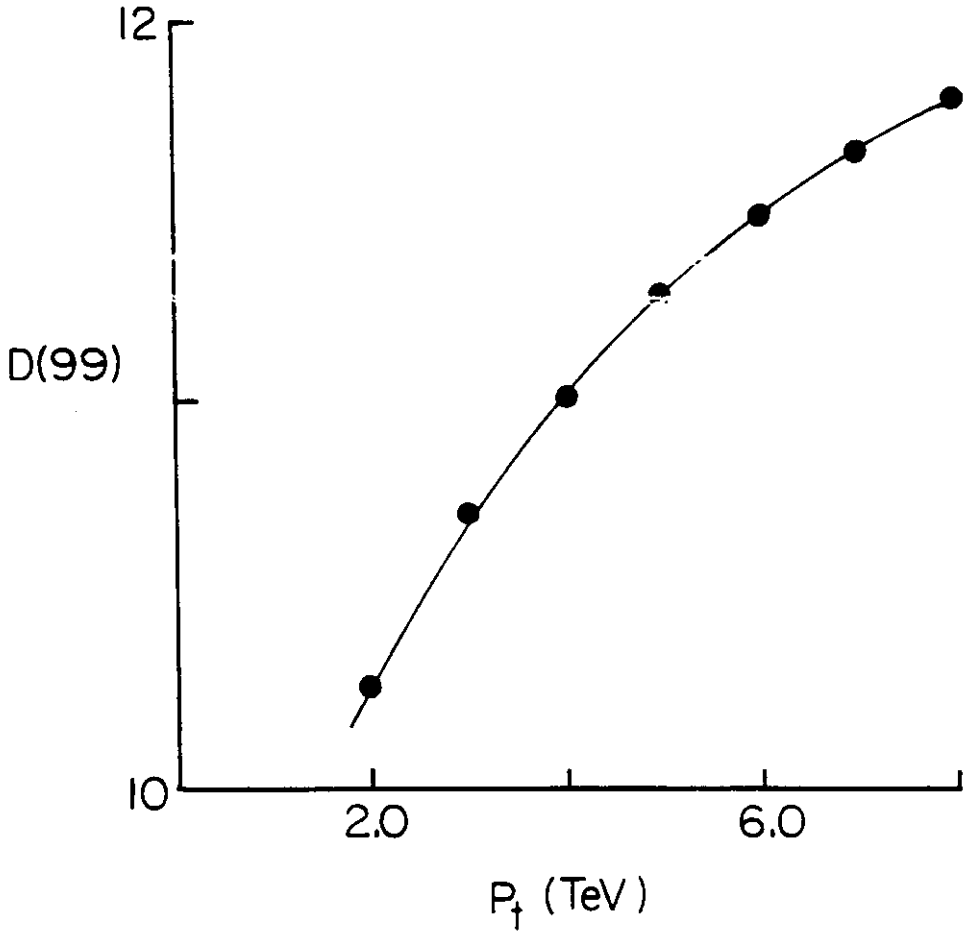
12
D(99)
10
2.0
6.0
P_t (TeV)

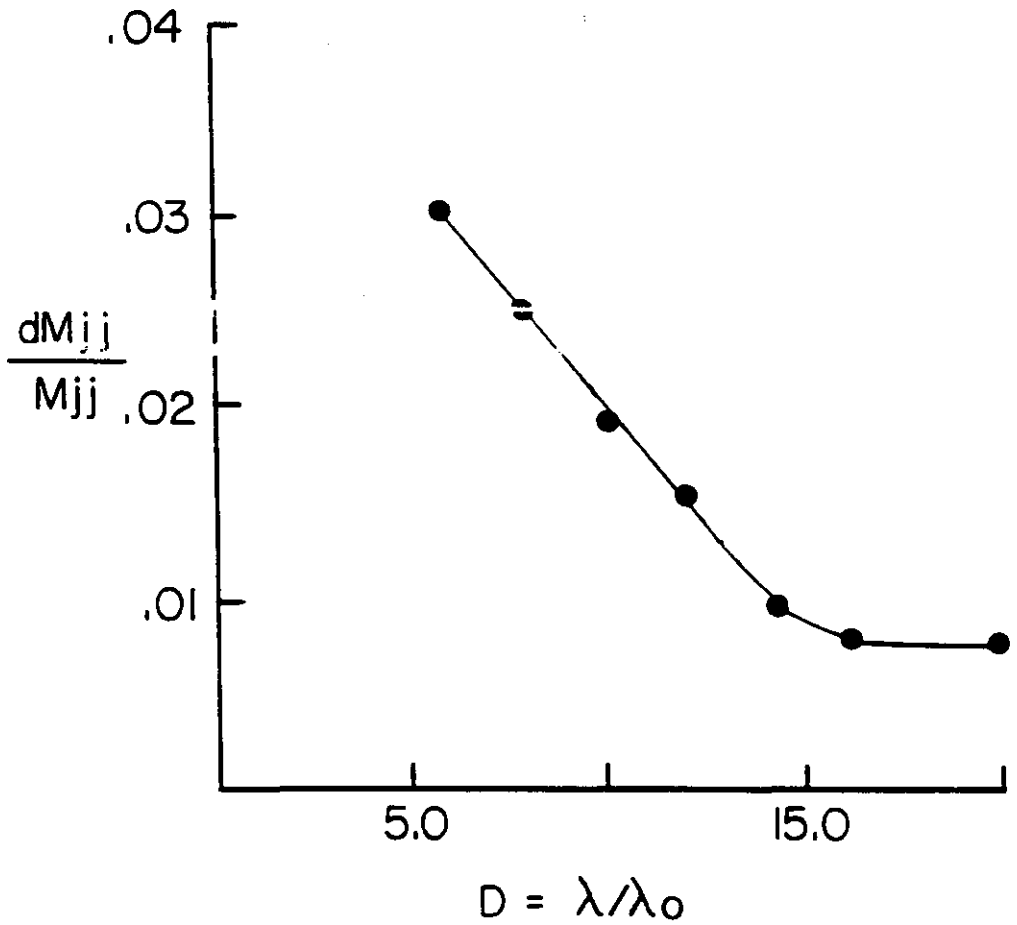
.04
.03
.02
.01
dMjj / Mjj
5.0
15.0
D = λ/λo

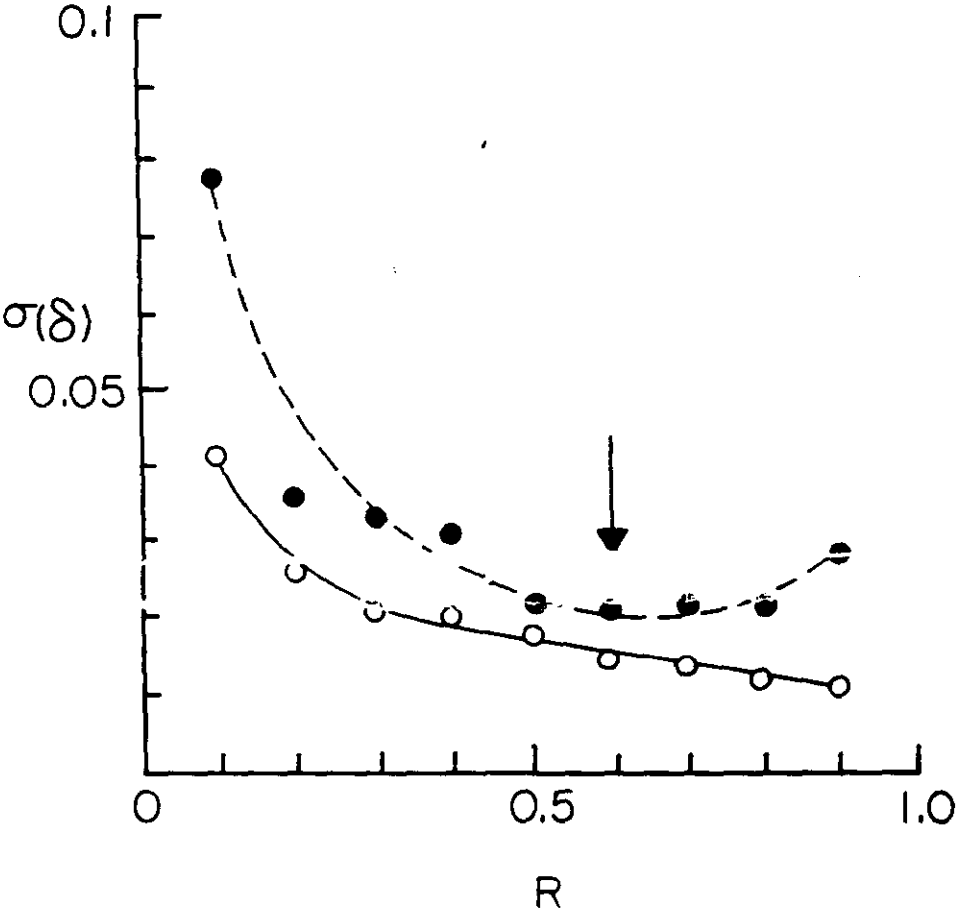
0.1
σ(δ)
0.05
0
0.5
1.0
R

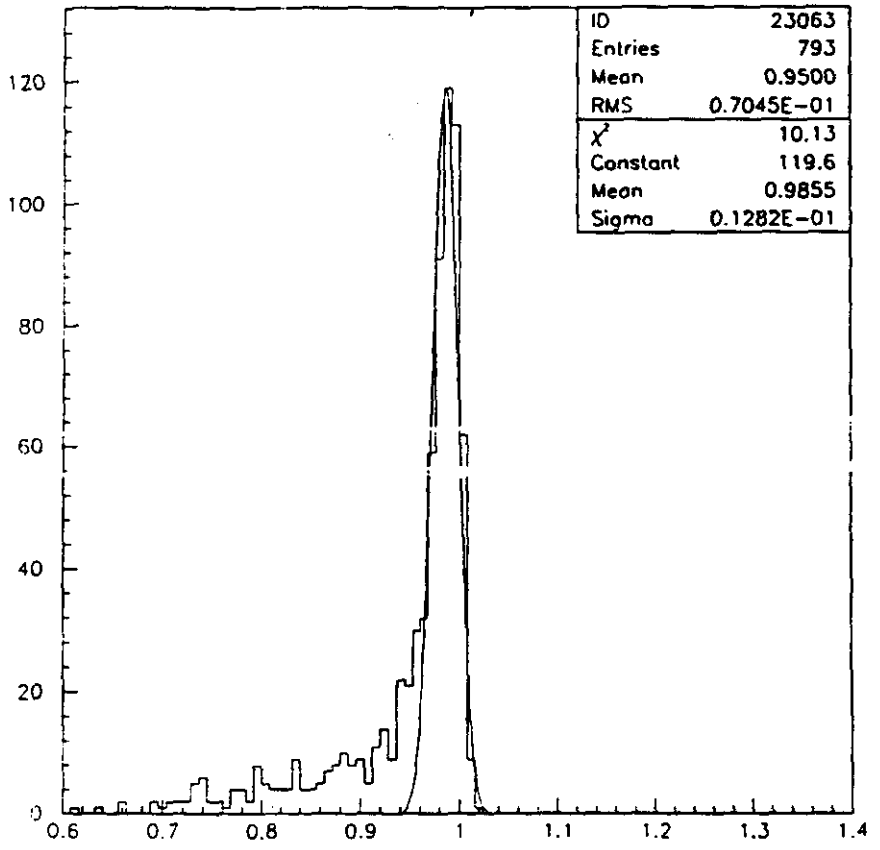

RATIO OF RECONSTRUCTED/GENERATED MASS FOR Z0 FOR RAD=0.60

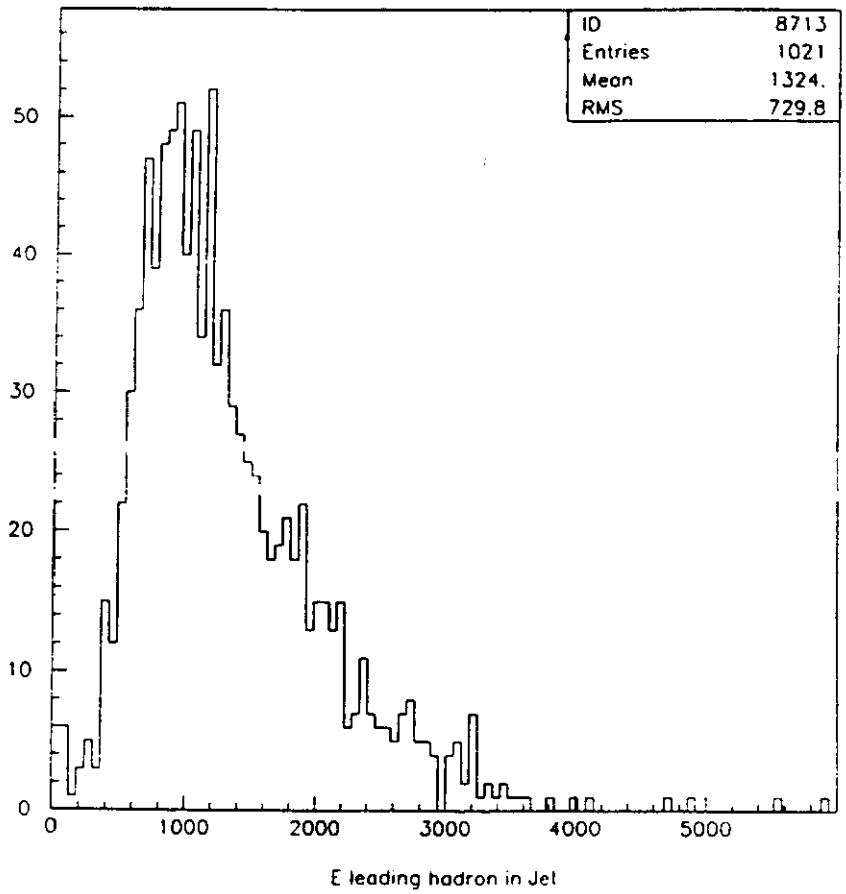
ID 8713
Entries 1021
Mean 1324.
RMS 729.8
50
40
30
20
10
0
0
1000
2000
3000
4000
5000
E leading hadron in Jet

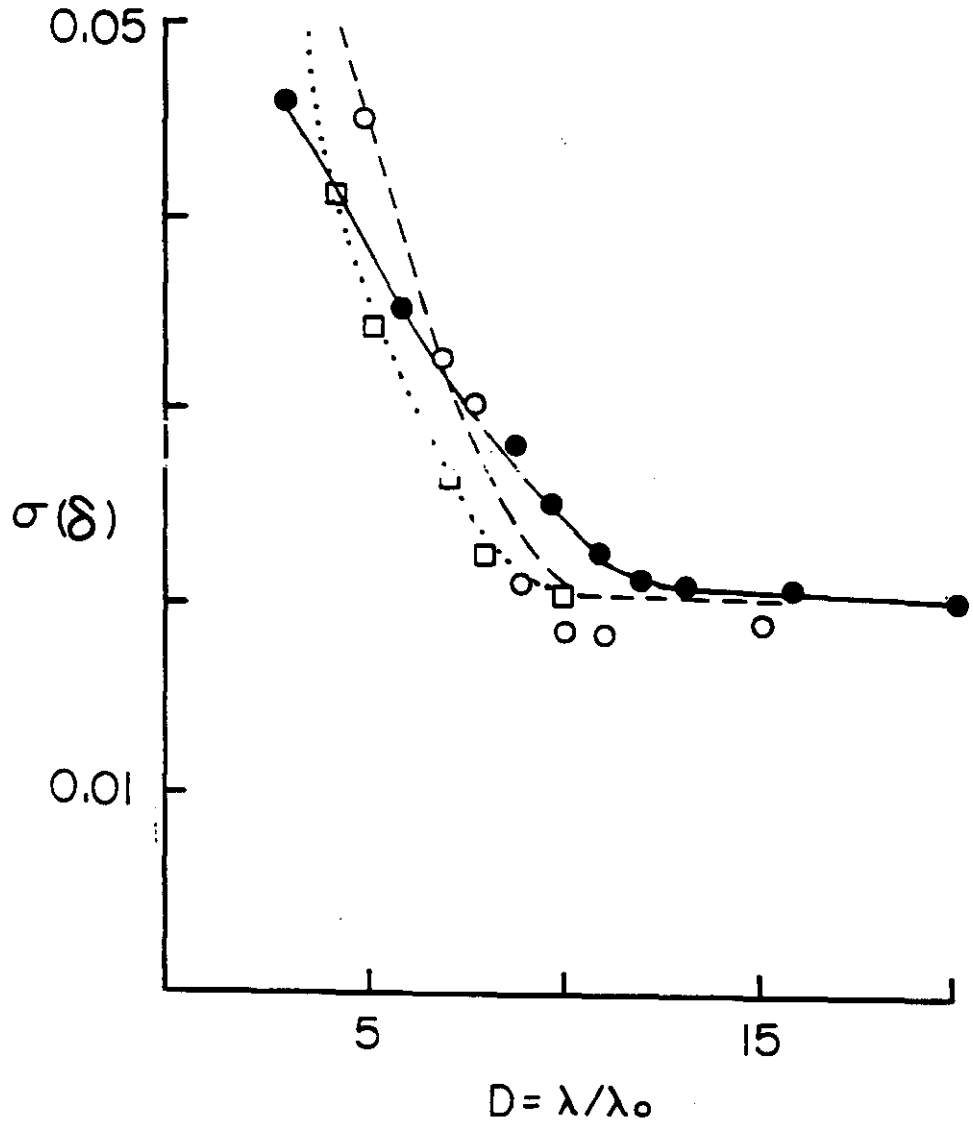
0.05
0.01
σ(δ)
5
15
D= λ/λo

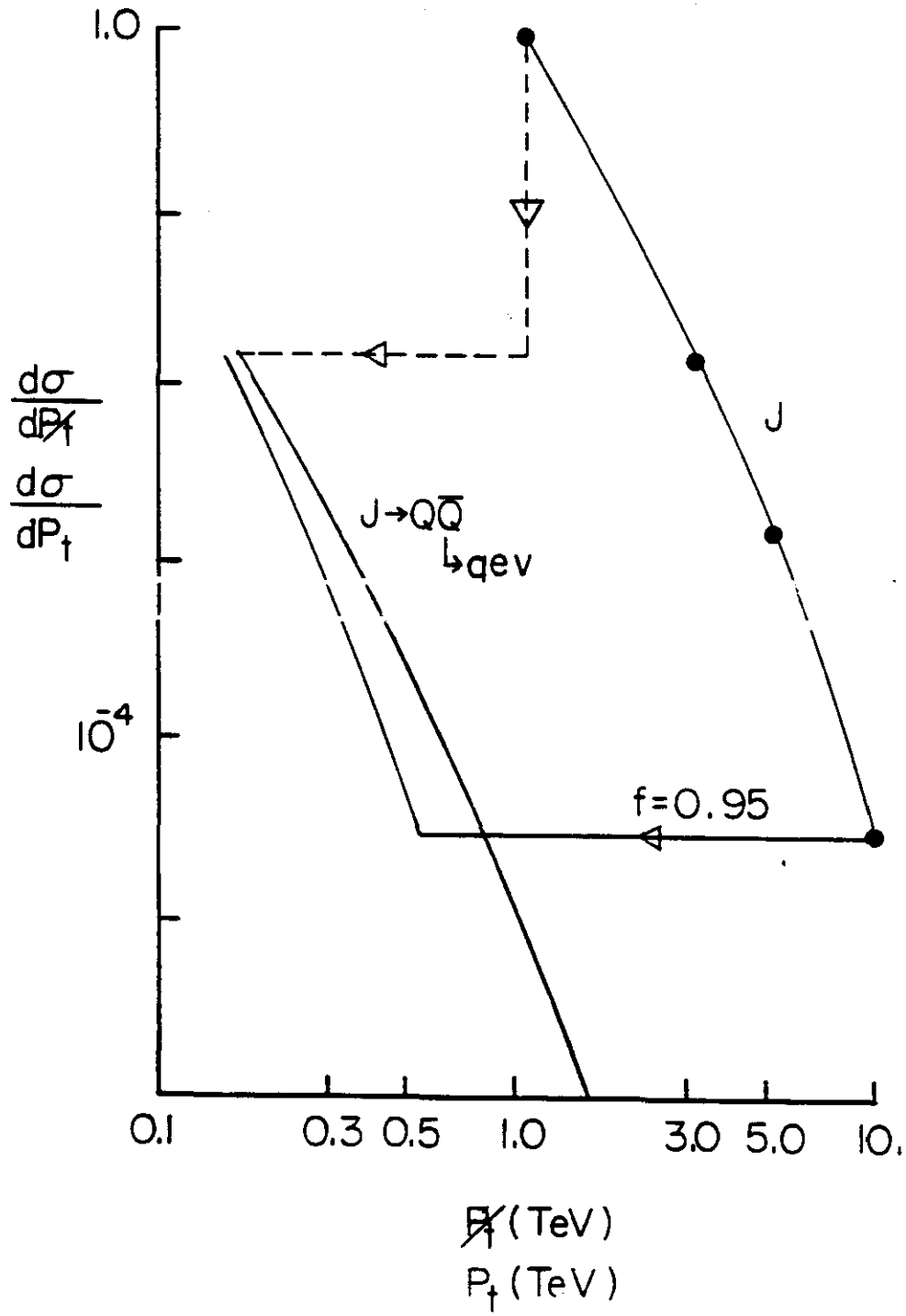
1.0
10^{-4}
$\frac{d\sigma}{d\not{P}_t}$
$\frac{d\sigma}{dP_t}$
J
$J \to Q\bar{Q}$
$\hookrightarrow qev$
f=0.95
0.1
0.3
0.5
1.0
3.0
5.0
10.
$\not{P}_t$ (TeV)
P_t (TeV)

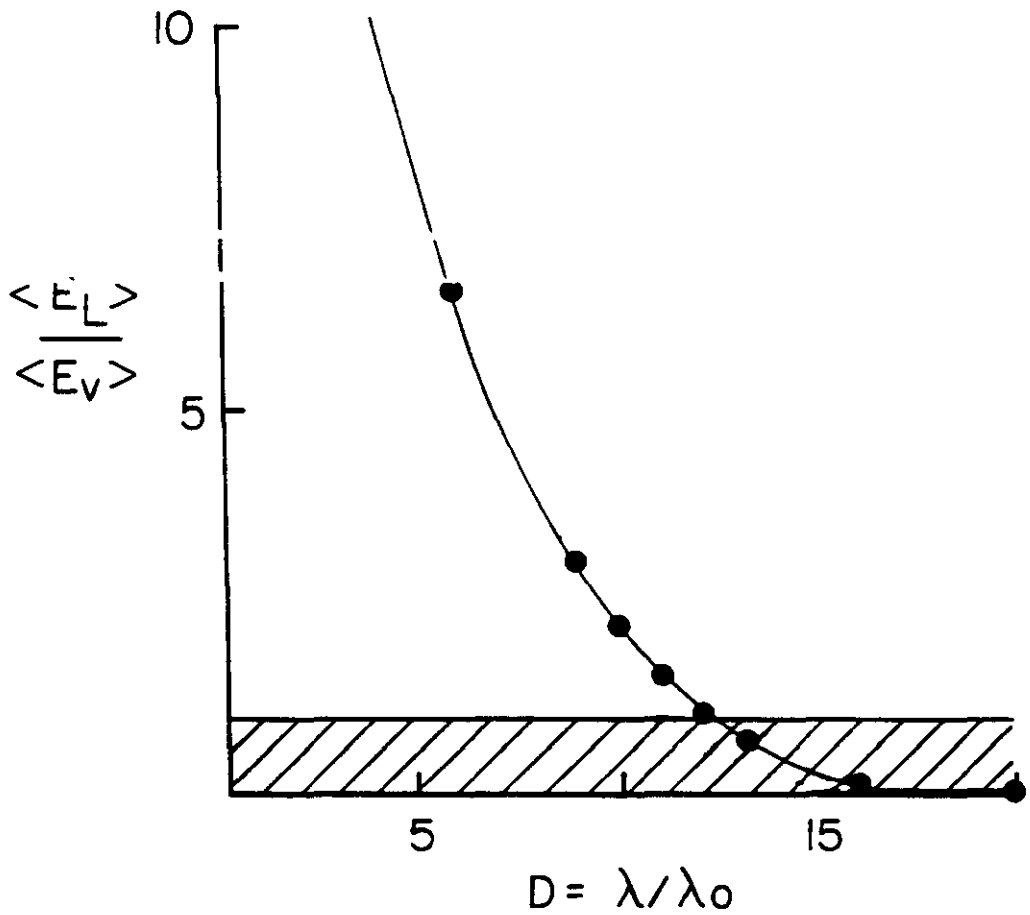
10
5
<E_L>
<E_V>
5
15
D = λ/λo

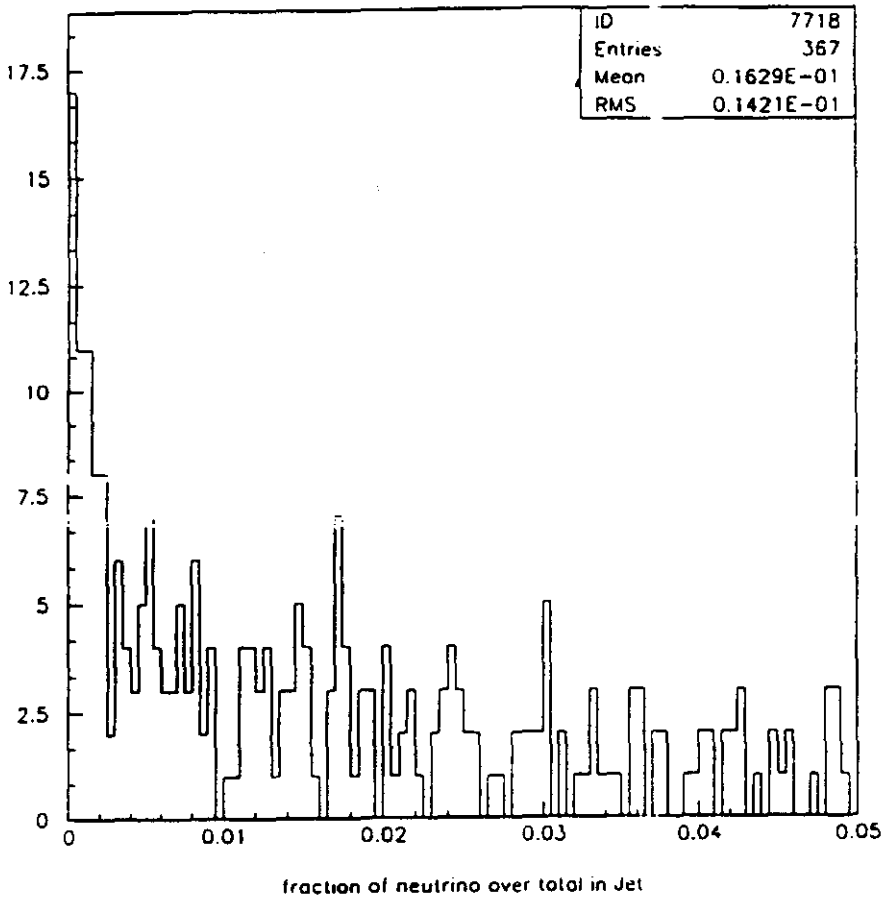
ID 7718
Entries 367
Mean 0.1629E-01
RMS 0.1421E-01
17.5
15
12.5
10
7.5
5
2.5
0
0
0.01
0.02
0.03
0.04
0.05
fraction of neutrino over total in Jet

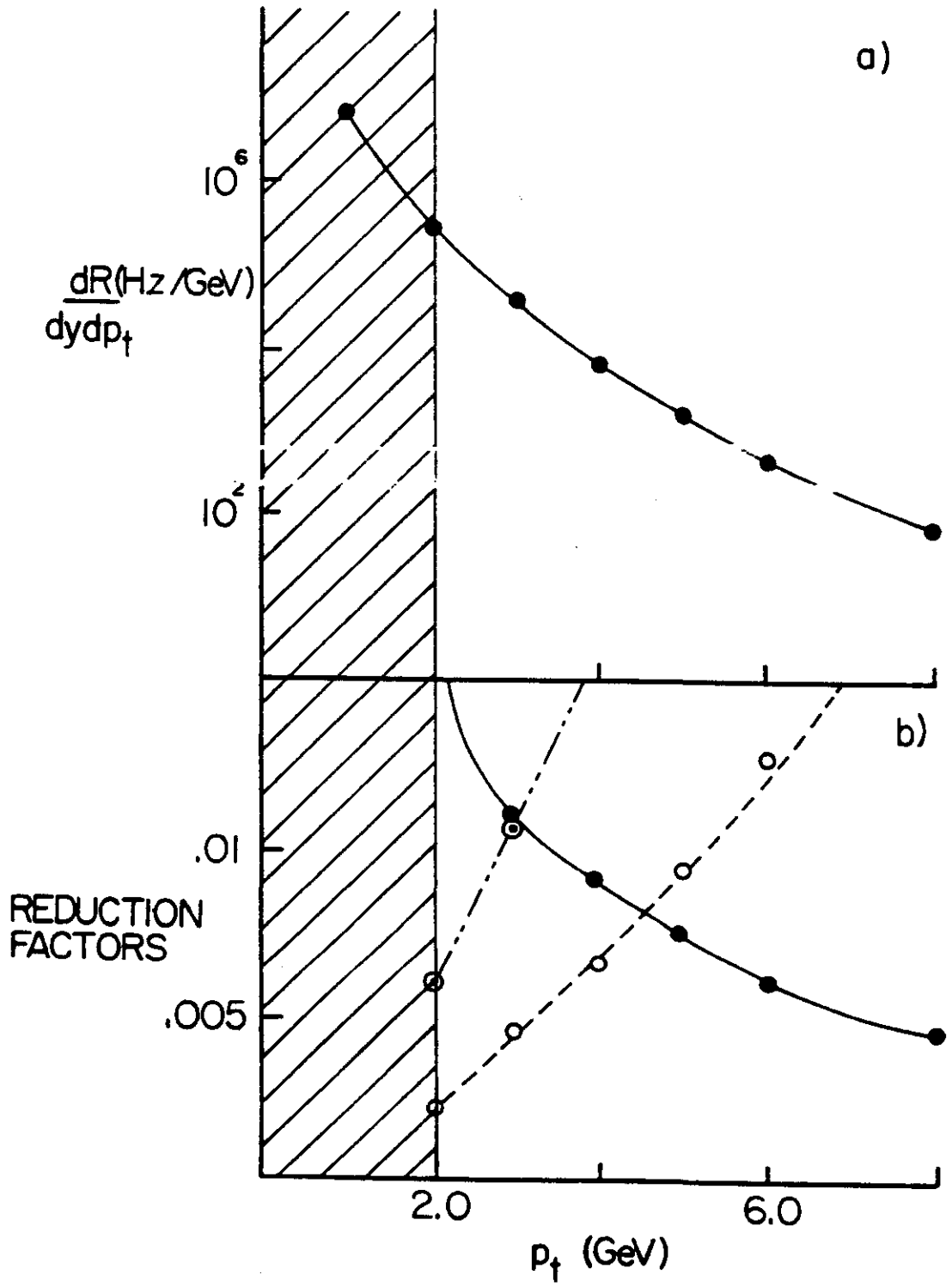
a)
10^6
$\frac{dR}{dydp_t}$(Hz/GeV)
10^2
b)
.01
REDUCTION FACTORS
.005
2.0
6.0
p_t (GeV)

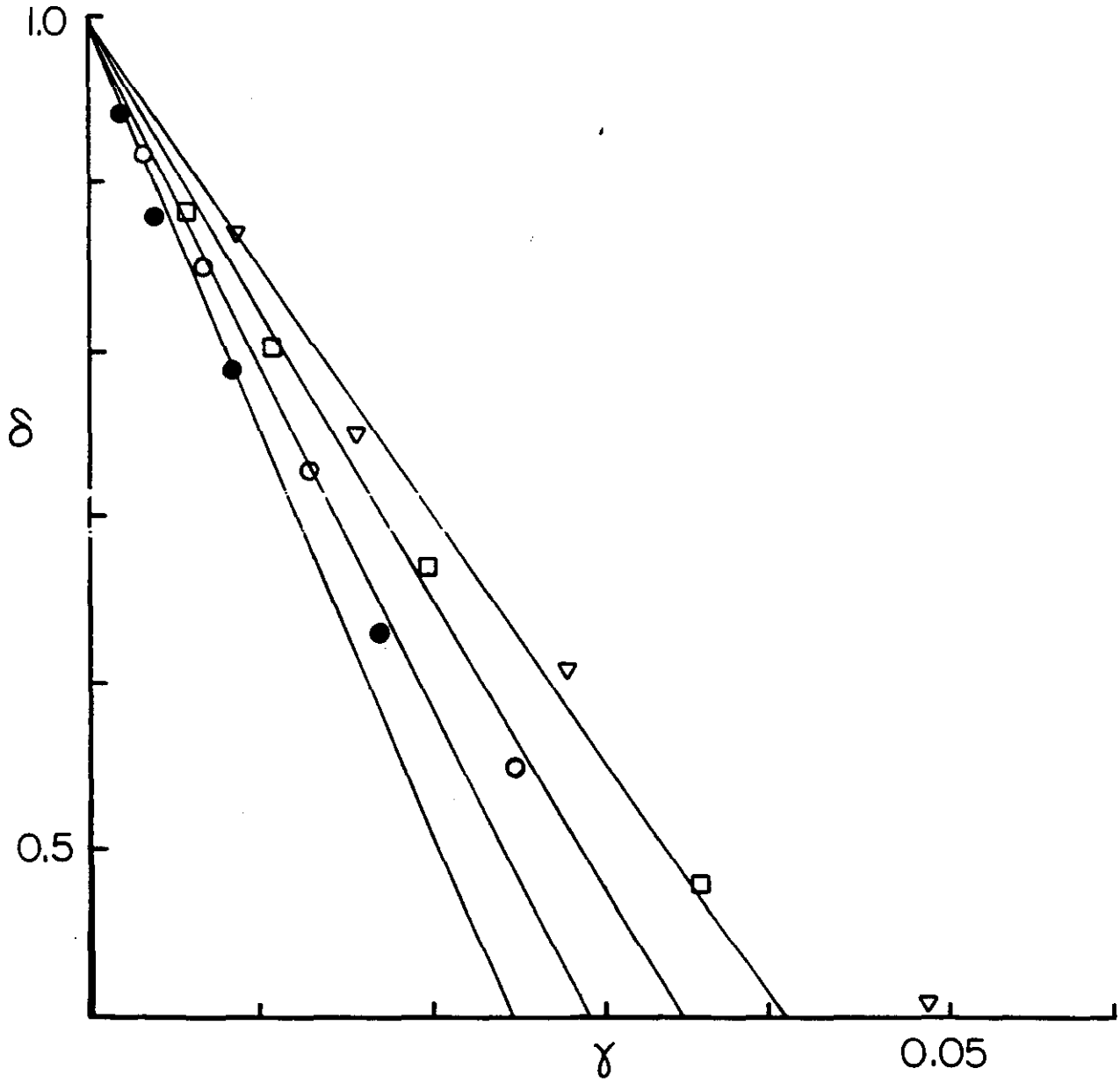
1.0
δ
0.5
γ
0.05

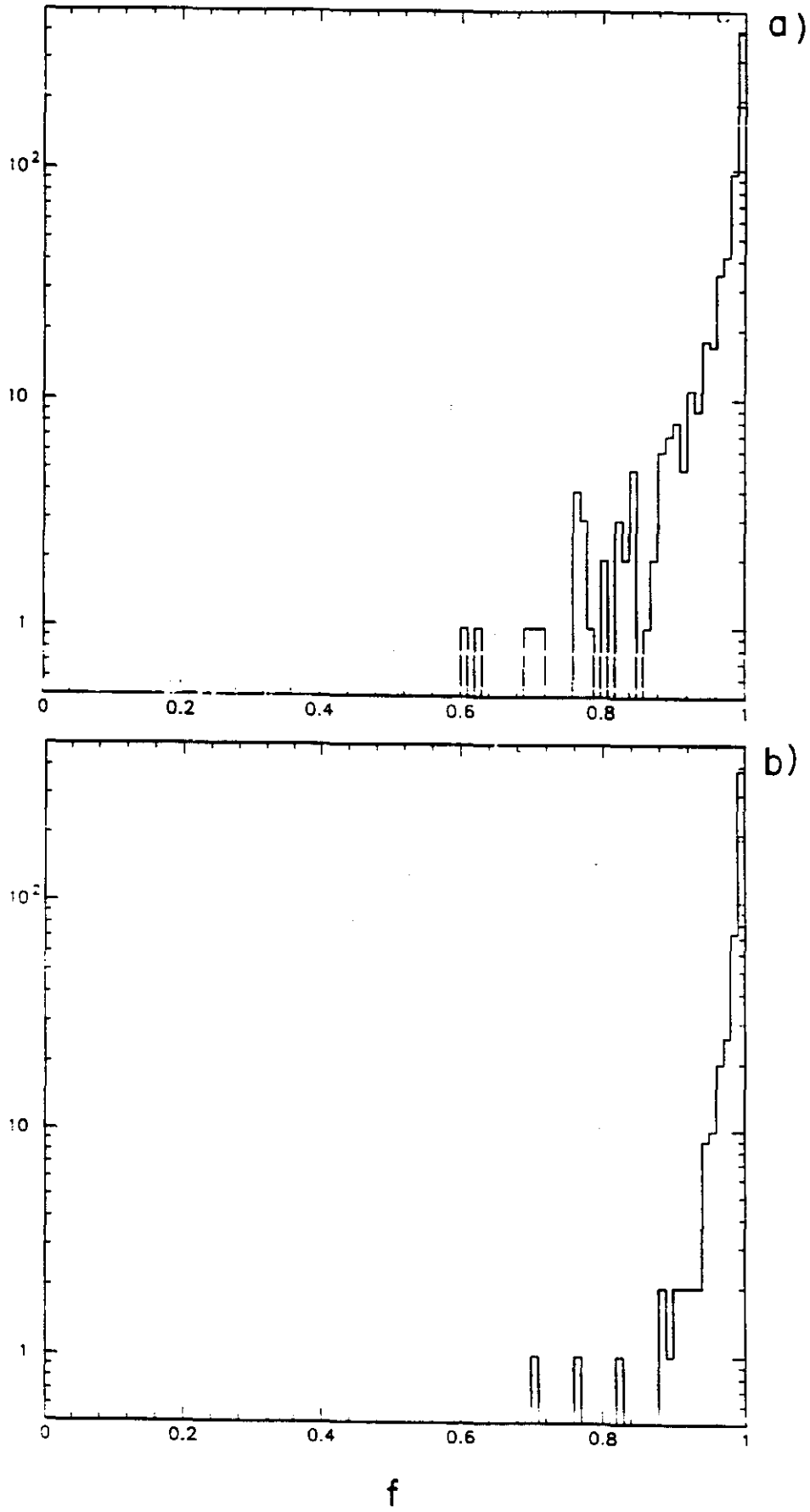
a)
10^2
10
1
0
0.2
0.4
0.6
0.8
1
b)
10^2
10
1
0
0.2
0.4
0.6
0.8
1
f

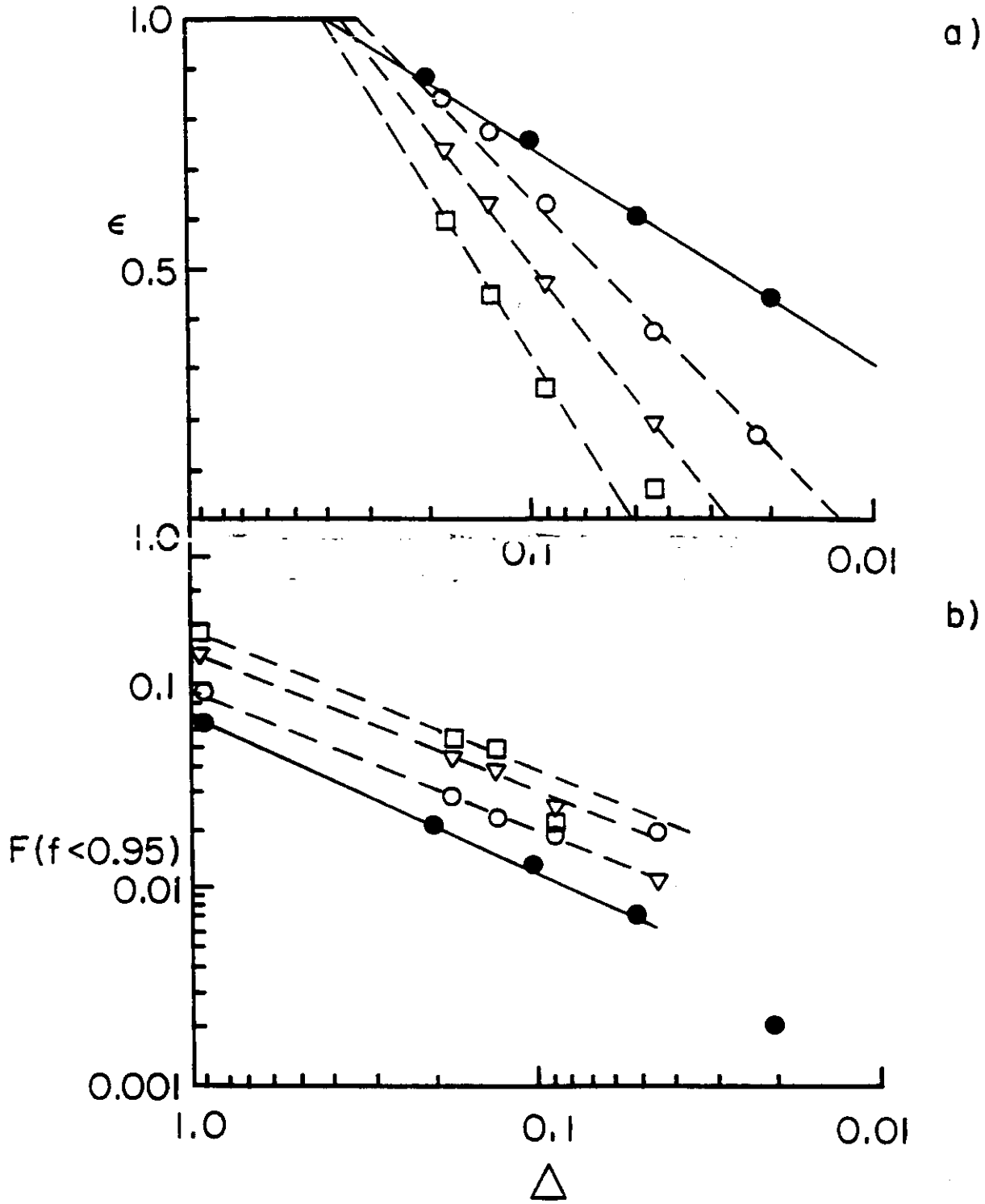
a)
1.0
ϵ
0.5
1.0
0.1
0.01
b)
0.1
F(f<0.95)
0.01
0.001
1.0
0.1
0.01
Δ

... last words?

Reasons to Choose Scintillating Fibers over Liquid Scintillator

Let's make decision today

1) Should not choose technology for which prototypes have not been built and tested

   SPACAL -- 6 different prototypes built and tested, 6 publications in NIM, 2 CERN reviews

   SSCintCAL -- 3 different prototypes, 2 tested 2 SSC R & D reviews, 1 TNRLC

   Liquid Scintillator -- No prototype (not even EM)
   .. despite visionary work, exemplary answers to critics

2) BaF_2/LXe may eventually not be selected ($$ or R & D results)

   Then only LAr and Liquid Scintillator remain -->
   no credible 6%/ √E EM backup
   if liquid scintillator is chosen instead of fibers

   Jetset performance

   Fibers provide both hadronic calorimeter and EM backup for same R & D $$

L. Sulak
GEM Calorimeter Meeting
9/6/91

3) Completion of fiber R & D cheaper (FY92 cash flow), faster (now 4 years into design & test beam program)

Mature fiber R & D program requires <= 3% R&D vs 11% ... ~ $6M savings

Liquid scintillator R & D program just starting.
Insufficient time to fully test design before technical design report in November 1992

4) Current liquid scintillator effort below critical mass

5) Preliminary costing shown first on Wednesday, 9/4

82M liquid
.04M fiber ORNL
77M fiber Draper

Difference between fibers/liquid ($22M) within errors
Draper Spaghetti estimate lower ($26M less than ORNL)

Liquid system costs not yet reviewed by GEM
No calibration system costed, etc. ← Release Kennyk from gag rule

... experience / 2 SSC contracts for ... fibers... double checked by Martin Marietta

6) Spaghetti behind BaF2/LXe yet to be optimized

Must be descoped because BaF2/LXe now in front
No longer 2 integrated systems in plan

Descoped Draper Cost $57M ...
using Bicron SBIR results...
$1.27/m fiber
auto threading of fibers

Fewer interaction lengths,
Courser segmentation,
Increased fiber diameter
} hadron cal overdesigned

TO AVOID UNPLEASANT SURPRISES CHOOSE THE SYSTEM WITH DEMONSTRATED PERFORMANCE CHARACTERISTICS

Survivability of Synthetic Calorimeter

η	[illegible]	Dose* (Gy/yr)	Time 1% [illegible]
0	9°	[illegible]	565
1	40°	[illegible]	[illegible]4
2	15°	[illegible]	31
3	6°	2.1 k	3

* Dose at shower max

assume
no annealing
no fiber improvements

INITIAL ESTIMATE for 9/4 Meeting
DRAPER

GEM DETECTOR

SCINTILLATING FIBER HADRON CALORIMETER

COST ANALYSIS A

	Category	Tot Un	$K Unit	Units	Costs $K
1.00	Towers				
1.10	Lead	2126	5.58	Mton	$11,855
1.20	Fiber	6.00E+06	.00127	Meters	$7,600
1.30	PMT's	13232	0.30	Each	$3,970
1.40	Sheathe + Cover Plate	3308	.40	Each	$1,323
1.50	Light Guides	13232	0.10	Each	$1,323
1.60	Spacer Plates	3308	0.20	Each	$662
2.00	Electronics	13232	0.25	Channels	$3,308
3.00	Structure	187,000	0.005	LBS	$935
4.00	Thermal Cont				$500
5.00	Fab & Ass.				
5.10	Fab. Ass. & Test	13.8	0.045	M-H/tower	$9,300
5.20	Tooling				$3,000
6.00	Testing				
6.10	Test Beam				$1,000
6.20	Test Equip				
7.00	Transport				$500
8.00	Installation				
8.10	Install. Labor	17,000	$45/MH	Man-Hour	$765
8.20	Install. Equip				$1000
DIRECT COST					$47,121
EDIA		25%			$11,780
BASE COST					$58,901
CONTINGENCY*		25%, 10%			$18,455
SUBTOTAL					$69,356
R&D		11%			$7,651
TOTAL					$77,206

*Contingency: 10% on lead, fiber, and steel
25% on other items

Draper estimate before attempted compromise with DRNE
$77M

Scintillating Fiber Hadron Calorimeter-Cost Analysis

	Catagory	Tot Uts	$K/UNIT	Units	Costs
1.00	Towers				
1.10	Steel	2126	5.58	Mton	$11,855
1.20	Fiber	6.60E+06	0.00145	Meters	$9,570
1.40	Bundles	3308	0.30	Each	$992
1.50	Light Guides	13232	0.10	Each	$1,323
1.60	Connors	3308	0.18	Each	$595
1.70	Grab. Loops	120	2.00	Each	$240
2.00	Readout				
2.10	PMT's	13232	0.30	Each	$3,970
2.20	Electronics	13232	0.25	Channels	$3,308
3.00	Structure	350000	0.008	Lbs	$2,800
4.00	Thermal Cont				$980
5.00	Fab & Ass.		—		
5.10	Fab.Ass & Test	23	0.045	M-H/tower	$13,440
5.20	Tooling		—		$3,000
6.00	Testing				$2,500
6.10	Test Beam				
6.20	Test Equip				
7.00	Transport.				$500
8.00	Installation				
8.10	Install. Labor	33,333	0.045	Man-Hour	$1,500
8.20	Install. Equip				$1,500
	Direct cost				$58,073
	EDIA	25%			$14,518
	Base Cost				$72,592
	Contingency	30%			$21,777
	Subtotal				$94,369
	R&D	11%			$10,381
	Total				$104,750

MARK RENNICH/OAK RIDGE NATIONAL LABORATORY/ 8/21/91

2weeks old now

Attempted compromise with ORNL

F. Ayer
22 Aug. '90

SCINTILLATING FIBER HADRON CALORIMETER
COST ANALYSIS

(Revision by BU & CSDL 22 August 1991)

	Category	Tot Uts	$K Unit	Units	Costs $K
1.00	Tonnage				
1.10	Lead	2126	5.58	Mton	$11,855
1.20	Fiber	6.40E + 06	.00174	Meters	$11,136
1.30	PMTs	13232	0.25	Each	$3,308
1.40	Sheaths	3308	.30	Each	$992
1.50	Light Guides	13232	0.10	Each	$1,323
1.60	Spacer Plates				$600
2.00	Electronics	13232	0.25	Channels	$3,308
3.00	Structure				$2,200
4.00	Thermal Cont				$800
5.00	Fab & Ass.				
5.10	Fab. Ass. & Test	18.7	0.045	M-H/tower	$11,210
5.20	Tooling				$8,160
6.00	Testing				
6.10	Test Beam				$1,856
6.20	Test Equip				$642
7.00	Transport				$500
8.00	Installation				
8.10	Install. Labor	30,350	50/MH	Man-Hour	$1500
8.20	Install. Equip				$300
DIRECT COST					$53786
EDIA		25%			$13,446
BASE COST					$67,232
CONTINGENCY*		10%, 25%			$13,368
SUBTOTAL					$80,600
R&D		11%			$8,867
TOTAL					$89,468

<-91

$89M

*Contingency 10% on lead & fiber 23,000k
25% on other items

Results of SBIR ... DoE/SSC "Project to Develope Mass Drawing of Scintillating Fibers

FAX TO: CHARLES STARK DRAPER LABORATORIES
ATTN: FRANCOIS AYER
FROM: CHUCK HURLBUT, BICRON CORPORATION
DATE: 3 SEPTEMBER 1991

SUBJECT: BUDGETARY PROPOSAL FOR SCINTILLATING FIBERS FOR THE "GRM" COLLABORATION.

This estimate is for budgetary purposes. It represents the work of several people at Bicron including myself, the two senior engineers which have been assigned to our fiber program for the last three years, our Engineering Manager and our accounting department. We consider this to be a serious estimate with a high degree of accuracy.

$1.45/m → $1.27/m

We propose to provide the following goods and services:

6,000,000 meters of 3 mm dia. Type BH-1 scintillating fibers cut and assembled into 3,124 "preform" subassemblies as described below.

Total Price:	$7,600,000
FOB Newbury, Ohio	

The preforms would consist of 3600 individual fibers inserted into a set of precision drilled metal plates. The hole pattern would be a 60 x 60 matrix. The set of plates would be close stacked together resembling a single unit without spaces between the layers. The fibers would be precision cut to various lengths depending on their position in the assembly. The central fibers would be the maximum length, and the fibers would be shorter as their position is closer to the edge of the array. The final assembly would resemble a truncated pyramid. One end of each fiber would be modified to a slightly larger diameter too prevent its falling through its hole when the assembly is held so the fibers hang vertically with the larger end of the array at the top. The longest fiber in each preform would be about 220 cm Each preform would be packaged in an individual wood crate with the precision plate stack still in its condenced configuration.

nailed

Delivery would take about twenty months with the first assemblies being shipped about five months after receipt of order.

CONFIDENCE IN MASS PRODUCTION COST EFFICIENCY
Bicron has recently completed an SBIR Phase II development project in which the major task was the development of a mass production system for manufacturing large quantities of scintillating and waveguide optical fibers for use in the SSC. Main elements of this investigation included the following:

- Total factory layout
- Large volume monomer purification and storage
- Polymerization system design to achieve high throughput and quality consistency
- High speed fiber fabrication

from 5m/min now to 50-100m/min

Major prototype process equipment was constructed and successfully operated, and some components for the final operation were procured.

Our estimates of the various cost factors in this proposal are based on our experience from the SBIR work which is now being conducted with Bicron internal funding.

MAJOR COST ELEMENTS IN THE PROPOSAL

A. Raw Materials: Allowances were made for all foreseeable efficiency problems including potential impact of international tensions affecting petroleum supplies and unforeseeable difficulties in starting up the full volume system required for this program.

B. Labor: A full independent factory operating around the clock is envisioned. Personnel considerations included such factors special maintenance staff, dedicated management, training expenses, and impact of efficiencies on total labor required.

C. Factory Overheads: All standard and special factory overheads for the entire time of dedicated operation were included. All costs were accumulated in a zero-based calculation.

D. Special Factory Equipment Costs: A major portion of the factory construction expenses are allocated against this project. Reasons for this include the fact that the factory as constructed will be highly specialized with very little opportunity for cost recovery aside from special SCC projects like this one. A second reason is that a special set of equipment for assembly of the "preforms" will be constructed with the particular costs fully allocated here.

3 machines... one spare all the time

E. Special Preform Assembly Equipment: The concept for this equipment is already well developed as the outcome of a meeting of four members of the Bicron technical staff, each person having over 20 years in manufacturing process design from a variety of backgrounds. Each instrument would inspect the fiber as it is made on the continuous fiber lines and reject it if appropriate. Good fiber would be cut to the appropriate lengths, inserted in the appropriate holes, and altered to have a large "head". It would be a computer controlled system. Three systems would be constructed with one kept in reserve for breakdowns.

ADDITIONAL CONTINGENCIES

Contingencies that SSC planners prefer to add on need not exceed ten percent since significant contingencies have been factored into the above prices.

Downscaled Dragon Lab Cost ... $57M

GEM CALORIMETER

SCINTILLATING FIBER HADRON CALORIMETER

COST ANALYSIS C

	Category	Tot Uts	$K Unit	Units	Costs $K
1.00	Towers				
1.10a	Cutalloy 50%	948	5.58	Mton	$5,290
1.10b	Lead Shot 50%	1139	.99	Mton	$1,128
1.20	Fiber	5.7E+06	.00127	Meters	$7,239
1.30	PMTs	3308	0.30	Each	$992
1.40	Sheaths + Cover Plate	3308	.40	Each	$1,323
1.50	Light Guides	3308	0.20	Each	$662
1.60	Spacer Plates	3308	0.20	Each	$662
2.00	Electronics	3308	0.26	Channels	$857
3.00	Structure	160,000	0.005	LBS	$800
4.00	Thermal Cont				$500
5.00	Fab & Ass.				
5.10	Fab. Ass. & Test	15.8	0.045	M-H/tower	$9,380
5.20	Tooling				$3,000
6.00	Testing				
6.10	Test Beam				$1,000
6.20	Test Equip				
7.00	Transport				$500
8.00	Installation				
8.10	Install. Labor	17,000	$45/MH	Man-Hour	$765
8.20	Install. Equip				$1000
DIRECT COST					$35,068
EDIA		25%			$8,767
BASE COST					$43,835
CONTINGENCY*		25%, 10%			$8,000
SUBTOTAL					$51,835
R&D		11% shall be 3%?			$5,765
TOTAL					$57,600

*Contingency: 10% on lead, fiber, and steel
25% on other items

... see presentation of Dan Sullivan / Francis Dyer after lunch

The Liquid Argon Calorimeter will not Fit Within the Allocated Volume

REMPICH

Comment on 1 mm Accordion Plates:

The Issue is not Cost.

The Issue is Feasibility

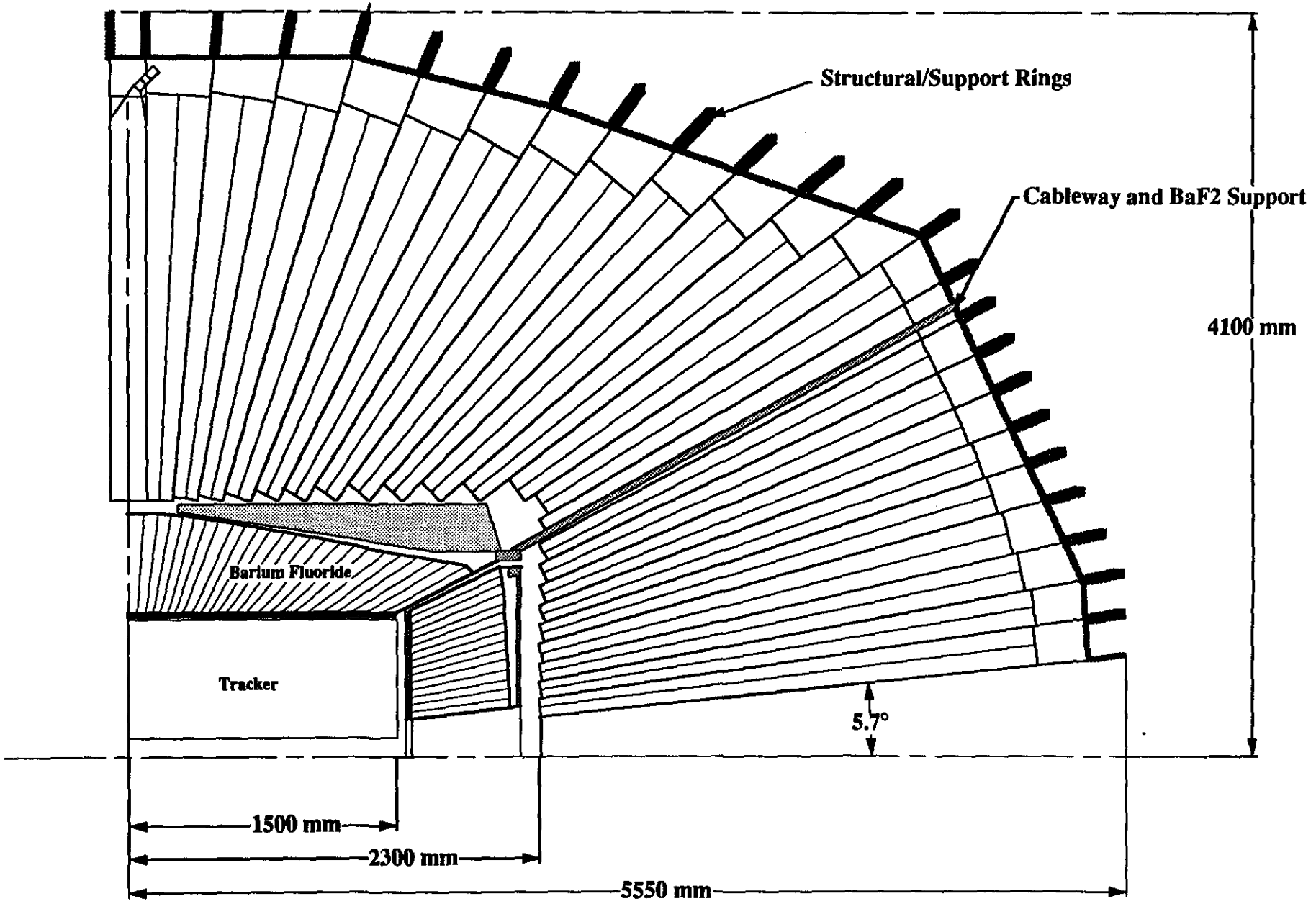

Spaghetti Hadron Calorimeter
Barium Fluoride EM Calorimeter

LS.03.SC.00037

Rennich

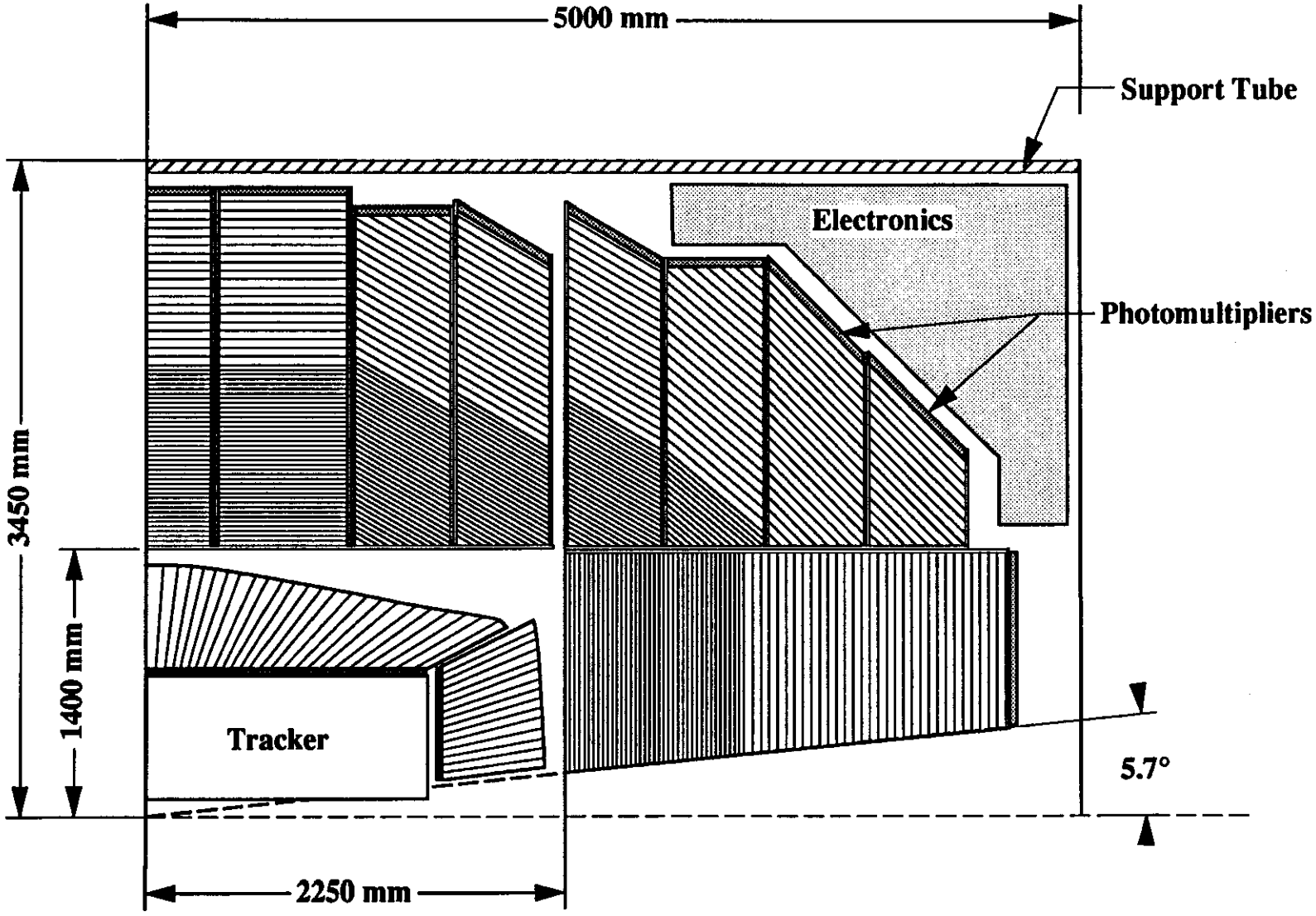

Liquid ScintillatorHadron Calorimeter
Barium Fluoride EM Calorimeter

COMPARISON OF HADRON CALORIMETER ESTIMATES

		Liquid Scintillator		Spaghetti
	Catagory	Conservative	Optimistic	Conservative
1.00	Material/Modules	$9,639	$7,914	$16,660
2.00	Sense Material	$468	$260	$6,600
3.00	Readout	$15,625	$15,625	$11,247
4.00	Structure	$400	$400	$1,600
5.00	Ass, Fab and Test	$16,262	$11,978	$16,695
6.00	Thermal Cont	$980	$980	$980
7.00	Oper. Testing	$2,500	$2,500	$2,500
8.00	Installation	$2,800	$2,350	$3,000
9.00	Shipping	$500	$500	$500
	DIRECT COST	$49,173	$42,506	$59,782
	EDIA	25%	25%	25%
	BASE COST	$61,466	$53,133	$74,728
	CONTINGENCY	25%	25%	25%
	SUBTOTAL	$76,833	$66,416	$93,410
	R&D	11%	11%	11%
	TOTAL	$85,285	$73,722	$103,685

Mark Rennich/Oak Ridge National Laboratory/9-5-91

COMPARISON OF 0.08 HADRON CALORIMETER ESTIMA

		Liq Scint	Spaghetti
	Catagory	Conservative	Conservative
1.00	Material/Modules	$9,809	$16,615
2.00	Sense Material	$468	$6,600
3.00	Readout	$8,016	$3,400
4.00	Structure	$400	$1,600
5.00	Ass, Fab and Test	$11,402	$16,500
6.00	Thermal Cont	$980	$980
7.00	Oper. Testing	$2,500	$2,500
8.00	Installation	$2,800	$3,000
9.00	Shipping	$500	$500
	DIRECT COST	$36,875	$51,695
	EDIA	25%	25%
	BASE COST	$46,094	$64,619
	CONTINGENCY	30%	25%
	SUBTOTAL	$59,922	$80,773
	R&D	11%	11%
	TOTAL	$66,513	$89,659

Conservative Scintillating Fiber Hadron Calorimeter-Cost Analysis

	Catagory	Tot Uts	$K/UNIT	Units	Costs
1.00	Towers				
1.10	Lead	2126	5.58	Mton	$11,855
1.20	Fiber	6.60E+06	0.00100	Meters	$6,600
1.40	Sheaths	3308	0.60	Each	$1,985
1.50	Light Guides	13232	0.10	Each	$1,323
1.60	Spacers	3308	0.18	Each	$595
1.70	Top Plate	3308	0.20	Each	$662
1.80	Calib. Loops	120	2.00	Each	$240
2.00	Readout				
2.10	PMT's	13232	0.60	Each	$7,939
2.20	Electronics	13232	0.25	Channels	$3,308
3.00	Structure	200000	0.008	Lbs	$1,600
4.00	Thermal Cont				$980
5.00	Fab & Ass.				
5.10	Fab,Ass & Test	23	0.045	M-H/tower	$13,695
5.20	Tooling				$3,000
6.00	Testing				$2,500
6.10	Test Beam				
6.20	Test Equip				
7.00	Transport.				$500
8.00	Installation				
8.10	Install. Labor	33,333	0.045	Man-Hour	$1,500
8.20	Install. Equip				$1,500
	Direct cost				$59,782
	EDIA	25%			$14,945
	Base Cost				$74,727
	Contingency	25%			$18,682
	Subtotal				$93,409
	R&D	11%			$10,275
	Total				$103,684

Revised Scintillating Fiber Hadron Calorimeter 0.08-Cost Analysis

	Catagory	Tot Uts	$K/UNIT	Units	Costs
1.00	Towers				
1.10	Lead	2126	5.58	Mton	$11,855
1.20	Fiber	6.60E+06	0.00100	Meters	$6,600
1.40	Sheaths	4000	0.60	Each	$2,400
1.50	Light Guides	4000	0.15	Each	$600
1.60	Spacers	4000	0.18	Each	$720
1.70	Top Plate	4000	0.20	Each	$800
1.80	Calib. Loops	120	2.00	Each	$240
2.00	Readout				
2.10	PMT's	4000	0.60	Each	$2,400
2.20	Electronics	4000	0.25	Channels	$1,000
3.00	Structure	200000	0.008	Lbs	$1,600
4.00	Thermal Cont				$980
5.00	Fab & Ass.				
5.10	Fab,Ass & Test	75	0.045	M-H/tower	$13,500
5.20	Tooling				$3,000
6.00	Testing				$2,500
6.10	Test Beam				
6.20	Test Equip				
7.00	Transport.				$500
8.00	Installation				
8.10	Install. Labor	17,000	0.045	Man-Hour	$765
8.20	Install. Equip				$2,235
	Direct cost				$51,695
	EDIA	25%			$12,924
	Base Cost				$64,618
	Contingency	25%			$16,155
	Subtotal				$80,773
	R&D	11%			$8,885
	Total				$89,658

Liquid Scintillator Hadron Calorimeter-Cost Analysis

	Catagory	Tot Uts	$K/UNIT	Units	Total Cost	
1.00	Modules					9638.6
1.10	Lead	1923	2.20	Mtons	4,231	
1.20	Fiber	2.08E+06	0.00035	Meters	728	
1.30	Shrouds	256	15.00	Each	3,840	
1.40	Trays	100000	0.002	each	200	
1.50	Liquid System	256	2.50	each	640	
2.00	Sense Material	26000	0.018	Liters	468	
3.00	Readout					15625
3.10	Electronics	50000	0.250	Channels	12,500	
3.20	PMT't	3125	1.000	each	3,125	
4.00	Structure				400	
5.00	Assembly					16261.5
5.10	Ass & Test	3.00E+05	0.045	MH	13,500	
5.20	Tooling				1,800	
5.30	Lead Processing	1923	0.50		962	
6.00	Thermal Cont				980	
7.00	Testing				2,500	
8.00	Installation					
8.10	Install. Manp	20000	0.045	MH	900	
8.20	Inst. Tooling				1,900	
9.00	Shipping				500	
	DIRECT COST				49,173	
	EDIA	25%			12,293	
	BASE COST				61,466	
	CONTINGENCY	25%			15,367	
	SUBTOTAL				76,833	
	R&D	11%			8,452	
	TOTAL				85,285	

Liquid Scintillator Hadron Calorimeter-"Optimistic" Cost Analysis

	Catagory	Tot Uts	$K/UNIT	Units	Total Cost
1.00	Modules				
1.10	Lead	1923	2.20	Mtons	4,231
1.20	Fiber	2.08E+06	0.00035	Meters	728
1.30	Shrouds	256	8.00	Each	2,048
1.40	Trays	133530	0.002	each	267
1.50	Liquid System	256	2.50	each	640
2.00	Sense Material	26000	0.010	Liters	260
3.00	Readout				
3.10	Electronics	50000	0.250	Channels	12,500
3.20	PMT't	3125	1.000	each	3,125
4.00	Structure				400
5.00	Assembly				
5.10	Ass & Test	800	0.045	MH/Tower	9,216
5.20	Tooling				1,800
5.30	Lead Processing	1923	0.50		962
6.00	Thermal Cont				980
7.00	Testing				2,500
8.00	Installation				
8.10	Install. Manp	10000	0.045	MH	450
8.20	Inst. Tooling				1,900
9.00	Shipping				500
	DIRECT COST				42,506
	EDIA	25%			10,627
	BASE COST				53,133
	CONTINGENCY	25%			13,283
	SUBTOTAL				66,416
	R&D	11%			7,306
	TOTAL				73,722

Liquid Scintillator Hadron Calorimeter 0.08-Cost Analysis

	Catagory	Tot Uts	$K/UNIT	Units	Total Cost
1.00	Modules				
1.10	Lead	1923	2.96	Mtons	5,692
1.20	Fiber	1.40E+06	0.00035	Meters	491
1.30	Shrouds	192	15.00	Each	2,880
1.40	Trays	133000	0.002	each	266
1.50	Liquid System	192	2.50	each	480
2.00	Sense Material	26000	0.018	Liters	468
3.00	Readout				
3.10	Electronics	25280	0.250	Channels	6,320
3.20	PMT's	1696	1.000	each	1,696
4.00	Structure				400
5.00	Assembly				
5.10	Ass & Test	1,000	0.045	MH/tower	8,640
5.20	Tooling				1,800
5.30	Lead Processing	1923	0.50		962
6.00	Thermal Cont				980
7.00	Testing				2,500
8.00	Installation				
8.10	Install. Manp	20000	0.045	MH	900
8.20	Inst. Tooling				1,900
9.00	Shipping				500
	DIRECT COST				36,875
	EDIA	25%			9,219
	BASE COST				46,094
	CONTINGENCY	30%			13,828
	SUBTOTAL				59,922
	R&D	11%			6,591
	TOTAL				66,513

COST TO WEIGHT RATIOS FOR MAJOR DETECTOR PROPOSALS

	Weight	Total Cost	Cost/Ton	Cost/Pound
L*- Liq Scintill**	2099	$89,112	$42K	$19
E/T-Spghetti	2378	$103,000	$43K	$20
E/T-Liq Argon	3075	$156,750	$51K	$23
SDC-Liq Argon	4700	$159,000	$34K	$15
SDC-Pla. Tile	5300	$198,300	$37K	$17
GEM -Spaghetti**	2322	$103,684	$45K	$20
Alternative				
0.08 Conservative	2322	$89,658	$39K	$18
0.08 Alternative				
GEM-Liquid Arg	3000	$155,000	$52K	$23
GEM-Liq Scint.**	2099	$85,285	$41K	$18
Optimistic	2099	$73,722	$35K	$16
0.08 Conservative	2099	$66,513	$32K	$14
CDF-Pb/Scint.				$14
ZEUS-Ur/Scint.				$29

Costs include Electronics
Costs include Therio Adjustment
GEM estimates are preliminary
****Does not include EM calorimeter**
Items included in CDF and ZEUS calorimeters are unknown

GEM-TN-91-7

INDEPENDENT COST ESTIMATE OF THE SPAGHETTI HADRON CALORIMETER

by

C.S. Draper Laboratory Inc.
Cambridge, MA
5 September 1991

F. Ayer
C. Elder
D. Sullivan
E. Womble

CSDL APPLICABLE EXPERIENCE

- Non-profit Research & Development Corporation
- 50 years of design, development and prototype fabrication experience
- 50 years experience transferring technology to industrial contractors
- Industrial engineering consultant to high volume industries: automotive, electronics
- Developer of industrial automation techniques and equipment for high volume applications: automation, apparel

DRAPER LABORATORY

DRAPER EXPERIENCE WITH TEXAS ET AND GEM COLLABORATIONS

• May - Aug '90	Scintillator Calorimeter Support Structural Design and Evaluation
• Sep - Dec '90	Tower Manufacturing and Costing for Scintillating fiber Calorimeters
• Feb - May '91	Supertower Prototype Development and Casting
• Aug '91	GEM Fiber Calorimeter Cost and Structural Analysis

DRAPER LABORATORY

CALORIMETER COST REDUCTION

- Fewer/larger towers
- Trade high labor costs for materials
- Build precision into tools
- Use of foundry type procedures/costs/efficiencies not skilled labor
- Apply automation where practical

DRAPER LABORATORY

COST ANALYSIS APPROACH

- Cost analysis format is derived from ORNL spread sheet
- Our unit costs are based on discussions with ORNL, BU, collaboration physicists (Hans Paar) and vendors for fibers, lead, steel, and fabrication.
- We present 3 cost analyses:

  A. Nominal design with new fiber cost and new contingency rationale

  B. Same as "A" but used 50% lead shot and a slightly smaller calorimeter

  C. Same as "B" with reduced physics segmentation

CSDL

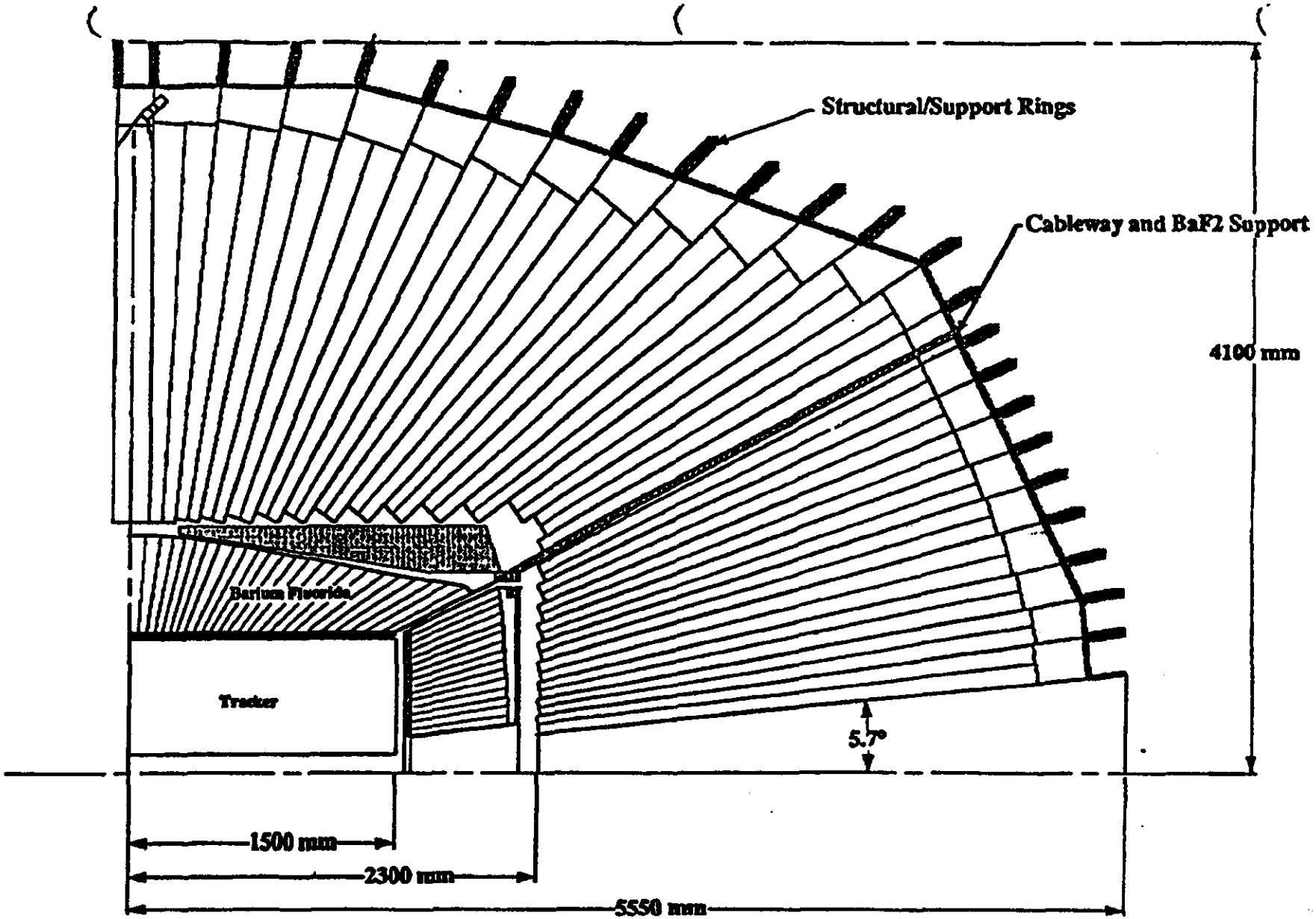

Spaghetti Hadron Calorimeter
Barium Fluoride EM Calorimeter

LS.03.SC.00037

Rennich

GEM Calorimeter Structures

The structural weight is estimated by extrapolation from our Texas calorimeter design, analysis, and evaluation (Aug. 90).

Texas Calorimeter		GEM Calorimeter	
• Ellipsoidal	20m long dia 10m short dia	"Ellipsoidal"	11m long dia 8m short dia
• Towers	Volume 753 m^3	Volume	273 m^3
• Structures	Tons		Tons
Shell Plate(2cm)	80	Plate (1.5cm)	30
Rings Circumfer.	64	Rings	25
and Longitudinal Supporting Frames	174	*Support to membrane	30
	318 Tons		85 Tons = 187,000 lbs

* The present design assumes a central membrane to support the calorimeter structure in the middle. Special structural members are required for a stable attachment. Our estimate is 30 tons.

CSDL

TEXAS CALORIMETER – STRUCTURAL SYSTEM

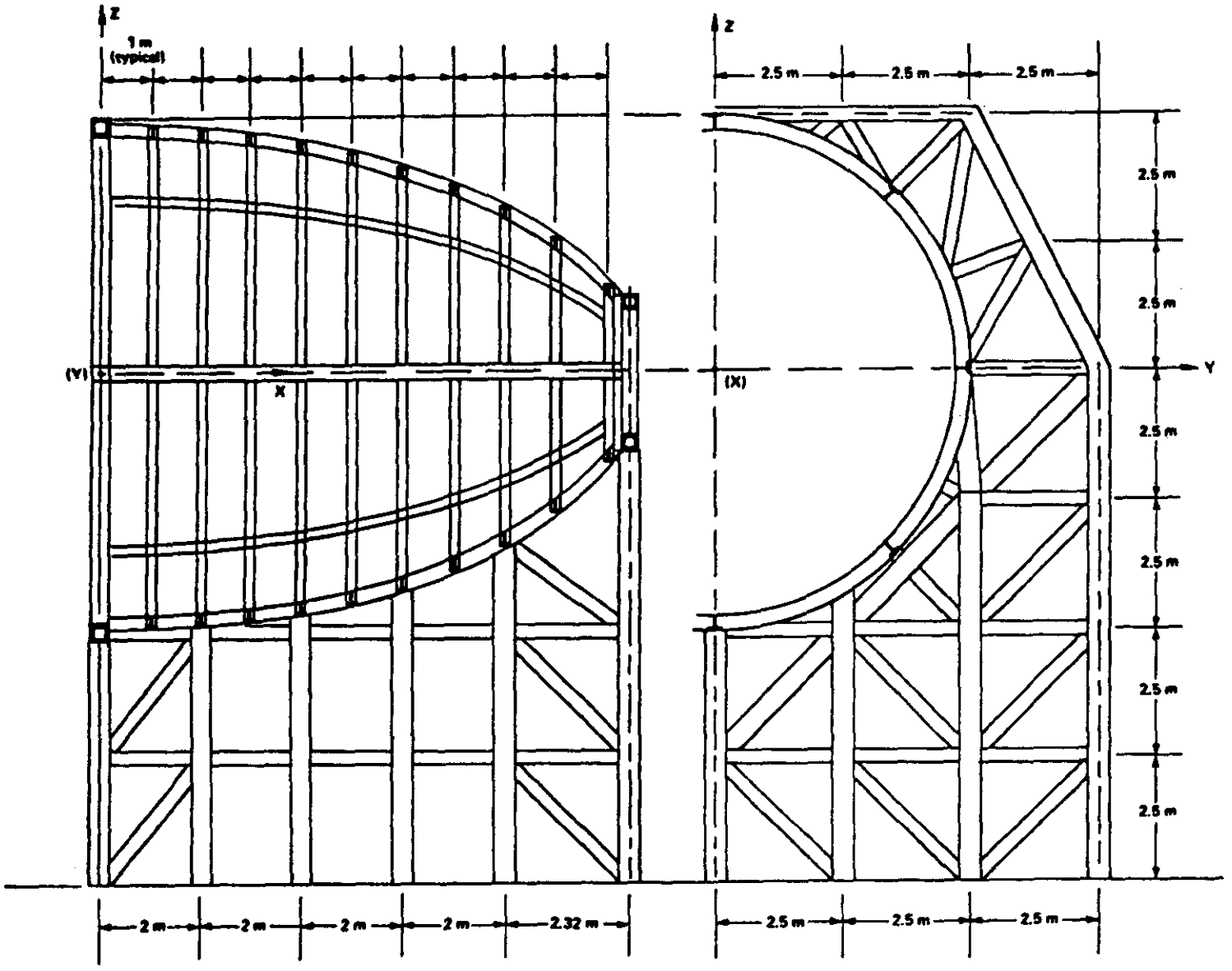

MATERIAL QUOTES

- **Fibers 3mm scintillating type RH-1**

  Bicron Corp.

  Quoted 7,600,000 for 6000km of fiber

  includes: fiber, trimming, heading, inserting into spacer plates, boxing, shipping, and wastage

  Contingency: Bicron suggests no more than 10%

  Note that this represents $1.27/m with labor previously counted in tower construction

  See attached Bicron letter for details.

- **Stainless Steel**

  Ryerson, Allston Ma, new line

  Quoted $2/lb. for 304 type ST. steel

  Used $5/lb for structural system and sheaths to account for fabrication processes. Contingency should be no more than 10%.

- **Lead Shot**

  Tarcorp Industries, Granite, Illinois

  Quoted $0.45/lb for dust shot of 0.6mm dia. average.

  Produces 30m lbs/year of lead shot

  Contingency should be no more than 10%

CSDL

GEM DETECTOR

SCINTILLATING FIBER HADRON CALORIMETER

COST ANALYSIS A

	Category	Tot Uts	$K Unit	Units	Costs $K
1.00	Towers				
1.10	Lead	2126	5.58	Mton	$11,855
1.20	Fiber	6.00E + 06	.00127	Meters	$7,600
1.30	PMT's	13232	0.30	Each	$3,970
1.40	Sheaths + Cover Plate	3308	.40	Each	$1,323
1.50	Light Guides	13232	0.10	Each	$1,323
1.60	Spacer Plates	3308	0.20	Each	$662
2.00	Electronics	13232	0.25	Channels	$3,308
3.00	Structure	187,000	0.005	LBS	$935
4.00	Thermal Cont				$500
5.00	Fab & Ass.				
5.10	Fab. Ass. & Test	15.8	0.045	M-H/tower	$9,380
5.20	Tooling				$3,000
6.00	Testing				
6.10	Test Beam				$1,000
6.20	Test Equip				
7.00	Transport				$500
8.00	Installation				
8.10	Install. Labor	17,000	$45/MH	Man-Hour	$765
8.20	Install. Equip				$1000
DIRECT COST					$47,121
EDIA		25%			$11,780
BASE COST					$58,901
CONTINGENCY*		25%, 10%			$10,654
SUBTOTAL					$69,555
R&D		11%			$7,651
TOTAL					$77,206

*Contingency: 10% on lead, fiber, and steel
25% on other items

GEM CALORIMETER

SCINTILLATING FIBER HADRON CALORIMETER

COST ANALYSIS B

	Category	Tot Uts	$K Unit	Units	Costs $K
1.00	Towers				
1.10A	Ostalloy 50%	948	5.58	Mton	$5,290
1.10B	Lead Shot 50%	1139	.99	Mton	$1,128
1.20	Fiber	5.7E + 06	.00127	Meters	$7,239
1.30	PMT's	13232	0.30	Each	$3,970
1.40	Sheaths + Cover Plate	3308	.40	Each	$1,323
1.50	Light Guides	13232	0.10	Each	$1,323
1.60	Spacer Plates	3308	0.20	Each	$662
2.00	Electronics	13232	0.25	Channels	$3,308
3.00	Structure	160,000	0.005	LBS	$800
4.00	Thermal Cont				$500
5.00	Fab & Ass.				
5.10	Fab. Ass. & Test	15.8	0.045	M-H/tower	$9,380
5.20	Tooling				$3,000
6.00	Testing				
6.10	Test Beam				$1,000
6.20	Test Equip				
7.00	Transport				$500
8.00	Installation				
8.10	Install. Labor	17,000	$45/MH	Man-Hour	$765
8.20	Install. Equip				$1000
DIRECT COST					$41,188
EDIA		25%			$10,297
BASE COST					$51,485
CONTINGENCY*		25%, 10%			$9,912
SUBTOTAL					$61,397
R&D		11%			$6,754
TOTAL					$68,151

*Contingency: 10% on lead, fiber, and steel
25% on other items

GEM CALORIMETER

SCINTILLATING FIBER HADRON CALORIMETER

COST ANALYSIS C

	Category	Tot Uts	$K Unit	Units	Costs $K
1.00	Towers				
1.10A	Ostalloy 50%	948	5.58	Mton	$5,290
1.10B	Lead Shot 50%	1139	.99	Mton	$1,128
1.20	Fiber	5.7E + 06	.00127	Meters	$7,239
1.30	PMT's	3308	0.30	Each	$992
1.40	Sheaths + Cover Plate	3308	.40	Each	$1,323
1.50	Light Guides	3308	0.20	Each	$662
1.60	Spacer Plates	3308	0.20	Each	$662
2.00	Electronics	3308	0.25	Channels	$827
3.00	Structure	160,000	0.005	LBS	$800
4.00	Thermal Cont				$500
5.00	Fab & Ass.				
5.10	Fab. Ass. & Test	15.8	0.045	M-H/tower	$9,380
5.20	Tooling				$3,000
6.00	Testing				
6.10	Test Beam				$1,000
6.20	Test Equip				
7.00	Transport				$500
8.00	Installation				
8.10	Install. Labor	17,000	$45/MH	Man-Hour	$765
8.20	Install. Equip				$1000
DIRECT COST					$35,068
EDIA		25%			$8,767
BASE COST					$43,835
CONTINGENCY*		25%, 10%			$8,000
SUBTOTAL					$51,835
R&D		11%			$5,702
TOTAL					$57,537

*Contingency: 10% on lead, fiber, and steel
25% on other items

SUMMARY

- Calorimeter design, fabrication, assembly, and testing are still preliminary and evolving.
- Cost estimates are based on realistic enquiries (quotes) to specialists and vendors.
- Quantities (lead, fiber) have been checked and structural system is based on sound previous work.
- Contingencies for materials (10%) reflect vendors inputs.
- Other costs (labor, tooling, testing etc.) are more difficult to estimate and a higher (25%) contingency is appropriate.

CSDL

FAX TO: CHARLES STARK DRAPER LABORATORIES
ATTN: FRANCOIS AYER
FROM: CHUCK HURLBUT, BICRON CORPORATION
DATE: 5 SEPTEMBER 1991

SUBJECT: BUDGETARY PROPOSAL FOR SCINTILLATING FIBERS FOR THE "GEM" COLLABORATION.

This estimate is for budgetary purposes. It represents the work of several people at Bicron including myself, the two senior engineers which have been assigned to our fiber program for the last three years, our Engineering Manager and our accounting department. We consider this to be a serious estimate with a high degree of accuracy.

We propose to provide the following goods and services:

6,000,000 meters of 3 mm dia. Type RH-1 scintillating fibers cut and assembled into 3,124 "preform" subassemblies as described below.

Total Price: $7,600,000
FOB Newbury, Ohio

The preforms would consist of 3600 individual fibers inserted into a set of precision drilled metal plates. The hole pattern would be a 60 x 60 matrix. The set of plates would be close stacked together resembling a single unit without spaces between the layers. The fibers would be precision cut to various lengths depending on their position in the assembly. The central fibers would be the maximum length, and the fibers would be shorter as their position is closer to the edge of the array. The final assembly would resemble a truncated pyramid. One end of each fiber would be modified to a slightly larger diameter too prevent its falling through its hole when the assembly is held so the fibers hang vertically with the larger end of the array at the top. The longest fiber in each preform would be about 220 cm Each preform would be packaged in an individual wood crate with the precision plate stack still in its condenced configuration.

Delivery would take about twenty months with the first assemblies being shipped about five months after receipt of order.

CONDIFENCE IN MASS PRODUCTION COST EFFICIENCY

Bicron has recently completed an SBIR Phase II development project in which the major task was the development of a mass production system for manufacturing large quantities of scintillating and waveguide optical fibers for use in the SSC. Main elements of this investigation included the following:

- Total factory layout
- Large volume monomer purification and storage
- Polymerization system design to achieve high throughput and quality consistency
- High speed fiber fabrication

Major prototype process equipment was constructed and successfully operated, and some components for the final operation were procurred.

Our estimates of the various cost factors in this proposal are based on our experience from the SBIR work which is now being continued with Bicron internal funding.

MAJOR COST ELEMENTS IN THE PROPOSAL

A. Raw Materials: Allowances were made for all forseeable efficiency problems including potential impact of international tensions affecting petroleum supplies and unpredictable difficulties in starting up the full volume system required for this program.

B. Labor: A full independent factory operating around the clock is envisioned. Personnel considerations included such factors special maintenance staff, dedicated management, training expenses, and impact of efficiencies on total labor required.

C. Factory Overheads: All standard and special factory overheads for the entire time of dedicated operation were included. All costs were accumulated in a zero-based calculation.

D. Special Factory Equipment Costs: A major portion of the factory construction expenses are allocated against this project. Reasons for this include the fact that the factory as constructed will be highly specialized with very little opportunity for cost recovery aside from special SCC projects like this one. A second reason is that a special set of equipment for assembly of the "preforms" will be constructed with the particular costs fully allocated here.

E. Special Preform Assembly Equipment: The concept for this equipment is already well developed as the outcome of a meeting of four members of the Bicron technical staff, each person having over 20 years in manufacturing process design from a variety of backgrounds. Each instrument would inspect the fiber as it is made on the continuous fiber lines and reject it if appropriate. Good fiber would be cut to the appropriate lengths, inserted in the appropriate holes, and altered to have a large "head". It would be a computer controlled system. Three systems would be constructed with one kept in reserve for breakdowns.

ADDITIONAL CONTINGENCIES

Contingencies that SSC planners prefer to add on need not exceed ten percent since significant contingencies have been factored into the above prices.

CURRENT ACTIVITY/INTEREST

L. OSBORNE	STREAMER TUBES MUON LAB
C. BROMBERG	SPAGHETTI MP
H. KOBRAK	BaF_2 NT
F. PLASIL	LIQ. SCINT — ?
W. BUGG	SILICON — ?

KOBRAK

FERMILAB TEST BEAMS

1991 NOW TIL ~15 DEC (? JAN 92)
1994 6 - 10 MONTHS

POLICY ISSUES

1) ONLY APPROVED ACTIVITIES
   (APPROVAL ⇒ REQUEST BY GEM
   ⇒ DETAILED PROPOSAL BY CONTACT PERSON
   ⇒ MOU)
2) NO "SUPPORT" BY FERMILAB
   WE PAY FOR EVERYTHING
   ⇒ "FULL COST RECOVERY"
3) NO BOOTLEGGING
4) ID, SAFETY, ETC.

Superconducting Super Collider Laboratory

Physics Research Division
2550 Beckleymeade Avenue
Mail Stop 2001
Dallas, TX 75237-3946
(214) 708-9000 • FAX (214) 708-0006

6 September 1991

Professor John Peoples, Director
Fermi National Accelerator Laboratory
P. O. Box 500
Batavia, IL 60510

Dear John:

As spokesman of the GEM collaboration at the Superconducting Super Collider, I wish to request access to beam areas at Fermilab for the purpose to test prototypes for components of the GEM detector. These tests will be an important element in making our final decision on GEM detector technologies.

For the period of the current Fermilab Fixed Target period, the following efforts would greatly benefit from test beam time.

Barium Fluoride Calorimetry
Contact person: H.Kobrak, U. of California, San Diego.
A proposal (T-849) has been submitted to Fermilab.

Scintillating Fiber Calorimetry
Contact person: C. Bromberg, Michigan State University.
A proposal (T-840) has been submitted to Fermilab.

Limited Streamer tracking tubes.
Contact person: L. Osborne, MIT.
A proposal (T-819) has been accepted by Fermilab.

Preshower detector
Contact person: C. Rosenfeld, U. of South Carolina.
A proposal (T-841P) has been accepted by Fermilab.

(*) Silicon Electromagnetic Calorimeter
Contact person: W. Bugg, U. of Tennessee.
A detailed proposal will be submitted to Fermilab.

(*) Liquid Scintillator Calorimeter
Contact person: F. Plasil, Oak Ridge National Laboratory. A detailed proposal will be submitted to Fermilab.

Requests marked (*) are conditional to final decisions to be taken by the GEM collaboration by 19 September 1991.

For the 1994 fixed target period, I anticipate that the GEM collaboration will want to request further test beam time. Details of these requests are currently under discussion in the collaboration. We expect submit a set of proposals by Spring of 1992.

For my GEM colleagues and myself. I wish to express our appreciation for your help and that of Fermilab.

Sincerely

Bary

Bary Barish Spokesman,
GEM collaboration

Question (6) What provision has been made for the rejection of pi-zero gammas from unfavorable jet fragmentations? (The rate of such fragmentation has large uncertainties, and these may dominate the Higgs –> gamma gamma background.) If very fine lateral segmentation is proposed, this must be included in the baseline cost.

The following devices are being considered for the rejection of π^o γ's:

1. Drift diodes: Rehak/BNL,

2. Milli-Strip detector:

   - scale from UV-diodes: 14k strip detector at 100$ each,
   - scale from micro-strips: 13k$/5k ch = 3$/ch
   - 30 ch each with 5 bit ADC = 3 $ * 30 * 2 = 18$
   - 280 x 14k = 5 M$.

3. Scin. Fibre: J. Brau

4. TPC Wire chamber: E. Aprile, T. Doke, T. Ypsilantis

The cost is basically included in the baseline, which over-estimates by 4M$ (40% contingency) or 9 M$ (25% contingency).

CHE2

Noble Liquid Calorimeters
LAr/LXe/Kr Calorimeters

- Raiation hard
- Depth measurement
- γ vertex and direction measurement
- Calibration
- Active precision pre-radiator
- Ultra-high resolution:
  - $\delta E/E = 0.8\%$ at 40 GeV
  - $\delta E/E = 0.6\%$ at 100 GeV
  - Same as BGO test beam
- Scintilation fast veto pile up
- Upgradable to LXe precision calorimeter with $\delta E/E = 0.25\%$
- Compatiable with high B-field. enditemize

H. Newman

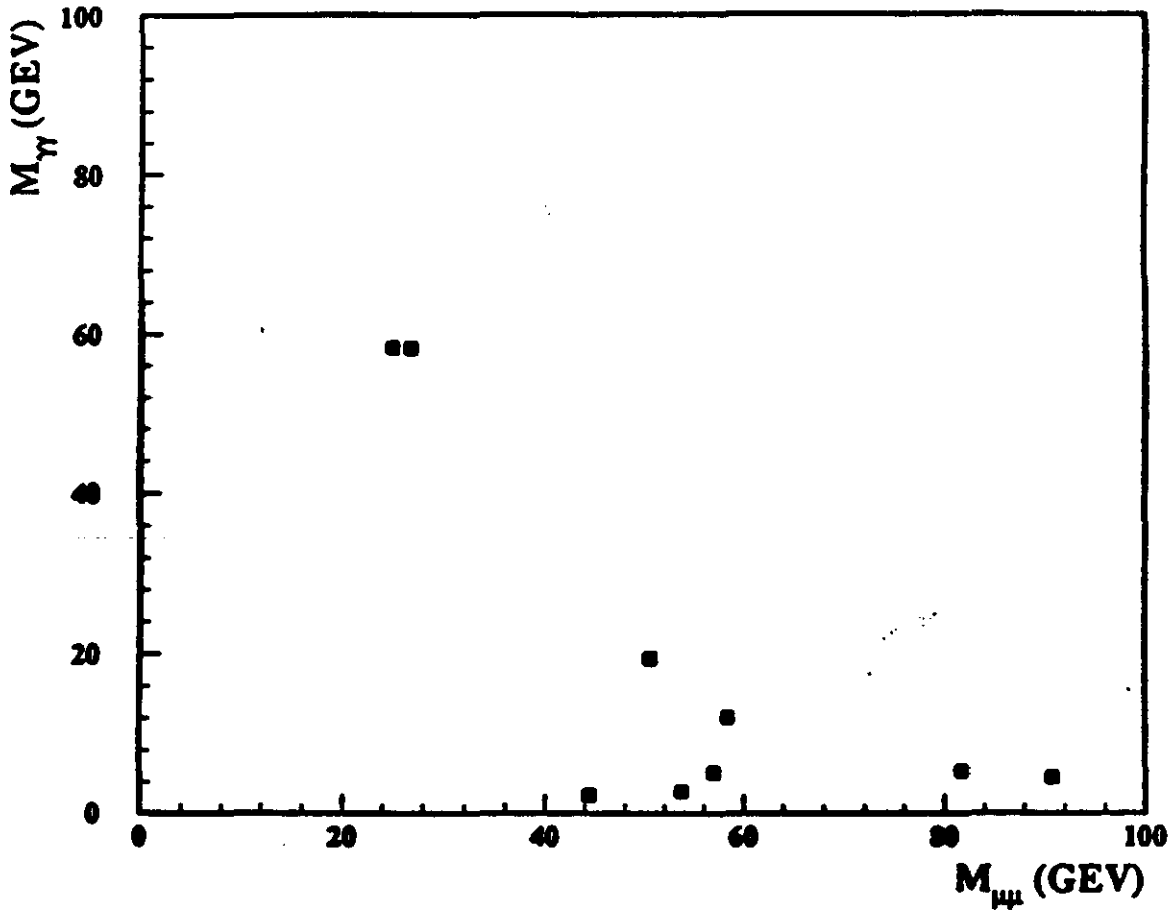

Figure 5.18: Scatterplot of $M_{\gamma\gamma}$ versus $M_{\mu\mu}$ for $\mu\mu\gamma\gamma$ events recorded with the L3 detector.

$\mu^+\mu^-\gamma\gamma$ Events in L3

(WITH BGO ENDCAPS in '91)

→ 2 in 220 K Hadrons

→ $m_{\gamma\gamma}$ = 58.8 GeV; 58.9 GeV
$\sigma \sim 0.6$ GeV

- MC Study $E_{\gamma_1}, E_{\gamma_2} > 1$ GeV
  Isolation Cut $> 5°$

- YFS (3.02) (JADACH & WARD): Prelim.
  Predict 19.3 Events
  See 19 Events
  } $M_{\gamma\gamma}^{MAX} < 25$ GeV

- $P_1 (M_{\gamma\gamma} > 50) = 1\%$ Expect (0.15 ev)
  $P_2 (M_{\gamma\gamma} > 40) = 5.6\%$ Expect (0.38 ev)

- Expectation: 0.035 events Per 1 GeV Bin

- STRANGE: NOTHING in $ee\gamma\gamma$ $q\bar{q}\gamma\gamma$ channels

- But if get 3rd & 4th events:
  EFFECT ESTABLISHED

Run # 311104 Event # 4744 Total Energy : 97.68 GeV

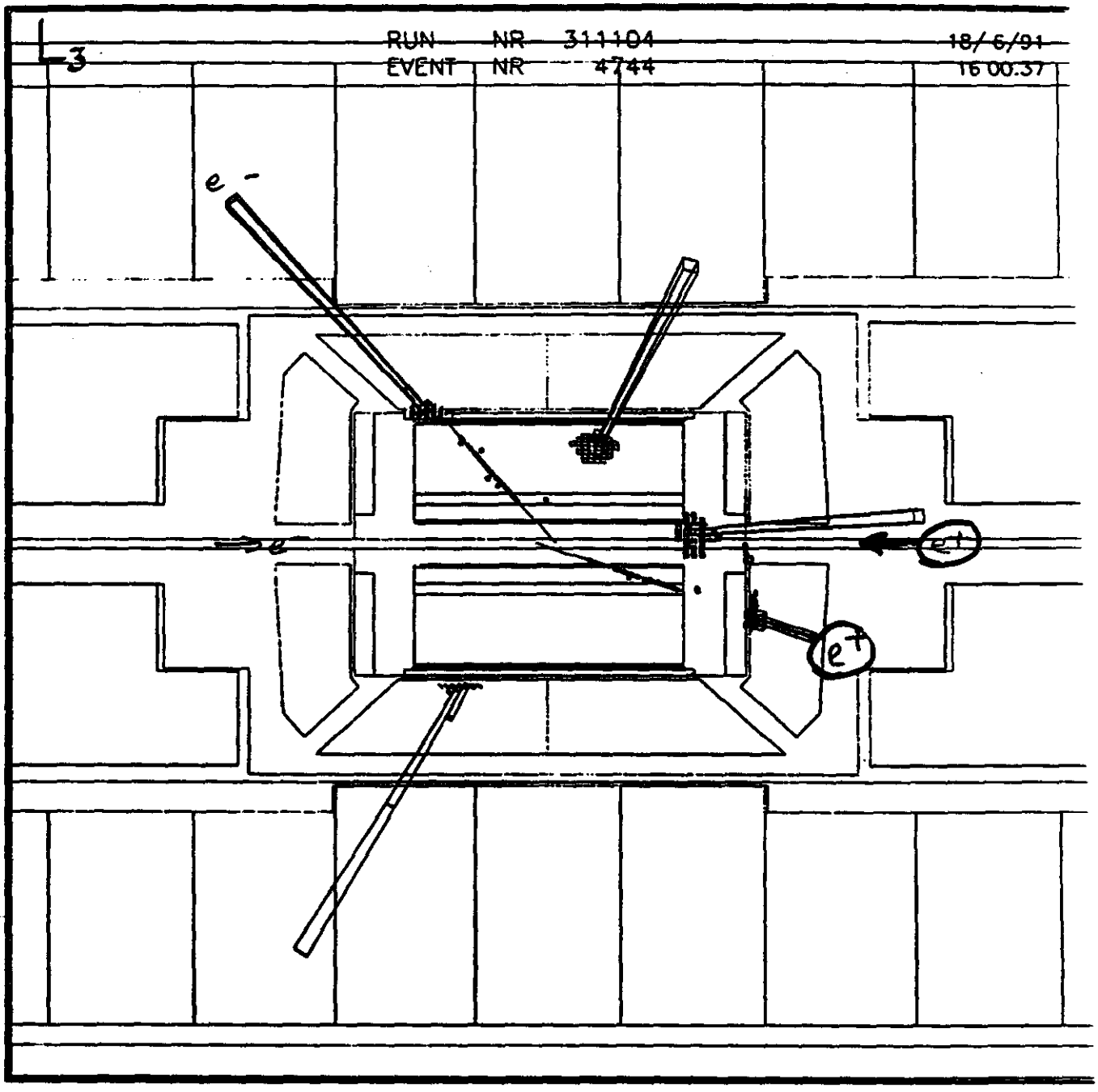

Transverse Imbalance :	0.03 GeV	**Longitudinal Imbalance :**	0.01 GeV
Thrust : 0.6932	**Major :** 0.5962	**Minor :** 0.3037	
Printed Date :	*Sunday, June 23, 1991 17:34: 2*		

Run # 318101 Event # 4813 Total Energy : 88.32 GeV

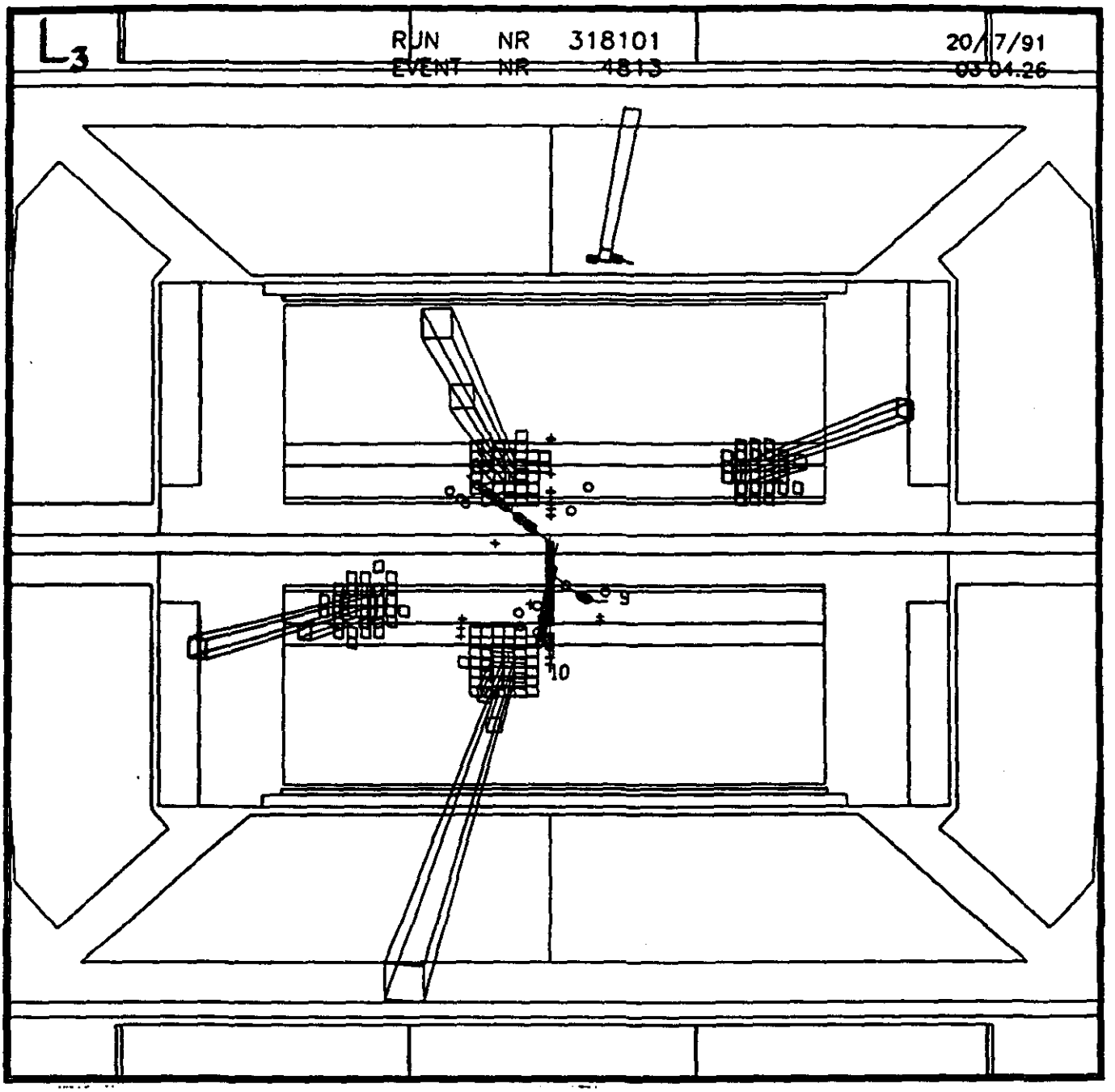

Transverse Imbalance :	94.05 GeV	**Longitudinal Imbalance :**	0.01 GeV
Thrust : -.0965	**Major :** 0.9182	**Minor :** 0.2396	
Printed Date :	*Saturday, July 27, 1991 15:17:28*		

Run # 311104 Event # 4744 Total Energy : 105.18 GeV

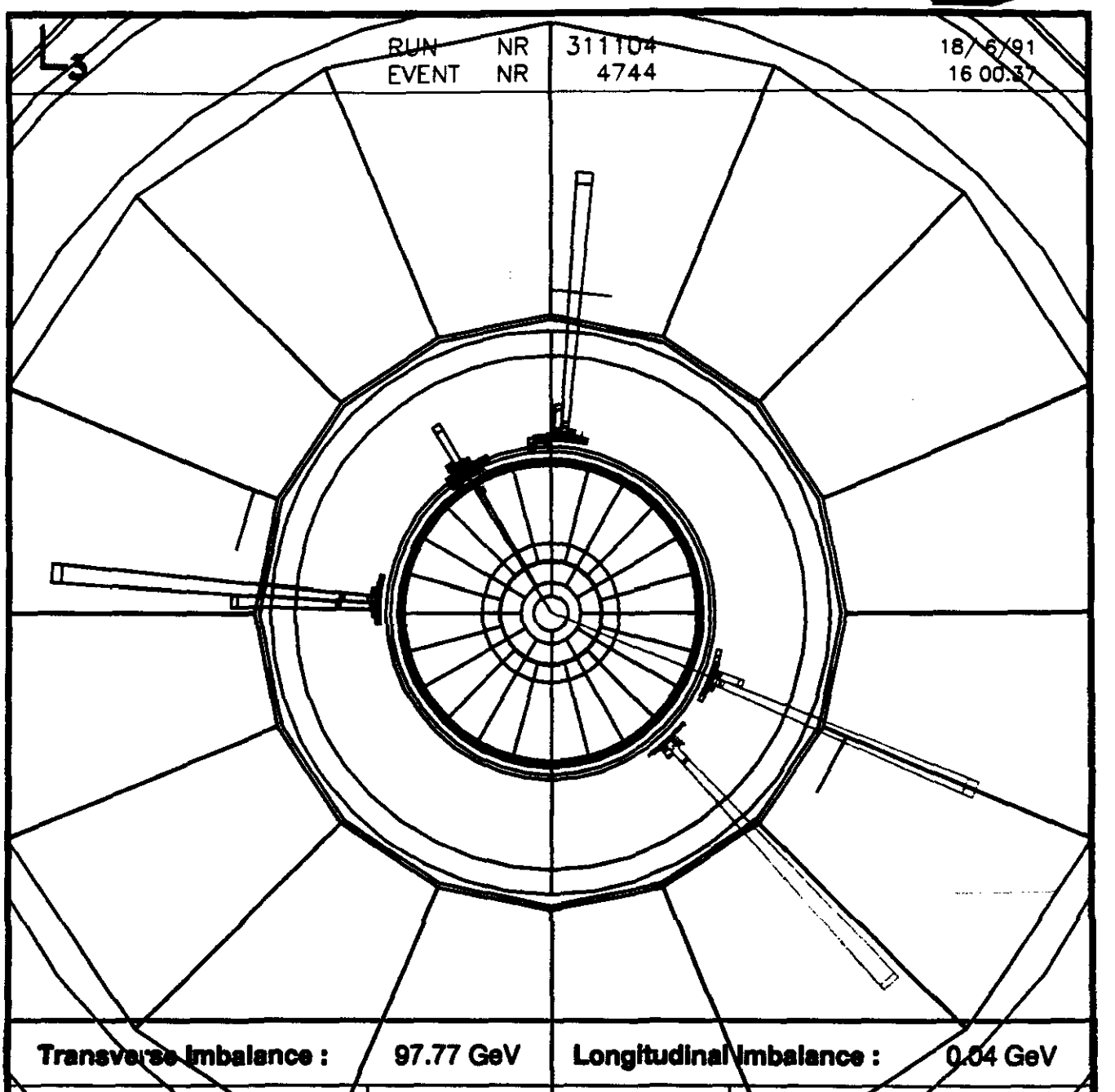

Transverse Imbalance :	97.77 GeV	**Longitudinal Imbalance :**	0.04 GeV

Thrust : -.0323	**Major :** 0.5993	**Minor :** 0.5846

Printed Date : *Friday, June 28, 1991 17:23:18*

HJN

PHYSICS of ELECTRONS and PHOTONS At The TeV SCALE

ISOLATE NEW PHYSICS SIGNALS

from "Standard" Physics Backgrounds

- **Cleanly Separate Leptons and Photons from Jets and Single Hadrons.**
- **Reconstruct Multilepton, Multiphoton, and Lepton-Photon Invariant Masses Precisely**

BARIUM FLUORIDE CALORIMETER CALIBRATION

- **Minimum Ionizing Particles (MIPs) from pp Collisions**
  - Pass Through Crystals Longitudinally
  - Calibrate to 0.4% in 12 Hours

- **Verify With Inclusive** e^+e^- From Z^0, Υ, J
  - Reconstruct Mass: Use RFQ + MIP Results
  - 200 e^+ or e^- from Υ, 20 from Z^0 Per Crystal Per Week

Peak at 226 MeV ⇒ 9.42 MeV/cm
Δ ≈ 5 bin of 8 MeV ⇒ 38 MeV
σ ≈ 16 MeV σ⁻ ≈ 13.6 MeV
σ/E ≈ 7.1% σ⁻/E ≈ 6.0%

L3 / B.G.O
JULY 90
S. T. + D.B.

~ 30 000 μ⁺ tracks
~ ½ of 1990
~ 5100 MIP

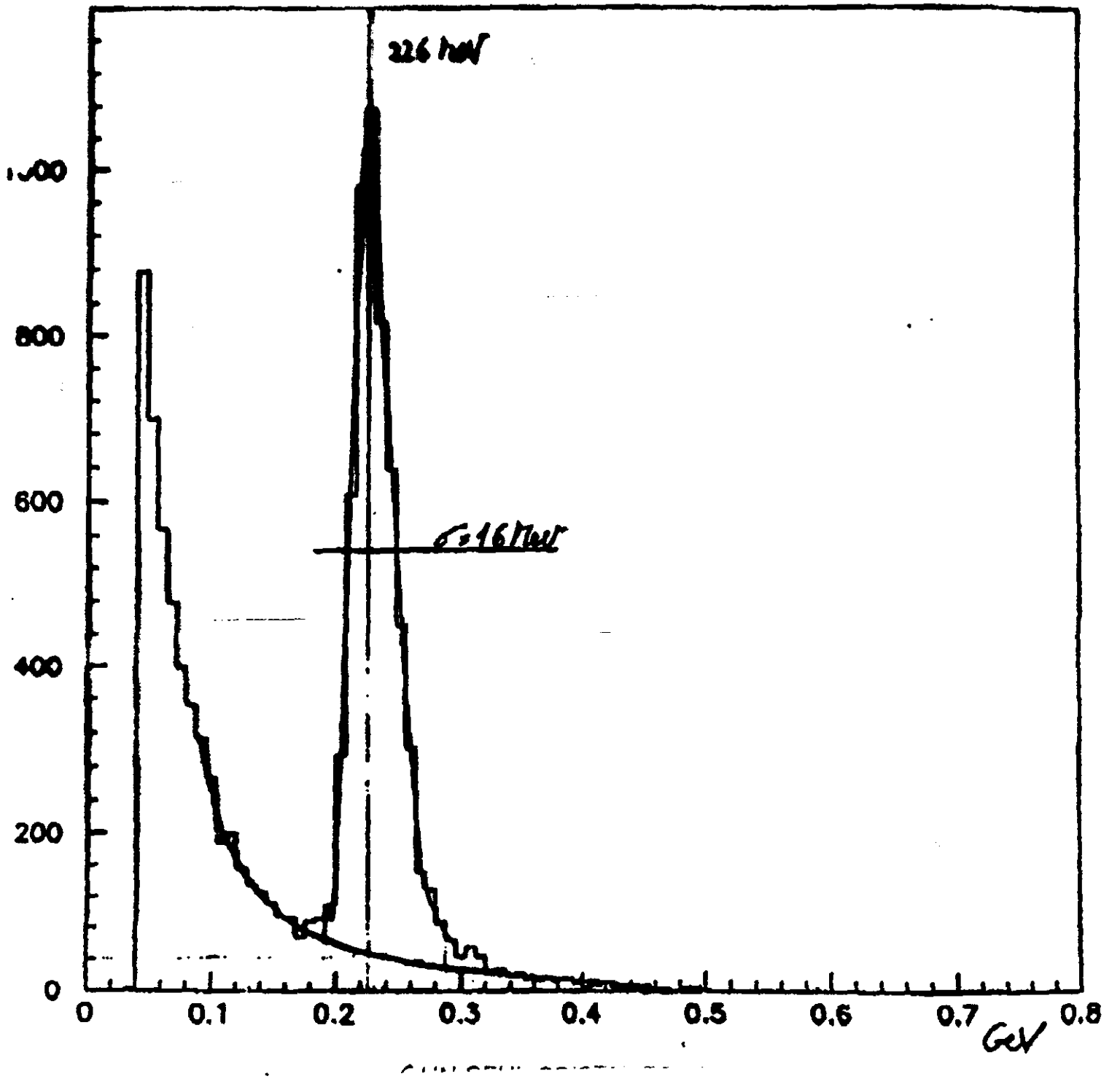

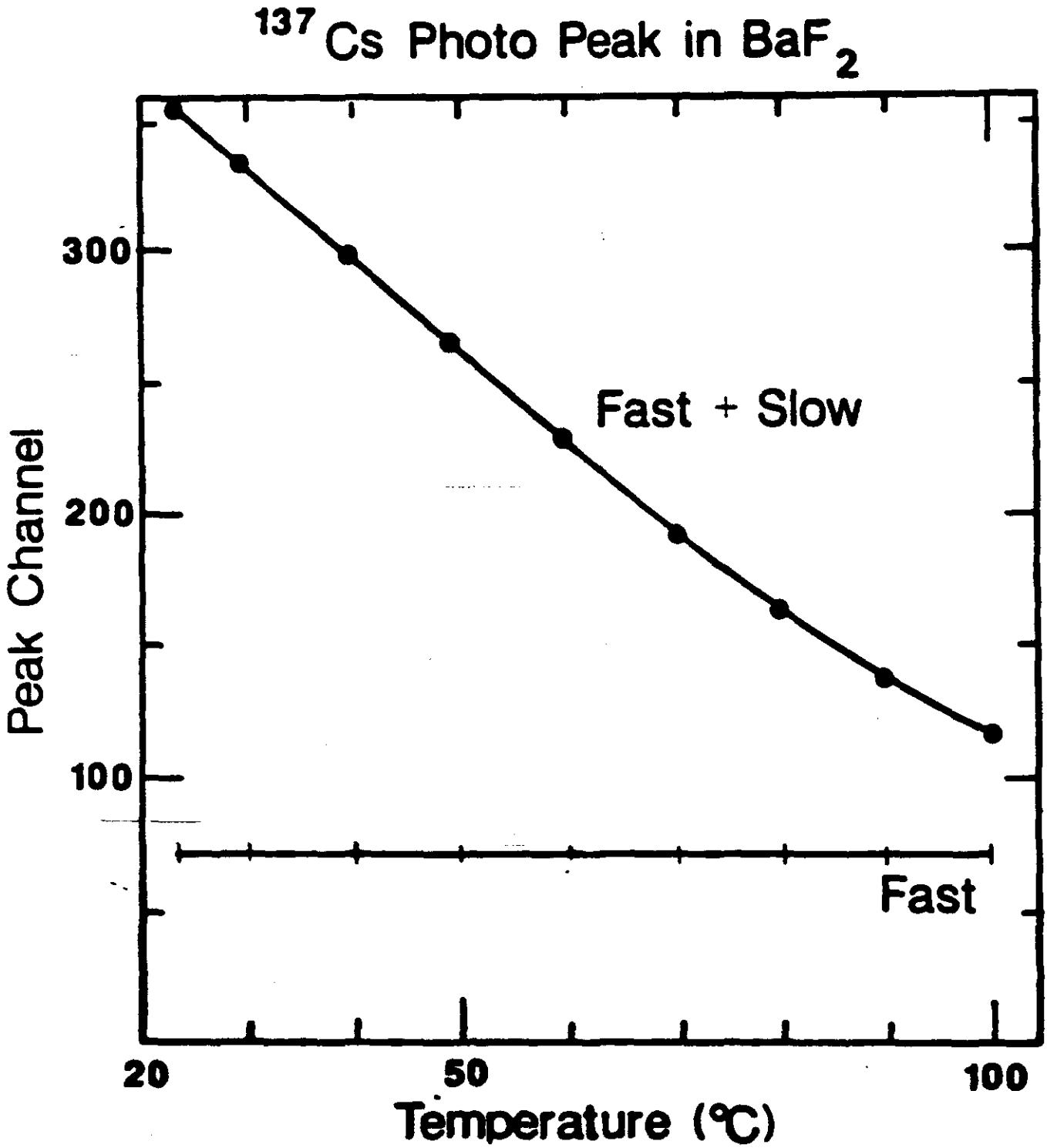
^{137}Cs Photo Peak in BaF_2
Peak Channel
300
200
100
Fast + Slow
Fast
20
50
100
Temperature (°C)

Electron Energy Smeared at Generator Level

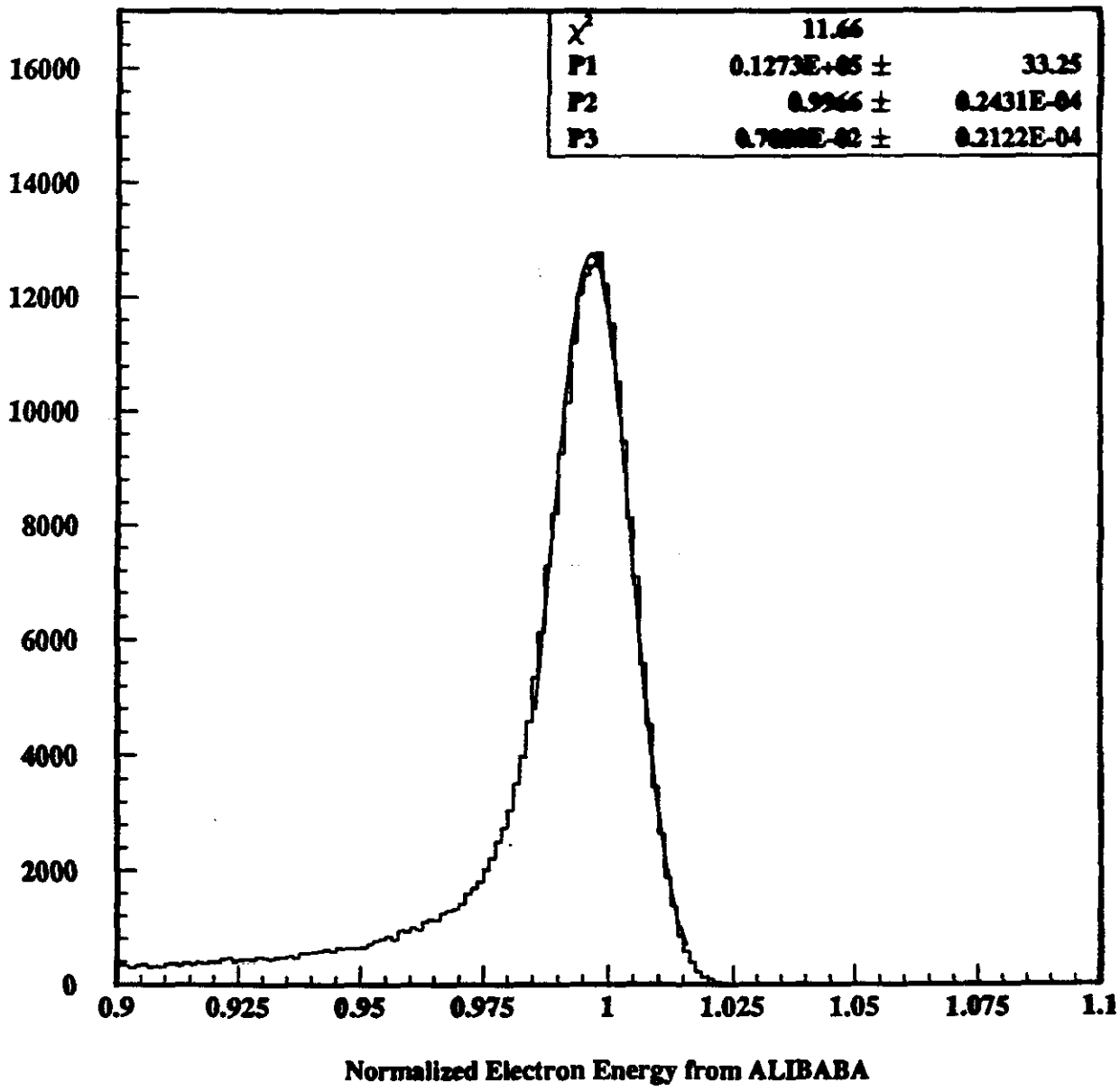

tully.l3.none.1FD23

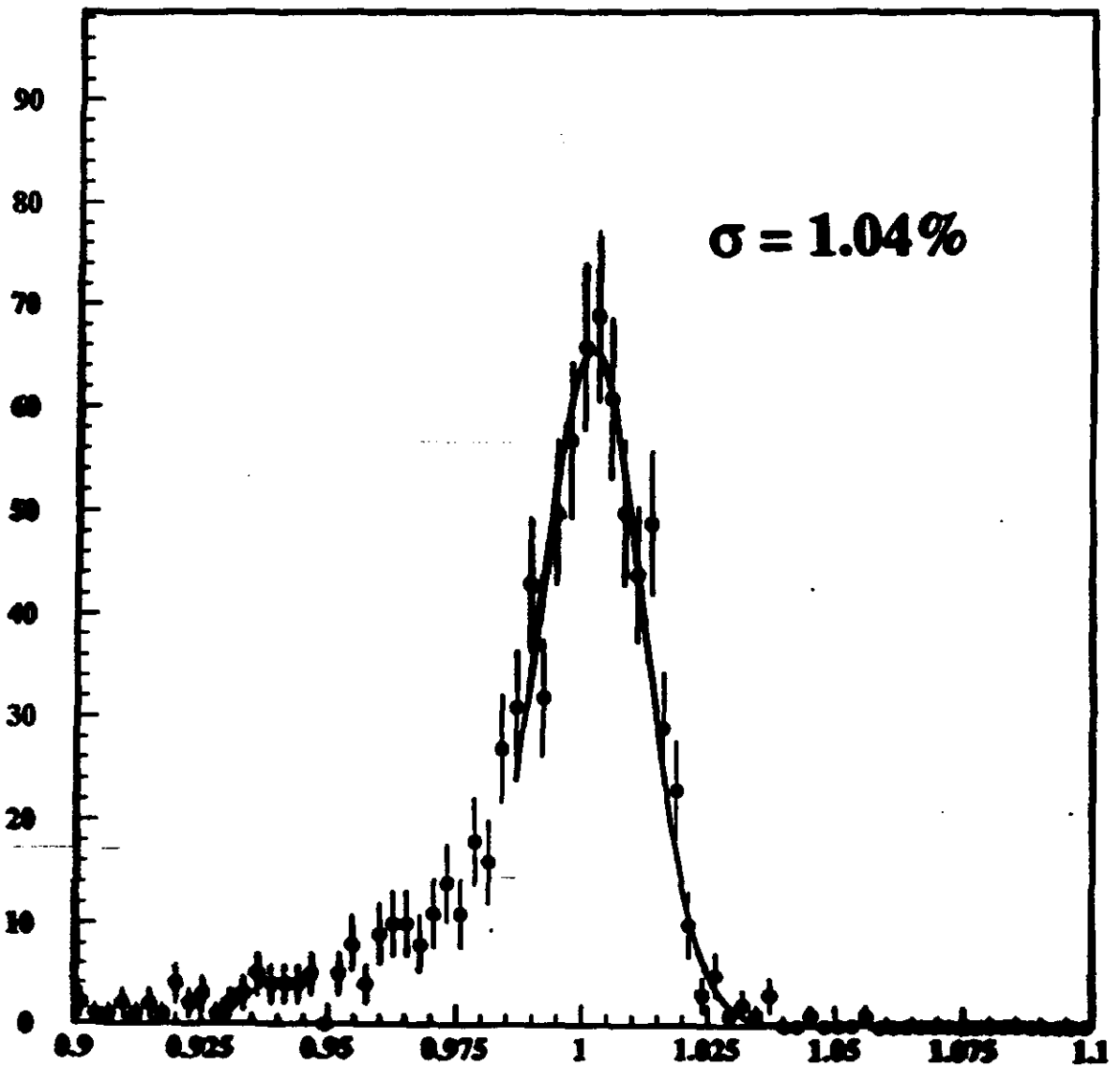
σ = 1.04%
90
80
70
60
50
40
30
20
10
0
0.9
0.925
0.95
0.975
1
1.025
1.05
1.075
1.1

Position Dependence for 90ab and 91a Data

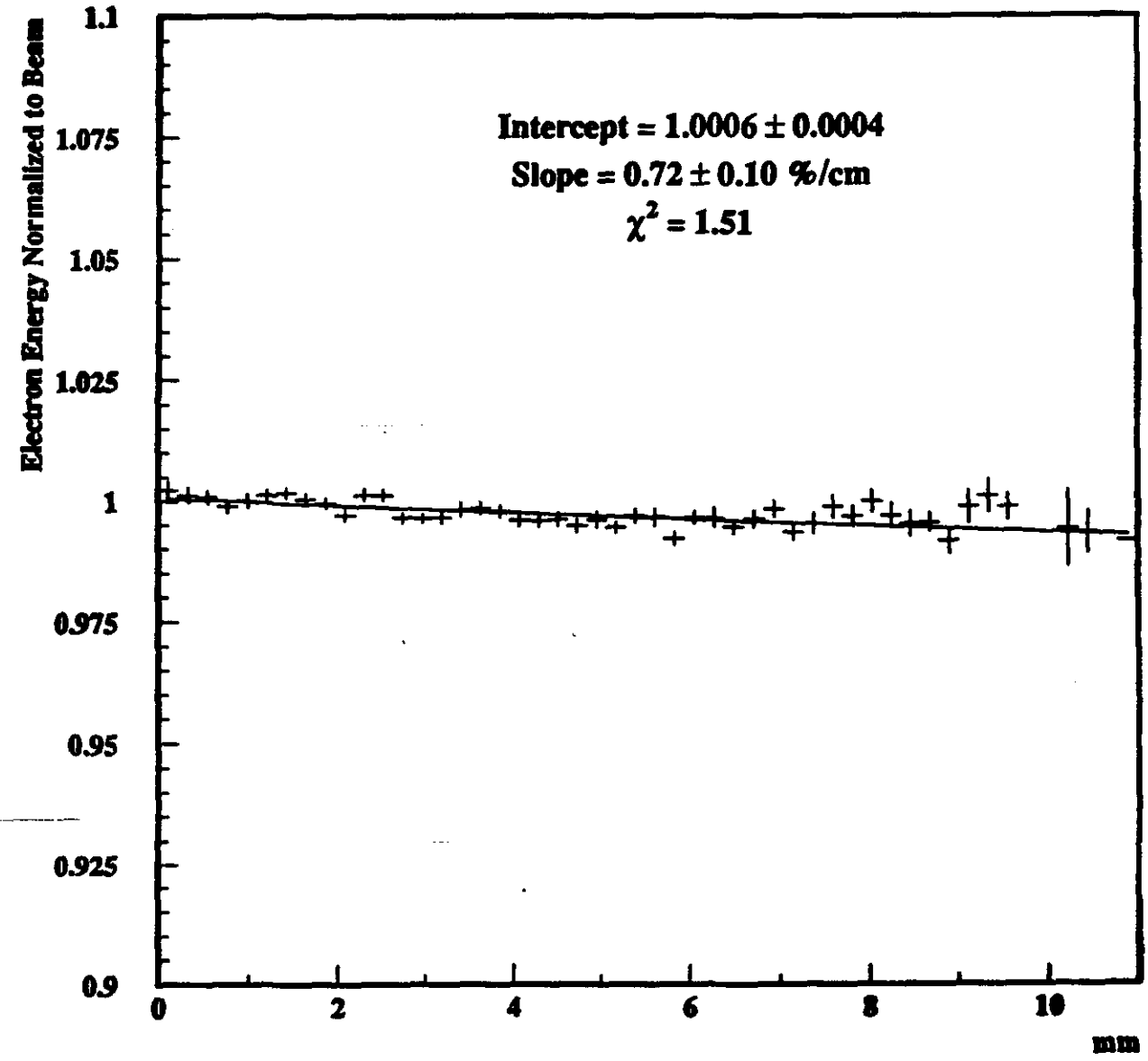

Electron Energy Measured in L3 BGO Calorimeter

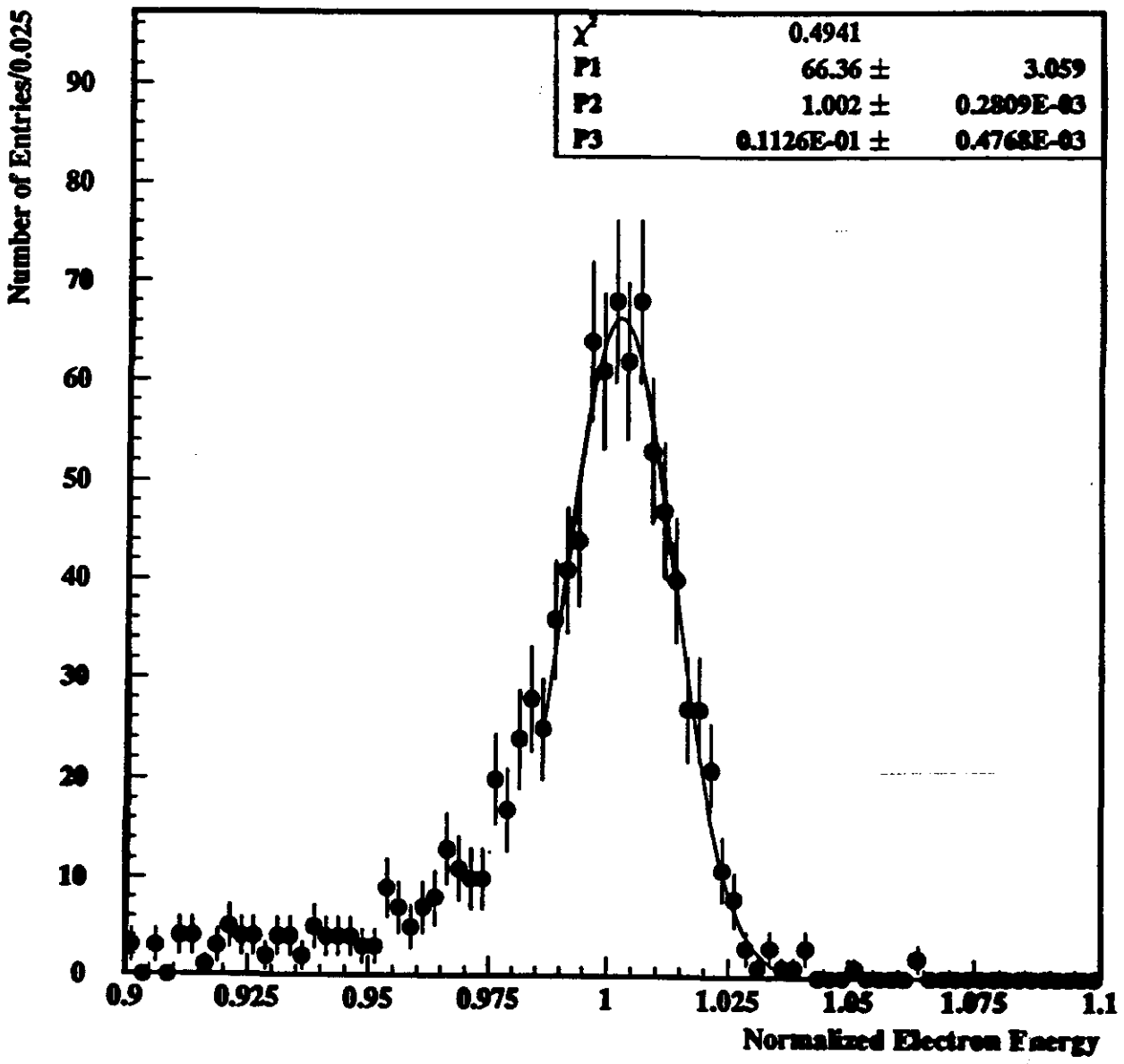

HW

BGO energy measurement resolution

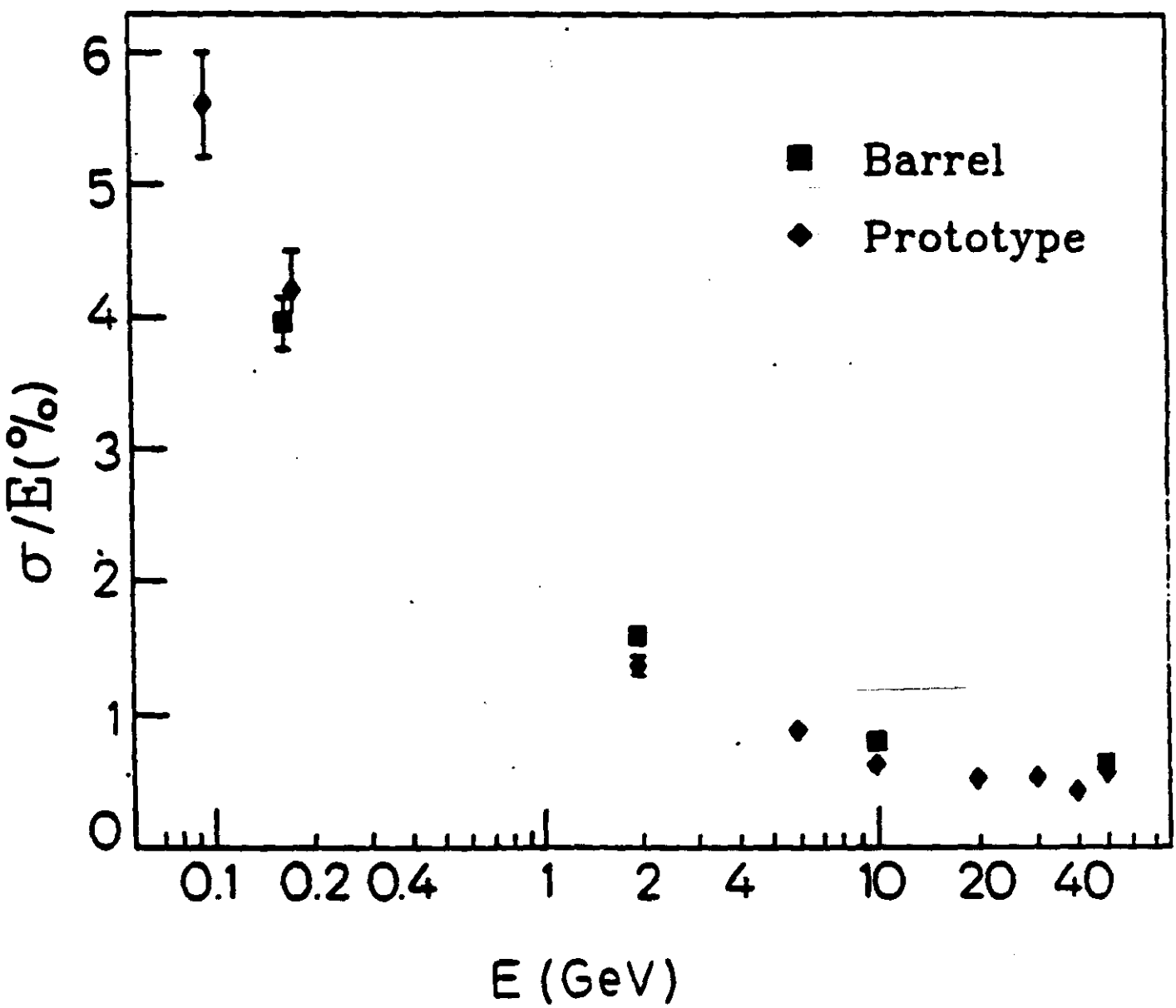

- Studies of the BaF_2 Radiation Damage Mechanism at SIC

- **Light Collection Uniformity**
  - EGS Study of Light Uniformity Requirements in Coupled Crystals

- **Test Beams**
  - Beam Requirements
  - Test Beam Status at Fermilab

- **BaF_2 Calorimeter Performance**
  - Position Resolution
  - Energy Resolution

- **R&D Budget**

- **Attachment: Progress Report on BaF_2 R&D at BNL**

APPENDICES

- **Mass Production of BaF_2 Crystals in China**
  - UV Transmittance of the Crystals
  - Memorandum of Understanding Between Caltech, SIC and BGRI for BaF_2 Crystal Mass Production in China
  - Production Capacity and Investments in China
- **Structural Design of the BaF_2 Calorimeter, and the Final Prototype**
  - Design Concept
  - Carbon Fiber Structure
  - Structure for the Final Prototype
  - Materials Study for the Structure
  - Other Design Aspects: Electronics Placement, Cable Routing and Thermal Control
- **BaF_2 Radiation Resistance**
  - Measurements of BaF_2 Radiation Damage Phenomena in the BaF_2 Collaboration
  - Studies of Doped Crystals, and Correlation of Radiation Damage With Impurities
  - Studies of Radiation Damage Effects on Transmission and Light Output at BNL

BaF_2 Questions and Answers - Part II

Q11(a) COMPARE BaF_2 to High Z, Sampling Calorimeter (HZSC), for e/π, e/Jet, γ/Jet ...

- HZSC Definition : p. 2
- Level of e/π, e/Jet, γ/Jet in BaF_2 : p. 2-4 (Shower Shape p. 3); + "qqγ" Slides available

Q11(b) Electron & Photon Identification : p. 5-7 (Fig.).
L3 Examples : γ/π^0 Separation to 30 GeV
Inclusive b decays: 10 mrad isolation
⊕ Physics ⇔ Isolation

Q11(c) Shower Spread in BaF_2 versus an HZSC.

- EM Shower: 1.6 TIMES in Angle : p. 8
- Hadron Shower : 1.2 TIMES in Angle : p. 9 (+ Zhu 8/91 Slides Available).

Q11(d) Possible Radial Space Savings with an HZSC : p. 10

Q12 : Higgs Vertex Selection With Charge Multiplicity p. 11; Figures p. 12, 13.

Q13 : Hadronic Energy Resolution ; Compensation

(a) e/h : p. 14
(b) Resolution Studies ⇒ 1.5% – 2.5%
Constant Term : p. 14-17 (Figs: 15, 16)

Appendix on e/Hadron Separation (e/π + e/Jet) : p. 18 ff.

BaF_2 QUESTIONS & ANSWERS Part I (Cont'd)

Q7: When will Fast Shaping Electronics Be Tested?
- Work at ORNL p. 20-21 : Prototype; Evolution
- Work by Princeton p. 21 : GaAs Preamp {FIGS: 22, 23}
- Work at Los ALAMOS: 21-22 : GaAs MESFETs

Q8: Justification for NO Depth Segmentation?
↳ (γ Direction; γ/π^0 Separation; e/π Separation)
- e/π Separation OK : p. 24 (+ Appendix Part II).
- Cost (Photodevice) : p. 25
- Detector Layout : pp. 25-26

Q9: BaF_2 Calorimeter Design; Including Space to Fit CRYSTALS in Support?
pp. 27-28 + Appendix B + Rennich & Moore Slides.

Q10(a) How to achieve Light Collection Uniformity, & high Enough light output to achieve the Resol'n?
PP. 29-33: Figs. p. 30, 32* + Table p. 31 (KE-103)
⇒ KE-103 Rad Hard

Q10(b)
↳ Effect of Shower Fluctuating into BaF_2 or Quartz Prism : p. 34

Q10(c): Phototubes With Sufficient Linearity, Dynamic Range 10^5, in B-Field? : p35

... + APPENDIX LIST

BaF_2 Questions & Answers

Part I p.3-4 + Appendix C ⇒ RAD. DAM

Q1: HOW LONG TO WAIT for RAD. DAMAGE SPECS?

Q2: HOW CONFIDENT of SUFFICIENT PRODUCTION AT \$2.5/cc ?: p. 5 + APPENDIX A.2, A.3

Q3a: FRAGMENTATION EFFECT On QCD BACKGROUND IN $H^0 \to \gamma\gamma$ SEARCH : p 6-8 (TABLE) ⇒ ZHU STUDY

Q3b: WHY CAN ELMUD NOT SEE $H^0 \to \gamma\gamma$ for $M_H = 90$ GeV p. 9 (+ELMUD FIGURES AVAILABLE)

Q4: Radiation Effects in BaF_2?
How to Achieve Uniformity If Rad. Damage?
p. 10,11 + Appendix C (Rad Damage) + p. 29 ff:
Light Uniformity + Appendix H (BNL Study)

Q5: Detector Calibration (I): pp. 12-13
(a) Cost : Included in Baseline (RFQ + UV Monitor)
(b) UV Monitor System
(c) MIP Calibration.

Q6: RFQ System : Detector Calibration (II):
(a) Description : pp. 14-16 + Fig. on 18
(b) Schedule : pp. 17
(c) γ's STOP Towards Front? : pp. 18-19

BaF_2 Questions and Answers - Part II

Q11(a) COMPARE BaF_2 to High Z, Sampling Calorimeter (HZSC), for e/π, e/Jet, γ/Jet ...

- HZSC Definition : p.2
- Level of e/π, e/Jet, γ/Jet in BaF_2 : p.2-4 (Shower Shape p.3); + "qqγ" Slides available

Q11(b) Electron & Photon Identification : p.5-7 (Fig.).
L3 Examples : γ/π^0 Separation to 30 GeV
Inclusive b decays: 10 mrad isolation
⊕ Physics ⇔ Isolation

Q11(c) Shower Spread in BaF_2 versus an HZSC.

- EM Shower: 1.6 TIMES in Angle : p.8
- Hadron Shower : 1.2 TIMES in Angle : p.9 (+ Zhu 8/91 Slides Available).
- → Optimization of $\Delta\eta, \Delta\varphi$ for any calorimeter

- **Q11(d)** Possible Radial Space Savings with an HZSC : p.10

Q12 : Higgs Vertex Selection With Charge Multiplicity p.11; Figures p. 12, 13.

- **Q13** : Hadronic Energy Resolution ; Compensation
  (a) e/h : p.14
  (b) Resolution Studies → 1.5% – 2.5%
  Constant Term : p.14-17 (Figs: 15, 16)

Appendix on e/Hadron Separation (e/π + e/Jet) : p.18ff.

- Studies of the BaF_2 Radiation Damage Mechanism at SIC

- **Light Collection Uniformity**
  - EGS Study of Light Uniformity Requirements in Coupled Crystals

- **Test Beams**
  - Beam Requirements
  - Test Beam Status at Fermilab

- **BaF_2 Calorimeter Performance**
  - Position Resolution
  - Energy Resolution

- **R&D Budget**

- **Attachment: Progress Report on BaF_2 R&D at BNL**

APPENDICES

- • **Mass Production of BaF_2 Crystals in China**
  - UV Transmittance of the Crystals
  - Memorandum of Understanding Between Caltech, SIC and BGRI for BaF_2 Crystal Mass Production in China
  - Production Capacity and Investments in China
- • **Structural Design of the BaF_2 Calorimeter, and the Final Prototype**
  - Design Concept
  - Carbon Fiber Structure
  - Structure for the Final Prototype
  - Materials Study for the Structure
  - Other Design Aspects: Electronics Placement, Cable Routing and Thermal Control
- • **BaF_2 Radiation Resistance**
  - Measurements of BaF_2 Radiation Damage Phenomena in the BaF_2 Collaboration
  - Studies of Doped Crystals, and Correlation of Radiation Damage With Impurities
  - Studies of Radiation Damage Effects on Transmission and Light Output at BNL

BaF_2 Questions & Answers

Part I p.3-4 + Appendix C ⇒ RAD. DAM

- **Q1**: How long to wait for RAD. DAMAGE SPECS?

- **Q2**: How confident of sufficient production at \$2.5/cc?: p. 5 + APPENDIX A.2, A.3

* **Q3a**: FRAGMENTATION EFFECT on QCD BACKGROUND IN $H^0 \to \gamma\gamma$ SEARCH : p 6-8 (TABLE) ⇒ ZHU STUDY

Q3b : WHY CAN ELMUD NOT SEE $H^0 \to \gamma\gamma$ for $M_H = 90$ GeV p. 9 (+ELMUD FIGURES AVAILABLE)

→ * R. ZHU

- **Q4**: Radiation Effects in BaF_2?
  How to Achieve Uniformity If Rad. Damage?
  p. 10,11 + Appendix C (Rad Damage) + p. 29 ff:
  Light Uniformity + Appendix H (BNL Study)

Q5: Detector Calibration (I): pp. 12-13
- (a) Cost : Included in Baseline (RFQ + UV Monitor)
- (b) UV Monitor System
- (c) MIP Calibration.

Q6: RFQ System : Detector Calibration (II):
- (a) Description : pp. 14-16 + Fig. on 18
- (b) Schedule : pp. 17
- (c) γ's STOP Towards Front? : pp. 18-19

BaF_2 QUESTIONS & ANSWERS Part I (Cont'd) NEWMAN

Q7: When will Fast Shaping Electronics Be Tested?
- Work at ORNL p. 20-21 : Prototype; Evolution
- Work by Princeton p. 21 : GaAs Preamp {FIGS: 22, 23}
- Work at Los ALAMOS: 21-22 : GaAs MESFETs

Q8: Justification for No Depth Segmentation?
↳ (γ Direction; γ/π⁰ Separation; e/π Separation)
- e/π Separation OK : p. 24 (+ Appendix Part I).
- Cost (Photodevice) : p. 25
- Detector Layout : pp. 25-26

Q9: BaF_2 Calorimeter Design; Including Space to Fit CRYSTALS in Support?
pp. 27-28 + Appendix B + Rennick & Moore Slides.

- Q10(a) How to achieve Light Collection Uniformity, & high enough light output to achieve the Resol'n.?
pp. 29-33: Figs. p. 30, 32* + Table p. 31 (KE-103)
⇒ KE-103 Rad Hard

Q10(b)
↳ Effect of Shower Fluctuating into BaF_2 or Quartz Prism. : p. 34

Q10(c): Phototubes With Sufficient Linearity, Dynamic Range 10^5, in B-Field? : p35

... + APPENDIX LIST

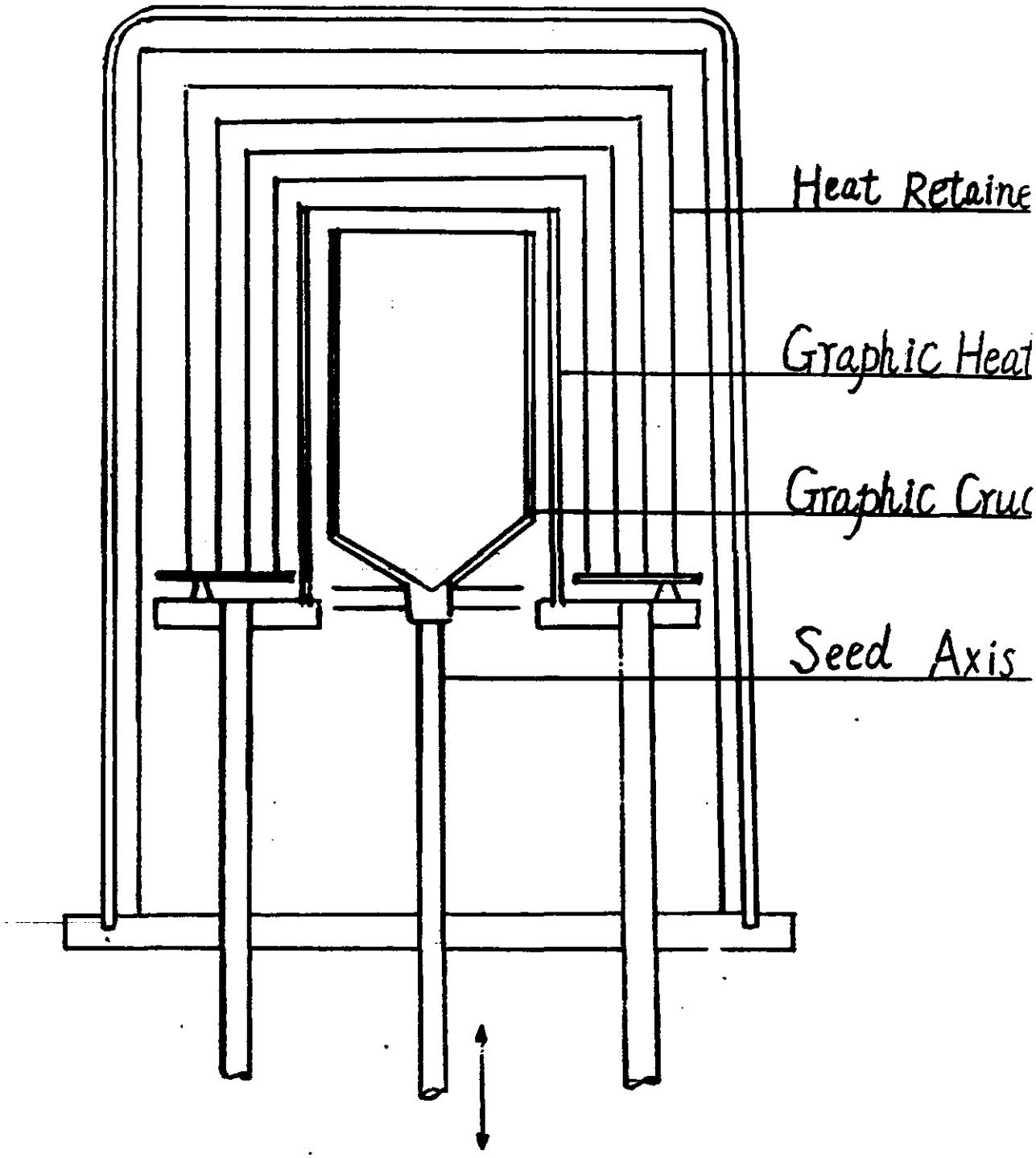

Fig. 1. Schematic representation of the crystal growth system.

BaF_2 CRYSTAL PRODUCTION At SHANGHAI and BEIJING

- **PRODUCTION: 1991 - 1992**
  - 6/91: FIVE FURNACES; 50 PIECES PER MONTH
  - 12/91: ~~NINE~~ 10 FURNACES; ~~120~~ 130 PIECES PER MONTH
- **MASS PRODUCTION PLAN**
  - 800 PIECES Per MONTH: 1993 - 1997
  - PRICE \$ 2.5/cm^3 By End 1992
- **MANPOWER**
  - R&D PHASE (1990-1992): 28 (SIC) + 21 (BGRI); 18 FTE's by 6/91
  - MASS PRODUCTION PHASE: Total 80 - 100 FTE's

BGRI and SIC will invest US$750,000 separatly in creasing the production capacity of BaF_2 scintillation crystals up to 2x2.5 tons per year (2x0.5M^3/year) and the amount of BaF_2 crystals will be 2x2 tons during 1992.

1993-1997:

After receiving the order of L* project, BGRI and SIC will invest US$3,000,000 respectively in setting up the factory of BaF_2 scintillation crystal with production capacity of 2x5 tons per year so as to increase the output up to 2x7.5 tons/year.

Wen Ou

Wen Ou

June 6,1991

THE RESEARCH AND DEVELOPMENT OF BaF_2 SCINTILLATION CRYSTAL IN BEIJING GLASS RESEARCH INSTITUTE

DIRECTOR: WEN OU

BEIJING GLASS REASERCH INSTITUTE

C. BGRI agrees to carry out a production demonstration of a crystal-pair of full size, consisting of two crystal pieces approximately 35*cm* and 15*cm* long. The crystals will have the trapezoidal shape characteristic of the final calorimeter. The crystal pair will also be required to meet the usual transmission requirements before irradiation of production quality crystals.

At a later stage, following the successful demonstration of 35*cm* finished crystals, SIC and BGRI will try to meet the radiation damage specifications given above.

B. Studies of radiation damage in BaF_2 crystals indicate that the damage may be associated with an absorption peak at $288nm$. This peak is suspected to be caused by Cerium or O_2 in the crystals. SIC and BGRI will pursue a systematic series of studies to eliminate this absorption peak.

SIC and BGRI will therefore determine the source of Cerium as a trace element, and eliminate it from further crystal batches.

SIC and BGRI also will continue to pursue tests that will determine the effect of Oxygen(O_2) dissolved in the crystals. SIC, BGRI, Caltech, engineers from ORNL, and engineer M. LeBeau will work together to improve the growing conditions, so as to remove O_2 down to a level where it does not lead to significant absorption in the UV following irradiation. In order to achieve this, the vacuum systems of the ovens may be improved. A production oven with improved pumping, to achieve a vacuum in the 10^{-6} to 10^{-7} Torr range, will be set up with the assistance of Caltech and the engineers.

SIC and BGRI will investigate the use, and necessity of the use, of very pure raw materials in the crystal growth. This step is recognized to be useful only once effective methods of analysis down to a trace element level of $\leq 10^{-7}$ (molar fraction) have been established.

2. CRYSTAL QUALITY CONTROL

A. SIC and BGI agree to apply their best efforts to produce a radiation hard crystal-pair of size $(2 \times 2) \times (4 \times 4) \times 50cm^3$ long (two $25cm$ long pieces). The radiation hardness specification is that the crystals shall show a change in transmission of 25% or less, following a dose of several megarads of gamma-rays (Co^{60}), or a dose of $10^{13} neutrons/cm^2$. The damage effect is expected to be saturated, such that further doses up to $10^7 Rads(Co^{60})$ or $10^{14} neutrons/cm^2$, do not lead to substantial further damage.

The target date for production of the first radiation hard crystal pair is 12/91 or earlier. The target for production of a radiation-hard full size subarray, conposed of 5×5 crystal cells, or more is 6/92 or earlier.

1. PROJECT GOALS

Following discussions at the Barium Fluoride Precision EM Calorimeter Meeting in Shanghai, the undersigned parties agree to apply their best efforts towards successful development of the calorimeter, and to carry out the steps listed below.

The immediate goal is to complete the construction of a first round prototype during the summer of 1991, demonstrating the requisite energy resolution.

The principal short term goal is to develop a production-quality prototype, composed of radiation hard crystals of final size, integrated with an optimized carbon fiber mechanical structure and high rate electronics readout, by the Summer of 1992.

The long term goal is to develop and construct a complete calorimeter composed of 18,000 crystal-cells, using production methods that will allow the undersigned to set the price at $2.5/cc. The production of the full calorimeter at this price is forseen starting in 1993, at a full production rate of 800 crystal pieces per month.

MEMORANDUM OF UNDERSTANDING

BETWEEN

THE SHANGHAI INSTITUTE OF CERAMICS (SIC)
THE BEIJING GLASS RESEARCH INSTITUTE (BGRI)
THE CALIFORNIA INSTITUTE OF TECHNOLOGY (CALTECH)

FOR THE DEVELOPMENT OF A HIGH PRECISION BARIUM FLOURIDE ELECTROMAGNETIC CALORIMETER

May 29, 1991

BaF_2 PRECISION ELECTROMAGNETIC CALORIMETER WORKSHOP

SHANGHAI and BEIJING, CHINA

MAY 27-JUNE 1, 1991

Content	Speaker
1, Welcome address	D. S. Yan
2, Motivation of the workshop	H. Newman
3, Physics requirements on precision of electromagnetic calorimeter at the SSC	R. Zhu
4, Status of BaF_2 R & D at U. S.	H. Newman
5, Progress in production and quality control of BaF_2 crystals in SIC and BGRI	J. K. Guo
6, Some aspects on the growth of large size BaF_2 crystals	J. Zhang
7, BaF_2 and other scintillating crystal at BNL	C. Woody
8, Front-end electronics for BaF_2	M. Bauer
9, Mechanical design of L*EMC	M. Rennich
10, BaF_2 EMC prototype	J. Moore
11, L3 BGO experence	M. Lebeau
12, On the radiation damage of Barium Fluoride Crystals	Z. W. Yin
13, The optical and radiation damage properties of BaF_2	L.M. Wang
14, Studies on trace elements in BaF_2crystal by using ICP and NAA	P. Kong
15, Spectral properties of Ce-doped Barium Fluoride crystal	Y. Dong
16, Studies on decay time of fluorescence from a series of Ce-doped BaF_2crystals	Z. Z. Xu
17, Radiation damage and recovery of doped crystals (no full text)	J. T. He
18, Positron annihilation in Ce-doped BaF_2crystal	J. Chang
19, Temperature dependence of luminescence from $BaF_2:Ce^{3+}$ crystals	Y. W. Tang
20. Radiation hardness studies of Teflon materials	Y. C. Zhu

BARIUM FLUORIDE PRECISION EM CALORIMETER MEETING

Shanghai Institute of Ceramics

Beijing Glass Research Institute

Beijing IHEP

May 27, 1991 - June 1, 1991

- A High Resolution Detector To Do Unique Physics at Future Hadron Colliders
- BaF_2 CRYSTALS:
  - Transmission, Uniformity, Rad Hardness;
  - Mechanics, Size, Production, Price
- Status of BaF_2 Prototype Matrix R&D
  - Crystal Test Results
  - UV-selective Photosensitive Devices
  - Electronic Readout
  - Optical Coupling
  - Mechanics for Crystal Production
  - Mechanical Tests; Structure Design
- BaF_2 and Other Crystals at BNL
- Lessons from the L3 BGO Detector

BaF_2 PRICE

NOW AT $ 3.5/CC
FOR 81 FULL-SIZE
CRYSTAL PAIRS

AGREEMENT:

MASS PRODUCTION
AT $ 2.5/CC

BaF_2 CRYSTAL PRODUCTION
R&D Program At Shanghai and Beijing

- Analysis of Impurities in Raw Materials and Crystals
- Pre-Treatment of Raw Materials for High Purity
- → Optimize Crystal Growth Technology
- Study Effect of Impurities on Transmittance, Radiation Hardness
- → Study Mechanical Processing of Large Crystals
- Study Crystal Doping For High Luminosity Running at SSC

P. Lecoq

.Table 1: Crystals characteristics

Crystal	Density	Radiation length cm	Moliere radius cm	Decay time nsec	Peak emission nm
BGO	7.13	1.11	2.33	300	480
BaF2	4.89	2.06	3.39	0.6 620	210 310
CeF3	6.16	1.68	2.63	5 20	300 340
YAP:Ce	5.35	2.83	2.82	35	390
GSO:0.5%Ce	6.71	1.39	2.42	55	435
GSO:2.5%Ce	6.71	1.39	2.42	31	450
ThF4	6.32	1.18	2.71	≤ 25	315,330,450
BaLiF3	5.24	2.13	3.13	≤ 25	435
LiYbF4	6.09	1.56	2.70	≤ 25	≈ 450
PbF2	7.66	.94	2.24	-	-

Beijing Glass Research Institute (BGRI)

long history for synthetic crystal growth technology

especially on fluorides such as

BaF_2 crystal

for infrared field application at early stage

for scintillating application 6 years ago

1986 ϕ 60 mm BaF_2 have been grown scale up

1987 300 mm length

HN

BaF_2 CRYSTAL PRODUCTION
Shanghai and Beijing Collaboration

- **Shanghai Institute of Ceramics (SIC)**
  - 50 Kinds of Synthetic Crystals: Electro-Optical, Acousto-Optical, Piezoelectric, and Scintillators
  - 200 Faculty, 500 Research Staff 300 Skilled Support Personnel
  - 11,000 Crystals for L3: Peak Production 400 Per Month
  - Large Vacuum Furnace Facility For BaF_2 Developed Since 1989.

- **Beijing Glass Research Institute (BGRI)**
  - 6 Years Growing Large BaF_2 Crystals; Large Vacuum Furnace Facility.
  - Large Diameter BaF_2 Crystals Boules Up To 45 cm Long Finished Crystals to 35 cm Long.

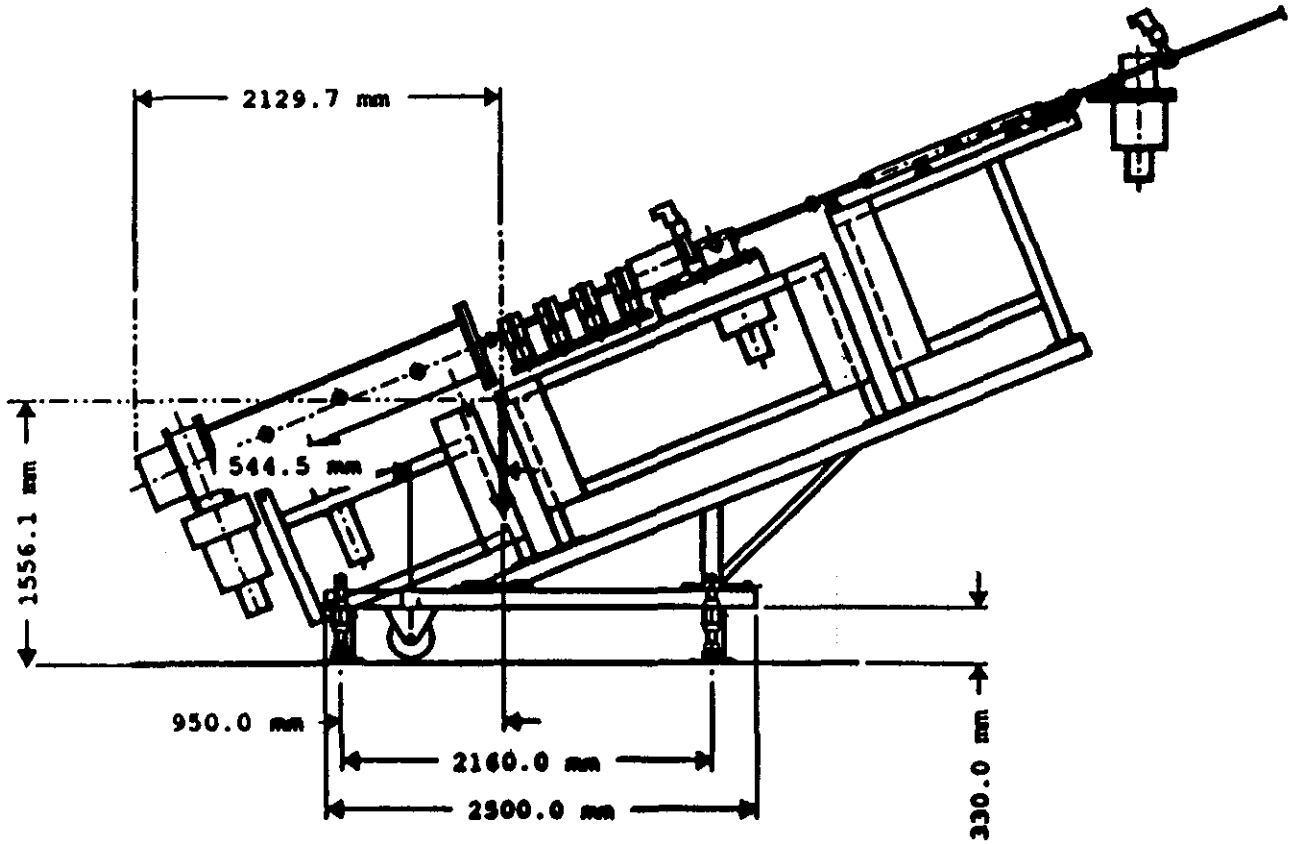

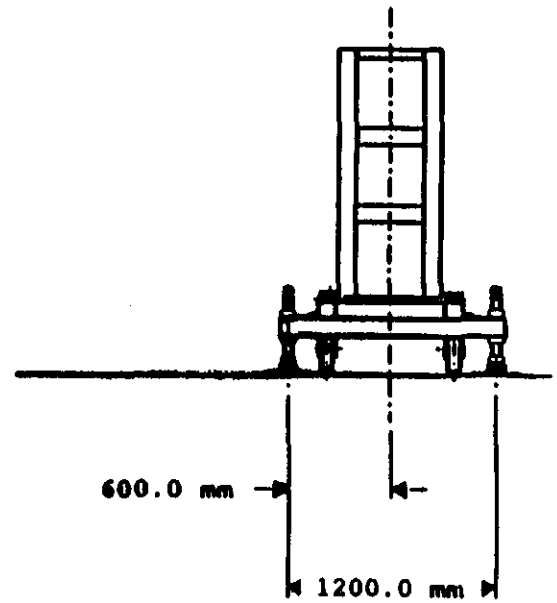

RFQ;ENSEMBLE SUPPORT Modele B

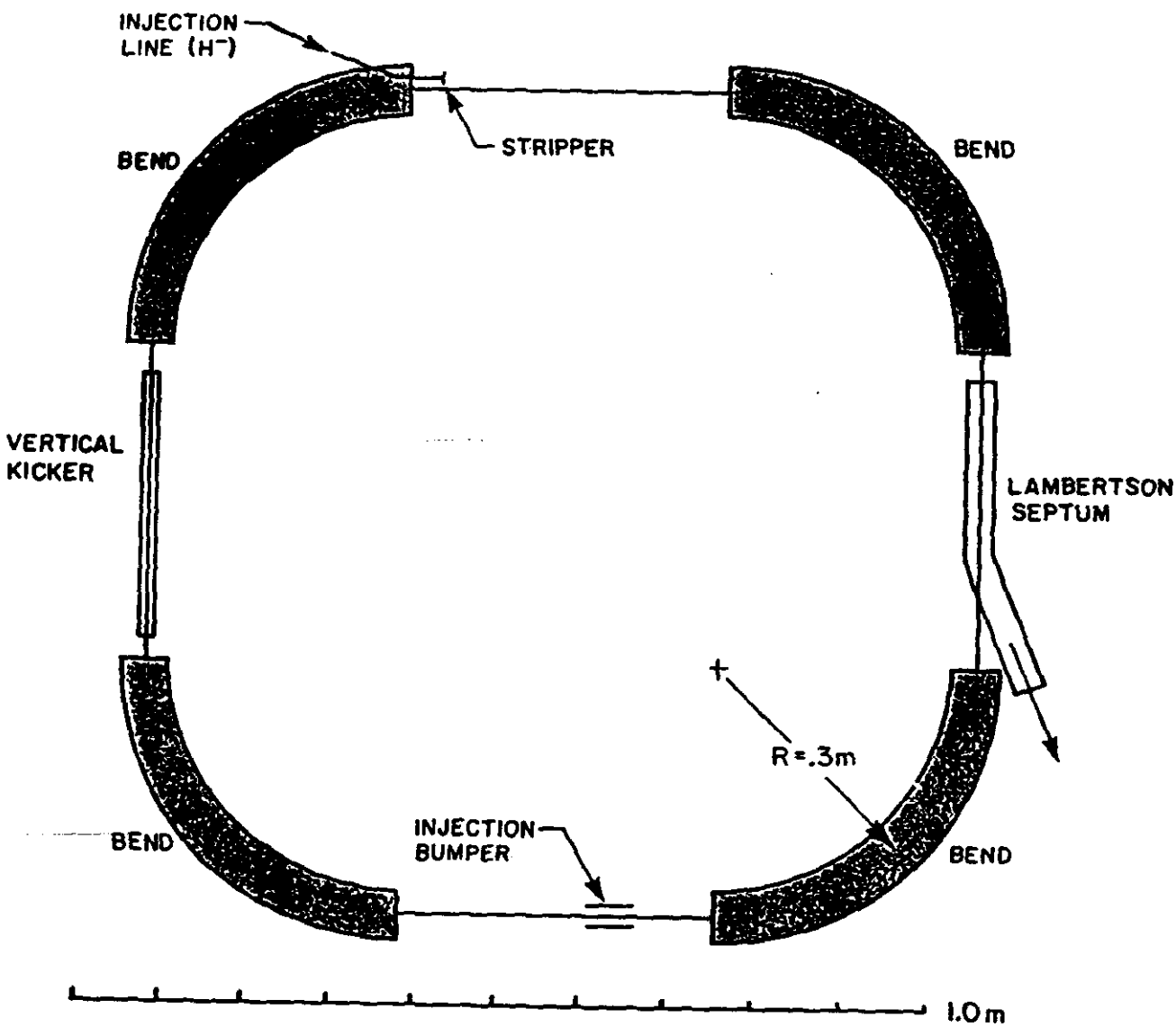

Fig. 15. Compact layout of storage ring designed for the SSC calorimeter calibration system

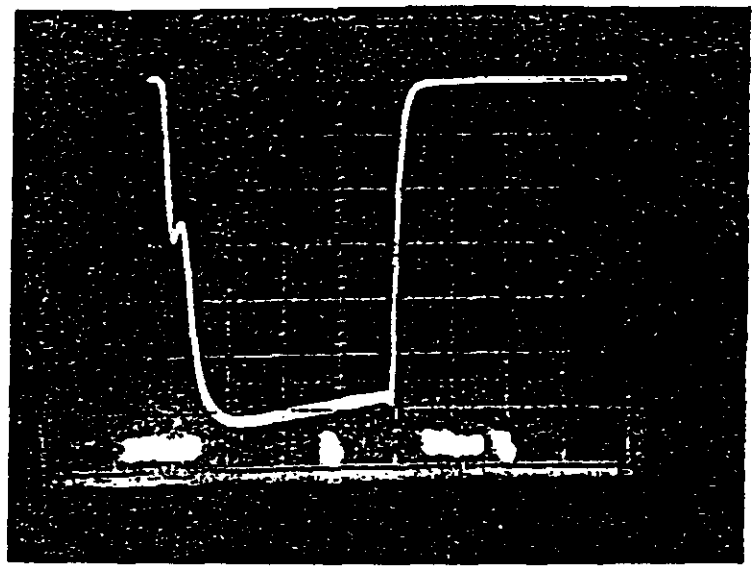

Fig. 11. H^- ion current measured with external spectrometer

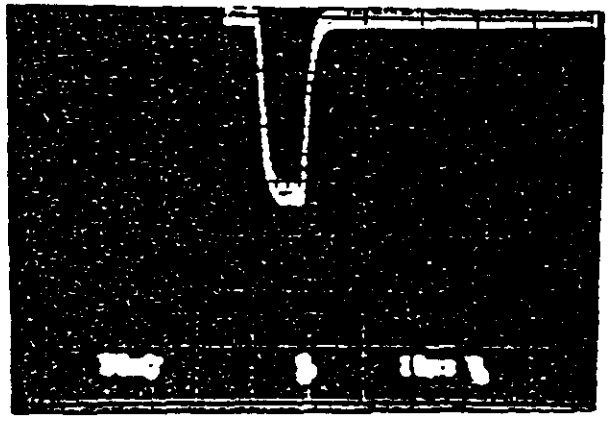

Fig. 12. H^- ion current from RFQ linac at entrance to neutralizer

Fig. 18

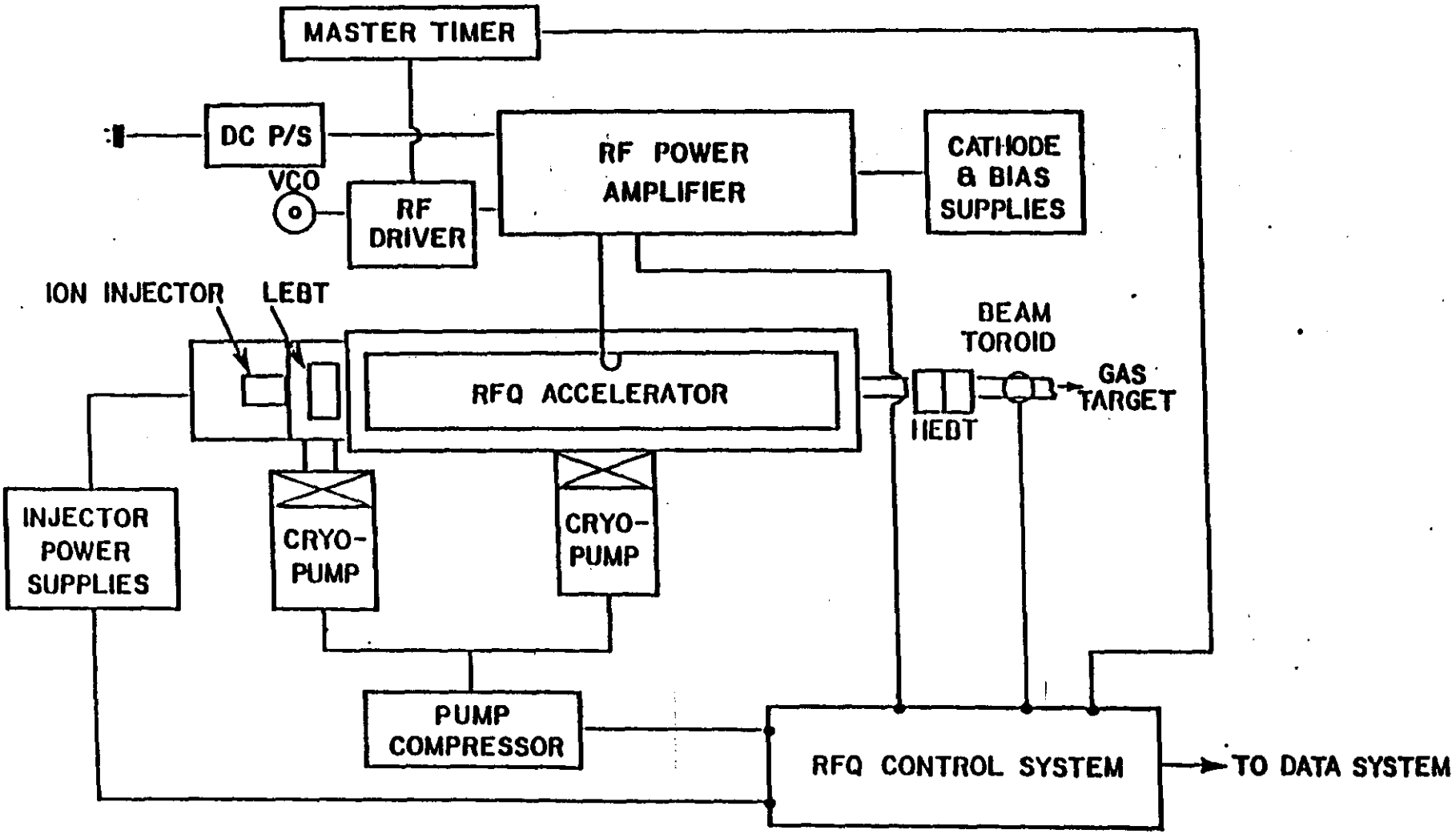
MASTER TIMER
DC P/S
VCO
RF DRIVER
RF POWER AMPLIFIER
CATHODE & BIAS SUPPLIES
ION INJECTOR
LEBT
RFQ ACCELERATOR
BEAM TOROID
HEBT
GAS TARGET
INJECTOR POWER SUPPLIES
CRYO-PUMP
CRYO-PUMP
PUMP COMPRESSOR
RFQ CONTROL SYSTEM
TO DATA SYSTEM

Fig 1

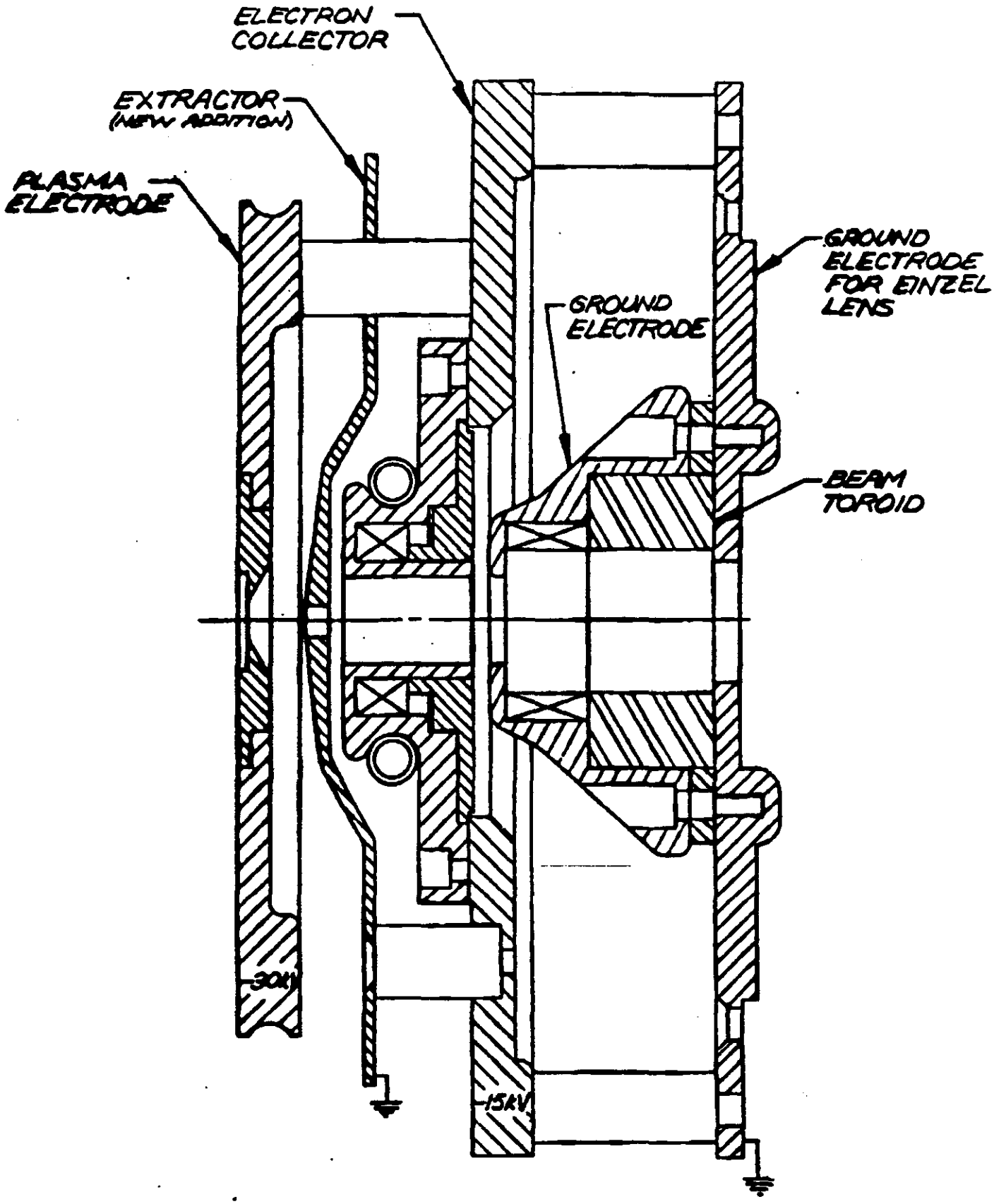

H^- INJECTOR ELECTRODES (ACCEL-DECEL)

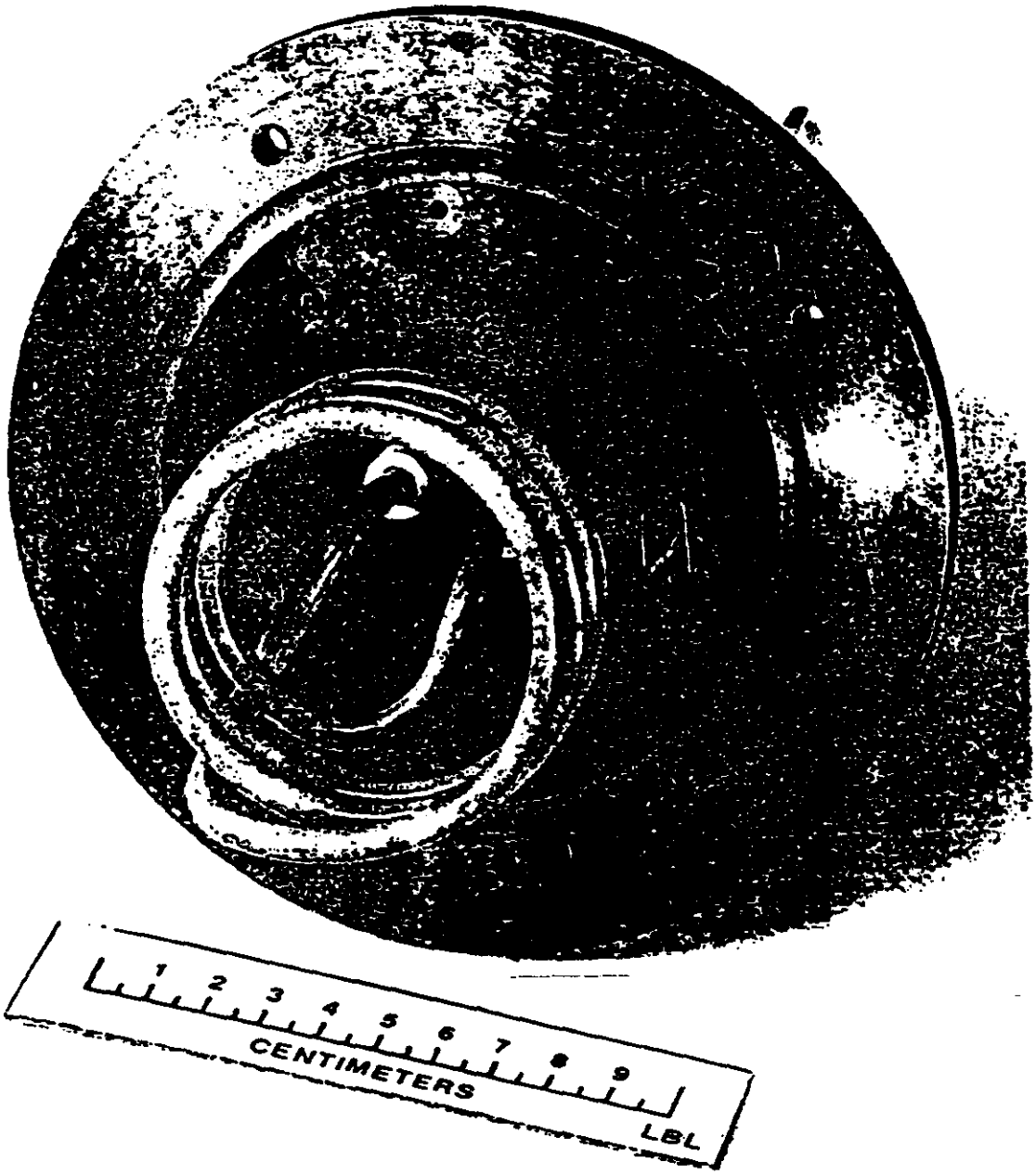

Fig. 4. Antenna and "starter" filament in the LBL rf-driven H^- ion source

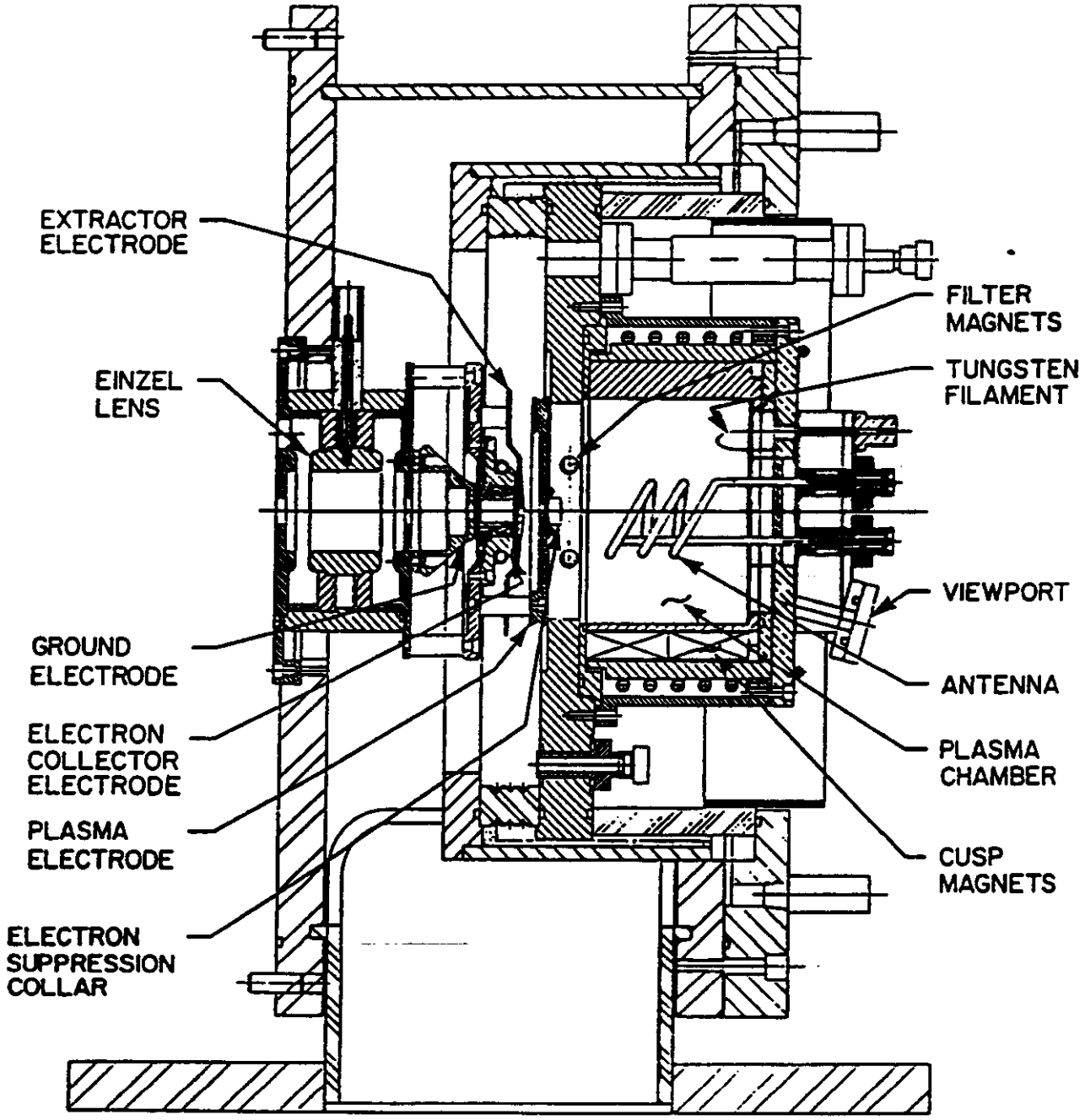

Fig. 7. Cross-sectional view of H^- ion injector

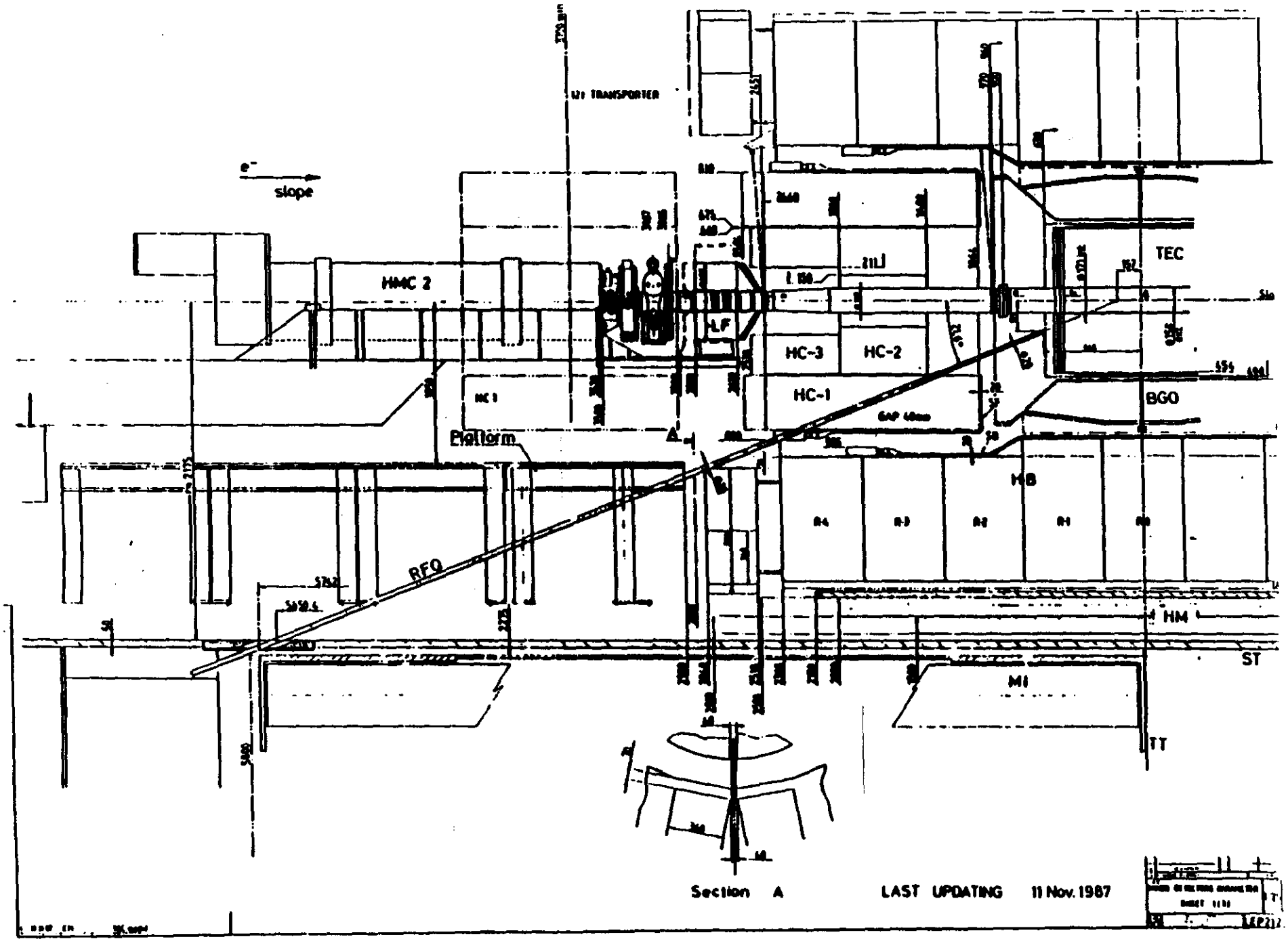
e⁻
slope
TRANSPORTER
HMC 2
LF
HC-3
HC-2
HC-1
HC 1
TEC
BGO
HB
Platform
A
RFQ
HM
ST
MI
TT
Section A
LAST UPDATING 11 Nov. 1987

Gas Stripping Efficiency

1.5 MeV H^- on H_2O

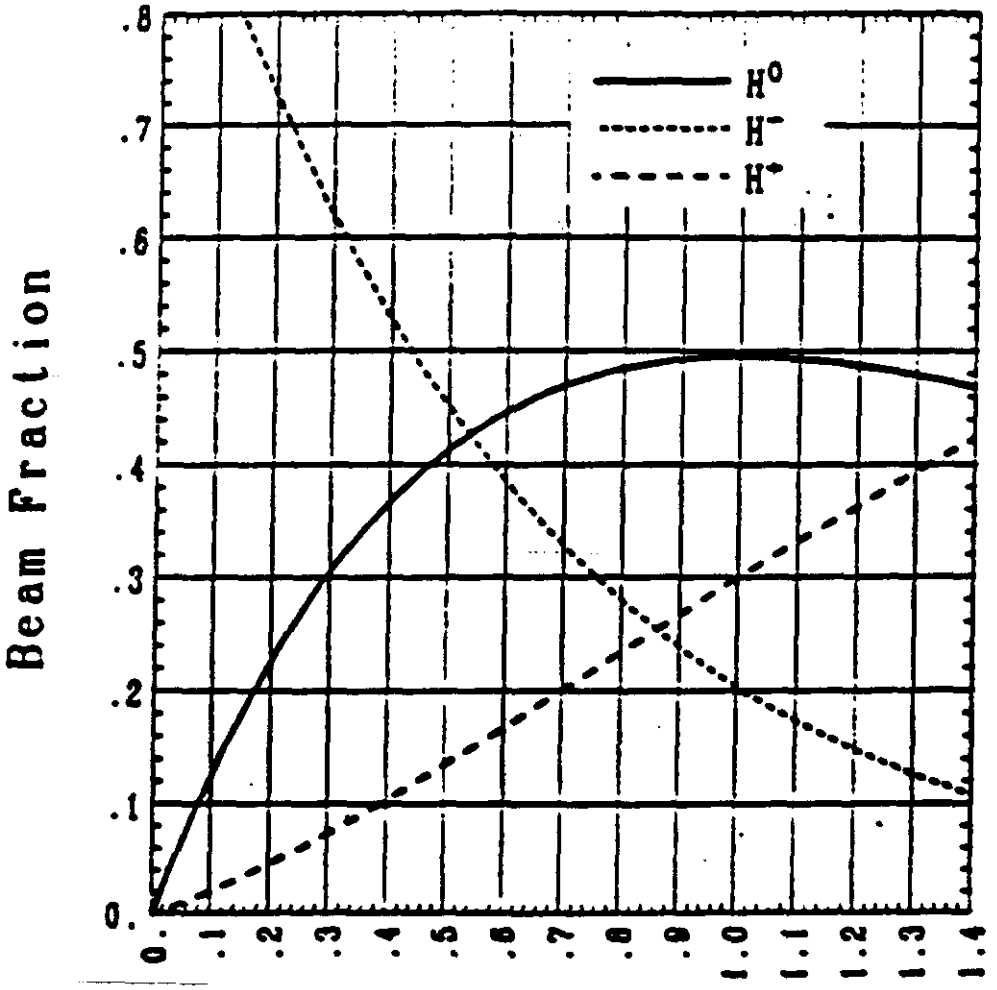

Target Thickness/Optimum

Optimum Thickness
5.73×10^{15} mol./cm^2

BARIUM FLUORIDE CALORIMETER CALIBRATION

- **Minimum Ionizing Particles*** **(MIPs) from pp Collisions**
  - Pass Through Crystals Longitudinally
  - Calibrate to 0.4% in 12 Hours
    COSMIC RAY TEST BENCH; BEAM TESTS
- **Verify With Inclusive** e^+e^- From Z^0, Υ, J
  - Reconstruct Mass:
    Use RFQ + MIP Results

  → 200 e^+ or e^- from Υ,
  20 from Z^0 Per Crystal Per Week

Table II. Budgetary Cost for SSC Calorimeter Calibration Syste

Model PL-4 RFQ linac	$ 450,(
Model 12TW 350 RF amplifiers (2 req'd.)	600,(
H^- ion injector (per Phase II design)	350,(
Control system, integration and documentation	100,(
100 nsec accumulator ring (incl. power supplies)	600,(
Total	$2,100,(

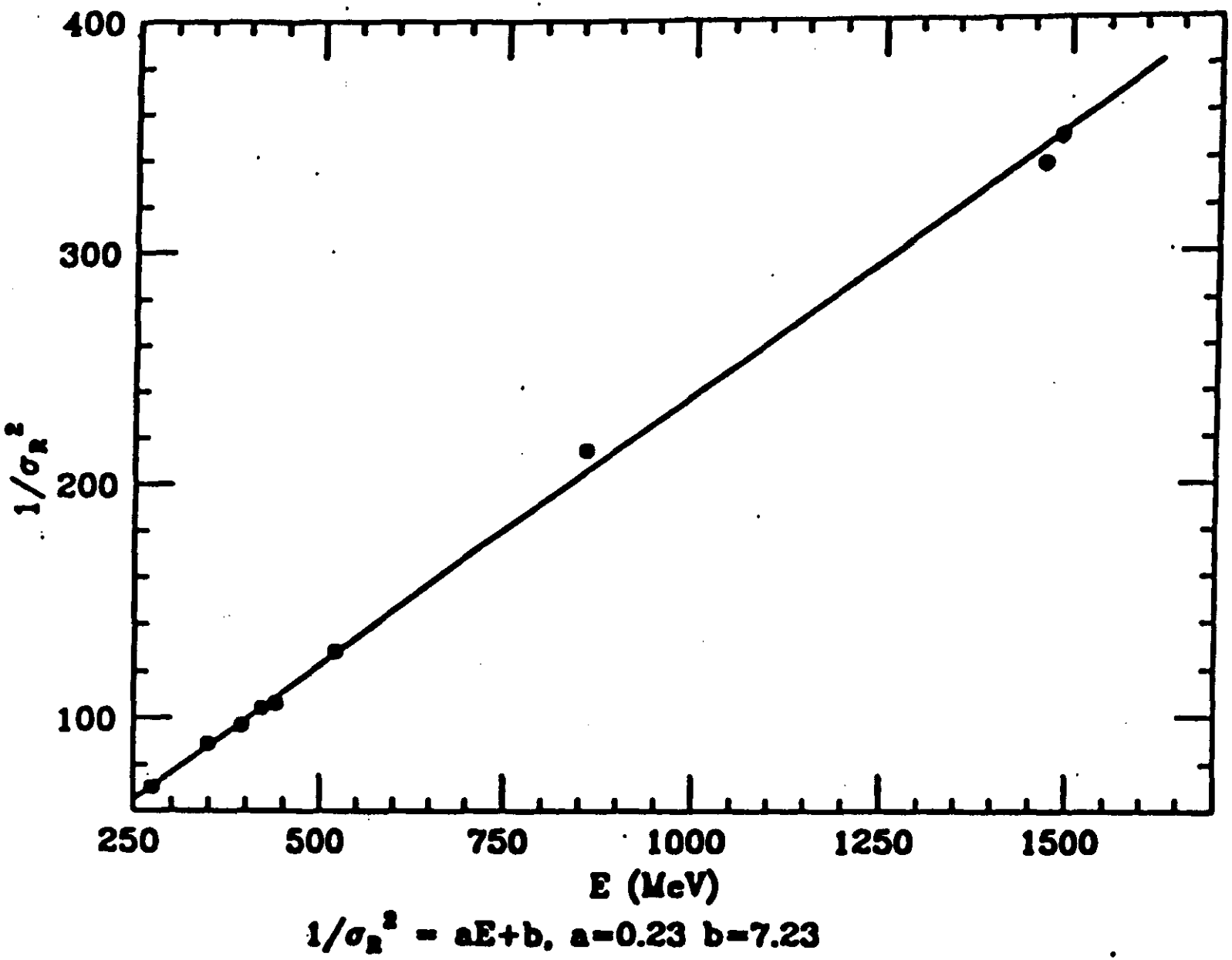

Figure 10: Correlation between the relative r.m.s. and the average energy in BGO Crystal 32.

Distribution of Normalized ADC (Run 49)

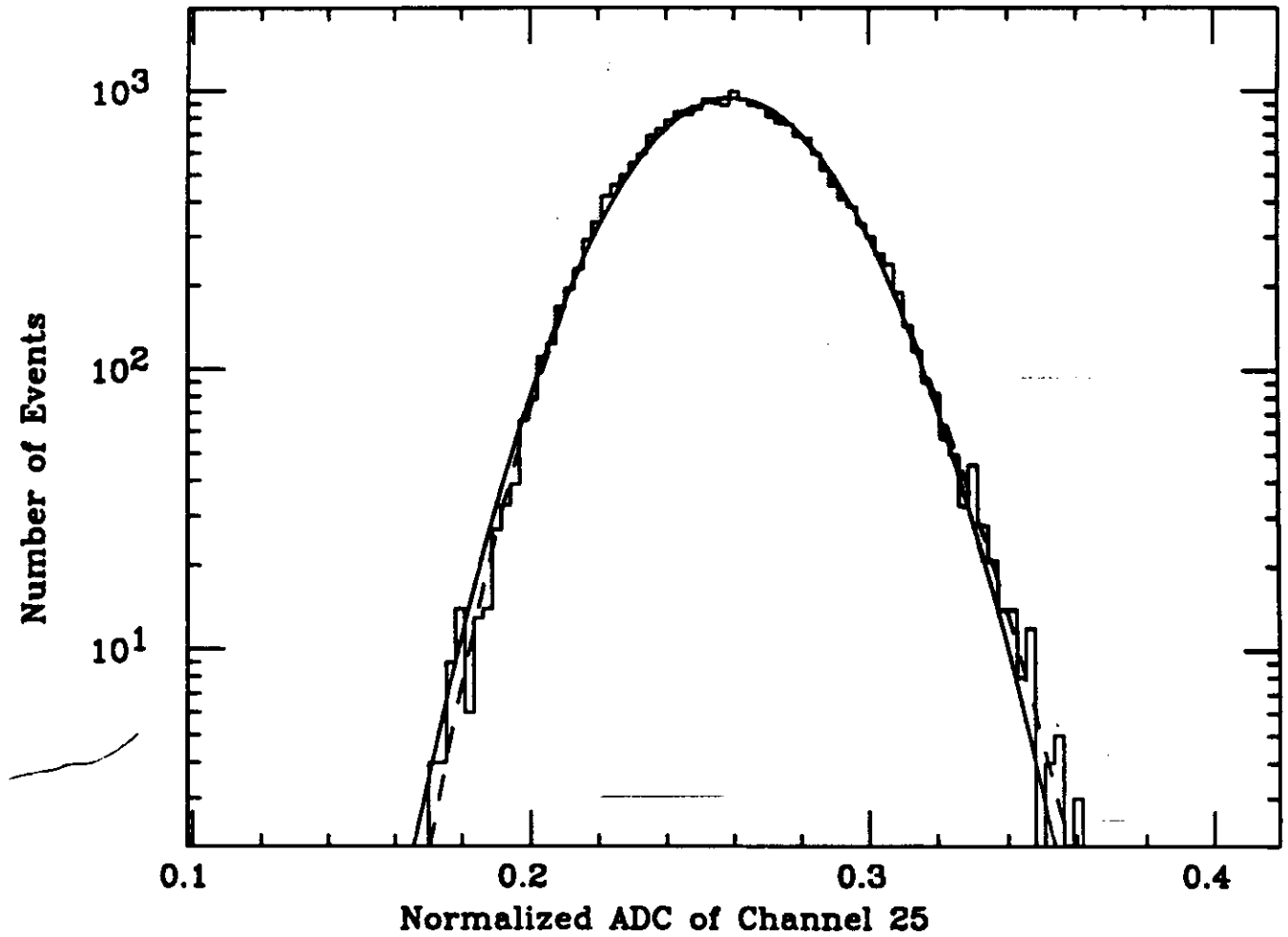

Gaussian(solid): Peak= 0.2597, σ= 0.02675(10.3%), χ^2/DoF =1.3

Poisson(dash): N = $1/\sigma^2$ = 94

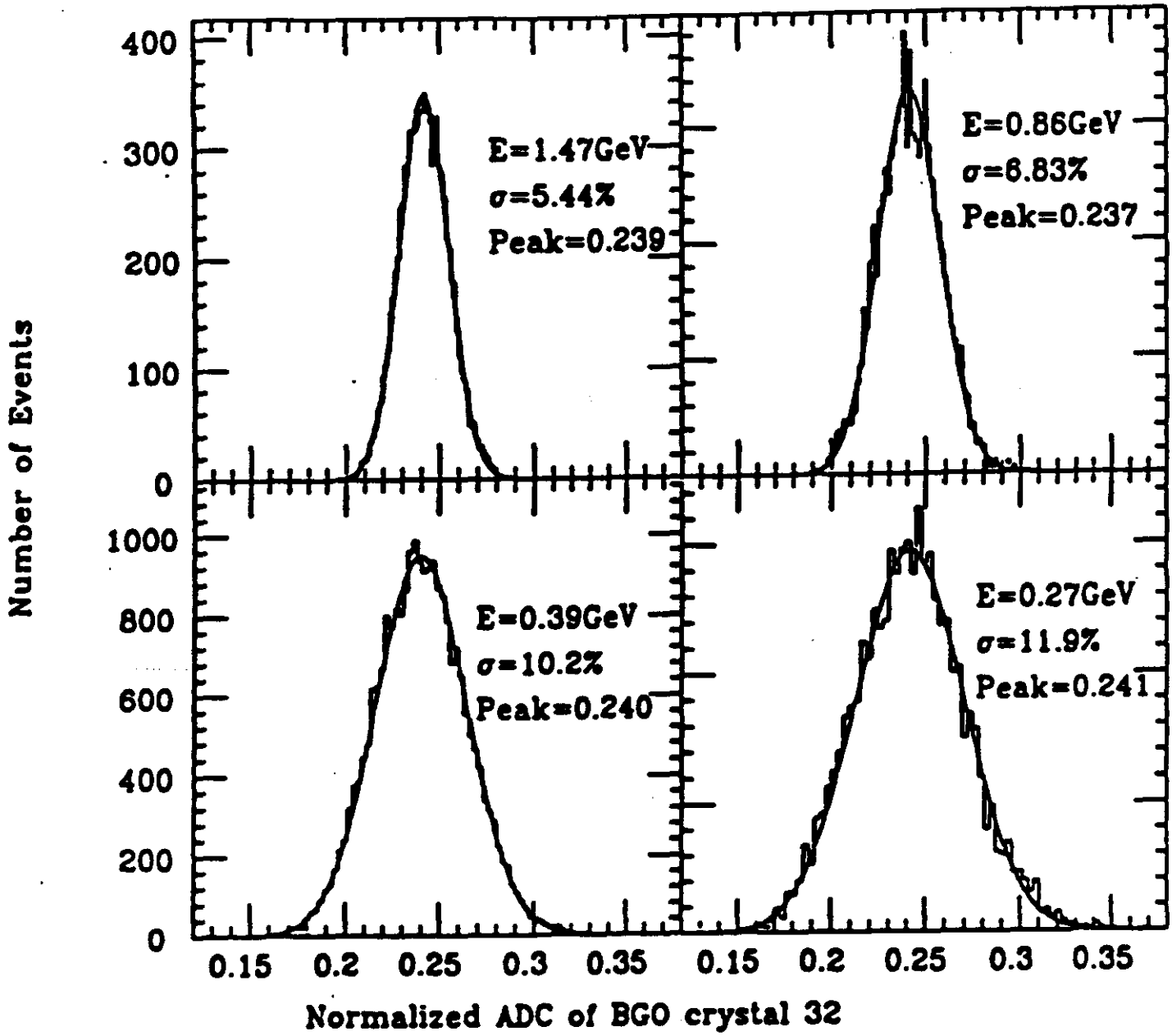
Number of Events
400
300
200
100
0
1000
800
600
400
200
0
E=1.47GeV
σ=5.44%
Peak=0.239
E=0.86GeV
σ=6.83%
Peak=0.237
E=0.39GeV
σ=10.2%
Peak=0.240
E=0.27GeV
σ=11.9%
Peak=0.241
0.15
0.2
0.25
0.3
0.35
Normalized ADC of BGO crystal 32

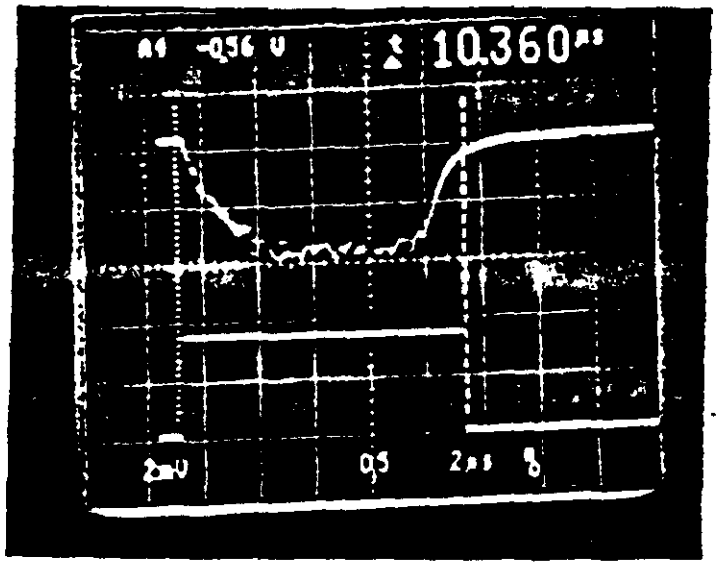

Figure 7(a)

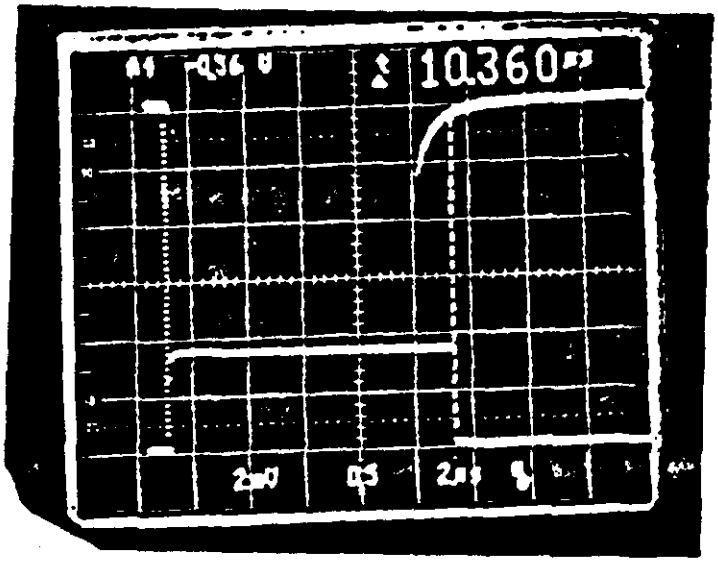

Figure 7(b)

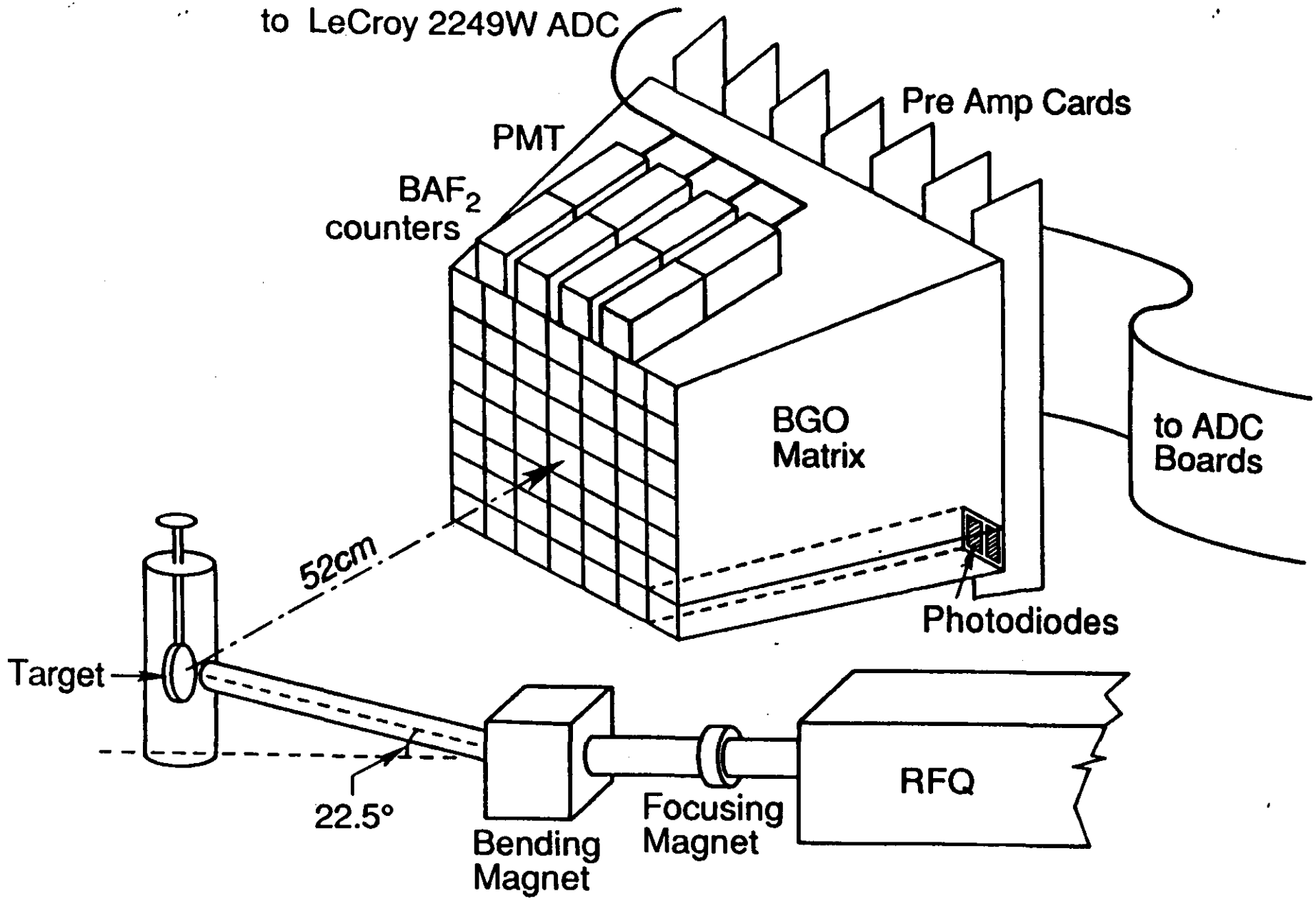
to LeCroy 2249W ADC
Pre Amp Cards
PMT
BAF2
counters
BGO
Matrix
to ADC
Boards
52cm
Photodiodes
Target
22.5°
Bending
Magnet
Focusing
Magnet
RFQ

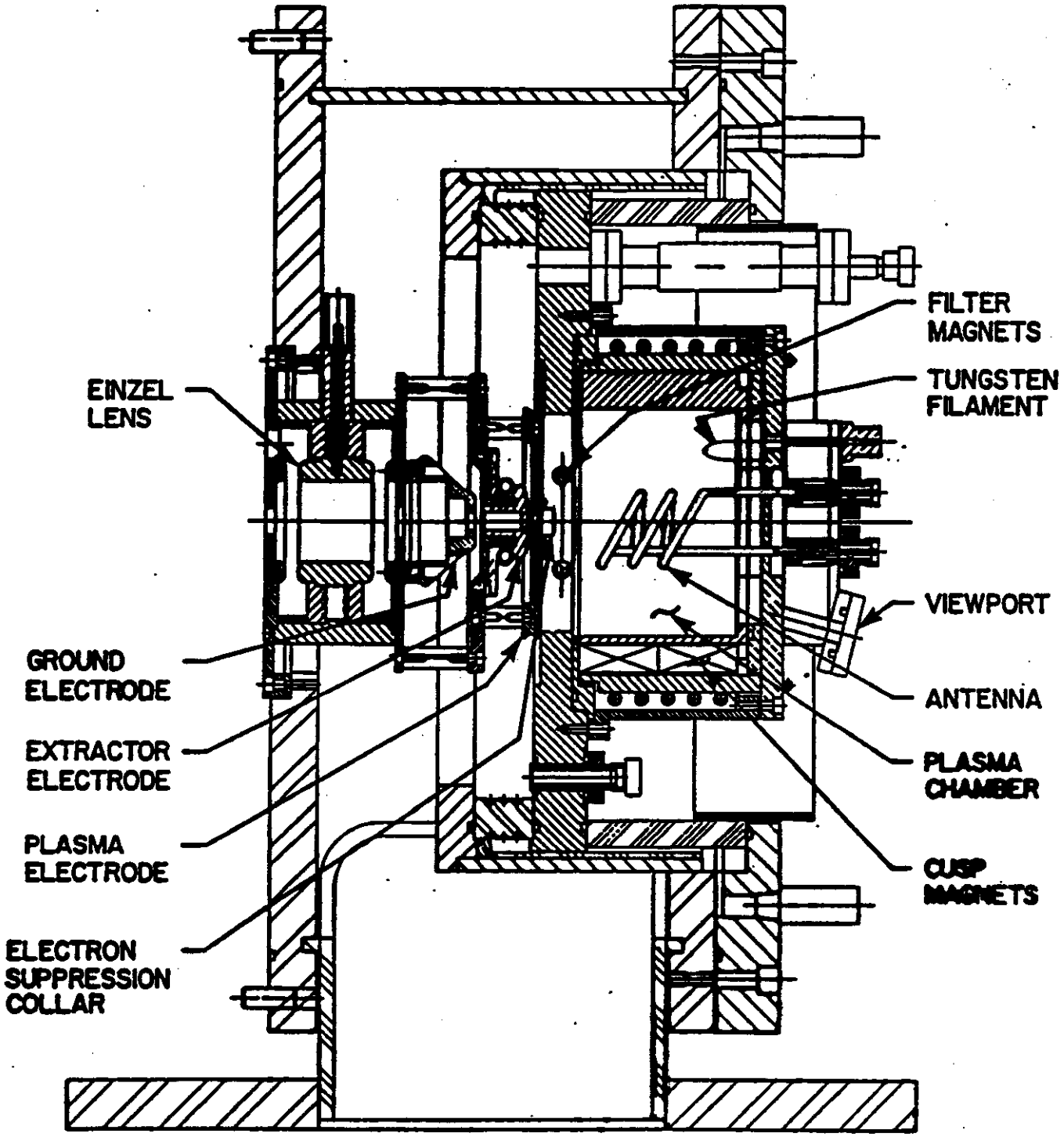
FILTER MAGNETS
TUNGSTEN FILAMENT
EINZEL LENS
VIEWPORT
GROUND ELECTRODE
ANTENNA
EXTRACTOR ELECTRODE
PLASMA CHAMBER
PLASMA ELECTRODE
CUSP MAGNETS
ELECTRON SUPPRESSION COLLAR

HIGH ENERGY PHYSICS DETECTOR CALIBRATION SYSTEM

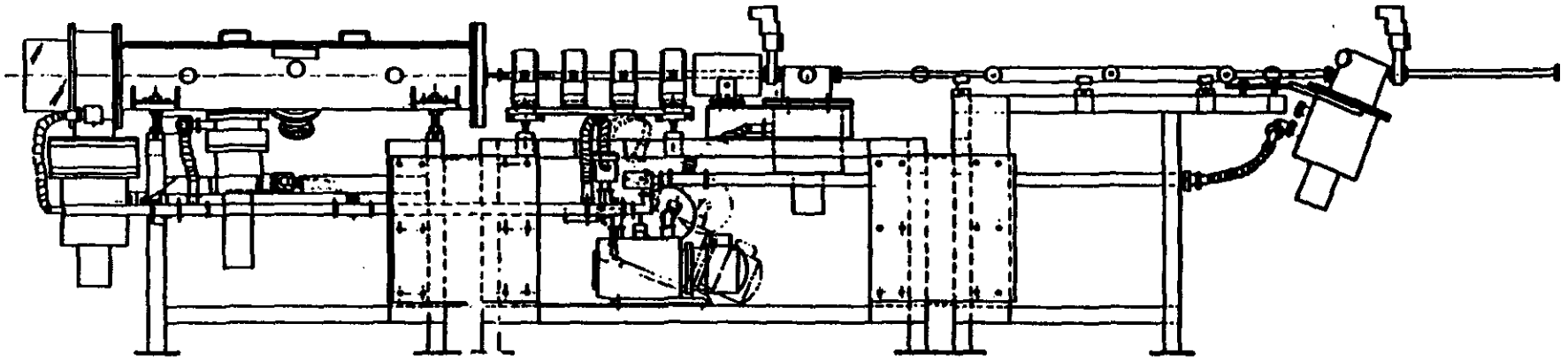

ACCSYS
TECHNOLOGY, INC

FIGURE 4

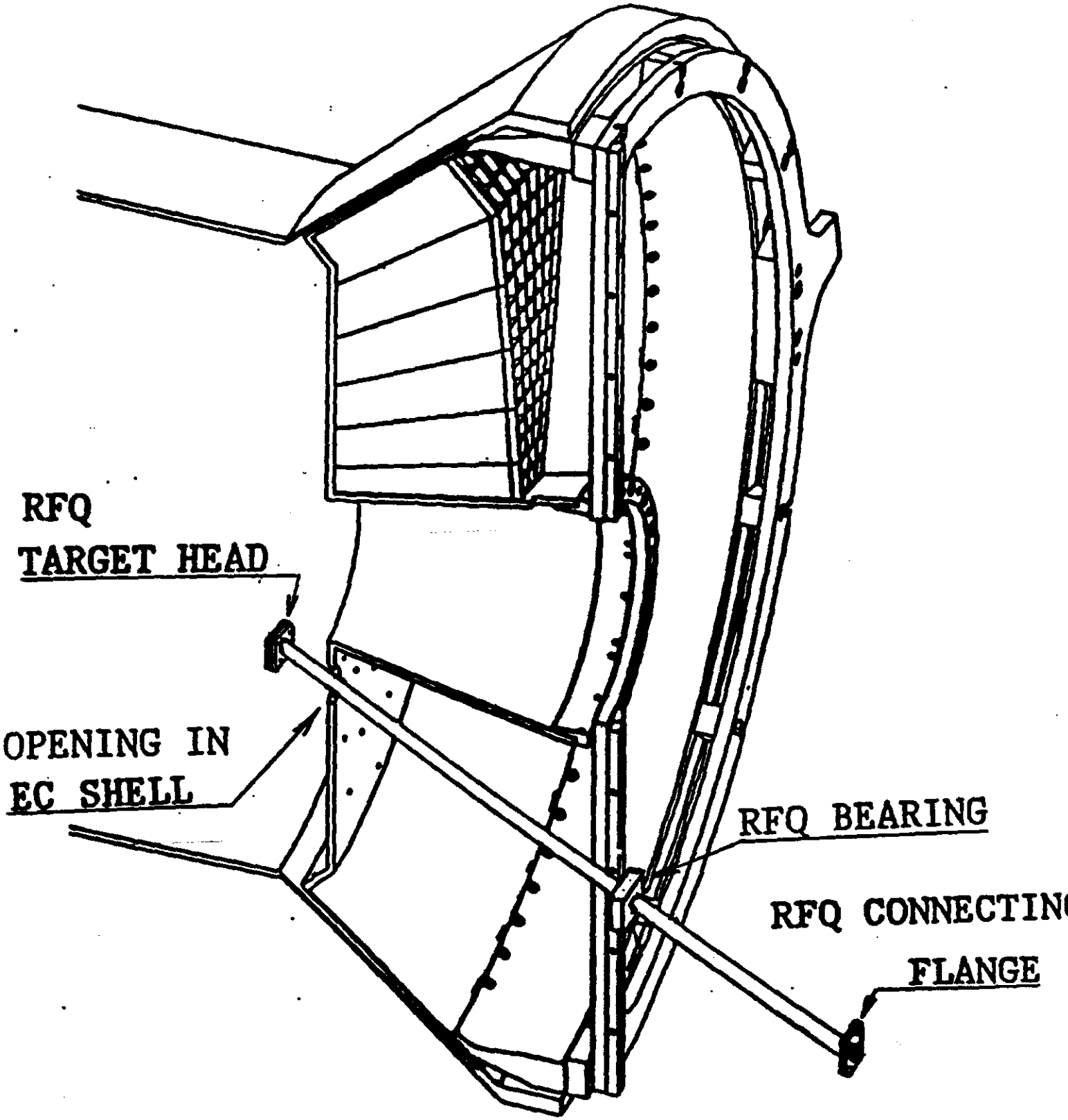

1/2 EC ISOMETRIC VIEW (after PM/LAPP)

30 10 89 MU

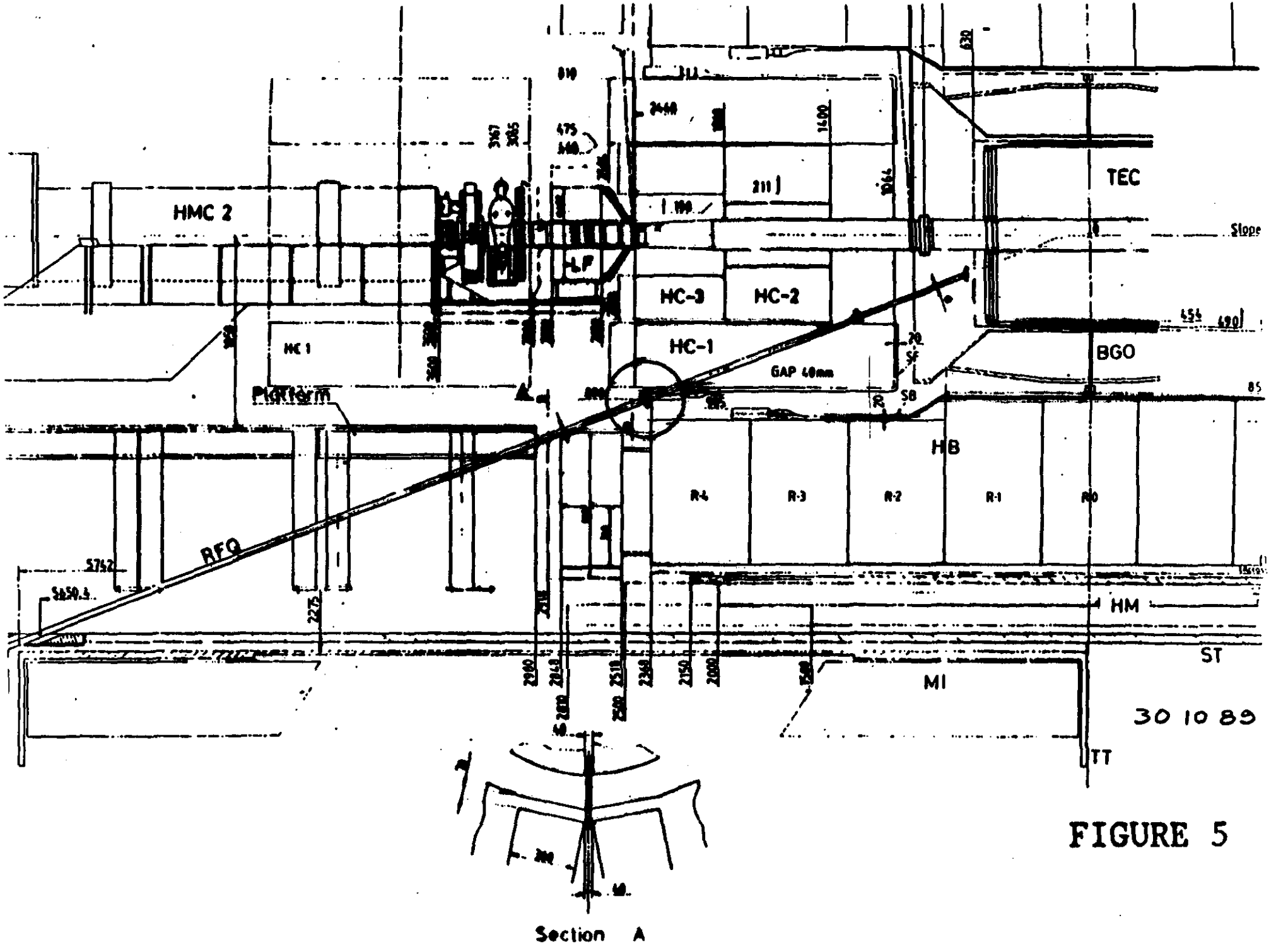
HMC 2
HC 1
Platform
RFQ
HC-3
HC-2
HC-1
GAP 40mm
TEC
BGO
HB
R-4
R-3
R-2
R-1
R-0
HM
ST
MI
TT
Slope
30 10 89
Section A

FIGURE 5

HIGH ENERGY PHYSICS DETECTOR CALIBRATION SYSTEM

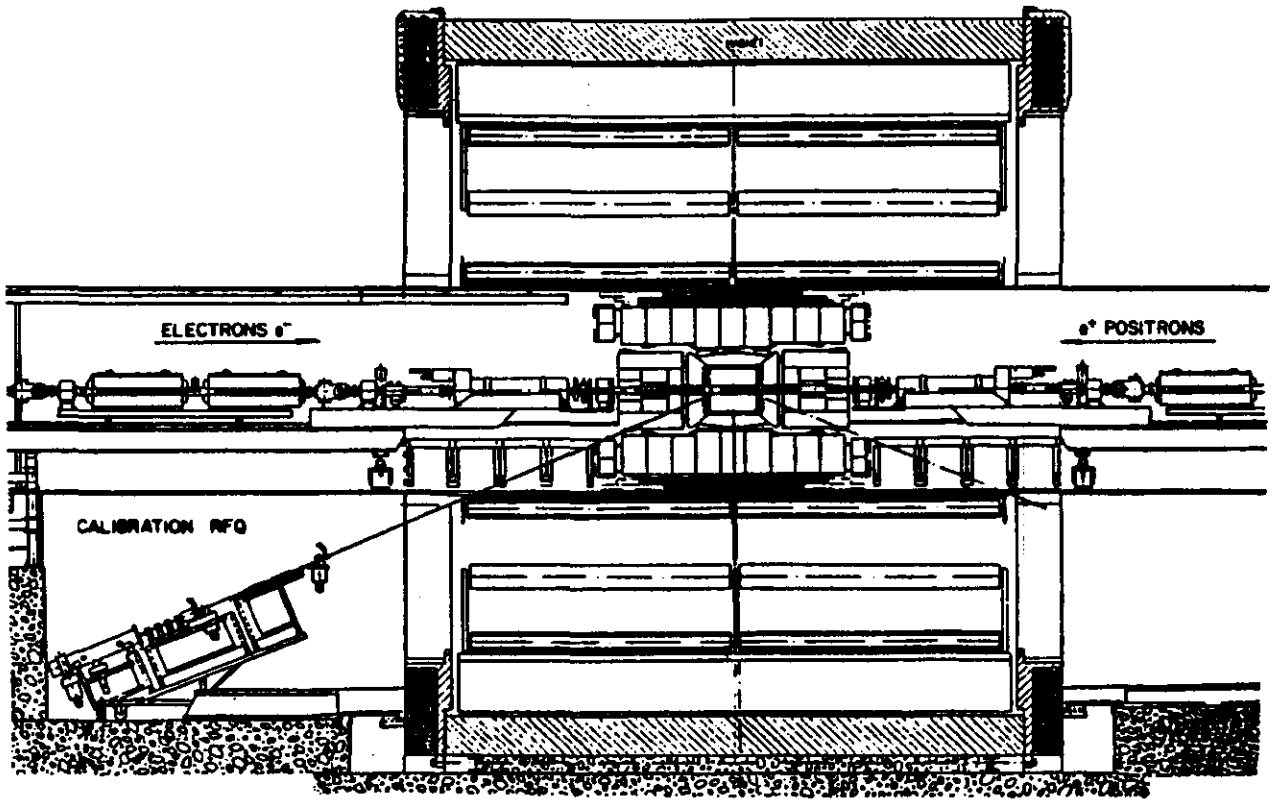

L3 DETECTOR

ACCSYS TECHNOLOGY, INC

RFQ TEST at AccSys (1988)

- 4 BaF_2 Sample Crystals (8 cm Deep)
- 49 L3 BGO Crystal Array
- 1.9 MeV Beam Energy: Up to 10 GeV Equivalent Per Pulse
- Narrow Clean Gaussian Distributions: Width 2.0% at 10 GeV
- Calibration Point: Peak Position

Deviation (%) of Peak Position

CRYSTAL	Run 1	Run 2	Run 3	Run 4	Run 5
BaF 1	0.32	0.00	0.19	0.06	-0.57
BaF 2	-0.31	-0.36	0.11	0.53	0.04
BaF 3	-0.12	-0.09	0.11	0.14	0.24
BaF 4	0.62	-0.19	0.04	-0.12	-0.36

RESULT: Rms Deviation of Peak in BaF_2 Crystals = 0.29%
(in BGO Crystals = 0.34%)

BARIUM FLUORIDE CALORIMETER CALIBRATION

Precise Frequent Calibration *in situ* is Essential to Maintain the High Resolution

RADIOFREQUENCY QUADRUPOLE ACCELERATOR (RFQ)

- **3.9 MeV Proton Beam**
- **Radiative Capture in Fluoride Target**
  - Bursts Of 6 MeV Radiative Capture Photons
  - Up To 40 GeV Equivalent Per Crystal Per Beam Pulse (300 TeV Per Pulse Over 4π)
- **TEST RESULT (1988)**
  - Calibrate All Crystals to 0.4% in a Few Minutes

HW

CALIBRATION IN SITU

RFQ

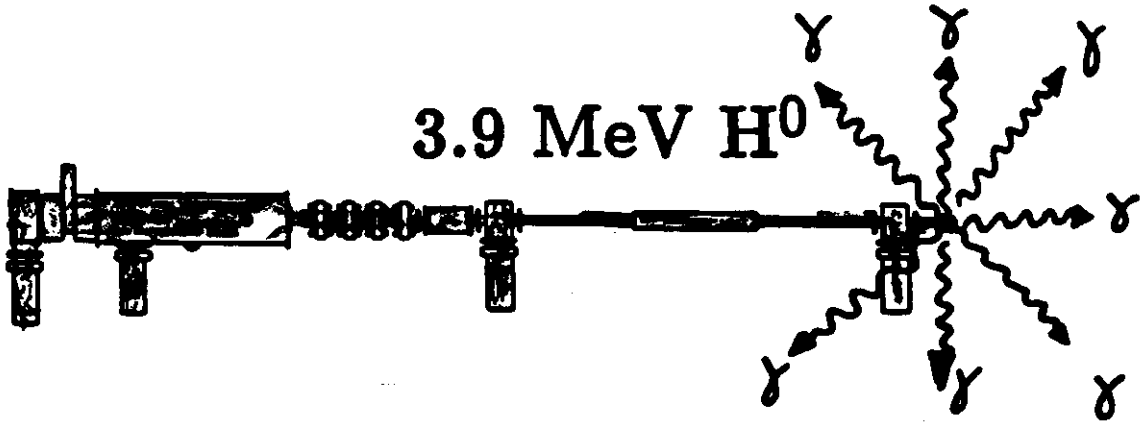

Up To 40 GeV Equivalent Per Crystal
Per 1 μsec RFQ Beam Pulse

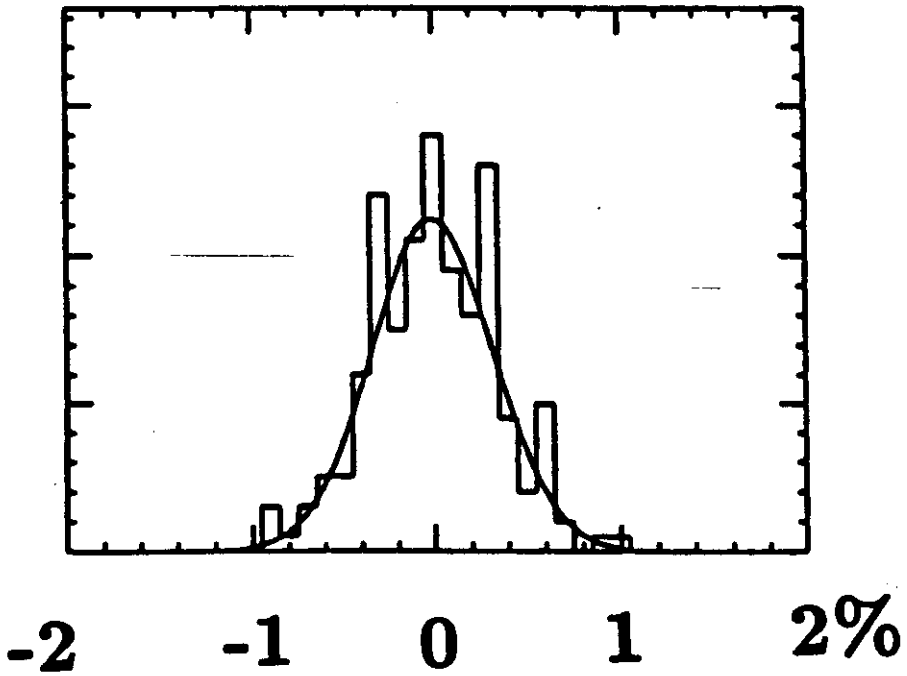

TEST RESULT:
RMS DEVIATION of PEAK= 0.3%

HW

BaF_2 RADIATION DAMAGE TESTS

At Caltech, UC Irvine, BNL, JPL

- To 2×10^7 Rads γ's;
  To 2×10^{14} n/cm^3
- Saturation Effect Observed
  $\Rightarrow$ Small Change to 10^5 Rads
  $\Rightarrow$ No Further Change to 10^7 Rads
- No Permanent Damage:
  Complete Recovery at 500°C
- Results Show Radiation Damage
  Is from External Impurities
- Electron Diffraction, Doping and Growth
  Studies at SIC, BGRI Indicate Ce, O_2

BaF_2 RADIATION RESISTANCE

Cross Scintillation Mechanism

- **Studied in Many Fluoride Crystals**
  - Fast UV Light
  - Weak Temperature Dependence
  - Effects of e, γ, n, p Irradiation Similar (Measured in Space Program)
- **High Purity Crystals: Hard to $\geq 10^7$ Rads**

R&D RESULTS
BaF_2 Radiation Resistance

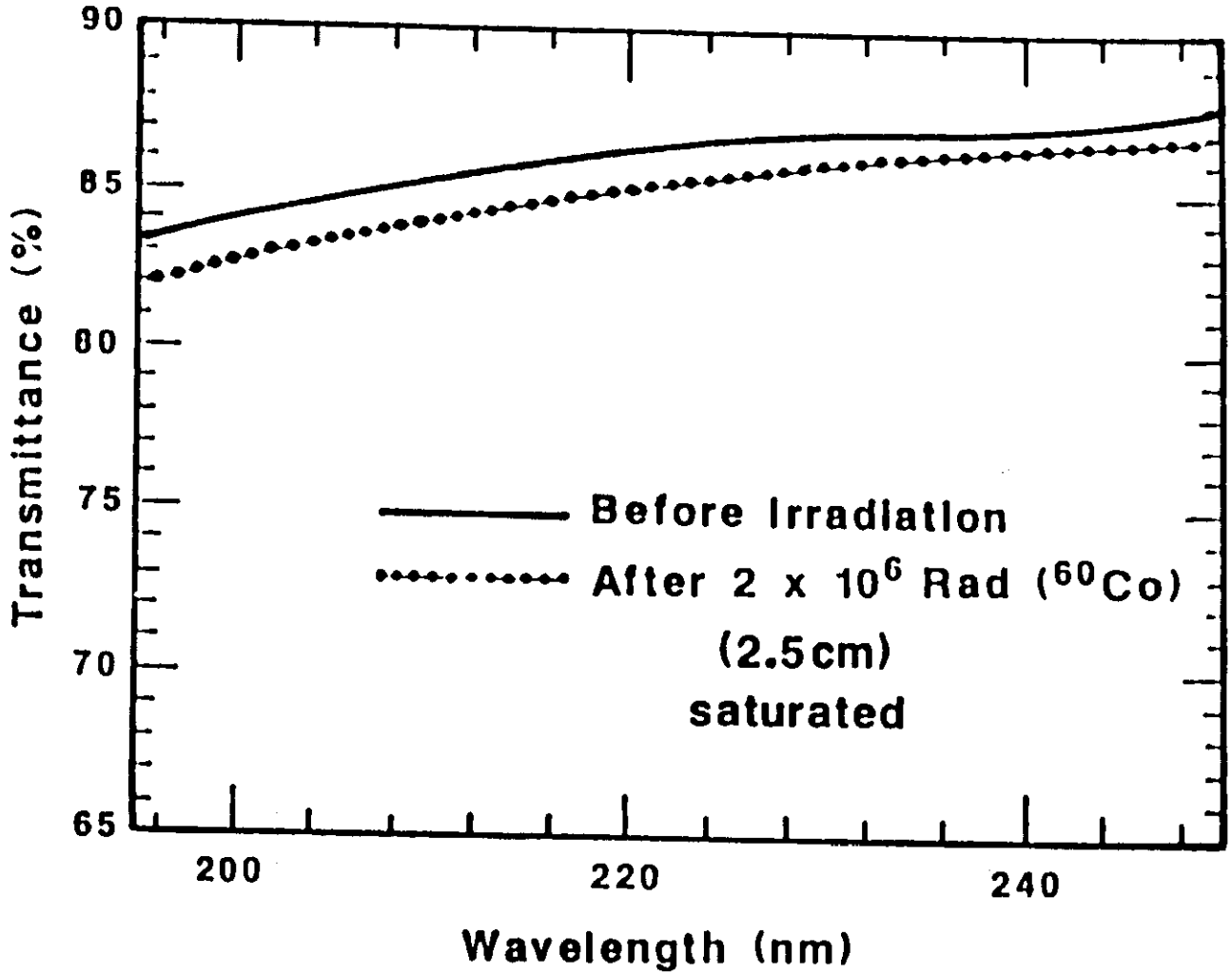

At 200nm effect equals to 1%

This implies a 20% effect for 50cm (acceptable)

BaF_2 CRYSTAL PRODUCTION and RADIATION RESISTANCE

- **Studies on Critical Impurities and Radiation Hardness**
  - at SIC, BGRI, CMU and Caltech
- **Purify Raw Materials:**
  - Eliminate Selected Metals (Ce, Pb, Co) To < 1 ppm
  - Specifically Eliminate Pb, O_2, OH^- During Pre-Treatment and Growth

Impurity	Crystal	Raw Material
NiO	1.7×10^{-6}	8.3×10^{-6}
MnO	1.5×10^{-7}	5.2×10^{-7}
CaO	3.6×10^{-7}	2.8×10^{-7}
Cr_2O_3	8.4×10^{-7}	1.4×10^{-5}
Fe_2O_3	9.2×10^{-6}	2.0×10^{-5}
MgO	1.9×10^{-6}	1.0×10^{-5}
CoO	1.0×10^{-5}	1.3×10^{-6}

Table.1. Impurity quantities of raw material and crystal respectively

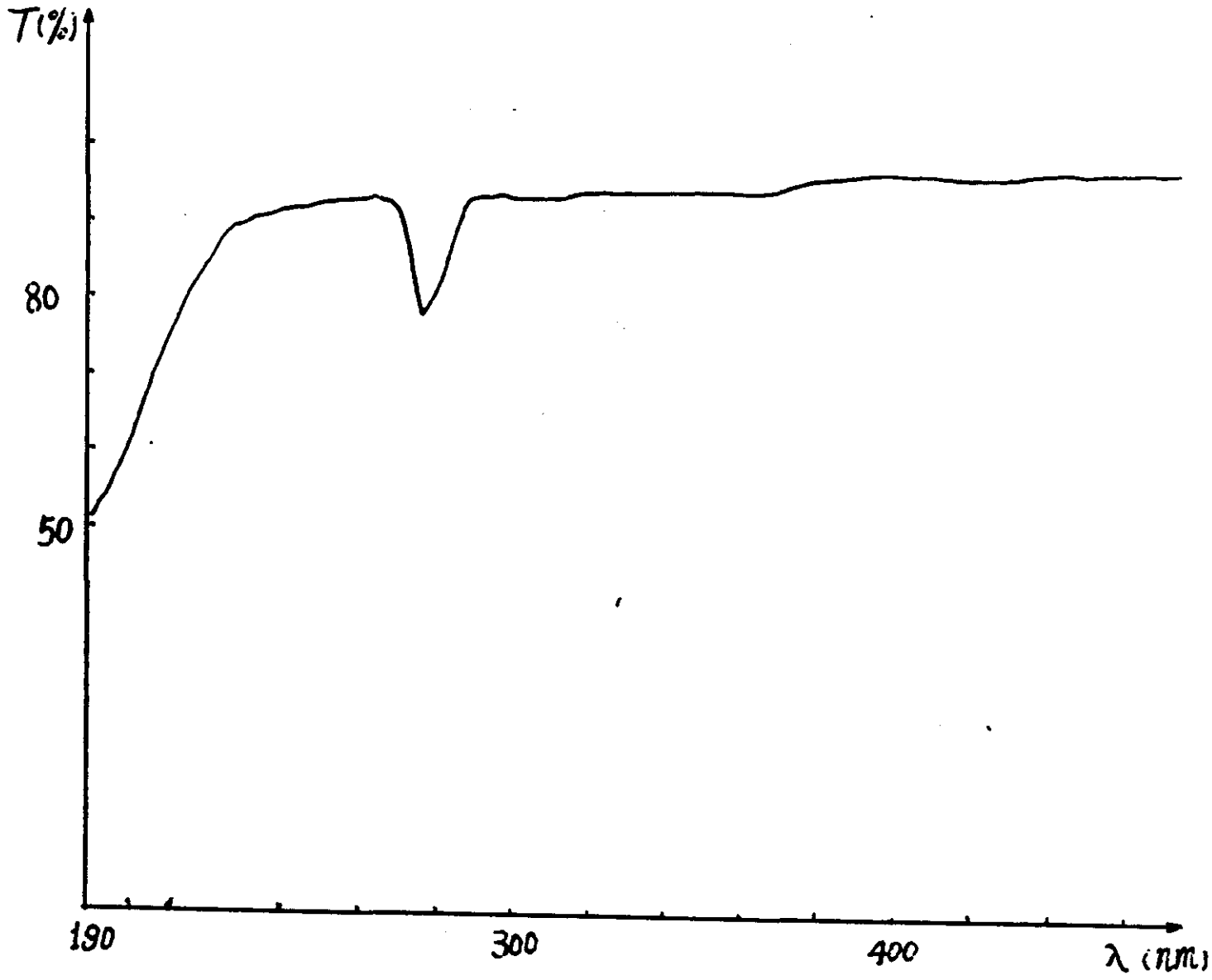

Fig. 2. The transmission curve of a BaF_2 Crystal. (sized. 4x4. 3x3. x25 cm^3).

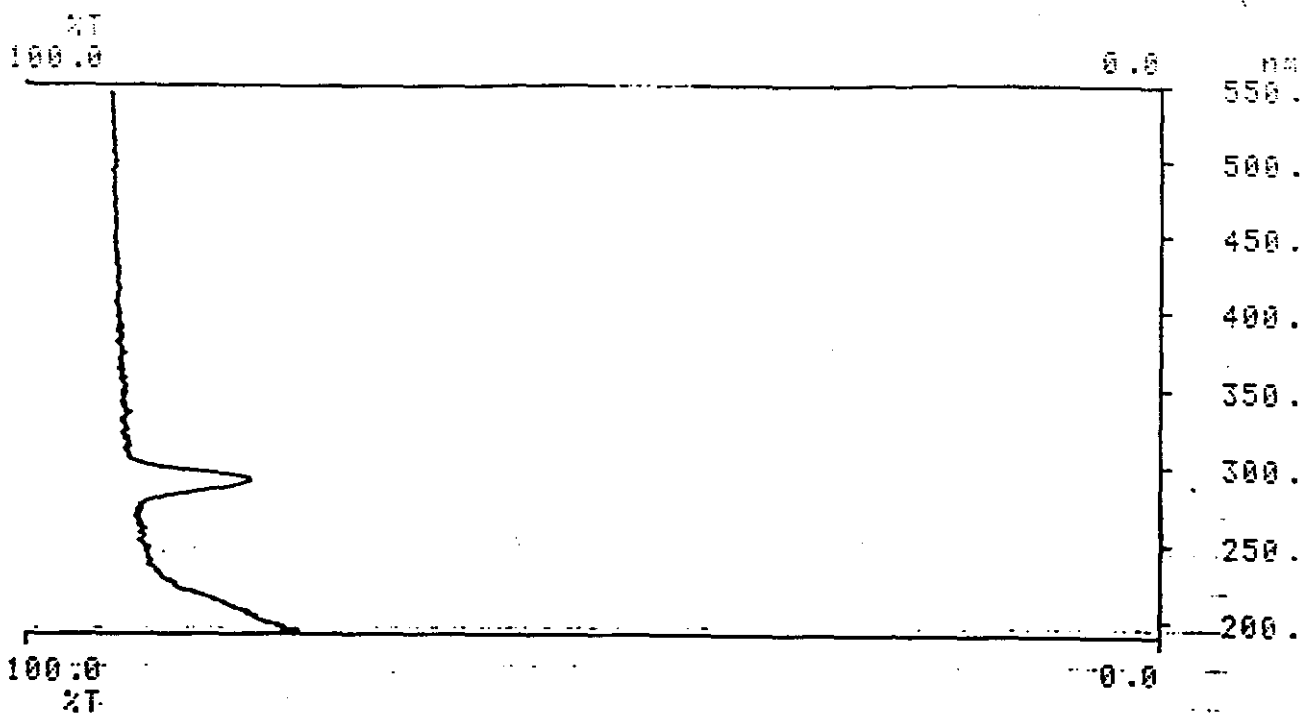

TITLE: S2A007.DT
SCAN SPEED: 60.0 nm/min
BANDPASS: 5.00nm

5:26 PM 5/13/91
RESPONSE: MEDIUM

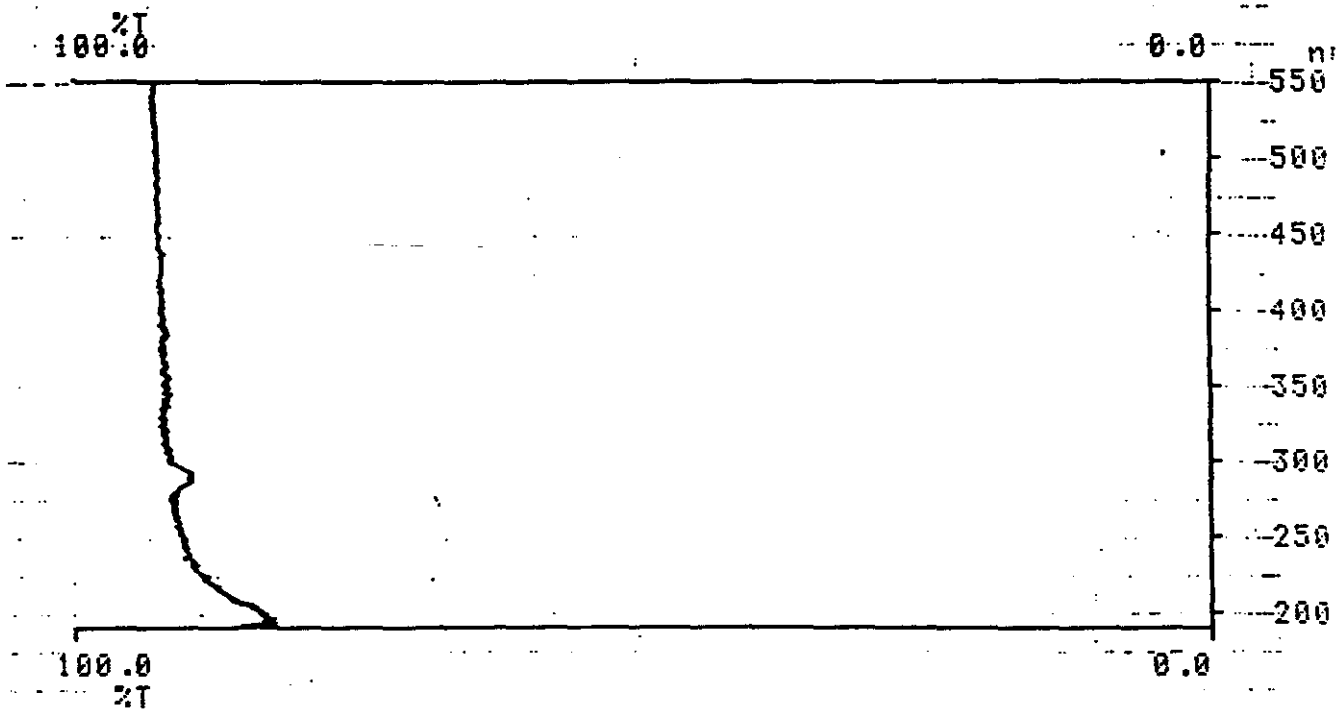

TITLE: S2A006.DT
SCAN SPEED: 60.0 nm/min
BANDPASS: 5.00nm

6:33 PM 5/13/91
RESPONSE: MEDIUM

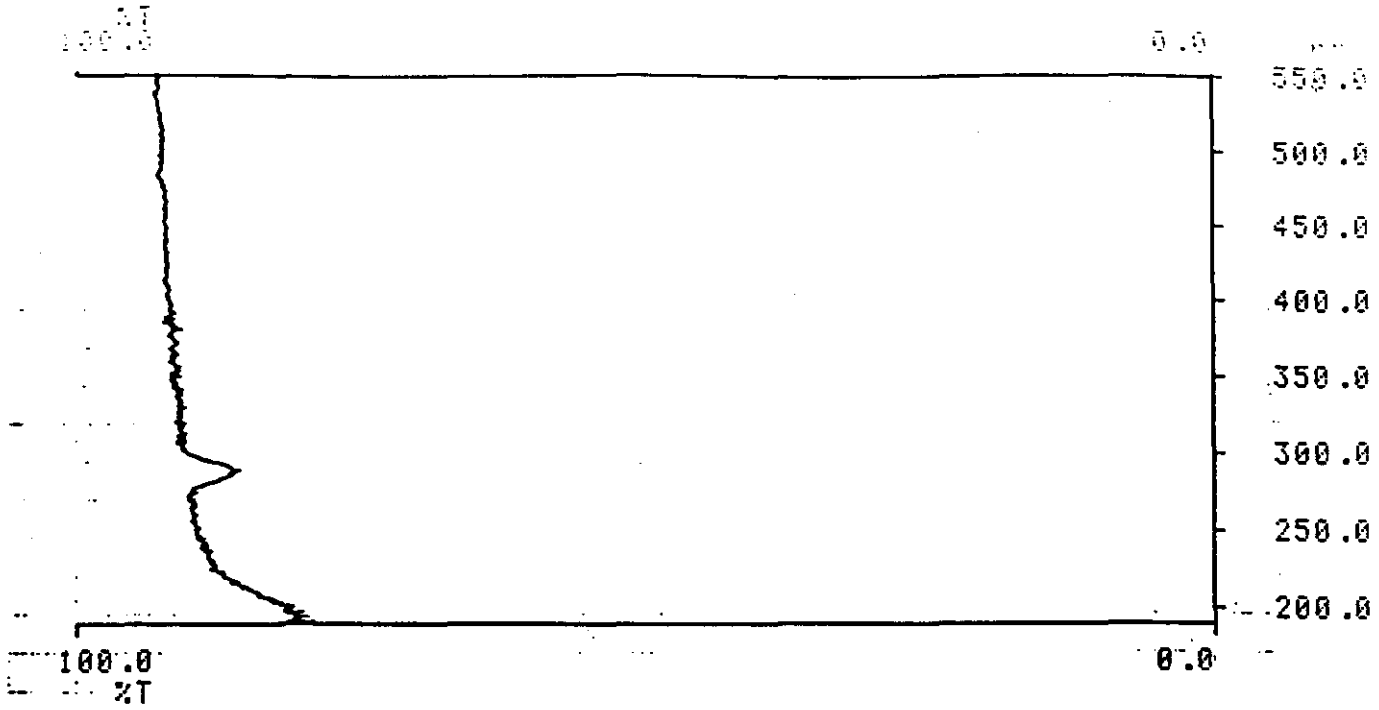

TITLE: S1A002.DT 2:58 PM 5/16/91
SCAN SPEED: 60.0 nm/min RESPONSE: MEDIUM
BANDPASS: 5.00nm

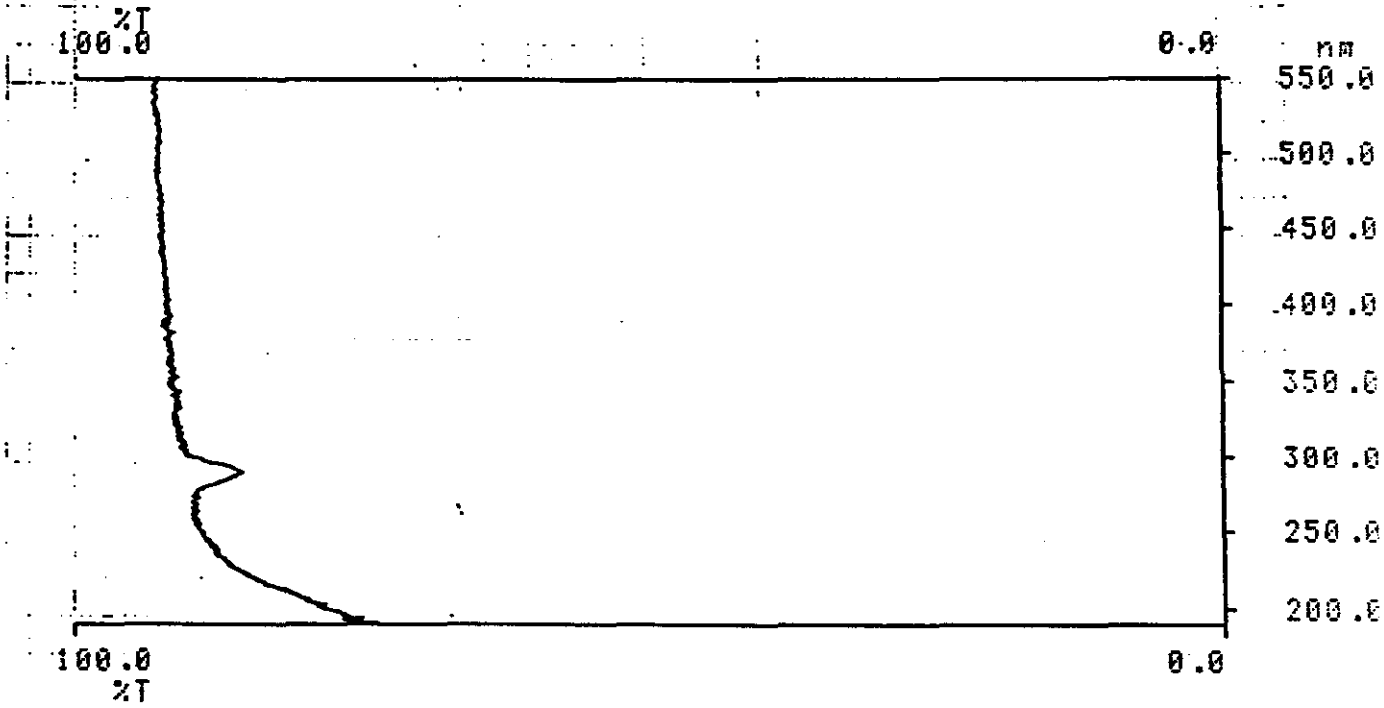

TITLE: S1A001.DT 2:48 PM 5/16/91
SCAN SPEED: 60.0 nm/min RESPONSE: MEDIUM
BANDPASS: 5.00nm

HITACHI NO. 228-1050

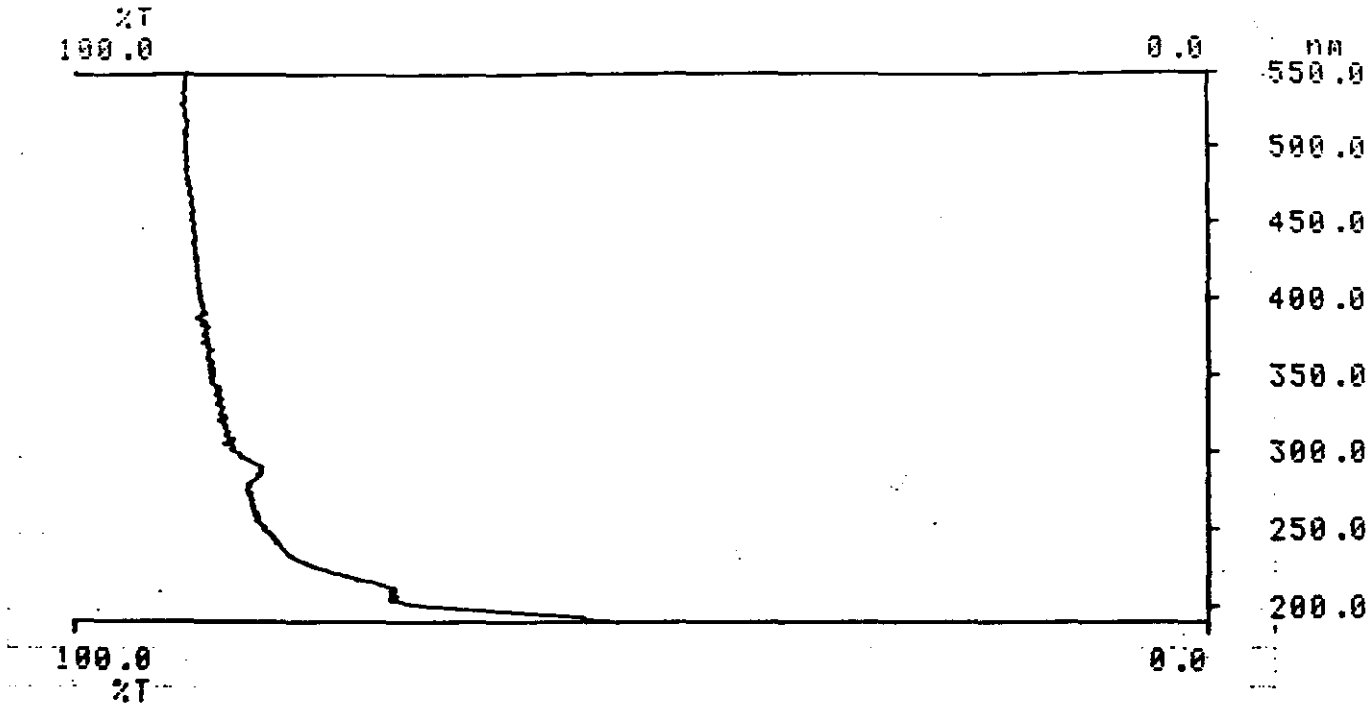

TITLE: S18006.DT
SCAN SPEED: 60.0 nm/min
BANDPASS: 5.00nm

12: 2 PM 5/16/91
RESPONSE: MEDIUM

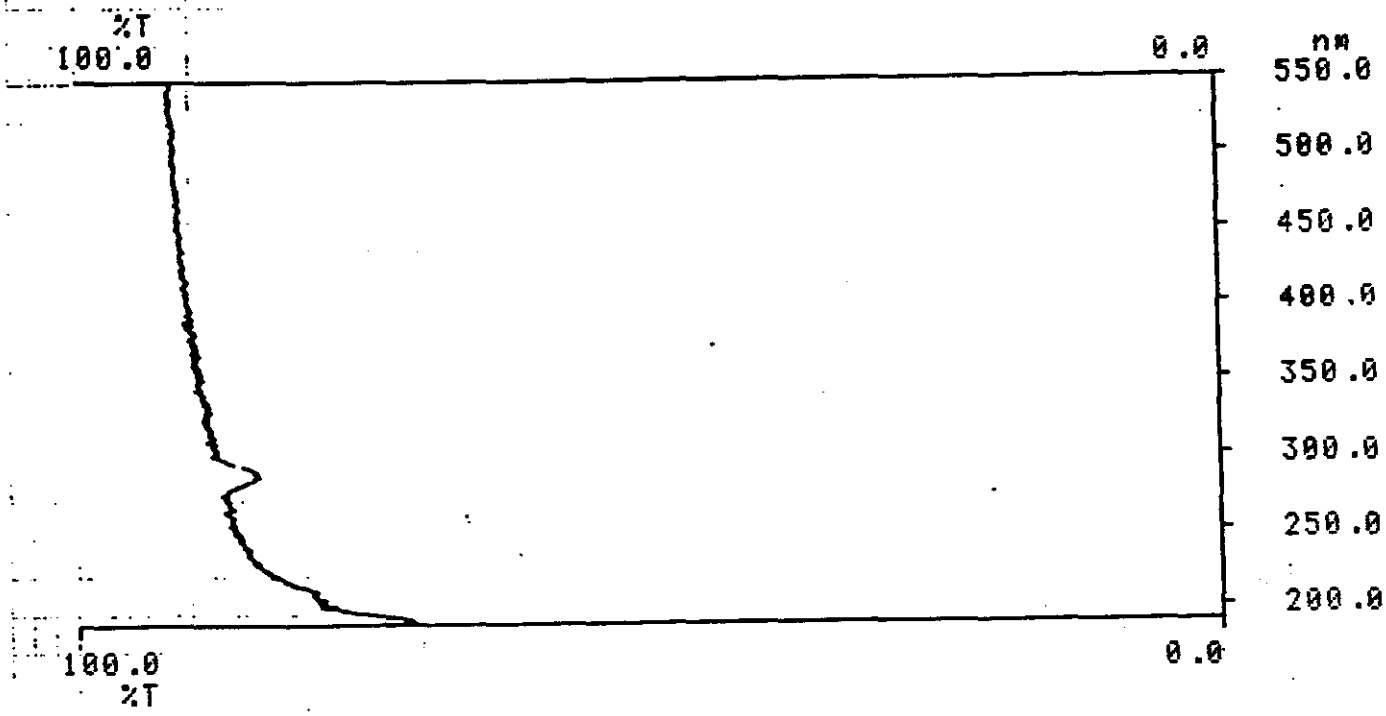

TITLE: S18005.DT
SCAN SPEED: 60.0 nm/min
BANDPASS: 5.00nm

11:21 AM 5/16/91
RESPONSE: MEDIUM

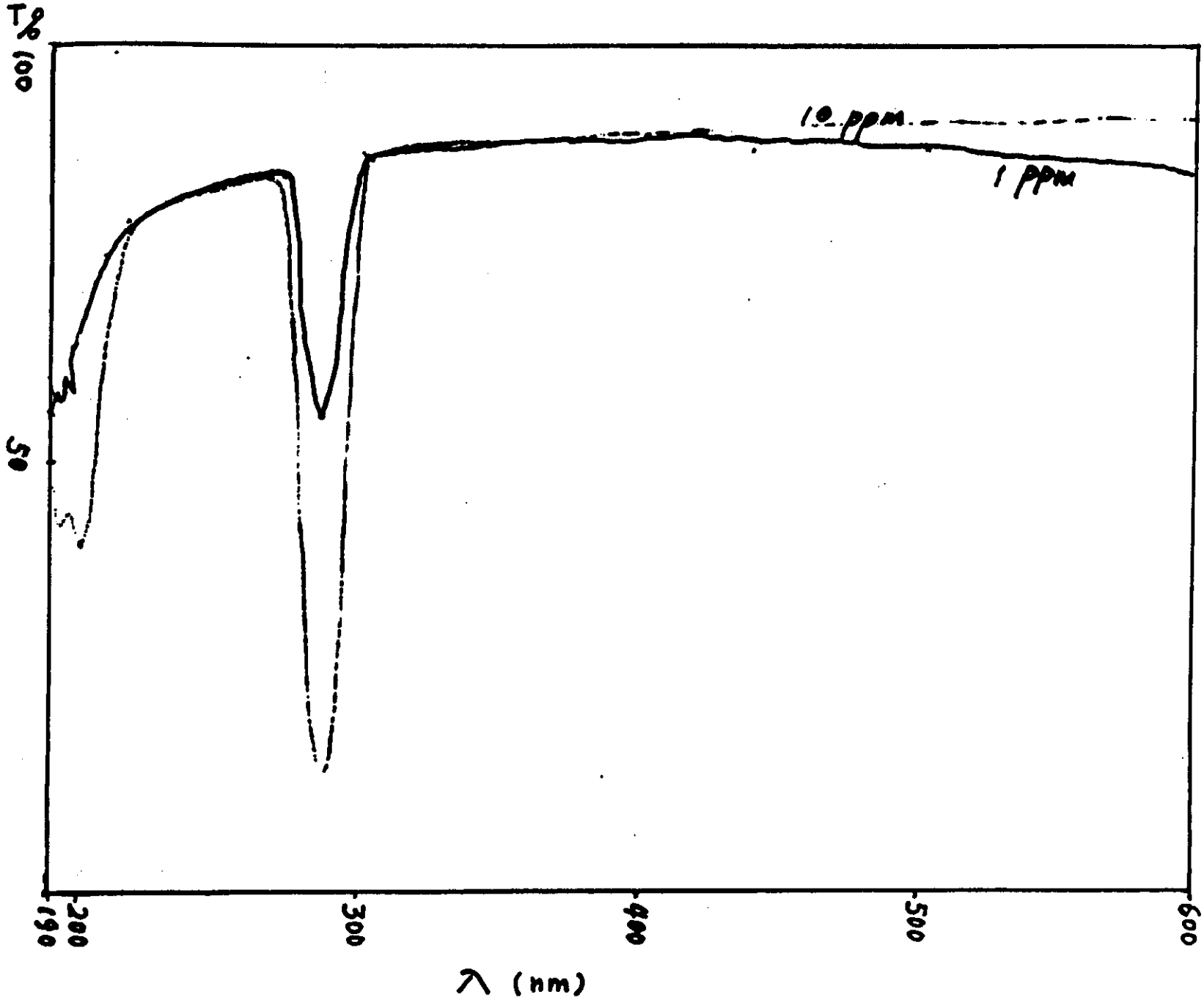

Fig. 8 Transmittance of Ce doped BaF crystal

Optovac 1" x 1" diameter

1% LaF_3 doped BaF_2 –sample 1

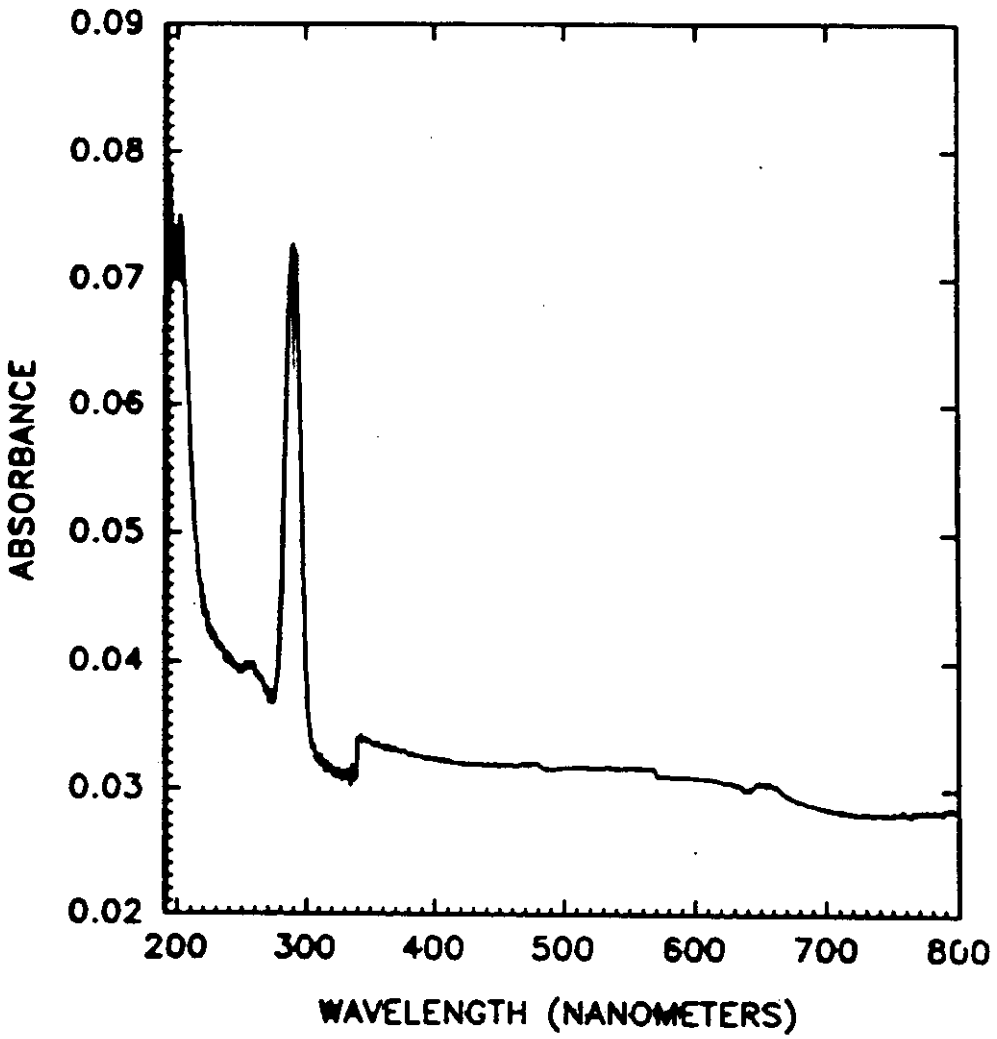

6-5-90
BALA1.SPC

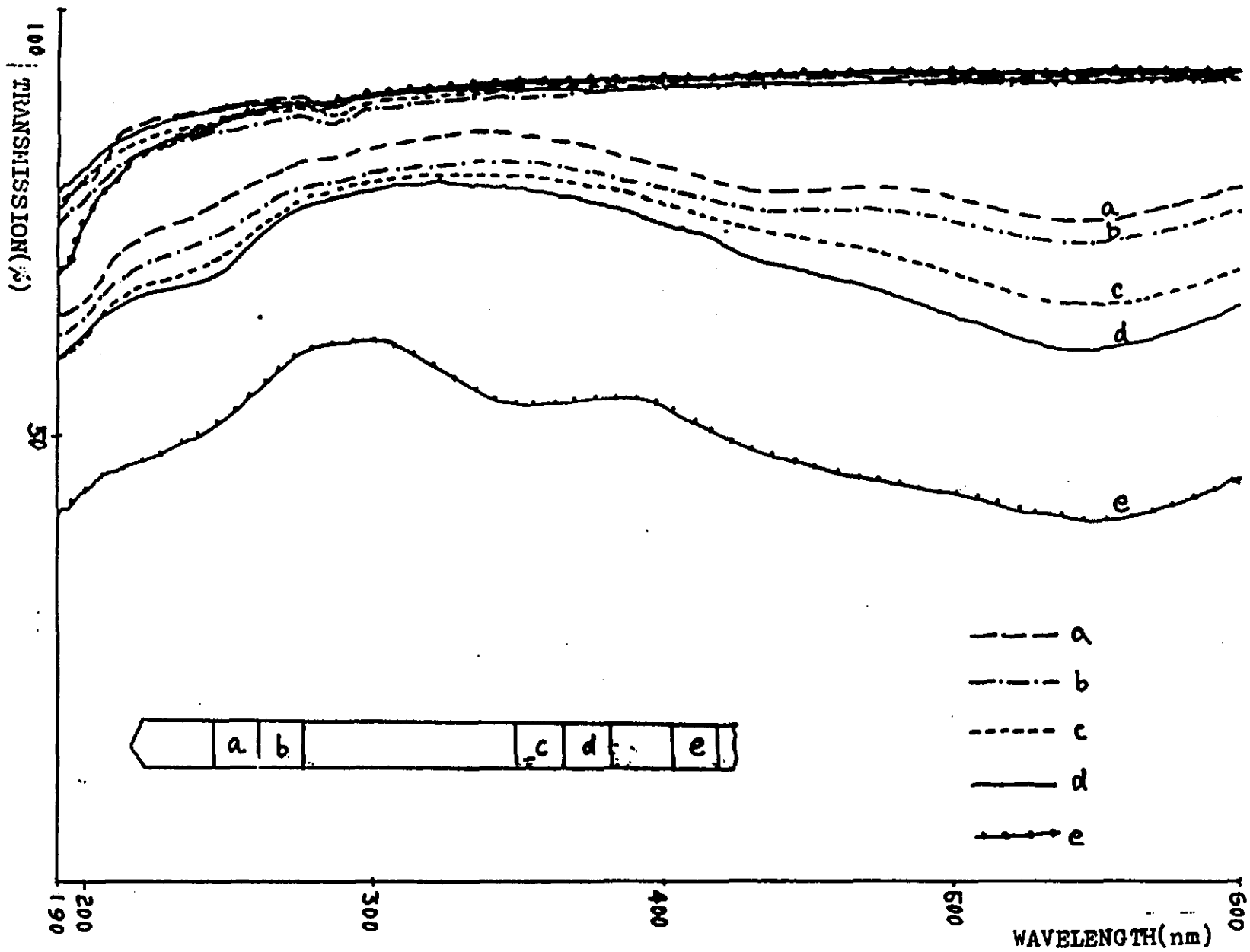

Fig.2 25 mm long crystal, r-ray irradiation: 1.6 MRad.
BaF_2 crystal cut from different sites of a 300 mm crystal

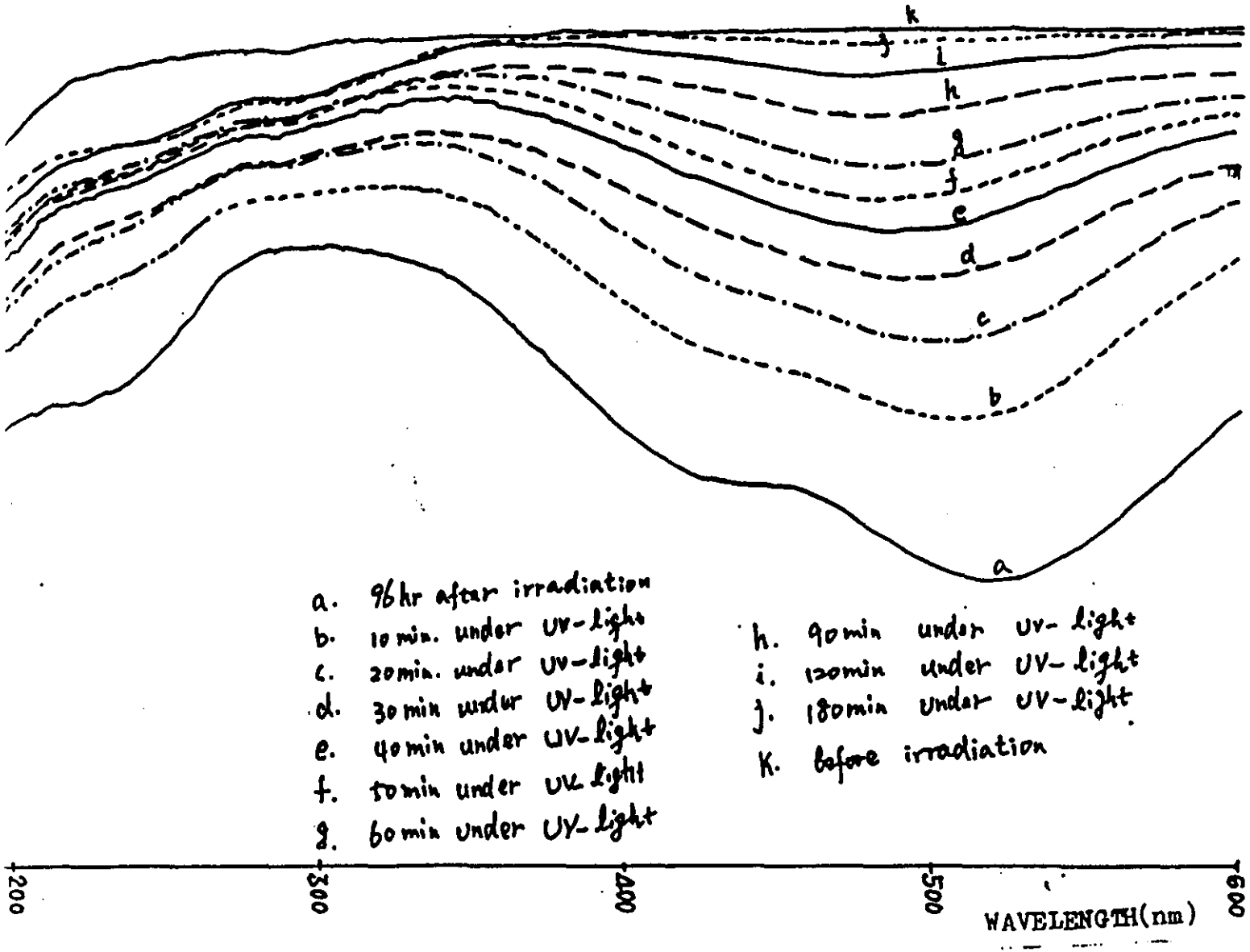

Fig.10 Bleaching effect of damaged BaF_2 crystal by UV light

---> **WAVELENGTH SCAN REPORT** <---

Date : 02-26-1991
Time : 19:54:06
Operator : Not Entered

File Name : C:\hp8452\DATA\sict1011.WAV

Sample Name : SICT1
Solvent Name :
Concentration : 0
Units :

Function : % Transmittance
Wavelength Range : 190 to 820 nanometers
Integration Time : 1 seconds
Std Deviation : ON

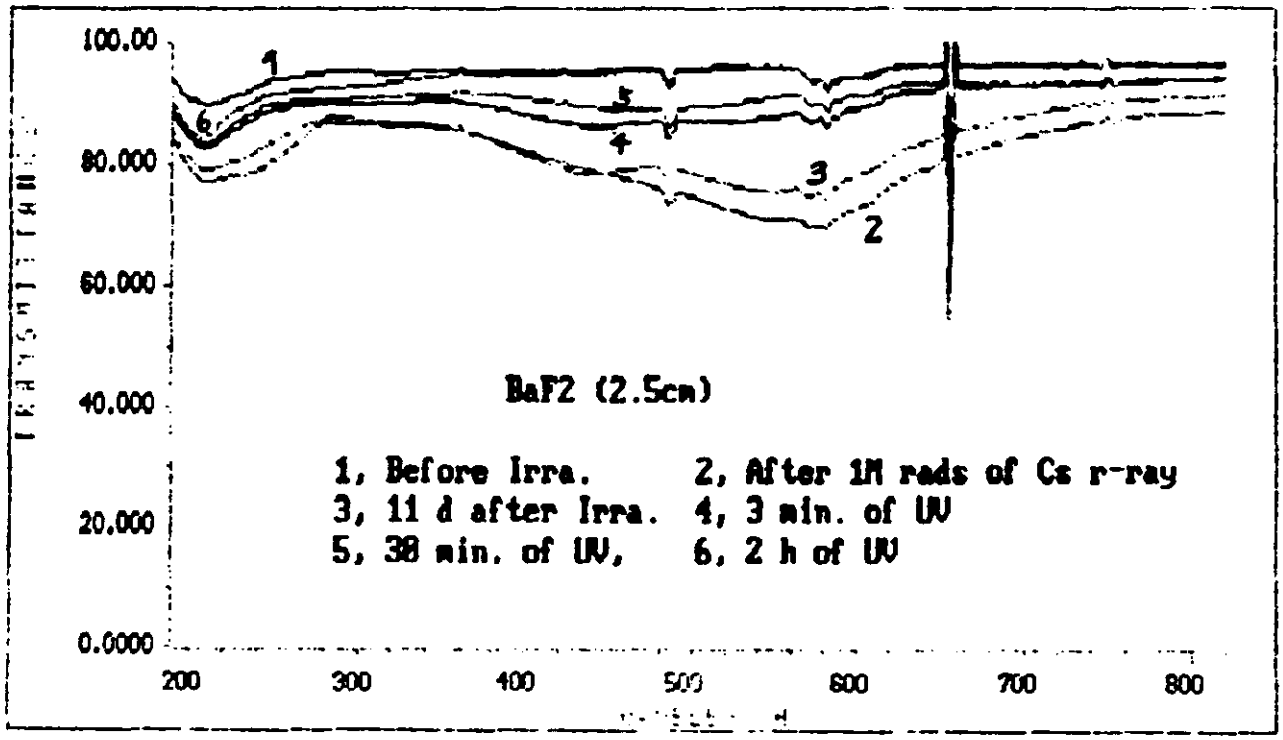

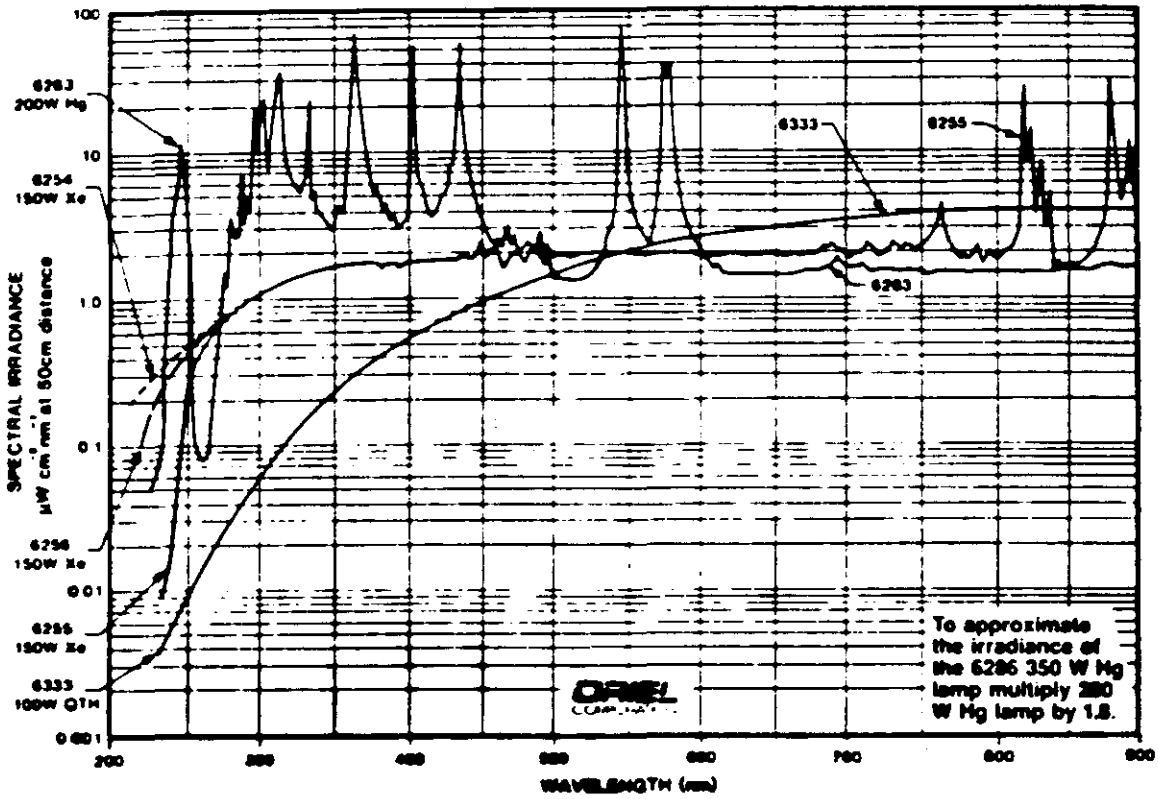

Fig. 2 Spectral irradiance of 200 W Hg, 150 Xe, and 100 W QTH Lamps.

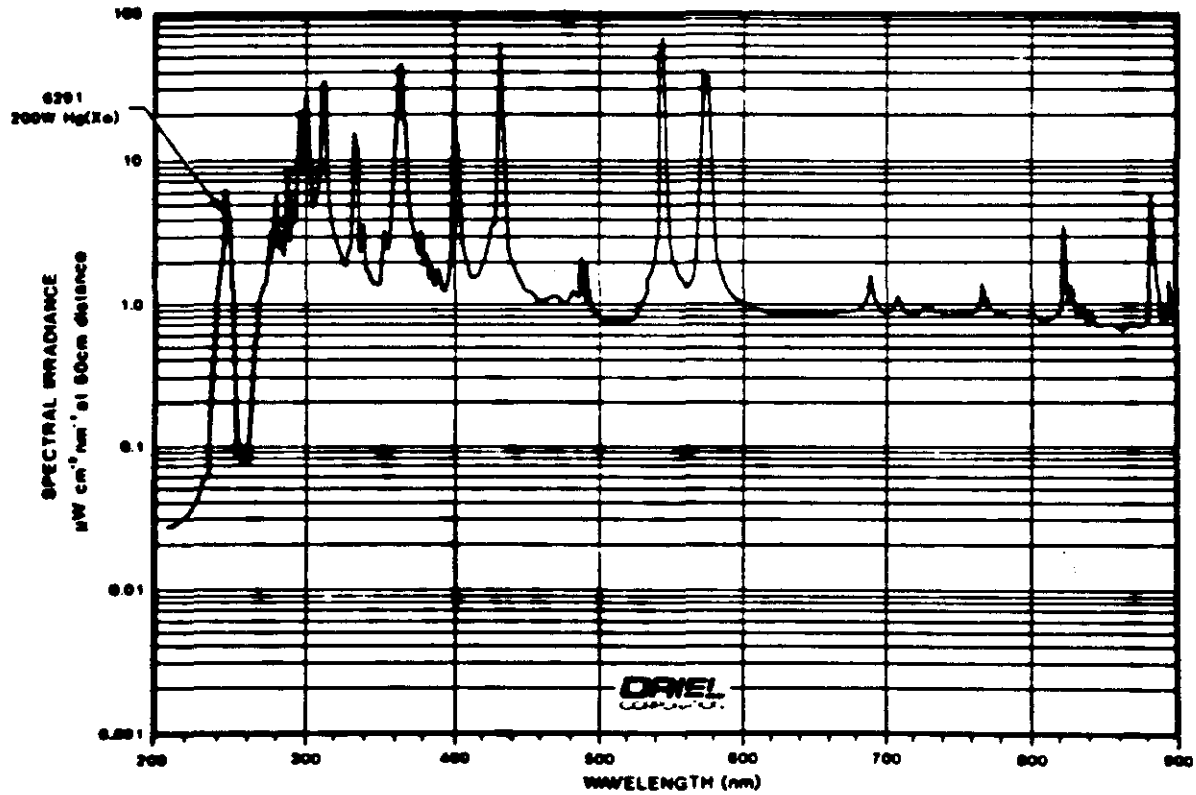

Fig. 3 Spectral irradiance of 200 W Hg(Xe) Lamp.

II. On the Mechanism of Optical Absorption and Radiation Damage of BaF_2 Crystals

1. Optical absorption of hydrogen and oxygen in BaF_2 crystals

* Hydrogen and oxygen are easy to enter BaF_2 crystals as impurities. they form OH^{-1} ions and OH^{-1}-X_i^0 defect complexes, Lone O^{-2} ions or O^{-2} ion pairs and O^{-2}-F^+ (F^+ is fluorine vacancy X_v) dipoles.

* For free OH^{-1}, its absorption band located in the infrared region at 3630 cm^{-1} corresponding to the stretching vibration of OH^{-1} dipoles[1].
  For OH^{-1}-X_i^0 (in BaF_2 crystal X_i^0 is institutial fluoride atom)(2,3), its absorption band appeared between 2900-3700 cm^{-1}.
  Besides, OH^{-1} also create far ultra-violet absorption bands 60 nm[4], 62 nm[5] and 65 nm[6] in CaF_2, SrF_2 and BaF_2 crystals, respectively. However, they are not correlated to the absorption bands in the 190-300 nm UV region.

* So, we assumed that the absorption bands located between 190-250 nm are created due to the lone O^{-2} ions or O^{-2}-O^{-2} ion pairs; and the absorption band located near 290 nm is due to the transition of O^{-2}-F^+ or $2O^{-2}$-$2F^+$ dipoles.

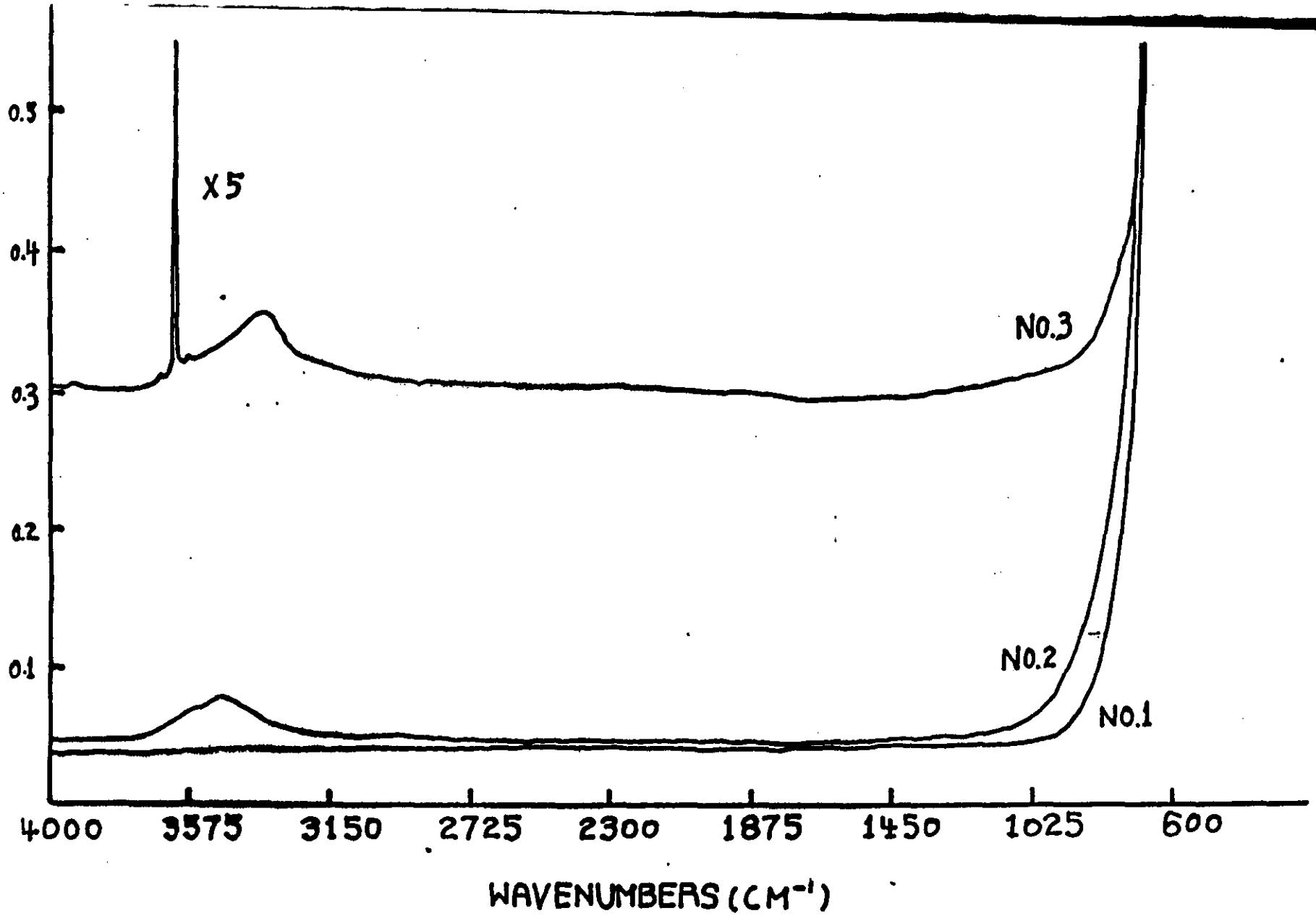

Fig.11 Infrared spectra of BaF_2 crystal with different content of OH^{-1} ions

* Oxygen containing fluorides can be considered as a mixed crystal of MF_2 and MO, for example, can consider oxygen containing SrF_2 crystal as a mixed crystal of SrF_2 and SrO. It was known that the UV absorption band of SrO is located at 215-217 nm[7], and it is 205-209 nm (about 6 e.V) for BaO. They are due to the transition from O_{2p} state to conduction band of Ba^{+2} or Sr^{+2} ions.

* When oxygen containing BaF_2 crystals were irradiated by r-ray radiation, O^{-2}-F^{+} dipoles decomposed:

$$O^{-2}\text{-}F^{+} \longrightarrow O^{-2} + F^{+}$$

which will increase the concentration of lone O^{-2} ions and O^{-2} ion pairs so as to increase the absorption in the 190-250 nm region. F^{+} vacancies are easy to capture electrons to form F centers which are responsible to the absorption in the visible region. In the mean time, the hollow at 290 nm was reduced or disappeared due to the decomposition of O^{-2}-F^{+} dipoles.

* When the damaged crystal was irradiated by UV, the electrons trapped in the F centers are easily escaped from the F^+, the crystal was bleached due to the destroy of F centers. The F^+ could associate again with O^{-2} ion to form O^{-2}-F^+ dipoles so as to decrease the concentration of O^{-2} ions and O^{-2} ion pairs in the crystal. The absorption in the 190-250 nm region also decreased.

* An experimental result of electron diffraction study (Fig.15) gave us an idea that probably there is a certain amount of oxygen (either in atom or molecule state) dissolved in the BaF_2 crystals.
Figure shows that just after the electron beam hitting the crystal, a very pure BaF_2 pattern was shown, however, after certain times, BaO rings appeared associated with the BaF_2 diffraction pattern. We assume that is the result of oxygen atoms or molecules transforming to oxygen ions during the electron beam bombardment.

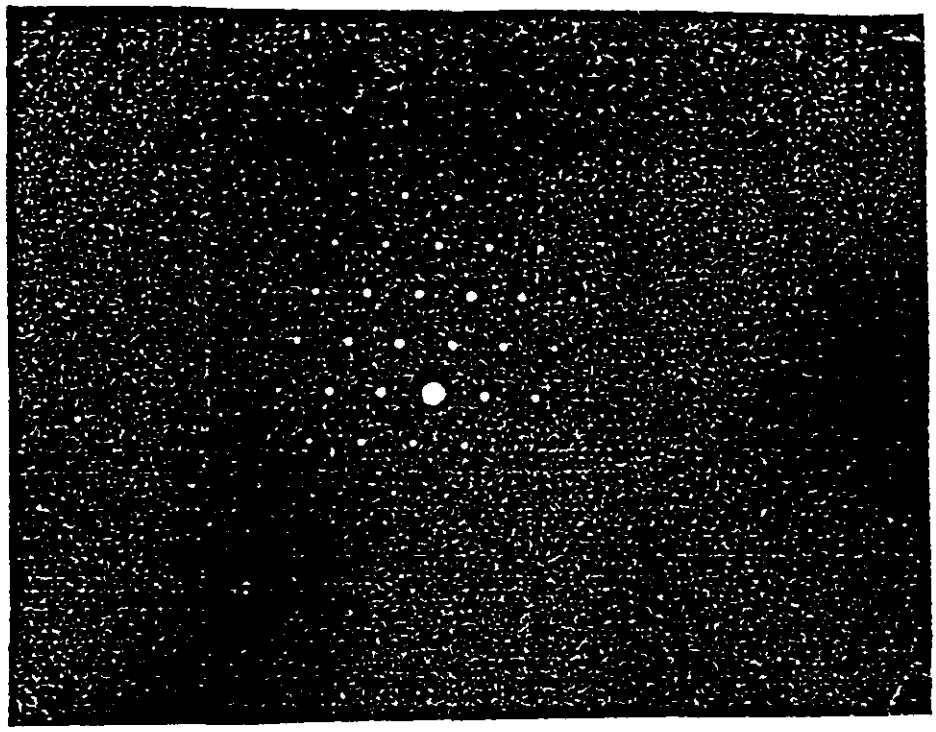

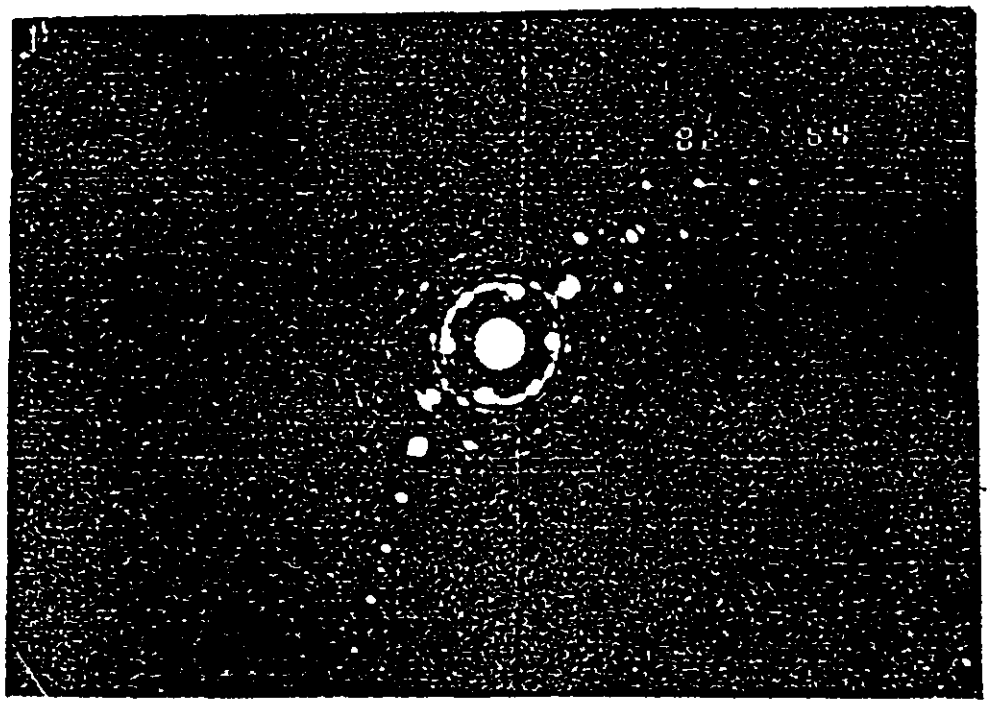

Fig.12 Electron diffraction patterns of BaF_2 crystal

(a) Just start bombardment of electron beam on crystals
(b) After certain time of bombardment of electron beam, pattern shows appearance of BaO rings

FIRST ROUND TEST:
7×7 ARRAY (8/91 - 11/91)

HW

- **ELECTRON RESOLUTION**
  To Demonstrate $\sigma_E/E = (1.3/\sqrt{E} + 0.5)\%$
  With Electrons from 10 GeV to $\geq$ 100 GeV
  - Calibrate the gain for each crystal + phototube.
  - Scan the beam across the central crystal to establish the (position corrected) uniformity of response.
  - Check the stability of a period of weeks.
  - Compare to GEANT predictions for resolution, energy sharing distributions, and position reconstruction accuracy as a function of the impact point.
- **PION RESPONSE**
  From 10 GeV to $\geq$ 100 GeV
  - Using data taken at the same time as for the electrons above.
- **ELECTRON-PION SEPARATION**
  Note: because of the limited transverse size of the first round crystal array, we will be able to test our electron selection criteria, but we will not have a complete test of e/π separation.
  - Test (Sum of 25)/(Sum of 49)
    Note: This is like (Sum of 9)/(Sum of 25) with the final crystal sizes.
  - E (electromagnetic energy) versus p (Momentum),
    using the drift chamber spectrometer.
  - Possibly: Veto on the energy in the backup calorimeter.
    Note: This may or may not be possible given the thickness of the calorimeter plates. A better HCAL module is needed.
- **MIPs CALIBRATION TEST**
  - Calibrate the crystals using minimum ionizing particles (MIPs) going along the long axis of a crystal. The mean energy for a MIP is expected to be 330 MeV.
- **ELECTRONICS DEVELOPMENT**
  - Test the resolution without a large electronic-noise contribution (with Cs-Te PMT's).
  - Isolate the contribution of noise using vacuum phototriodes and a first-round preamp and shaper matched to standard FASTBUS ADC's.
  - Develop mounting, shielding and grounding techniques to reach an acceptable noise level.
  - Possibly: Test a second-round of preamps and shapers with a shaping time $\sim$ 10 nsec or less, lower noise, and higher rate capability, used together with custom ADC's.
  - Test a Switched Capacitor Array readout module (Marlow).

SECOND ROUND TEST: 9×9 ARRAY (Summer 1992)

- ELECTRON RESOLUTION
  Demonstrate $\sigma_E/E = (1.3/\sqrt{E} + 0.5)\%$
  With Electrons from 10 GeV to > 100 GeV
  - * Calibrate the gain for each crystal + phototube.
  - * Scan the beam across the central crystal to establish the (position corrected) uniformity of response, with the carbon fiber prototype structure, and full-size crystals.
  - * Check the stability of a period of weeks.
  - * Check the resolution, and the absolute response, as a function of the rate.
  - * Compare to GEANT predictions for resolution, energy sharing distributions, and position reconstruction accuracy as a function of the impact point.
- PION RESPONSE From 10 GeV to > 100 GeV
  - * Using data taken at the same time as for the electrons above.
- ELECTRON-PION SEPARATION
  - * Test (Sum of 9)/(Sum of 25): Transverse shower shape.
  - * E (electromagnetic energy) versus p (Momentum), using the drift chamber spectrometer.
  - * Veto using an HCAL module from our Collaboration, placed behind the crystal array.
- ELECTRONICS DEVELOPMENT
  - * Use proximity-focused few-stage tube from Hammamatsu. Cross check against a separate run with high gain tubes or the previously-used phototriodes.
  - * Use monolithic preamp + shaper circuits, with lower noise than in 1991 tests; speed compatible with complete separation of signals from each SSC beam crossing.
  - * Develop mounting, shielding and grounding techniques to reach an acceptable noise level for the full-scale calorimeter.
  - * Test SCA or other higher level (e.g. FADC) trigger and readout modules.

THIRD ROUND TEST:
12×12 CRYSTAL ARRAY
and HCAL MODULES
Spring 1993

Note: This test will include further developments along the lines specified in the second-round test above, plus the following.

- ELECTRON-PION SEPARATION
  - Test (Sum of 9)/(Sum of 25), and other algorithms to fit jointly for the energy and position (analogous to a test of γ/π separation.
  - Check simulated results on side and rear leakage from the crystal array.
- ELECTRONICS DEVELOPMENT
  - Use latest UV-selective photodevice. Cross check against runs with previous devices.
  - Use monolithic preamp + shaper circuits, with final noise and pulse-spacing capability, corresponding to separation of signals from each SSC beam crossing.
  - Test trigger and digital readout modules.
- COMPENSATION
  - Measure the constant term in the resolution.
  - Develop optimized weighting methods, to minimize the constant term.
  - Check results on the energy distributions in the crystals and the HCAL, and their correaltions, against GEANT (GHEISHA) simulations. Check against other simulations (e.g. HETC) if necessary.

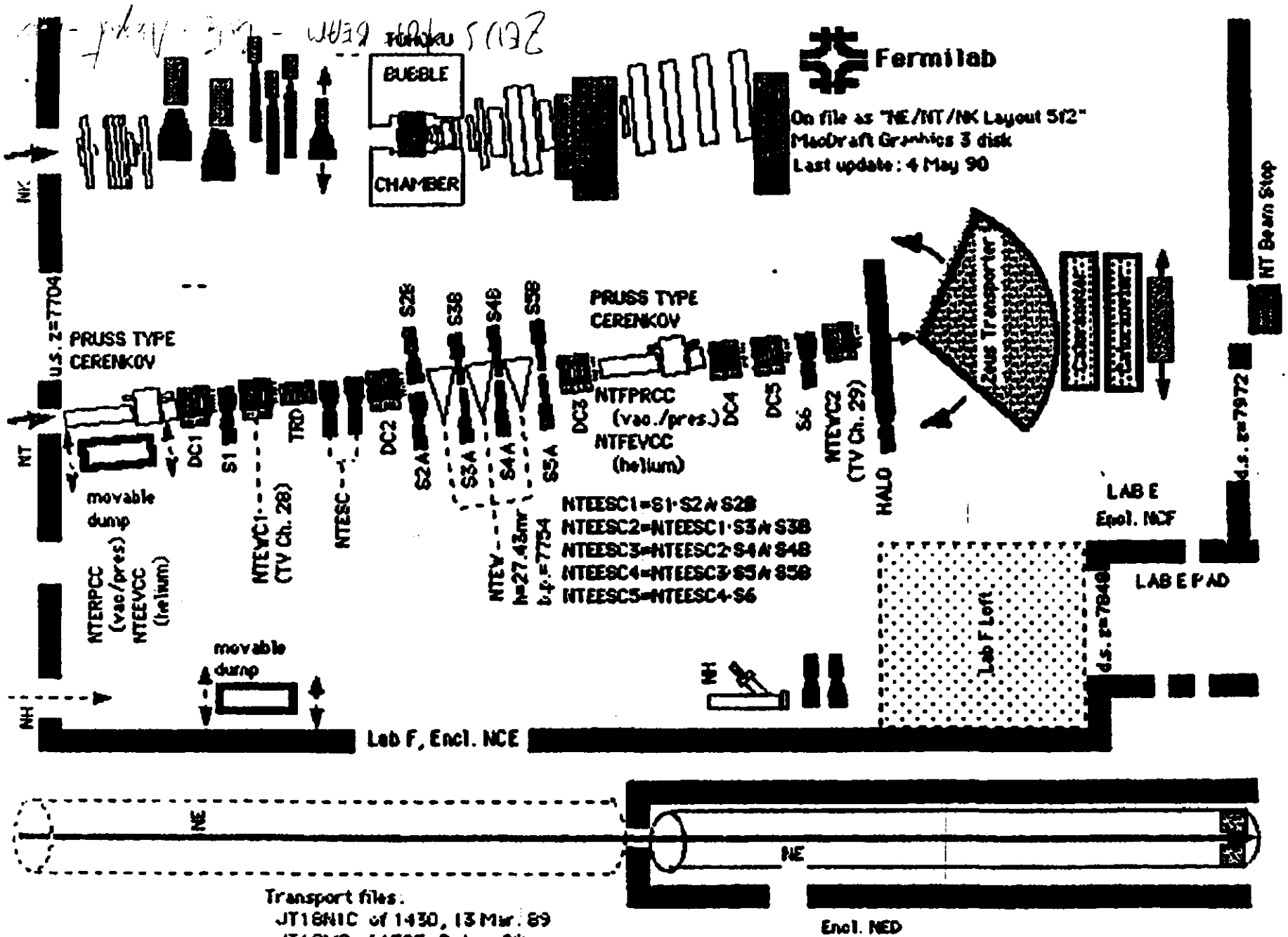
Fermilab
On file as "NE/NT/NK Layout 5f2"
MacDraft Graphics 3 disk
Last update: 4 May 90
BUBBLE
CHAMBER
NK
NT
NH
NE
u.s. z=7704
PRUSS TYPE
CERENKOV
movable
dump
NTERPCC
(vac/pres)
NTEEVCC
(helium)
DC1
S1
NTEVC1
(TV Ch. 28)
TRD
NTESC
DC2
S2B
S3B
S4B
S5B
S2A
S3A
S4A
S5A
NTEV
h=27.43mr
d.s.=7754
PRUSS TYPE
CERENKOV
DC3
NTFPRCC
(vac./pres.)
NTFEVCC
(helium)
DC4
DC5
S6
NTEVC2
(TV Ch. 29)
HALO
Zeus Transporter
NTEESC1=S1·S2∧S2B
NTEESC2=NTEESC1·S3∧S3B
NTEESC3=NTEESC2·S4∧S4B
NTEESC4=NTEESC3·S5∧S5B
NTEESC5=NTEESC4·S6
movable
dump
Lab F, Encl. NCE
Lab F Loft
d.s. z=7840
LAB E
Encl. NCF
LAB E PAD
d.s. z=7972
NT Beam Stop
Encl. NED
Transport files:
JT18N1C of 1430, 13 Mar. 89
JT18f12 of 1505, 8 June 88
NTCAL3B of 1855, 25 Nov. 88
NEP16S1 of 1843, 18 Dec. 88
GT18C of 1620, 9 Aug. 89
Halo file: BCHAL02 of 0925, 9 June 88

L* MONTE CARLO RESOLUTION

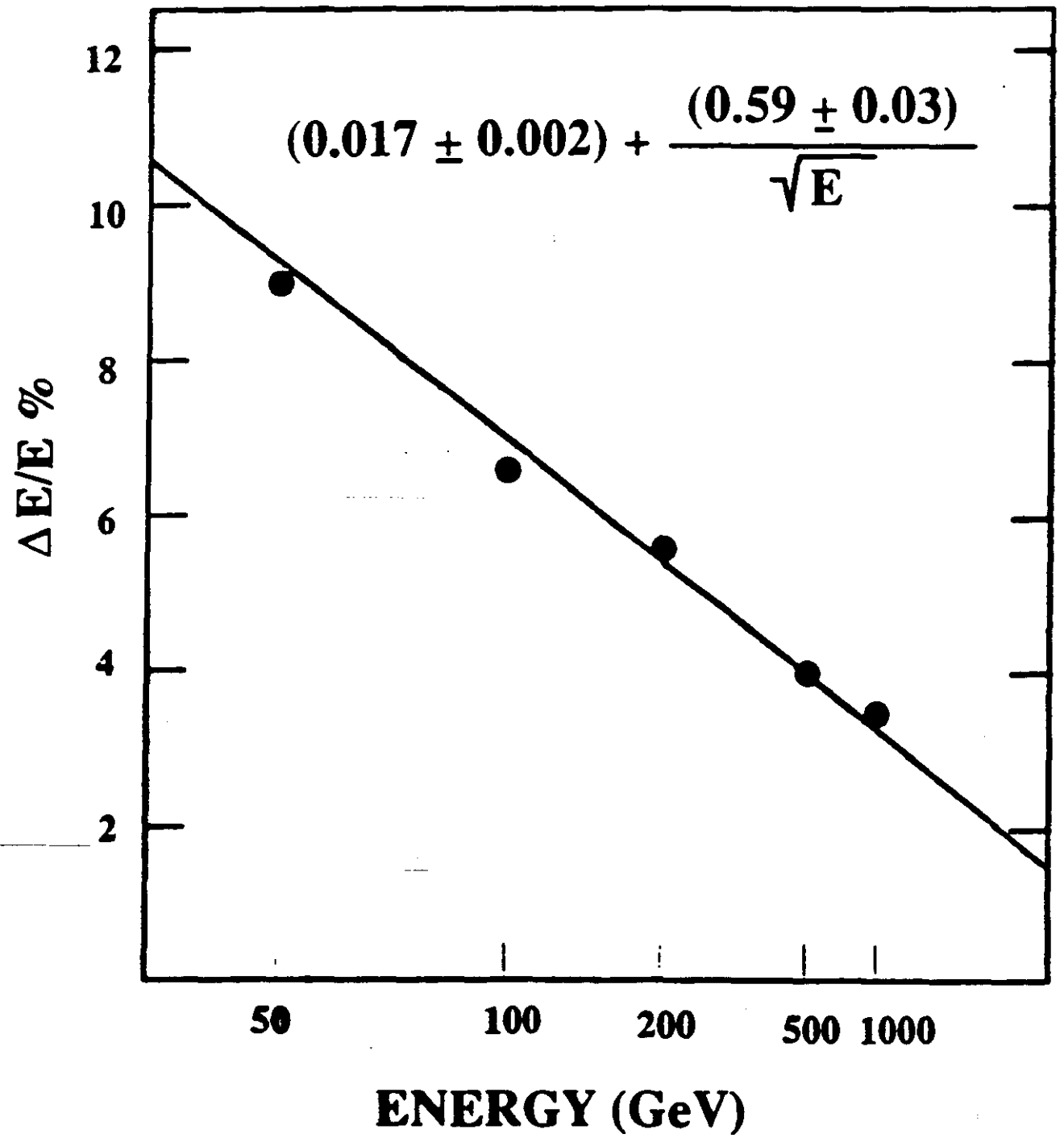

The energy resolution of calorimeters of different design has been extensively studied with the GHEISHA code [4]. Typical examples are shown in Fig.4.5 to 4.9 for incident jets as a function of energy in the 10 to 500 GeV range.

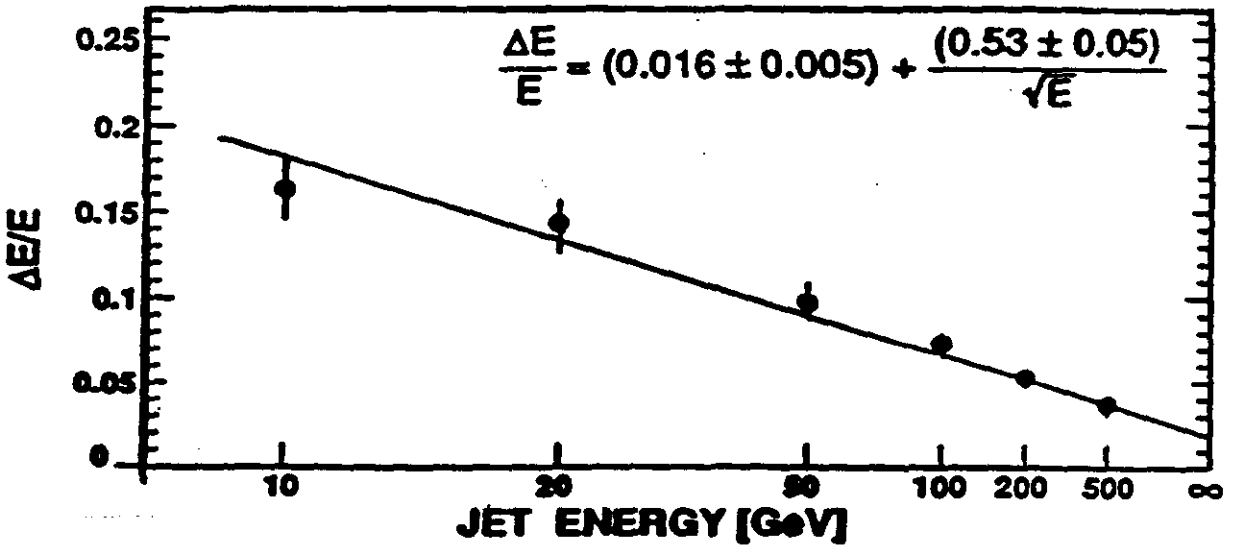

Fig.4.5 Jet energy resolution of BaF_2 (1.7λ) followed by 10.7λ of 2 cm Pb/0.5 cm scintillator.

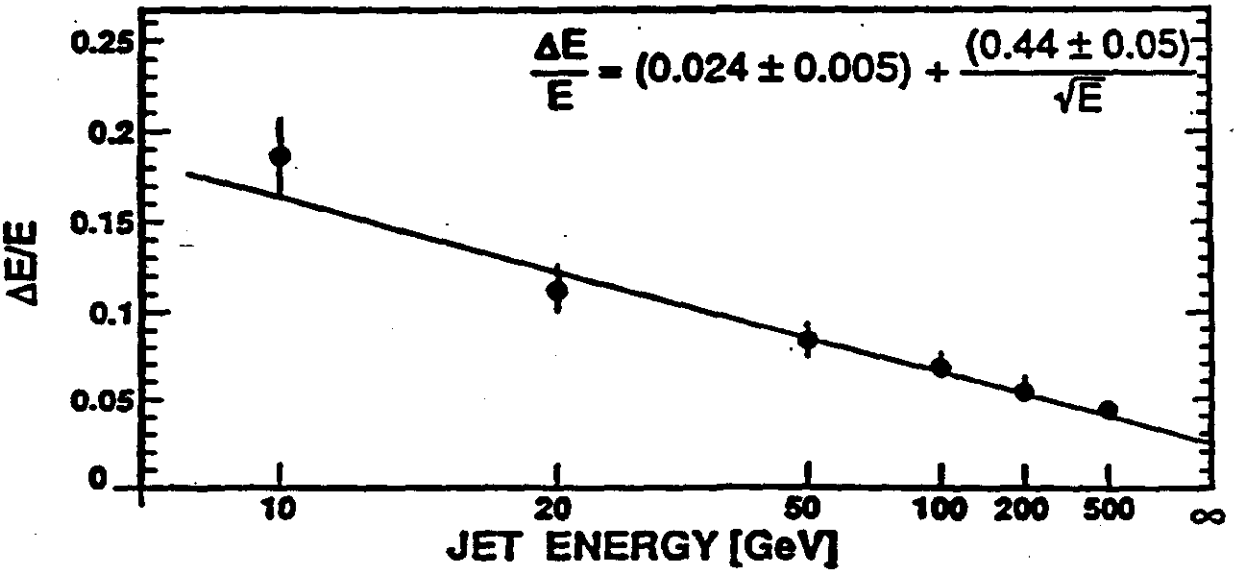

Fig.4.6 Jet energy resolution of BaF_2 (1.7λ) followed by 10.7λ of 1 cm Pb/0.5 cm scintillator.